Vol.: 48(2)
June, 2024
ISSN: 0250-4758
Online ISSN: 0973-970X

IJVP-2024

INDIAN JOURNAL OF VETERINARY PATHOLOGY

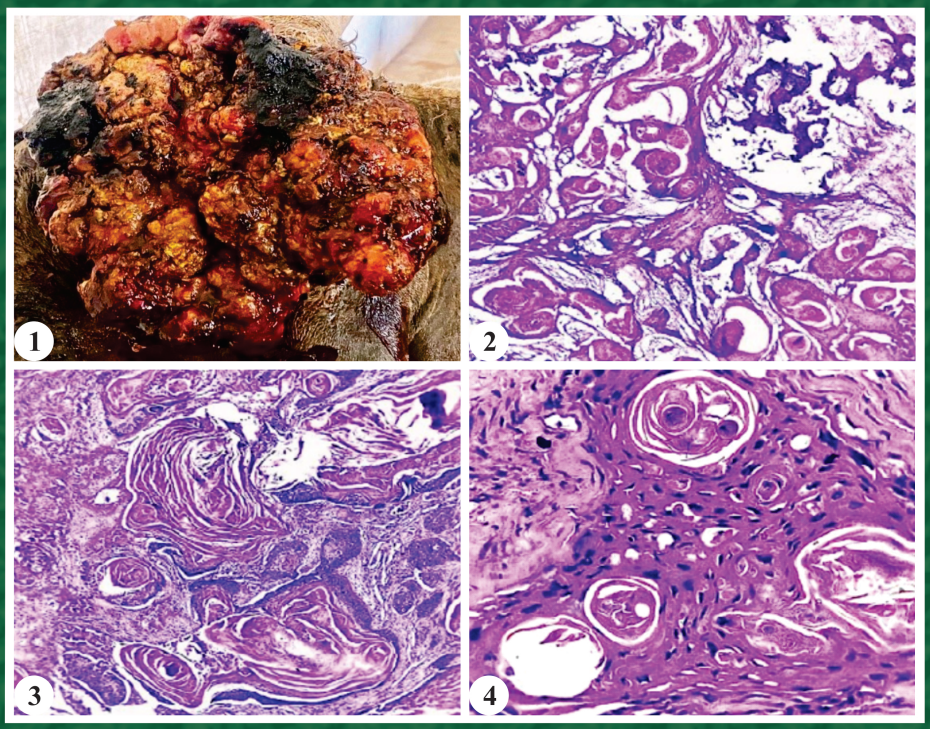

INDIAN ASSOCIATION OF VETERINARY PATHOLOGISTS
(Registered under article 21 of Societies Act 1860)

Visit us at: **www.iavp.org**
Journal available at: **www.indianjournals.com**

Vol. 48 (2)
June, 2024
ISSN: 0250-4758

INDIAN JOURNAL OF VETERINARY PATHOLOGY

Department of Veterinary Pathology, College of Veterinary Science,
Sri Venkateswara Veterinary University, Tirupati-517502, Andhra Pradesh
Mobile: +91-9441185383; E-mail: 7aakumar@gmail.com

INDIAN JOURNAL OF VETERINARY PATHOLOGY

Membership Fee and Subscription of Journal

- Individual life membership — Rs. 3,000/- (India) — US$ 600/- (Foreign)
- Individual Annual Membership (for foreign only) — US $ 60/- (with free online access; no hard copy of journal)
- Library, Institutions, etc. (Annual) — Rs. 12,000/- (India) — US$ 400/- (Foreign)
- Individual Patron of IAVP — Rs. 1,00,000/- (Life member - paid patron for 5 years)
- Govt./Non-Govt./Corporate/ Institution Patrons — Rs. 5,00,000/ (for 5 years)

Advertisement Tariff

	Black and White	Full Colour
Regular full page	Rs. 4,000	Rs. 6,000
Regular half page	Rs. 2,000	Rs. 3,000
Inside front & back cover page	–	Rs. 10,000
Back cover page	–	Rs. 15,000

Note:

- Those submitting advertisement for two/four/six issues of the IJVP will be extended 15%/20%/25% discounts, respectively, on the above rates.
- The membership fee must be paid through Cash/Online/Crossed cheque or DD in favour of Treasurer "Indian Association of Veterinary Pathologists" payable at SBI, CARI Branch, Bareilly.

Contents

INDIAN JOURNAL OF VETERINARY PATHOLOGY

INDIAN ASSOCIATION OF VETERINARY PATHOLOGISTS
(Estd. 1974)

Cover Page Photo : Squamous Cell Carcinoma in horn in cattle. **Fig. 1.** A well-differentiated squamous cell carcinoma, a tumourous mass of about 20 cm diameter at the base of horn in a bullock. **Fig. 2.** Depicting numerous epithelial pearls with areas of mineralization. **Fig. 3.** Many keratin micro cysts. **Fig. 4.** Keratin pearls, keratin cysts and numerous mitotic figures.

Indian J. Vet. Pathol., 48(2) : 99-105, 2024: DOI: 10.5958/0973-970X.2024.00019.4

REVIEW ARTICLE

Control of Newcastle disease: Do we need to change vaccine candidate

Nitin V. Kurkure* and Megha P. Kaore
Department of Veterinary Pathology, Nagpur Veterinary College, Maharashtra Animal & Fishery Sciences University, Nagpur-440 006, India

Address for Correspondence
Nitin V. Kurkure, Director of Research, Department of Veterinary Pathology, Nagpur Veterinary College, Maharashtra Animal & Fishery Sciences University, Nagpur-440 006, India, E-mail: nitinkurkure@rediffmail.com

Received: 26.3.2024; Accepted: 23.4.2024

ABSTRACT

Newcastle disease (ND) is one of the most economically devastating infectious diseases affecting the poultry industry globally. ND is vaccine-preventable but is a persistent threat to the poultry industry. The amino acid sequence of the cleavage site of the F protein has primarily determined the molecular basis for the pathogenicity of NDV. The F cleavage site reversion from avirulent to virulent has been reported for infectious clones after just one passage in chicken brains. Currently, the most widely used ND vaccines belong to early genotypes I and II, which were isolated approximately 70 years ago. Nevertheless, the prevalent NDV strains in poultry belong to late genotypes, including genotype V in America, genotype VII in Asia and Africa, which are genetically and antigenically distinct from traditional vaccines. Live ND vaccines, which include lentogenic and mesogenic vaccines, are commonly used to prevent and control the disease. Current live vaccines' mismatch with the dominant viruses is a major concern. Although NDV belongs to a single serotype, there are great genetic and antigenic variations between conventional live vaccines and viruses present in the field. Commercial rNDV genotype VII.1.1 vaccines based on the LaSota strain induced a protective immune response; however, GII-based vaccines failed to prevent virus shedding efficiently. A commercial live vaccine composed of recombinant NDV expressing the F and HN genes from genotype V NDV is more effective in reducing viral excretion than the LaSota strain. Genotype VII vaccine had a significantly higher protection rate than the LaSota vaccine against genotype VII NDV. A novel genotype VII-matched vaccine strain, generated by reverse genetics, induces a stronger cell-mediated immune response that blocks the viral shedding and provides full protection to chickens than LaSota in chickens. Looking towards the persistent threat of ND, we need to think about changing the vaccine strain or the use of genotype-matched vaccines for ND outbreaks in India.

Keywords: F and HN genes, Genotype VII, LaSota, ND vaccine, Poultry, Wild birds

INTRODUCTION

Newcastle disease (ND) is one of the most economically devastating infectious diseases affecting the poultry industry globally, even a century after its first description in Newcastle upon Tyne, UK, in Indonesia in 1926[1]. In India, ND is considered as enzootic and is commonly known as the Ranikhet Disease (RD) among poultry farmers and veterinarians. Though ND is vaccine-preventable, it is a persistent threat to the poultry industry across the globe. The disease is highly contagious and, without an adequate control strategy, causes high morbidity and mortality rates in naive or poorly vaccinated chickens, as well as drops in egg production in well-vaccinated layers[2]. Newcastle disease has a wide host range among avian species; at least 250 species classified in 27 of the 50 orders of birds are susceptible to ND[3]. The transmission of NDV is primarily through aerosol or oral routes. Based on the available literature, NDV ecology can be divided into two host systems: wild waterfowl harboring lentogenic strains[4] and domestic poultry, in which outbreaks occur due to mesogenic/velogenic strains. The highly pathogenic strains seem to arise during replication of the virus in high-density poultry populations[2]. Though vaccines were developed decades ago and have reduced morbidity and mortality-related losses, repeated ND outbreaks in chickens are reported even in vaccinated populations across the globe. Due to the lack of routine surveillance programs in India, there is a considerable knowledge gap on circulating NDV strains in apparently healthy birds, and epidemiological features associated with ND outbreaks.

How to cite this article : Kurkure, N.V. and Kaore, M.P. 2024. Control of Newcastle disease: Do we need to change vaccine candidate. Indian J. Vet. Pathol., 48(2) : 99-105.

Newcastle disease virus (NDV) belongs to the order Mononegavirales, family Paramyxoviridae, and to the genus Orthoavulavirus, recently renamed by the International Committee on Taxonomy of Viruses (ICTV). NDV, formerly known as the Avian paramyxovirus 1 or the Avian avulavirus1, is formally known since 2018 as the *Avian orthoavulavirus 1*. NDV is an enveloped virus with a single-stranded, negative-sense, non-segmented RNA genome.

The NDV genome encodes six viral proteins: the nucleoprotein (NP), phosphoprotein (P), matrix (M), fusion (F), haemagglutinin-neuraminidase (HN) and large (L) proteins[5]. M, HN and F form the envelope. The M protein is located at the inner face of the viral membrane and is responsible for driving the viral budding and virion assembly process. Proteins HN and F, are surface glycoproteins anchored to the viral envelope. The HN protein mediates the attachment of the virus to the host cell receptor, and the F protein mediates the fusion of viral and host cell membranes. Based on the pathogenicity of susceptible chickens, NDV can be classified into three pathotypes: velogenic, mesogenic, and lentogenic. Velogenic strains are further classified into viscerotropic velogenic and neurotropic velogenic strains. Viscerotropic velogenic strains produce lethal haemorrhagic lesions in the visceral organs, whereas neurotropic velogenic strains cause neurological and respiratory disorders. Lentogenic NDV strains cause subclinical infection with mild respiratory or enteric disease and are considered low-virulent. Strains with an intracerebral pathogenicity index (ICPI) ≥ 0.7 are defined as virulent strains according to the World Organization for Animal Health standards[6].

Panzootics of ND

ND is an important infectious disease with a history of nearly a century that has caused at least four panzootics globally. The first panzootic, from the 1930s to 1960s, was caused by viruses of genotypes I, II, III and IV. The second panzootic, from the late 1960s to 1973, was mainly caused by genotype V and VI viruses. In 1975, the third panzootic started in pigeons and spread to various regions around the world. Genotype VI NDV was responsible for this panzootic. In the late 1980s, genotype VII NDV originated from the Far East and spread throughout the world, causing the fourth panzootic. Currently, genotype VII NDV is endemic in many countries in Asia and Africa, posing a great threat to the poultry industry because of high infectivity and mortality rates and the ability for rapid spread, strains of subgenotype VII.2 (former VIIi) have been regarded as the possible cause of the fifth and latest ND panzootic[7].

Molecular basis of pathogenicity and virulence of NDV

The amino acid sequence of the cleavage site of the F protein has primarily determined the molecular basis for the pathogenicity of NDV. The F protein is a membrane glycoprotein that mediates virus-cell fusion. It is synthesized as a precursor, F0, and is fusogenic only after cleavage into disulfide-linked F1 and F2 polypeptides by host-cell proteases[8]. Thus, NDV becomes infective only when the precursor glycoprotein F0 is cleaved into F1 and F2. The ability to cleave F0 varies among different strains of NDV and has been determined to be a main determinant of NDV virulence. Virulent (mesogenic and velogenic) strains have the polybasic amino acid motif, 112 R/K- R- Q- K/R- R- F 117 (R-arginine; K-lysine; Q-glutamine; F-phenylalanine), allowing cleavage by proteases ubiquitously present in cells throughout the body, resulting in pantropic or systemic infection. In contrast, avirulent (lentogenic) and asymptomatic strains have fewer basic amino acids in the same region of 112 G/E- K/R- Q- G/E- R- L 117 (E-glutamate; G-glycine; L-leucine) and require a trypsin-like enzyme for cleavage. These viruses, therefore, appear to be restricted to replication primarily in the respiratory and intestinal tracts[6]. The F cleavage site reversion from avirulent to virulent has been reported for infectious clones after just one passage in chicken brains[9].

Transmission of NDV

The natural infection of birds occurs by the respiratory or the intestinal routes following either inhalation or ingestion of an infectious virus. Inhalation of infectious viruses may occur as the result of the presence of either large droplets or fine aerosols containing the virus. Since large amounts of virus particles are excreted in feces, ingestion of feces results in infection; this is the principal method of bird-to-bird spread without respiratory disease. Following the infection, the incubation period of ND after natural exposure has been reported to vary from 2-15 days (average 5-6 days). The speed of manifestation of clinical disease is variable depending on the infecting virus, the infected host, and environmental conditions[10].

Clinical signs

Clinical manifestation of disease depends on the virus's effects on respiratory, enteric, and/or nervous systems. Many factors related to the host (species, age and immune status), virus strain (pathotype, dosage, and route of infection), environmental stress and concurrent diseases can influence the severity and the course of the disease[11]. Respiratory signs of gasping, coughing, sneezing, and rales predominate in infections with the low virulence NDV widely used as live vaccines. Nervous signs of tremors, paralyzed wings and legs, torticollis, circling, clonic spasms, and complete paralysis may accompany but usually follow, the respiratory signs in neurotropic velogenic disease[12,13].

Gross and microscopic lesions

Gross lesions and the organs affected in birds infected with NDV are also dependent on the strain and pathotype of the infecting virus. No pathognomonic lesions are associated with any form of the disease. Gross lesions may also be absent. The presence of hemorrhagic lesions in the intestine of infected chickens has been used to distinguish very virulent Newcastle disease viruses (VVNDV) from non-virulent Newcastle disease viruses. The combined presence of gross lesions such as tracheal hemorrhage/necrosis, hemorrhage/necrosis of the proventriculus, and necrosis and/or ulceration of the gut-

associated lymphoid tissue (GALT) is considered highly indicative of VVNDV[14,15]. Gross pathologic changes are not always present in the respiratory tract, but when observed they are predominantly as mucosal hemorrhage and marked congestion of the trachea. Airsacculitis may be present even after infection with relatively mild strains and thickening of the air sacs with catarrhal or caseous exudates is often observed in association with secondary bacterial infections. Microscopic lesions are also more severe with VVNDV and are generally characterized by extensive depletion and necrosis of lymphoid organs and aggregates (mostly in GALT)[16]. In the respiratory system, the effect of NDV infection on membranes of the upper respiratory tract may be severe and related to the degree of respiratory distress. In the mucosa of the upper respiratory tract, congestion, edema, and dense cellular infiltration of lymphocytes and macrophages may be seen, particularly following aerosol exposure. Lesions may extend throughout the length of the trachea and comprise hyperplasia of the goblet cells, lymphocyte infiltration, disorientation and deformation of the cilia, and deciliation of the epithelium. A secondary bacterial infection increases the severity of respiratory lesions. Typical gross lesions are not usually observed in birds infected with the non-virulent Newcastle disease virus pathotype. Histologically, most noticeable findings are confined to the central nervous system and the cerebellum is more commonly involved. The lesions are characterized by mononuclear perivascular cuffing (mostly lymphocytes and plasma cells), neuronal degeneration and necrosis mainly of the Purkinje cells, endothelial cells hypertrophy, and gliosis[16]. Pneumonia, lymphoid depletion, and myocarditis also occur in birds infected with NVNDV isolates. Mesogenic virus infection causes perivascular cuffing, gliosis, and neuronal cuffing in the brain[12]. Minimal lesions may be present in birds infected with lentogenic NDV isolates, affecting mostly the respiratory tract.

Diagnosis

For effective disease management, it is important to identify birds that are infected with NDV and distinguish vaccine viruses from virulent viruses. Isolation and identification of NDVs and their subsequent characterization are important. The embryonating chicken egg is used almost universally for the propagation of NDV and allantoic fluid is harvested for virus isolation[6]. The presence of a virus can be detected by a hemagglutination (HA) test. Molecular diagnostic techniques have been developed in recent years. Direct detection of viral RNA isolated from swab samples or tissues may be tested using RT-PCR. Real-time RT-PCR assays cannot only distinguish APMV-1, but some tests can distinguish virulent NDV from lentogenic NDV[3]. Diagnostically, serology is most often used to measure the effectiveness of a vaccination program. Commercial ELISA kits are also available and are used to evaluate the uniformity of vaccination for a poultry flock.

Evolution of NDV

Nearly 100 years after its discovery, NDV has undergone a remarkable evolution, resulting in high diversity in terms of genetics, virulence, antigenicity, and host range. First, similar to other non-segmented RNA viruses, genomic changes in NDV mainly stem from the error-prone nature of the polymerase, which generates genetic variants known as quasi-species. Virus quasi-species harboring site mutations accumulating in the NDV genome can lead to apparent changes in viral phenotypes under selection pressure, representing a primary mechanism of virus evolution[17]. Novel genotypes may emerge with the accumulation of genetic variations, which may explain the association between each ND panzootic and the emergence of new genotypes. In addition to natural genetic evolution, antibodies in poultry flocks immunized with NDV vaccines exert high immune pressure on virus survival, especially in countries where extensive and frequent ND vaccination is performed. Mutations in the two surface glycoproteins, F and HN, contribute to viral escape from antibody immunity[18]. Second, the change in the host range is also an important outcome of virus evolution. Chickens are the major host of NDV, but there has been substantial expansion of the host range after ND panzootics. Waterfowl are the natural hosts of lentogenic NDV and are thought to be resistant to virulent NDV. However, during the fourth panzootic, outbreaks in geese caused by genotype VII NDV occurred in China, demonstrating the spillover of NDV from terrestrial to aquatic birds[19]. Subsequently, ND outbreaks in ducks were reported more frequently than before, highlighting an increased threat of NDV to waterfowl[20]. Another unique feature of the NDV host range is virus circulation in pigeons. Since the third panzootic, the primary genotype spreading in pigeons has been genotype VIb, and this genotype mainly infects pigeons under natural conditions. This finding indicates that genotype VIb (New classification, VI.1.1) viruses have established steady host specificity in pigeons since the third panzootic[21].

Genotypes of Newcastle disease virus

In the past, various schemes have been concurrently used to classify NDV based on their genetic information. However, each system was based on different approaches and lacked objective criteria for the classification of NDV isolates into different genetic groups. An international consortium of experts generated curated, up-to-date, complete fusion gene class I and class II datasets of all known NDV for public use, performed comprehensive phylogenetic Neighbor-Joining, maximum-likelihood, Bayesian and nucleotide distance analyses, and compared

these inference methods[22]. It provides updated, unified classification and nomenclature criteria for NDV.

Strains of NDV are divided into two classes, class I and class II, with class II further divided into different genotypes. Class I viruses are typically isolated from wild birds and all reported strains are of low virulence. The class I isolates are all grouped into a single genotype and three subgenotypes. The class II isolates are a mixture of viruses with diverse virulence potentials ranging from the most popular vaccine strains used for disease control to the highly virulent strains that cause outbreaks in different parts of the world. Class II isolates are classified into genotypes I-XXI, with majority of the genotypes being further subdivided into various subgenotypes. Genotype I isolate which are globally distributed are composed of three subgenotypes: I. 1.1 (former 1a), I.2 (former 1b), and I.1.2.1 (former 1c), I.1.2.2 (former 1d), most of which are considered lentogenic[22]. Indeed, the widely reported Queensland V4 and Ulster/chicken/Ireland/1967 vaccine strains are all grouped under this genotype. The genotype II isolates are a mixture of velogenic and lentogenic viruses such as LaSota and B1 strains used globally for disease control. Isolates in this genotype have been majorly recovered from domestic fowl, chicken, and wild birds found in North and South America, Africa, Asia, and Europe. Isolates belonging to genotypes III, IV, V, and VI are all predicted or pathotyped to be virulent in chicken. The genotype III isolates, which include the popular mesogenic Mukteshwar strain used as a vaccine strain, were recovered from birds in Japan as early as the 1930s and also in Pakistan around the mid-1970s before they subsequently resurged in China less than two decades ago[23]. Likewise, the genotype IV isolates occurred among the European poultry before the 1940s and include the extensively characterized Herts/33 strain. As for the genotype V isolates that emerged for the first time around the 1970s in America and spread to the European continent in the 1980s. So far, isolates in this genotype have been divided into four distinct subgenotypes (Va, Vb, Vc, and Vd) because of their within-the-group heterogeneity. However, the genotype VI isolates, which are cosmopolitan in distribution, are much more heterogeneous genetically. They were divided into subgenotypes VIa-k because of their enormous genetic diversity: VI.2.1.1.1 (VI a), VI.1.1 (VI b), VI.1.2.2.2 (VI e), VI.1.2.2.1 (VI f), VI.1.2.1.2 (VI h), VI.2.1.1.2.1 (VI j), VI.2.1.1.2.2 (VI k)[22].

Genotype VII isolates are arguably the most important group of NDV reported in the 21st century. From the year 2000 to date, these viruses have been incriminated in several economically important disease outbreaks in Asia, the Middle East, and some parts of America and South Africa. The viruses responsible for the fourth NDV panzootic grouped together and based on nucleotide distance, are classified into a single genotype (VII.1.1) [combining former sub-genotypes VIIb, VIId, VIIe, VIIj, and VIII]. An exception is former sub-genotype VIIf, which is classified as a separate sub-genotype, namely VII.1.2. This complex genetic diversity of genotype VII NDV highlights the need to monitor the epidemiological dynamics of the emerging viruses so that an effective vaccination program can be designed. Unlike the genotype VII isolates, members of the genotype VIII taxon are less diverse both genetically and in terms of spatial distribution. Apart from the report on their occurrence in Malaysia, Singapore, China, Turkey, Argentina, and South Africa between the 1960s and 1990s, no report exists on their emergence in other parts of the world in the recent times. Hence, they are thought to currently cease circulation in domestic birds. In contrast, the genotype IX isolates are still evolving in wild birds and domesticated poultry since survey of NDV between 2008 and 2011 revealed their presence in China. Nevertheless, they are still considered to be among the early genotypes, having been isolated as early as 1940s. However, unlike members of this genotype (genotype IX) which are mostly virulent in chicken, genotype X isolates are all predicted to be in the lentogenic class. Despite their restricted geographic distribution, they are still maintained between the turkeys and wild birds in Argentina and the United States of America. They are, however, among the less genetically diverse groups of NDV. The most geographically restricted group of NDV is the genotype XI isolates. They have only been reported from Madagascar, where they are believed to circulate between wild birds and domestic chickens. Although they are all predicted to be virulent based on the chemistry of their F cleavage site, there are reports of their isolation from apparently normal unvaccinated birds in Madagascar. Meanwhile the genotype XII isolates, which are all predicted to be virulent, have been reported from both China and America in geese and chicken, respectively. The epidemiological connection between the isolates in America and those in China is, however, still not clear since migratory birds have not so far been incriminated in carrying these viruses.

Genotype XIII isolates, which have been recovered from birds in Europe, Asia, and Africa, are all predicted to be virulent based on the amino acid composition of their F cleavage site. They are thought to be continuously evolving especially in Asia and the Middle East. Previously, they were divided into subgenotypes XIIIa, XIIIb, XIIIc, and XIIId based on old (year 2012) classification[24]. As per the new classification proposed[22], genotype XIIIa into XIII.1.1 and XIII.1.2, and XIIIb into XIII.2.1 and XIII.2.2, respectively, because of the addition of new sequences from recent studies[25]. Viruses isolated from different countries in Africa between 1995 and

2015 formed sub-genotype XIII.1.1, while viruses from Sweden, Russia, India, and Iran from 1997 to 2011 are classified in XIII.1.2. Viruses isolated in the last decade from Pakistan and India formed XIII.2.1 and XIII.2.2, respectively. Isolates from genotypes XIV, XVII, and XVIII have been recovered mainly from domesticated birds such as chickens, turkeys, and guinea fowls. The new NDV nomenclature proposal classified the viruses previously classified as members of sub-genotype Va are separated into a new genotype XIX[22]. Previous subgroups VIai and VIaii encompassed the early strains circulating in poultry but not pigeons into the new genotypes XX and XXI, whereas PPMV-1 remained in genotype VI with several sub-genotypes.

Currently available Vaccines

Currently, the most widely used ND vaccines belong to early genotypes, such as I and II, isolated approximately 70 years ago. Nevertheless, the prevalent NDV strains in poultry belong to late genotypes, including genotype V in America, genotype VII in Asia and Africa, and genotype VI in pigeons on different continents, which are genetically and antigenically distinct from traditional vaccines. Live ND vaccines, which include lentogenic and mesogenic vaccines, are commonly used to prevent and control the disease. Lentogenic live vaccines are the most widely used globally, and La Sota and B1 are the representative strains. These viruses belong to genotype II and show high similarities at the genetic and antigenic levels. Lentogenic vaccines can induce protective antibody responses, although they differ in chicken tissue tropism and replication patterns. The LaSota strain shows high tropism to the respiratory system and replicates to high levels in chickens. Antibody titers induced by LaSota are generally high, and this vaccine is thus suitable for use in countries where virulent NDV is endemic. The VG/GA vaccine is characterized by a dual tropism to the respiratory tract and intestine, with a higher tropism to the latter, and can elicit strong mucosal. In addition, the B1 vaccine has a very low virulence and is highly safe for chicks, and it is usually used under low-level infection or in chicks. Another type of lentogenic live vaccine is based on genotype I, and V4 and I-2 represent this type. These strains present low virulence and good safety in chickens of all ages. Moreover, V4 and I-2 are typical thermo-stable vaccines with the unique advantage of being used in remote country areas with limited cold chain facilities. They can be administered through drinking water or feed[26].

Need forgenotype-matched vaccines

Many studies have consistently verified that conventional ND vaccines protect against morbidity and mortality rather than reducing virus shedding from vaccinated chickens. In these circumstances, field viruses can still be silently disseminated in poultry flocks and cause nontypical diseases[2]. Most current vaccines and vaccination regimes primarily aim to mitigate clinical disease. Current live vaccines mismatch with the dominant viruses is a major concern. Although NDV belongs to a single serotype, there are great genetic and antigenic variations between conventional live vaccines and viruses present in the field.

In India, genotypes VI.2.1.1.1 (VI) and VII.1.1 (VII), XIII.2.2 (XIIIe) from Tamilnadu[25,28], genotype XIII.2.2 from Gujarat[29,30], genotype VII 1.1 (VII) and XIII.2.2 (XIIIb) from Central India[31,32], genotype VIIi and XIII.2.2 (XIIIb) from Uttar Pradesh[33] and recently novel genotype XIII.2.2, XXII.1 and XXII.2 from North-East region of India[34] have been reported. Similarly, in Latin America, the most frequent genotypes affecting poultry farms correspond to genotypes V, VI, VII, XII and XVI, and revealed that the amino acid sequence homologies of the F and HN proteins between the LaSota strain and genotype VII strains range from 87-89% and 87-88%, respectively[35]. Administration of live ND vaccines homologous to circulating viruses is beneficial for reducing virus shedding in the flock. Notably, reducing virus shedding is a key parameter for evaluating the efficacy of a novel recombinant genotype VII NDV vaccine in China. Two commercial rNDV genotype VII.1.1 vaccines based on the LaSota strain backbone or VG/GA strain backbone induced a protective immune response; however, genotype II-based vaccines failed to prevent virus shedding efficiently. Additionally, the noticeable superior performance of the rNDV vaccine based on the VG/GA strain backbone may be attributed to the enterotropic nature of the VG/GA strain, which makes it replicate more efficiently in both the respiratory and intestinal tracts of chickens[36]. Accordingly, a commercial live vaccine composed of recombinant NDV (rNDV-P05) expressing the F and HN genes from genotype V NDV are more effective in reducing viral excretion than the LaSota strain[37]. Recombinant rLS1-XII-2 and the commercial vaccine strain LaSota induced 100% protection. However, rLS1-XII-2 virus significantly reduced viral shedding, both in the number of shedding birds and in quantity of shed virus[38]. Genotype VII SG10 vaccine had a significantly higher protection rate than the LaSota vaccine against genotype VII NDV, regardless of intramuscular (IM) or eye drop/intranasal (ED/IN) route of SG10 challenge[39]. Recombinant genotype-matched VII NDV inactivated vaccine and a live attenuated vaccine can reduce virus shedding and improve egg production in commercial layers challenged with a velogenic genotype VII (Chicken/USC/Egypt/2015) virus under field conditions[40]. A novel genotype VII-matched vaccine strain G7M, generated by reverse genetics, induces a stronger cell-mediated immune response, blocks the viral shedding and provides full protection to chickens than LaSota in chickens[41]. Two main strategies are employed to

generate genotype-matched live vaccines. Some virulent strains have been attenuated using reverse genetics and engineered to obtain modified live vaccines. Virulent strains are attenuated by modifying the F cleavage site, and extra specific mutations in the L protein can further guarantee the safety of the attenuated virus. The other strategy is to replace a lentogenic virus's protective F and HN antigens with the corresponding proteins from prevalent virulent strains, and the F cleavage site is usually mutated. Several live recombinant NDV vaccines of this type have been commercialized in Korea (Himmvac Dalguban N$^+$ Live Vaccine), Egypt (live attenuated RINNOVAC™ELI-7) and Mexico (Genovax N5).

As different genotypes are circulating in India and currently used genotype II vaccines are unable to control the virus shedding despite proper and repeated vaccination, genotype-matched vaccines may prove beneficial in reducing virus shedding and thereby controlling Newcastle disease in India.

REFERENCES

1. Bello MB, Yusoff K, Ideris A, Hair-Bejo M, Peeters BP and Omar AR. 2018. Diagnostic and vaccination approaches for Newcastle disease virus in poultry: The current and emerging perspectives. *Biomed Res Int* 56-62.
2. Alexander DJ, Bell JG and Alders RG. 2004. A technology review: Newcastle disease, with special emphasis on its effect on village chickens.
3. Sahoo N, Bhuyan K, Panda B, Behura NC, Biswal S, Samal L, Chaudhary D, Bansal N, Singh R, Joshi VG and Jindal N. 2022. Prevalence of Newcastle disease and associated risk factors in domestic chickens in the Indian state of Odisha. *PloS One* **17:** 1-12.
4. Jindal N, Chander Y, Chockalingam AK, De Abin M, Redig PT and Goyal SM. 2009. Phylogenetic analysis of Newcastle disease viruses isolated from waterfowl in the upper midwest region of the United States. *Virol J* **6:** 1-9.
5. Shabbir MZ, Malik AN, Wajid A, Rehmani SF and Munir M. 2013. Newcastle disease virus: disease appraisal with global and Pakistan perspectives. *J Infect Mol Biol* **1:** 52-57.
6. OIE. 2018. Manual of diagnostic tests and vaccines for terrestrial animals: mammals, birds and bees. World Organization for Animal Health, Paris.
7. Mousa MR, Mohammed FF, El-Deeb AH, Khalefa HS and Ahmed KA. 2020. Molecular and pathological characterization of genotype VII Newcastle disease virus on Egyptian chicken farms during 2016-2018. *Acta Vet Hung* **68:** 221-230.
8. Dortmans JC, Koch G, Rottier P and Peeters BP. 2011. Virulence of Newcastle disease virus: what is known so far. *Vet Res* **42:** 122-130.
9. Seal BS, King DJ and Bennett JD. 1995. Characterization of Newcastle disease virus isolates by reverse transcription PCR coupled to direct nucleotide sequencing and development of sequence database for pathotype prediction and molecular epidemiological analysis. *J Clin Microbiol* **33:** 2624-2630.
10. Kapczynski DR, Afonso CL and Miller PJ. 2013. Immune responses of poultry to Newcastle disease virus. *Developmental & Comparative Immunology* **41:** 447-453.
11. Merino R, Villegas H, Quintana JA and Calderon N. 2011. Comparison of the virulence of pathogenic Newcastle disease viruses belonging to the same or different genotypes. *Int J Poult Sci* **10:** 713-20.
12. Wakamatsu N, King DJ, Kapczynski DR, Seal BS and Brown CC. 2006. Experimental pathogenesis for chickens, turkeys, and pigeons of exotic Newcastle disease virus from an outbreak in California during 2002-2003. *Vet Pathol* **43:** 925-933.
13. Susta L, Miller PJ, Afonso CL and Brown CC. 2011. Clinicopathological characterization in poultry of three strains of Newcastle disease virus isolated from recent outbreaks. *Vet Pathol* **48:** 349-360.
14. Cattoli G, Susta L, Terregino C and Brown C. 2011. Newcastle disease: a review of field recognition and current methods of laboratory detection. *J Vet Diagn Invest* **23:** 637-656.
15. Kaore MP. 2012. Pathology and molecular characterization of Newcastle disease virus in and around Nagpur. MVSc Thesis submitted to Maharashtra Animal & Fishery Sciences University, Nagpur, India.
16. Brown C, King DJ and Seal B. 1999. Detection of a macrophage-specific antigen and the production of interferon gamma in chickens infected with Newcastle disease virus. *Avian Dis* **98:** 696-703.
17. Meng C, Qiu X, Yu S, Li C, Sun Y, Chen Z, Liu K, Zhang X, Tan L, Song C and Liu G. 2016. Evolution of Newcastle disease virus quasi species diversity and enhanced virulence after passage through chicken air sacs. *Virol J* **90:** 2052-2063.
18. Gu M, Liu W, Xu L, Cao Y, Yao C, Hu S and Liu X. 2011. Positive selection in the hemagglutinin-neuraminidase gene of Newcastle disease virus and its effect on vaccine efficacy. *Virol J* **8:** 1-8.
19. Wan H, Chen L, Wu L and Liu X. 2004. Newcastle disease in geese: natural occurrence and experimental infection. *Avian Pathol* **33:** 216-221.
20. Putri N, Ernawati R, Rahmahani J, Suwarno S and Rantam FA. 2021. Phylogenetic relationship and genotype variation of six Newcastle disease viruses isolated from duck in Indonesia. *Vet World* **14:** 276-284.
21. Pchelkina IP, Manin TB, Kolosov SN, Starov SK, Andriyasov AV, Chvala IA, Drygin VV, Yu Q, Miller PJ and Suarez DL. 2013. Characteristics of pigeon paramyxovirus serotype-1 isolates (PPMV-1) from the Russian Federation from 2001 to 2009. *Avian Dis* **57:** 2-7.
22. Dimitrov KM, Abolnik C, Afonso CL, Albina E, Bahl J, Berg M, Briand FX, Brown IH, Choi KS, Chvala I and Diel DG. 2019. Updated unified phylogenetic classification system and revised nomenclature for Newcastle disease virus. *Infect Genet Evol* **74:** 103-917.
23. Miller PJ, Decanini EL and Afonso CL. 2010. Newcastle disease: Evolution of genotypes and the related diagnostic challenges. *Infect Genet Evol* **10:** 26-35.
24. Diel DG, da Silva L, Liu H, wang Z, Miller PJ and Afonso CL. 2012. Genetic diversity of avian paramyxovirus type 1: Proposal for a unified nomenclature and classification system of Newcastle disease virus genotypes. *Infect Genet Evol* **12:** 1770-1779.
25. Gowthaman V, Ganesan V, Gopala Krishna Murthy TR, Nair S, Yegavinti N, Saraswathy PV, Suresh Kumar G, Udhayavel S, Senthilvel K and Subbiah M. 2019. Molecular phylogenetics of Newcastle disease viruses isolated from vaccinated flocks during outbreaks in Southern India reveals circulation of a novel sub-genotype. *Transbound Emerg Dis* **66:** 363-72.
26. Habibi H, Firuzi S, Nili H, Asasi K and Mosleh N. 2020. Efficacy of thermostable Newcastle disease virus strain I-2 in broiler chickens challenged with highly virulent Newcastle virus. *Arch Razi Inst* **75:** 31-37.

27. Hu Z, He X and Deng J. 2022. Current situation and future direction of Newcastle disease vaccines. *Vet Res* **53:** 99-103.
28. Tirumurugaan KG, Kapgate S, Vinupriya MK, Vijayarani K, Kumanan K and Elankumaran S. 2011. Genotypic and pathotypic characterization of Newcastle disease viruses from India. *PloS One* **6:** 1-6.
29. Jakhesara SJ, Prasad VV, Pal JK, Jhala MK, Prajapati KS and Joshi CG. 2016. Pathotypic and sequence characterization of Newcastle disease viruses from vaccinated chickens reveals circulation of genotype II, IV and XIII and in India. *Transbound Emerg Dis* **63:** 523-39.
30. Khorajiya JH, Pandey S, Ghodasara PD, Joshi BP, Prajapati KS, Ghodasara DJ and Mathakiya RA. 2015. Patho-epidemiological study on Genotype-XIII Newcastle disease virus infection in commercial vaccinated layer farms. *Veterinary World* **8:** 372-380.
31. Gogoi P, Morla S, Kaore M, Kurkure NV and Kumar S. 2015. Complete genome sequence of a newcastle disease virus isolate from an outbreak in central India. *Genome Announ* **3:** e01418-14.
32. Morla S, Shah M, Kaore M, Kurkure NV and Kumar S. 2016. Molecular characterization of genotype XIIIb Newcastle disease virus from central India during 2006-2012: evidence of its panzootic potential. *Microb Pathog* **99:** 83-6.
33. Gowthaman V, Singh SD, Dhama K, Desingu PA, Kumar A, Malik YS and Munir M. 2016. Isolation and characterization of genotype XIII Newcastle disease virus from Emu in India. *Virus Dis* **27:** 315-8.
34. Rajkhowa TK, Zodinpuii D, Bhutia LD, Islam SJ, Gogoi A, Hauhnar L, Kiran J and Choudhary OP. 2023. Emergence of a novel genotype of class II New Castle Disease virus in North Eastern States of India. *Gene* **864:** 147-315.
35. Xiao S, Nayak B, Samuel A, Paldurai A, Kanabagattebasavarajappa M, Prajitno TY, Bharoto EE, Collins PL and Samal SK. 2012. Generation by reverse genetics of an effective, stable, live-attenuated Newcastle disease virus vaccine based on a currently circulating, highly virulent Indonesian strain. *PLoS One* **7:** e52751.
36. Dewidar AAA, Kilany WH, El-Sawah AA, Shany SAS, Dahshan A-HM, Hisham I, Elkady MF and Ali A. 2022. Genotype VII.1.1-Based Newcastle Disease Virus Vaccines Afford Better Protection against Field Isolates in Commercial Broiler Chickens. *Animals* **12:** 1696.
37. Absalon AE, Cortes-Espinosa DV, Lucio E, Miller PJ and Afonso CL. 2019. Epidemiology, control, and prevention of Newcastle disease in endemic regions: Latin America. *Trop Anim Health Prod* **51:** 1033-1048.
38. Lara IR, Chumbe A, Calderón K, Fernández-Díaz M and Vakharia VN. 2019. Genotype-matched Newcastle disease virus vaccine confers improved protection against genotype XII challenge: The importance of cytoplasmic tails in viral replication and vaccine design. *PLoS One* **14:** e0209539.
39. Yang HM, Zhao J, Xue J, Yang YL and Zhang GZ. 2017. Antigenic variation of LaSota and genotype VII Newcastle disease virus (NDV) and their efficacy against challenge with velogenic NDV. *Vaccine* **35:** 27-32.
40. Sultan HA, Talaat S, Elfeil WK, Selim K, Kutkat MA, Amer SA and Choi KS. 2020. Protective efficacy of the Newcastle disease virus genotype VII-matched vaccine in commercial layers. *Poultry Sci* **99:** 1275-1286.
41. Ji Y, Liu T, Du Y, Cui X, Yu Q, Wang Z, Zhang J, Li Y and Zhu Q. 2018. A novel genotype VII Newcastle disease virus vaccine candidate generated by mutation in the L and F genes confers improved protection in chickens. *Veterinary Microbiol* **216:** 99-106.

Indian J. Vet. Pathol., 48(2) : 106-115, 2024: DOI: 10.5958/0973-970X.2024.00020.5

RESEARCH ARTICLE

Histopathological studies on horn and ocular carinoma in bovines

Vivek Kumar*, Dhananjay Kumar Jolhe, Ratan Chandra Ghosh and Rukmani Dewangan[1]
[1]Department of Veterinary Surgery & Radiology, Department of Veterinary Pathology, Dau Shri Vasudev Chandrakar Kamdhenu Vishwavidyalaya, Anjora, Durg-491 001, Chhattisgarh, India

Address for Correspondence
Vivek Kumar, Department of Veterinary Pathology, Dau Shri Vasudev Chandrakar Kamdhenu Vishwavidyalaya, Anjora, Durg -491 001, Chhattisgarh, India, E-mail: vk561997@gmail.com

Received: 21.10.2023; Accepted: 28.11.2023

ABSTRACT

An investigation was carried out on eighteen clinical cases of neoplasm in bovines suspected of squamous cell carcinoma (SCC) in Durg, Dhamtari and Rajnandgaon districts of Chhattisgarh. The pathomorphological features of neoplasms observed at horn and eye were recorded. Neoplasms observed at horn were named as SCC of horn and at eye as ocular squamous cell carcinoma (OSCC). Unilateral large cauliflower like growths at the base of the horn and in ocular neoplasms, medium, unilateral firm cauliflower like growth, congested and reddish protruded mass of tissue covering the whole cornea were observed. Large nodular, hemorrhagic growth on limbus and lower eyelid with verrucous surface was also observed. Twelve out of eighteen cases (66.66%) were confirmatory for squamous cell carcinoma on the basis of histopathological examination of hematoxylin and eosin stained tissue sections. Histopathological findings were distinctive keratin pearls with concentric layers of keratinization observed in well differentiated SCC (n=5; 41.66%). Absence of epithelial pearls, although numerous mitotic figures with evidences of anaplasia and neovascularization were observed in poorly differentiated SCC (n=4; 33.33%), and moderate degree of keratinization at the center of neoplastic islets in moderately differentiated SCC (n=3; 25%). SCCs were classified as well, moderately and poorly differentiated types on the basis of histopathological scoring and grading.

Keywords: Epithelial pearls, eye and horn cancer, histopathology, pathological scoring, squamous cell carcinoma

INTRODUCTION

Squamous-cell carcinomas are malignant tumours of the stratified squamous epithelium - occur mostly in older animals[1]. Squamous Cell Carcinoma (SCC) is one of the most common cancer capable of metastatic spread and is observed in various forms across many animals[2-4]. Horn cancer is generally unilateral and is encountered in cattle between 5-10 years of age[5]. In India, horn cancer affects approximately 1% of the cattle population and accounts for 83.34% of total tumours reported[6]. Horn cancer is a sporadic, malignant neoplasm affecting the horn core epithelium and predominantly seen in aged zebu bullocks and rarely in buffaloes[7-9]. It is one of the most commonly encountered neoplastic conditions of economic importance in zebu bullock[10]. Anaplasia is one of the characteristic features of malignant neoplasms, also observed in SCC of horn. Microscopic examination of cancerous tissue collected from the region of horn core with typical keratinizing squamous cell carcinoma and characteristic formation of epithelial pearls, cell mass consists of concentric layer of squamous cells and gradual increase in keratinization towards the center was observed[11]. Abundance of connective tissue stroma along with numerous thin walled blood vessels[12], extension of neoplastic epithelial cells into dermis forming focal islands, cords and trabeculae showing variable degree of squamous differentiation. Epidermal hyperplasia, hyperkeratosis and fibrosis and keratin deposition as intracytoplasmic, eosinophilic fibrillar material with distinct keratin pearls[13] and numerous mitotic figures were observed with focal islands of neoplastic cells with moderate amount of basophilic cytoplasmare the characteristic histopathological findings of horn core carcinoma[22]. Well differentiated invasive type squamous cell carcinoma infiltrating into the basal layer and dermis with hyperkeratinization and squamous epithelial cells differentiated to form irregular islands of squamous epithelium surrounded by fibroblasts and collagen along with pleomorphic changes in the nuclei with cell nest formation or pearl like structure[14]. Another important form of SCC is ocular squamous cell carcinoma (OSCC), commonly referred as "cancer eye". Squamous cell carcinoma is by far the most common and most frequently diagnosed tumour afflicting the bovine eye. It is a primary neoplasm of epithelial origin occurring in different ocular and periocular tissues including the palpebral skin, epithelial surfaces of the cornea and conjunctiva, third eyelid and limbus[15]. Ocular squamous cell carcinomas were also reported in Indian buffaloes[7,11,16]. Microscopicaly, there is invasion of tumour cells in the region anterior uveal tissue forming small islands of keratinized cells

How to cite this article : Kumar, V., Jolhe, D.K., Ghosh, R.C. and Dewangan, R. 2024. Histopathological studies on horn and ocular carinoma in bovines. Indian J. Vet. Pathol., 48(2) : 106-115.

Fig. 1. Tumourous mass of about 20 cm diameter from the base of the horn in bullock (Case ID: BovHC4); **Fig. 2.** Large cauliflower-like growth on left horn of a cow (Case ID: BovHC3); **Fig. 3.** Profused bleeding from the tumourous mass in HF cow (BovEC3); **Fig. 4.** Wart like tumorous growth spreading from lateral canthus to the whole cornea (Case ID: BovEC6).

and keratin pearls in tumours of 3rd eyelid, cellular and nuclear atypia with several mitotic figures with assigned mitotic index (Table 1). Infiltration of inflammatory cells and intraepithelial neoplastic corneal cell projections with dermal stroma invasion and accentuated keratinization[15]. Grading of OSCCs according to the Broder's system based on the degree of keratinization and island formation of neoplastic cells centered on cellular differentiation, mitotic count, and degree of invasion[17].

SCCs are categorized into invasive and non-invasive types on the basis of histopathological findings. In noninvasive carcinoma, malignant transformation of the epithelial cells in the basilar layer or, less commonly, in the stratum spinosum[17]. Neoplastic cells with hyperchromatic nuclei, numerous mitotic figures, pleomorphism and loss of polarity[17]. Histopathological scoring is centered on cellular differentiation, mitotic count, and degree of invasion. Well-differentiated OSCCs characterized by neoplastic cells with abundant cytoplasm that commonly formed concentric laminated masses of keratin (keratin pearls). Moderately differentiated OSCCs that had a moderate degree of keratinization, small to medium-sized keratin pearls, smaller islands of neoplastic cells, and an increased number of poorly differentiated cells; neoplasms consisting of poorly differentiated cells without keratin pearls and only had individual cells undergoing keratinization. This communication reports the pathomorphological features of SCCs in 18 cases (17 in Cattle and 1 in Buffalo).

MATERIALS AND METHODS

The present study was conducted from January to June 2022 in the Department of Veterinary Pathology, College of Veterinary Science and Animal Husbandry (CVSc & AH), Durg (Chhattisgarh), India to explicate the histopathological alterations of squamous cell carcinoma in bovines (n=18). Following gross examination, the tissue samples were collected in 10% neutral buffered formalin from clinical cases suspected of neoplasms presented and operated at Veterinary Clinical Complex, CVSc & AH and Government Veterinary Hospitals of Durg, Dhamtari and Rajnandgaon districts of Chhattisgarh for histopathological studies.

Gross and Histopathological Examination

Growth observed in and around eye and cornua of horn suspected of SCC on the basis of gross pathology. Gross morphological features of tumours such as location, shape, colour and consistency of the tumour were recorded. Unique case identification number was given to each sample for further detailed study. The formalin fixed tissues were trimmed into pieces of 2-3 mm thickness and processed as per standard paraffin embedding technique. The paraffin embedded tissues were cut in 3-5 μm thickness and processed for Haematoxylin and Eosin (H&E) staining protocol[21].

Histopathological scoring/grading was done according to Broder's system on the basis of microscopical features such as degree of anaplasia, invasion into

Table 1. Histopathological scoring/grading system for squamous cell carcinoma (SCC) in bovines.

S.No.	Criteria for histological malignancy grade	Points	Features of malignancy
A.	Keratinization (formation of Keratin pearls and islands of neoplastic cells; K)	1	Complete absence of epithelial pearls, non-keratinizing type with small islands of neoplastic cells without keratin pearls and with absence of keratin deposition or only had individual keratinized cells
		2	Formation of keratin pearls/cytoplasmic/layered keratinization in 10-75 % of the tumour (Absence/formation of small to medium sized keratin pearls with moderate degree of keratinization and islands of keratin containing neoplastic squamous cells)
		3	Formation of large keratin/epithelial pearls; concentric laminated masses of keratin and large islands of neoplastic cells (>75%) containing large amount of keratin deposition in the tumour
B.	Degree of invasion, nuclear pleomorphism and Inflammation (I)	1	Slight or no Invasion of tumour cells; uniform or regular small nucleus and occasional nucleoli, slight or no inflammatory cells
		2	Slight to moderate invasion of tumour cells to the surrounding tissue with moderate variation in nuclear size and occasionally hyperchromatic nuclei seen, presence of fair amount of inflammation and mononuclear cell infiltration
		3	Marked invasion of tumourous cells with high variations in nuclear size, hyperchromatic nucleus, often with ≥1 prominent nucleoli, severe inflammation with abundance of mononuclear cells
C.	Mitoses per 10 high power field (Mitotic figures; M)	1	0-2 mitotic figures/10 HPF
		2	02-06 mitotic figures/10 HPF
		3	≥06 mitotic figures/10 HPF
	Histological malignancy grade	Points	Grade of malignancy
	Total scoring (K+M+I; KMI)	2-5	I (low, poorly differentiated)
		6-7	II (intermediate, moderately differentiated)
		8-9	III (high, well differentiated)

the surrounding tissue, degree of keratinization, formation of keratin pearls, nuclear pleomorphism, mitotic index (mitotic figures per high power field) and inflammatory cell infiltrations according to the method prescribed by Pugliese *et al*., (2014)[17] (Table 1). Malignancy grades of various tumours were also determined by sum of all histological findings (KMI score).

RESULTS

Gross Pathology

Horn cancer

Cauliflower-like growth at the base of horn were observed in most of the cases (n=9; Fig. 1 & 2). Large irregular cauliflower-like masses of about 20 cm diameter were recorded in BovHC3 and BovHC4 (Fig. 1 & 2). Most of these tumours were slightly soft to firm, friable, solid nodular growth. The surface of most of these tumours was irregular, rough and verrucous with poor demarcation. Cut surfaces of tumours showed variable colour such as whitish yellow, grayish white, grayish red to light brown with widespread hemorrhages and areas of necrosis (Fig. 2). Few of these masses were ulcerative with foul smelling purulent discharge (BovHC2 and BovHC10).

Eye cancer (ocular squamous cell carcinoma/OSCC)

Gross examination bovine eyes (6 numbers) BovEC 1-6 suspected of OSCC showed unilateral, small, pink colored, irregular growths, varied from soft to firm in consistency. Two animals BovEC1 and BovEC2 showed small, friable, haemorrhagic mass observed at lower eyelid. A large red colored hard protruded mass covering the whole cornea with severe hemorrhage was noticed in the right eye of yet another animal (Fig. 3). A wart-like tumorous growth spreading from lateral canthus covering the entire cornea was observed in left eye of buffalo (Case ID: BovEC6; Fig. 4).

Histopathology

Horn cancer

Histopathological features of horn

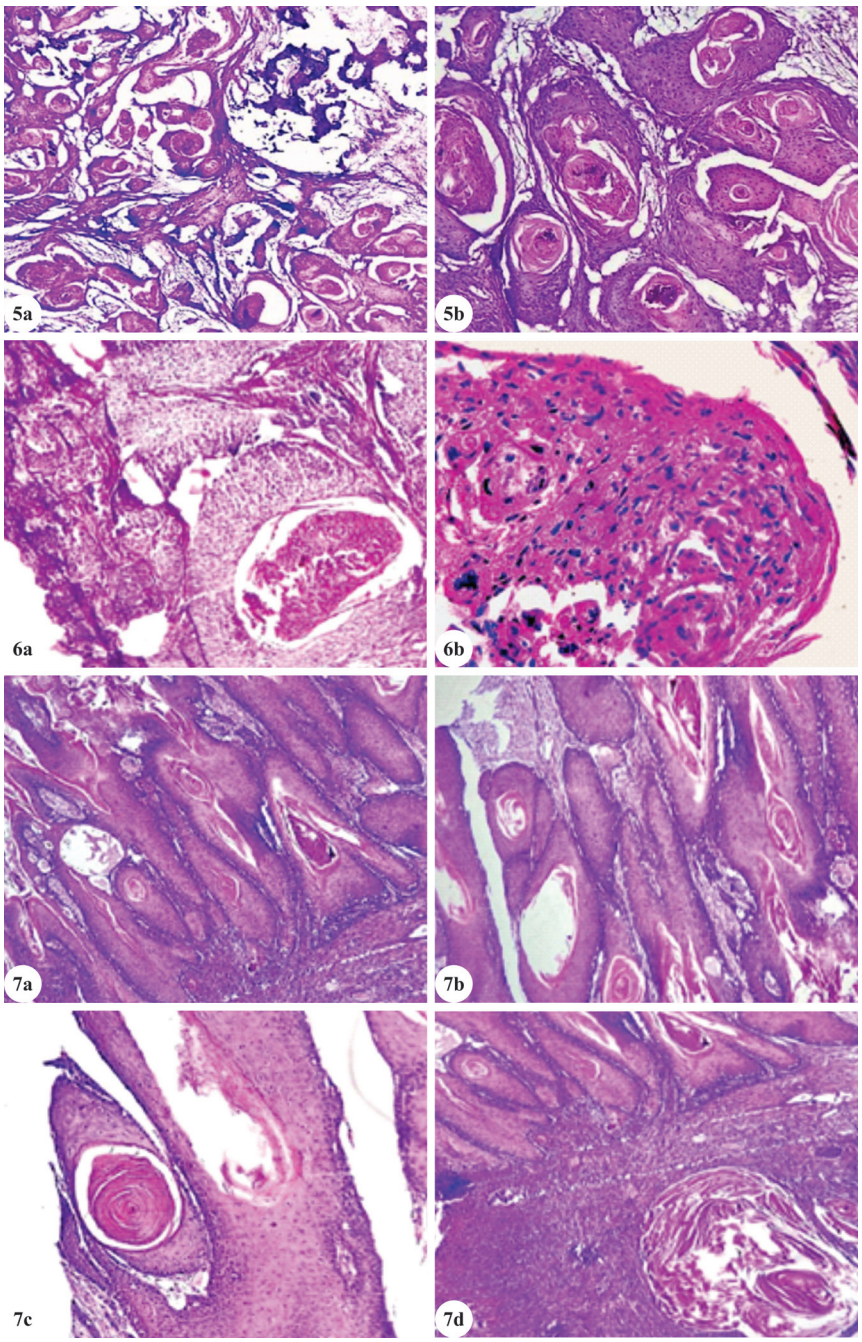

Fig. 5a. Well differentiated SCC of horn depicting formation of numerous epithelial pearls with mineralization (Case ID: BovHC6, H&E X40). **b.** Excessive keratinization of horn epithelium with concentric arrangement forming keratin pearls/Cell nests (Case ID: BovHC6, H&E X100); **Fig. 6a.** Moderately differentiated (Grade II) SCC showing large keratin pearl (BovHC1, H&E X100. **b.** H&E X400; **Fig. 7a.** Grade III SCC of horn with irregular shaped tumour islands in the epidermis invading deep into dermis layer with keratin pearls (BovHC3, H&E X100). **b.** Tumour islands containing well differentiated epithelial pearls. **c.** Illustrating characteristic epithelial pearl of well differentiated squamous cell carcinoma (Case ID: BovHC3, H&E X100). **d.** Large keratin cyst containing concentric cell nest (BovHC3, H&E X100).

cancer revealed keratinization of horn epithelium with formation of numerous epithelial pearls and mineralization. Well differentiated squamous cell carcinoma revealed characteristic epithelial pearl at the centre. Degree of keratin formation and formation of keratin pearls varies from animal to animal (Figs. 5a, b, 7b, c, 8a, 9a, 13b, 14b). Few caseses revealed a large keratin cyst containing concentric cell nest (Fig. 14a) and multiple keratin pearls with formation of keratin microcyst in well differentiated SCC (BovHC10; Fig. 8a). Layered keratinization was also observed [BovHC9; Fig. 13a-b]. Keratinization pattern is given in Table 1 & 2. Non-keratinizing type of SCC was also evident (BovHC4). Neoplastic cells formed irregular islands,

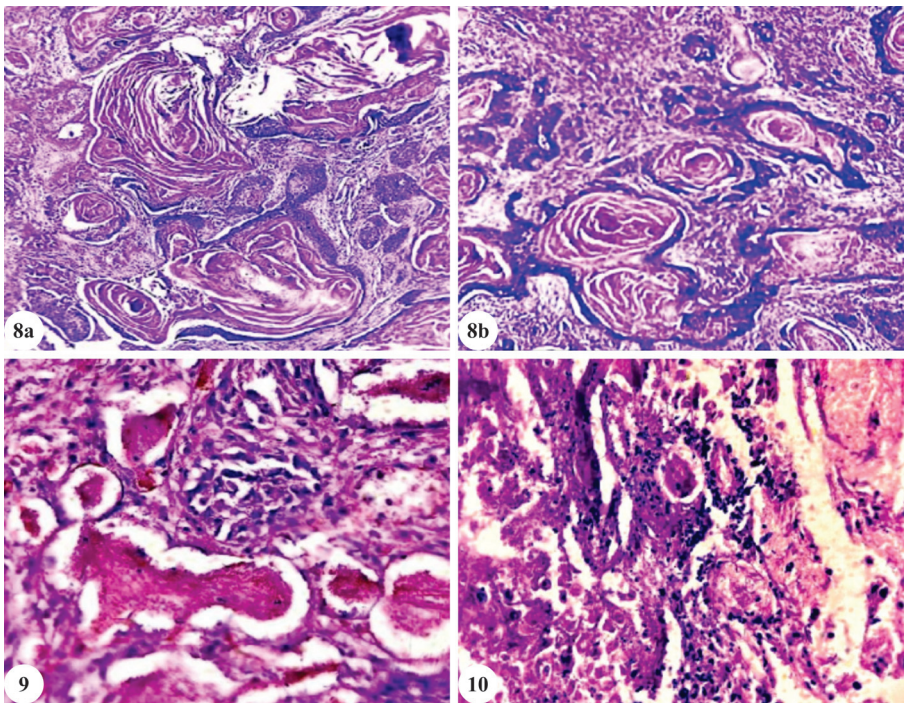

Fig. 8a. Multiple keratin pearls with formation of keratin microcyst in well differentiated SCC of horn (BovHC10, H&E X100). **b.** Concentric keratin pearls in well differentiated SCC with mineralization (BovHC10, H&E X100); **Fig. 9.** Poorly differentiated SCC of horn with severe hemorrhages (BovHC4, H&E X400); **Fig. 10.** Moderately differentiated (Grade II) SCC of horn with numerous mitotic figures with variable number of nucleoli (BovHC1, H&E X400).

which were invaded deep into dermis (BovHC3; Fig. 7a). These neoplastic islands revealed aplastic squamous cells with numerous mitotic figures, variable number of nucleoli (Figs. 5b, 7a, 10). Gradual thickening of keratin layer of epithelium was evidenced with infiltration of mononuclear cells (Fig. 11). Superficial epithelial cells revealed hyperplasia, hyperkeratosis (Figs. 5b, 7c). Few cases revealed moderately differentiated SCC with presence of epithelial pearls (BovHC8; Fig. 12) and large keratin pearl with numerous mitotic figures (BovHC1; Fig. 6a-b). Distinctive keratin pearls were not observed in few cases (BovHC2; Fig. 11, BovHC4; Fig. 16, BovHC5 and BovHC11). Most severe hemorrhages were reported in BovHC4 (Fig. 9), possibly due to inflammation and

Table 2. Histopathological scoring of horn cancer SCC.

Case ID	Degree of Keratinization (1)	Degree of Anaplasia, Nuclear pleomorphism and Mitotic figures (2)	Degree of Invasion and Inflammation (3)	Score with ref. to Table 1; Sum total (1+2+3)	Grade of Malignancy
BovHC1	1	2	3	6	Grade II (Moderately differentiated SCC)
BovHC2	0	1	2	3	Grade I (Poorly differentiated SCC)
BovHC3	3	3	3	9	Grade III (Well differentiated SCC)
BovHC4	0	3	3	6	Grade I (Poorly differentiated SCC), highly invasive and malignant
BovHC5	0	1	1	2	Not diagnosed as SCC
BovHC6	2	3	2	7	Grade III (Well differentiated SCC)
BovHC7	0	1	1	2	Not diagnosed as SCC
BovHC8	1	2	2	5	Grade II (Moderately differentiated SCC)
BovHC9	3	3	2	8	Grade III (Well differentiated SCC)
BovHC10	3	3	2	8	Grade III (Well differentiated SCC)
BovHC11	0	2	0	2	Not diagnosed as SCC
BovHC12	0	1	1	2	Not diagnosed as SCC

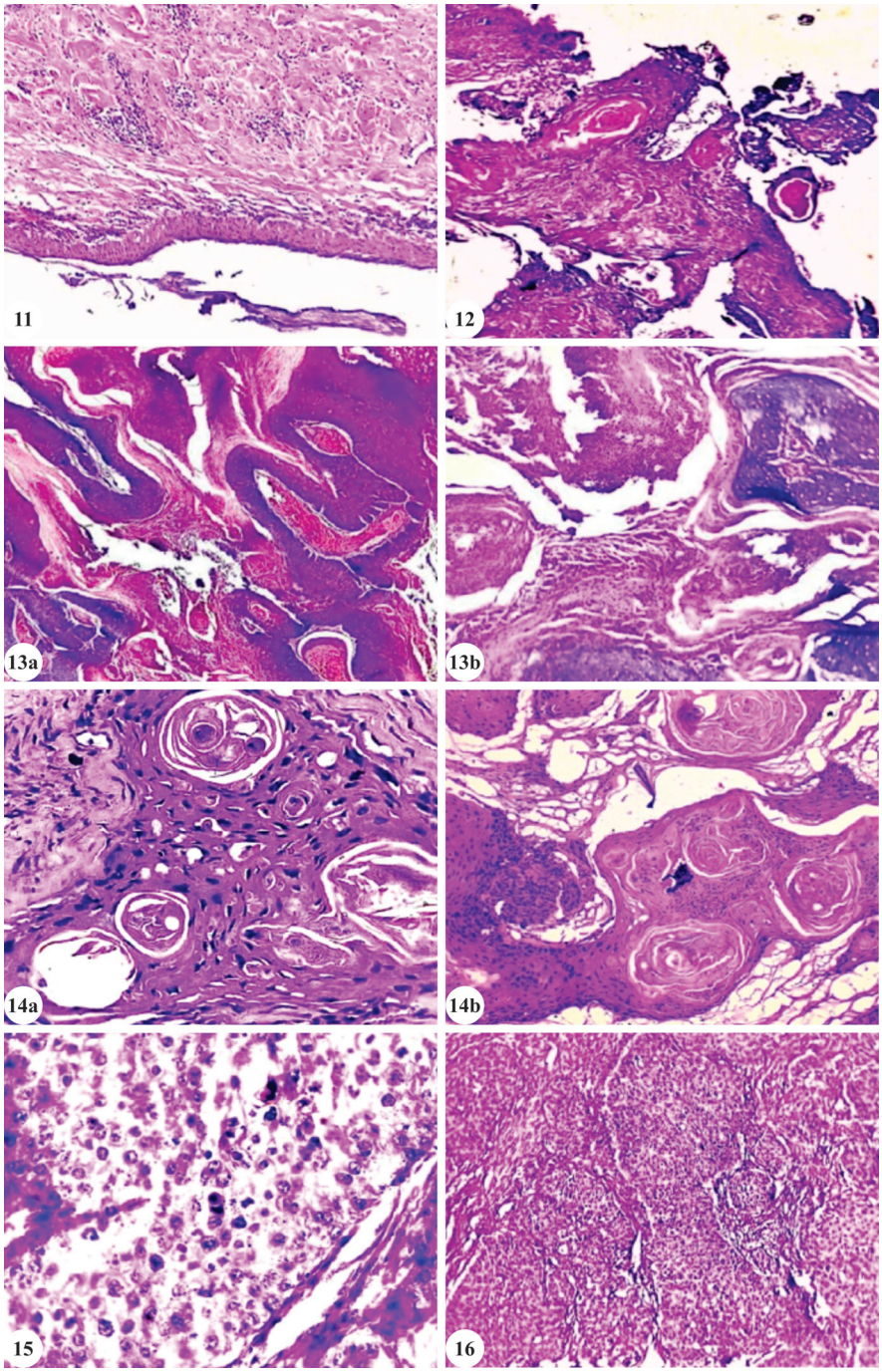

Fig. 11. Poorly differentiated SCC of horn, gradual thickening of keratin layer of epithelium with infiltration of mononuclear cells (BovHC2, H&E X100); **Fig. 12.** Moderately differentiated SCC of horn with presence of epithelial pearls (BovHC8, H&E X100); **Fig. 13a.** Well differentiated SCC of horn illustrating layered pattern of keratinization (BovHC9, H&E X100). **b.** Keratin pearls along with layered keratinization in SCC of horn (BovHC9, H&E X400); **Fig. 14a.** Well differentiated SCC of horn with keratin pearls as well as keratin cysts formation and numerous mitotic figures (BovHC6, H&E X400). **b.** Showing large epithelial pearls with mononuclear cells infiltration (H&E X100, BovHC6, H&E X100); **Fig. 15.** Abundance of mitotic figures and cells exhibiting anaplasia (H&E X400); **Fig. 16.** Poorly differentiated SCC (Grade I).

more blood supply to the malignant neoplasm due to angiogenesis. Distinctive keratin pearls were not seen in (BovHC2; Fig. 11, BovHC4, BovHC5 and BovHC11). Moderately differentiated SCC of horn was observed with presence of epithelial pearls (BovHC8; Fig. 12). Poorly differentiated SCC was observed with deep invasion from the primary site with areas of haemorrhage and inflammatory cell infiltrations predominantly neutrophils and lymphocytes in the stroma was observed in BovHC4 (Figs. 9, 11, 14b). Ballooning degeneration in

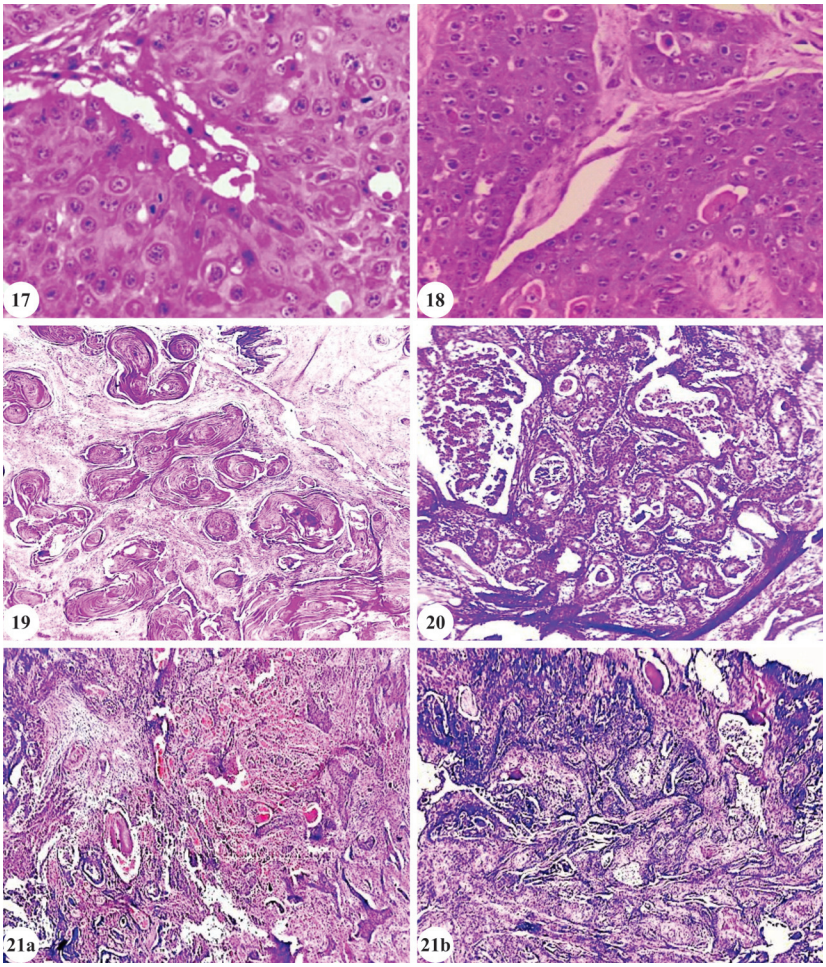

Fig. 17. Poorly differentiated SCC of horn with anaplastic cells and mitotic figures (BovHC4, H&E X400); **Fig. 18.** Well differentiated SCC of horn with ballooning degeneration in tumour cells in well differentiated SCC of horn (BovHC9, H&E X400); **Fig. 19.** Well differentiated OSCC with multiple epithelial pearls (BovEC3, H&E X100); **Fig. 20.** Cords of invasive tumour cells with mononuclear cell infiltration and keratinization at the center of neoplastic islets in OSCC (H&E X100); **Fig. 21a.** Poorly differentiated OSCC illustrating neovascularization (BovEC2, H&E X40). **b.** Poorly differentiated OSCC with absence of epithelial pearls (BovEC2, H&E X40).

tumour cells was observed in BovHC9 (Fig. 18).

Eye cancer

Histopathological findings in OSCC were distinctive keratin pearls with more keratin deposition towards the center in one case (BovEC4, Fig. 19) Mineralization was also observed around the periphery of keratin pearls (Fig. 19). Numerous mitotic figures were also noticed with evidences of severe anaplasia (BovEC3, Fig. 20) BovEC3 had a moderate degree of keratinization with keratin deposition at the center of neoplastic islets containing large anaplastic epithelial cells, multiple islands of tumourous squamous cells below the epidermal layer (Fig. 20). Neovascularization was evident in poorly differentiated OSCC (Fig. 21a). Poorly differentiated OSCC were characterized with absence of epithelial pearls (Fig. 21b). Cords of invasive tumour cells were clearly evident with mononuclear cell infiltration and keratinization at the center of neoplastic islets in OSCC (Fig. 22). Large tumour islands with mononuclear cell infiltration were also observed in moderately differentiated OSCC (Fig. 22). Moderately differentiated OSCC were characterized with few small keratin pearls and multiple patches of keratin deposition in the form

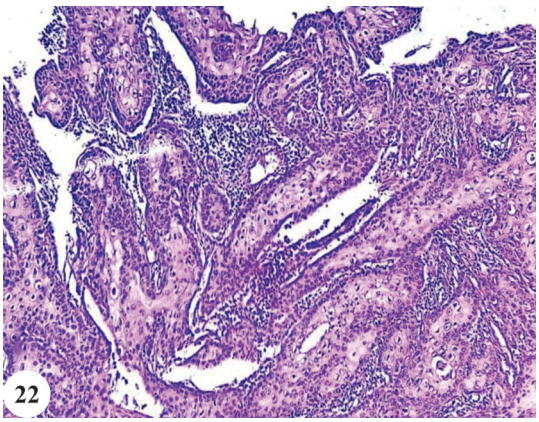

Fig. 22. Large tumour islands with mononuclear cell infiltration in OSCC (BovEC3, H&E X40).

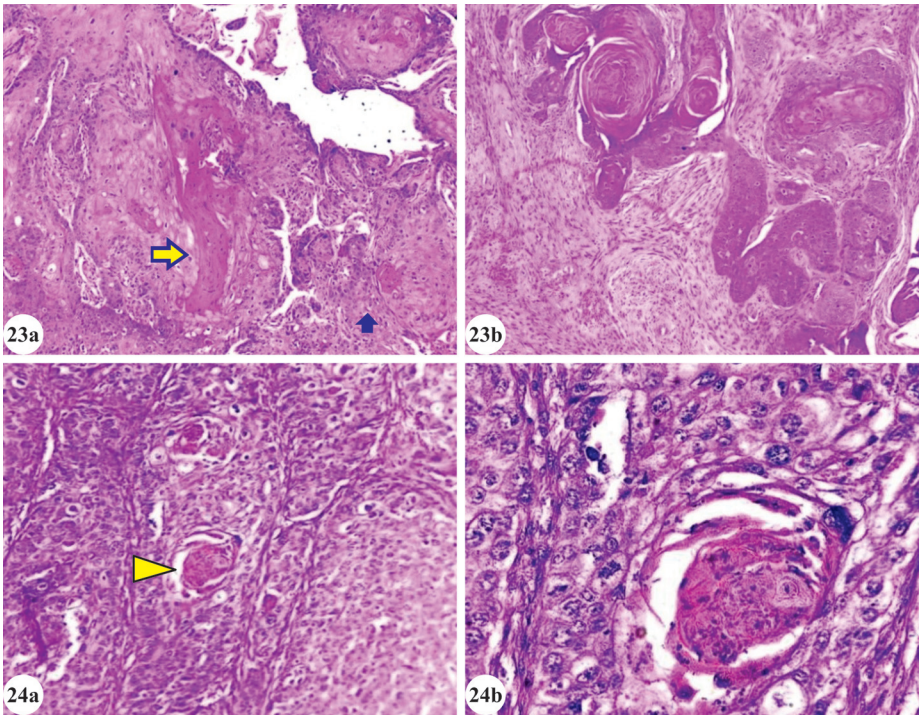

Fig. 23a. Moderately differentiated OSCC with linear keratinization along with keratin pearl (Arrows) (BovEC3, H&E X100). **b.** Moderately differentiated OSCC exhibiting few well differentiated cell nests with multiple islands of tumourous squamous cells (BovEC3, H&E X100); **Fig. 24a.** Moderately differentiated OSCC with few small keratin pearls and abundance of fibrous tissue (H&E X100). **b.** Small concentric keratin pearl peripheried by inflammatory cells in case of moderately differentiated OSCC (H&E X400).

of cell nests (Fig. 24a-b).

Histopathological scoring/grading

Histological malignancy grade of various tumours diagnosed as horn cancer on the basis of histopathology determined by sum of all histological findings (Degree of keratinization + degree of anaplasia and invasiveness + Mitotic figures; Table 1). BovHC3 was diagnosed as Grade III; most well differentiated SCC with score of 9 (Table 2), followed by BovHC9 & BovHC10 with score of 8 each; High score signified highly differentiated and malignant nature of SCC. Grading of SCC (horn) revealed a total of 2 cases as Grade I (poorly differentiated SCC); 2 cases as Grade II (moderately differentiated SCC) and 4 cases as Grade III (well differentiated SCC) (Table 4).

Histological malignancy grade of various tumours diagnosed as OSCC on the basis of histopathology were determined with score ranging from 2 to 8 in different cases by sum of all histological findings (degree of keratinization (K) + degree of anaplasia and invasiveness (I) + mitotic figures (M); KMI, K+M+I) are depicted in Table 3.

BovHC3 was diagnosed as Grade III; most well differentiated SCC with score of 9 (Table 3), followed by BovHC9 & BovHC10 with score of 8 each; High score

Table 3. Histopathological scoring of eye cancer.

Case ID	Degree of Keratinization (K)	Degree of Anaplasia, Nuclear pleomorphism and Mitotic figures (M)	Degree of Invasion and Inflammation (I)	Score with ref. to Table 1; Sum total (K+M+I)	Grade of Malignancy
BovEC1	0	1	1	2	Not diagnosed as OSCC
BovEC2	1	1	2	4	Grade I (Poorly differentiated OSCC)
BovEC3	1	3	3	7	Moderately differentiated OSCC
BovEC4	3	3	2	8	Grade III (Well differentiated OSCC)
BovEC5	0	1	1	2	Not diagnosed as OSCC
BovEC6	0	3	3	6	Poorly differentiated OSCC with no keratinization

Table 4. Grading of SCC (horn and eye) on the basis of histopathological scoring.

Grade of malignancy	Horn cancer	Eye cancer	Total
Grade I (Poorly differentiated SCC)	2	2	4
Grade II (Moderately differentiated SCC)	2	1	3
Grade III (Well differentiated SCC)	4	1	5

signified highly differentiated and malignant nature of SCC.

DISCUSSION

Gross pathological findings of neoplasm of horn like unilateral growth observed in all cases examined was in accordance with[14]. Pink cauliflower like soft, friable growth with bleeding at the base of the horn were also reported by[6,12,18], Rough and verrucous surface of the tumourous growth was also reported by[13]. Foul smelling purulent discharge observed in the present study was also reported by[18]. Firm consistency of tumours and scattered growth with poor demarcation observed in the present study was also reported by[2]. Wart-like tumourous growth observed in eye was also reported by[7].

Histopathological findings of the present study were consistent with the findings of earlier workers who had reported cell nests or keratin pearls in well differentiated squamous cell carcinoma of horn[22,19,6,9]. Anaplasia and neovascularization observed in squamous cell carcinomas of horn were in accordance with[6-7]. Histopathological findings such as islands of tumourous epithelial cells, proliferation of fibroblasts, connective tissue and infiltration of lymphocytes and plasma cells were also reported earlier in OSCCs[20,6,7]. Invasion of dermal stroma and highlighted keratinization with infiltration of neoplastic squamous cells observed in cases of OSCC in the present study were also reported by[7,15]. Histopathological findings of the present study such as anaplasia and neovascularization in squamous cell carcinomas were in accordance with[9,12,15]. Histological malignancy grade of various tumours diagnosed as horn cancer on the basis of histopathology determined by sum of all histological findings (Degree of keratinization (K) + degree of anaplasia and invasiveness (I) + Mitotic figures (M); Table 1). Histopathological scoring obtained as KMI score by summation forms the basis of categorization of SCC as well, moderate and poorly differentiated. BovHC3 was diagnosed as Grade III; most well differentiated SCC (Table 2) with presence of multiple large keratin pearls with irregular shaped tumour islands (K=3); high invasion deep into dermis layer (I=3); high mitotic index (M=3) contributing to high histopathological score (K+M+I) of 9 (Table 2), BovHC4 was categorized as Grade I (Poorly differentiated) with absence of epithelial pearls (K=0), extensive hemorrhages; presence of individually keratinized cells with deep invasion into the dermis layer (I=3) and abundace of mitotic figures (M=3). Well differentiated SCC with multiple keratin pearls and poorly differentiated SCC with complete abscence of keratin pearls were described by[17]. BovHC9 & BovHC10 with high KMI (K+M+I) score of 8 each characterised by cell nests (K=3) and high degree of inflammation (I=2). High histopathological score signified highly differentiated and malignant nature of SCC.

BovEC4 was diagnosed as well differentiated OSCC with a score of 8 followed by BovEC3 (moderately differentiated OSCC). BovEC2 and BovEC6 were diagnosed as poorly differentiated OSCC on the basis of histopathological score (K+M+I, Table 1 and 3) of 4 and 6 respectively (Table 3). Invasion of dermal stroma and highlighted keratinization with infiltration of neoplastic squamous cells observed in cases of OSCC in the present study were also reported by Fornazari *et al*., (2017)[15].Poorly differentiated OSCC (BovEC2) characterised by presence of individual keratinized cells scored as (K=1), no keratin pearls and less invasion to the surrounding tissue. Moderately differentiated OSCC (BovEC3) presence of tumour island, moderate keratinization scored as K=2; with evidence of invasion (I=3) resulting in KMI scoring of 7.

CONCLUSIONS

A total of 12 out of 18 samples collected were confirmed as SCC on the basis of histopathology. Eight were diagnosed as SCC of horn (n=8) out of 12 and four cases were of OSCC (n=4) out of 6, a total of 12 cases out of 18 were diagnosed as SCC on the basis of histopathological findings. Grading of SCC (horn & eye) based on histopathological scoring revealed a total of 4 cases (2 of horn; 2 of eye) as Grade I (poorly differentiated SCC); 3 cases (2 of horn; 1 of eye) as Grade II (moderately differentiated SCC) and 5 cases (4 of horn; 1 of eye) as Grade III (well differentiated SCC). Histopathologicaly, cell nests or keratin pearls with high degree of keratinization and layered pattern of keratinization were reported in well differentiated SCC of horn with anaplasia, numerous mitotic figures, tumour islands with severe inflammation, neovascularization, hemorrhages etc. Severe anaplasia with hyperchromatic tumourous cells or spindle shaped cells with little or no squamous differentiation or keratinization. Fibrosis with severe proliferated fibrous tissue was observed in BovEC6 along with squamous cells in connective tissue stroma. Histopathological scoring was centered on degree of keratinization, cellular differentiation, mitotic figures and degree of invasion. obtained as KMI (Degree of keratinization (K) + degree of anaplasia and invasiveness (I) + Mitotic figures (M); Table 1). This KMI score by summation forms the basis of categorization of SCC

as well, moderate and poorly differentiated squamous cell carcinoma of horn and eye. High KMI score signified highly differentiated and malignant nature of horn cancer as well as ocular squamous cell carcinoma.

ACKNOWLEDGEMENTS

The authors are thankful to the Dean, academic faculty of Veterinary Pathology and Veterinary Surgery in College of Veterinary Sciences, Dau Shri Vasudev Chandrakar Kamdhenu Vishwavidyalaya for providing necessary facilities for research work and in completion of this research article.

REFERENCES

1. Vegad JL. 2007. Neoplasia. In: A Textbook of Veterinary General Pathology, 2nd revised and enlarged edn. *International Book Distributing Co. Lucknow*, pp: 281, 376-377.
2. Thomson M. 2007. Squamous cell carcinoma of the nasal planum in cats and dogs. *Clin Tech Small Anim Pract* **22:** 42-50.
3. Tsujita H and Plummer CE. 2010. Bovine ocular squamous cell carcinoma. *Vet Clin North American Food Anim Pract* **26:** 511-529.
4. Yan W, Wistuba II, Emmert-Buck MR and Erickson HS. 2011. Squamous cell carcinoma-similarities and differences among anatomical sites. *American J Cancer Res* **1:** 275.
5. Tyagi RPS and Singh J. 2006. Ruminant Surgery, 1st edn., CBS Publisher and Distributors, New Delhi: 415-416.
6. Sharma S, Gupta RP, Jangir BL, Lather D and Hazari R. 2020. Pathomorphological studies and immunohistochemical expression of p53 and pancytokeratin in bovine epithelial tumors. *Indian J Vet Pathol* **44:** 1-6.
7. Kumar V, Jolhe DK, Ghosh RC, Sonkusale PM and Sharma S. 2023. Pathology and diagnosis of ocular squamous cell carcinoma in bovines. *Indian J Vet Sci & Biotech* **19:** 43-49.
8. Kumar R and Thilagar S. 2000. An unusual case of bilateral horn cancer in a buffalo. *Indian Vet J* **77:** 48-49.
9. Singh S and Singh G. 2005. Important aspects of horn cancer. *Scientific Econ J* **2:** 32-9.
10. Udharwar SV, Aher VD, Yadav GU, Bhikane AU and Dandge BP. 2008. Study on incidence, predisposing factors, symptomatology and treatment of Horn cancer in Bovine with special reference to Surgery and Chemotherapy. *Vet World* **1:** 7.
11. Lakshmi MP, Veena P, Kumar RS and Prameela RD. 2020. Clinical, pathological and immunohistochemical studies on bovine eye cancer. *The Pharma Innov J* **9:** 353-355.
12. Giri DK, Kashyap DK, Dewangan G, Tiwari SK, Ghosh RC and Sinha B. 2011. Squamous cell carcinoma of horn and its surgical management-a report of three cases. *Inter J Livestock Sci* **1:** 55-58.
13. Reddy KJM, Kumar VG, Ganesh S and Raghavender KBP. 2017. Unilateral horn cancer in cow and its surgical Management-a case report. *International J Curr Microbiol Appl Sci* **6:** 3349-52.
14. Kalim MO, Tiwari SK, Sharda R, Shakya S, Sannat C, Praveen K and Deshmukh SK. 2021. Studies on prevalence, predisposing factors and microscopic evaluation of bovine horn cancer. *Pharma Innov J* **10:** 268-270.
15. Fornazari GA, Kravetz J, Kiupel M, Sledge D, De Barros Filho IR and Montiani-Ferreira F. 2017. Ocular squamous cell carcinoma in Holstein cows from the South of Brazil. *Vet World* **10:** 1413.
16. Islam ST, Khurma J, Wani JM, Ganaie MY, Singh AK, Rashid H and Fayaz IB. 2017. Ocular squamous cell carcinoma in a female buffalo: A case report. *J Entomol and Zool Stud* **5:** 795-796.
17. Pugliese M, Mazzullo G, Niutta PP and Passantino A. 2014. Bovine ocular squamous cellular carcinoma: a report of cases from the Caltagirone area, Italy. *Veterinarski arhiv* **84:** 449-457.
18. Kumar V, Mathew DD, Kumar N and Arya RS. 2013. Horn cancer in bovines and its management. *Intas Polivet* **14:** 56-57.
19. Joshi BP, Soni PB, Ferar DT, Ghodasara DJ and Prajapati KS. 2009. Epidemiological and pathological aspects of horn cancer in cattle of Gujarat. *Indian J Field Vet* **5:** 65-67.
20. Patel PB, Mistry JN, Suthar DN and Patel JB. 2009. Surgical Management of ocular squamous cell carcinoma in buffalo calf. *Intas Polivet* **10:** 293-294.
21. Layton C, Bancroft JD and Suvarna SK. 2019. Fixation of tissues. *Bancroft's Theory* and *Practice of Histological Techniques*, 8th ed.; Suvarna SK, Layton C, Bancroft JD, Eds: 40-63.
22. Kumar V, Jolhe DK, Ghosh RC and Dewangan R. 2023. Patho-morphological and Immunohistochemical Studies on Bovine Horn Core Carcinoma. *Indian J of Anim Res* **57:** 1485-1496.

Indian J. Vet. Pathol., 48(2) : 116-122, 2024: DOI: 10.5958/0973-970X.2024.00021.1

RESEARCH ARTICLE

Co-infection of porcine circovirus 2 (PCV-2) with synergistic infections and their multisystemic pathological consequences

T. Princy, S.S. Devi*, K.S. Prasanna, I.S. Sajitha, R. Ambily[1], R. Bharathi and C. Udhayakumar

[1]Department of Veterinary Microbiology, College of Veterinary and Animal Sciences, Mannuthy, Thrissur-680 651, Kerala, Department of Veterinary Pathology, College of Veterinary and Animal Sciences, Mannuthy, Kerala Veterinary and Animal Sciences University, Pookode, Wayanad-680 656, Kerala, India

Address for Correspondence

S.S. Devi, Assistant Professor, Department of Veterinary Pathology, College of Veterinary and Animal Sciences, Mannuthy, Kerala Veterinary and Animal Sciences University, Pookode, Wayanad-680 656, Kerala, India, E-mail: deviss@kvasu.ac.in

Received: 9.10.2023; Accepted: 15.11.2023

ABSTRACT

The present study was aimed at screening synergistic infections in *Porcine circovirus* 2 (PCV2) infected pigs. Among the 80 cases studied, 18 were PCV2 positive and these positive samples were subsequently analysed for possible viral and bacterial co-infections. Further investigation revealed three PCV2 cases co-infected with *classical swine fever virus* (CSFV) infection, two cases with *porcine reproductive and respiratory syndrome virus* (PRRSV) and one with *porcine parvovirus* (PPV) infections. The present case describes the multisystemic pathological events observed in a case of concurrent infection with PCV2, CSFV, *Escherichia coli* (*E. coli*) and *Pasteurella* spp. in a six-month-old male cross-bred pig presented for necropsy to the Department of Veterinary Pathology, College of Veterinary and Animal Sciences, Mannuthy, Thrissur, Kerala, from an organised farm in Thrissur, Kerala. The animal had a history of weakness, reduced appetite, fever and diarrhoea. Necropsy revealed petechial to ecchymotic skin haemorrhages, congested and consolidated lungs, endocardial haemorrhages, splenic infarction, gastric ulcers, catarrhal enteritis and congested kidneys with petechiation. Microscopically, broncho-interstitial pneumonia, vascular changes like congestion, haemorrhages and thrombus formation together with degenerative and necrotic changes were evident in the lungs, heart, tonsil, testes, spleen, lymph nodes, kidney, skin and liver. Lymphoid depletion and histiocytic replacement were the characteristic lesions observed in lymphoid organs. Molecular detection of PCV2 by polymerase chain reaction (PCR) targeting the ORF-2 gene revealed an amplicon size of 481 bp. Similarly, in the case of CSFV, nested reverse transcription polymerase chain reaction (RT-nPCR) targeting the *E2* gene showed 271 bp sized amplicons and PCR for *Pasteurella* spp. expressed amplification of a 560 bp fragment of the *rpoB* gene. Sequencing was done to confirm the identity of the viruses and phylogenetic analysis for PCV2 was also performed. Bacteriological examination, culturing of tissue samples and biochemical tests confirmed the presence of *E. coli* as well. Such occurrences of combined infections warrant strict prophylactic and scientific management practices in swine rearing.

Keywords: Classical swine fever virus, *Escherichia coli,* polymerase chain reaction, porcine circovirus 2, synergistic infection

INTRODUCTION

Viral and bacterial synergistic infections, co-infections and sequential infections in pigs have been reported frequently during past few years. Currently, the most common co-infection pattern is thought to be associated with PCV2, an immunosuppressive virus, with PPV, PRRSV, CSFV, Swine influenza virus and other bacterial organisms like *Salmonella* spp., Mycoplasma hyopneumoniae, *Streptococcus suis 2*, *E. coli* and *Pasteurella* spp.[1-8]. Here, the pathology of a case with multiple infections involving PCV2, CSFV, E. coli and *Pasteurella* spp.is described. Porcine circovirus 2 is a non-enveloped, small, single-stranded circular DNA virus with icosahedral symmetry that comes under the genus *Circovirus* and the family *Circoviridae*[9]. It has a world-wide distribution and manifests different disease conditions, mainly post-weaning multisystemic wasting syndrome (PMWS), porcine dermatitis and nephropathy syndrome (PDNS), neurological diseases, reproductive failure, proliferative and necrotising pneumonia (PNP), porcine respiratory disease syndrome (PRDC) and enteritis[10,11]. Lymphoid depletion and associated immunosuppression induced by the virus is regarded as the primary reason which facilitates the occurrence of synergistic and or secondary viral and bacterial infections in affected pigs. In this study, the viral synergistic agent identified was CSFV. Classical swine fever (CSF) is a contagious viral disease of pigs associated with multisystemic haemorrhages, caused by a single-stranded positive-sense RNA virus of the genus Pestivirus belonging to the family *Flaviviridae*[12]. *Escherichia coli* is a Gram negative, rod shaped, facultative anaerobic coliform bacteria that comes under the family Enterobacteriaceae and the disease condition elicited by this bacterium in pigs is postweaning enteric colibacillosis[13]. Family *Pasteurellacea* consists of Gram

How to cite this article : Princy, T., Devi, S.S., Prasanna, K.S., Sajitha, I.S., Ambily, R., Bharathi, R. and Udhayakumar, C. 2024. Co-infection of porcine circovirus 2 (PCV-2) with synergistic infections and their multisystemic pathological consequences. Indian J. Vet. Pathol., 48(2) : 116-122.

Table 1. PCR conditions for amplification of PCV2 (*ORF-2* gene).

Steps		Temperature	Time
Initial denaturation		94°C	1 min
35 cycles	Denaturation	94°C	1 min
	Annealing	55°C	1 min
	Extension	72°C	1 min
Final extension		72°C	10 min

Table 2. PCR conditions for amplification of *Pasteurella* spp. (*rpoB* gene).

Steps		Temperature	Time
Initial denaturation		94°C	3 min
35 cycles	Denaturation	94°C	30 sec
	Annealing	54°C	30 sec
	Extension	72°C	30 min
Final extension		72°C	10 min

Table 3. Nested PCR conditions for amplification of CSFV (Outer reaction - *E2* gene).

Steps		Temperature	Time
Initial denaturation		95°C	2 min
35 cycles	Denaturation	95°C	30 sec
	Annealing	56°C	45 sec
	Extension	72°C	1 min
Final extension		72°C	5 min

Table 4. Nested PCR conditions for amplification of CSFV (Inner reaction - *E2* gene).

Steps		Temperature	Time
Initial denaturation		95°C	2 min
35 cycles	Denaturation	95°C	30 sec
	Annealing	58°C	45 sec
	Extension	72°C	45 sec
Final extension		72°C	5 min

negative, non-motile organisms often associated with respiratory infections, specifically atrophic rhinitis condition in pigs[14]. The combined pathogenesis of multiple infectious agents could enhance the severity of diseases and the occurrence of such conditions warrants the need for thorough surveillance, strict prophylaxis as well as scientific management practices in swine rearing.

MATERIALS AND METHODS

Carcass of a six-month-old male cross-bred pig from an organised farm in Thrissur, Kerala was presented to the Department of Veterinary Pathology, College of Veterinary and Animal Sciences, Mannuthy, Thrissur, Kerala, for necropsy. The animal had a history of weakness, reduced appetite, fever and diarrhoea. A detailed post-mortem examination was conducted and the gross lesions observed were recorded. Samples of the lungs, heart, stomach, intestine, spleen, kidney, skin, testes, lymph node and tonsils of the soft palate were collected and fixed in 10 percent neutral buffered formalin for histopathology. Heart blood smear was prepared and stained using Field stain. Pooled samples of lymphoid organs like spleen, lymph node, tonsil and thymus were also collected and stored at -80^{O}C for the molecular detection of different viruses using PCR and RT-PCR. Initially, DNA was extracted from the pooled lymphoid organ samples using commercially available DNA isolation kit (ORIonX Genomic DNA Kit), as per the manufacturer's instructions and screened for PCV2 by PCR targeting 481 bp of the ORF-2 region using the published primers (F - 5′-CGGATATTGTAGTCCTGGTCG-3′ and R - 5′-ACTGTCAAGGCTACCACGTA-3′) under appropriate PCR conditions[14] (Table 1). For the detection of *Pasteurella* spp., PCR was done with primers[15] (F - 5′-GCAGTGAAAGARTTCTTTGGTTC-3′) and (R - 5′-GTTGCATGTTNGNACCCAT-3′) targeting 560 bp fragment of the *rpoB* gene and used corresponding PCR conditions (Table 2). Further, we screened the sample for the detection of CSFV, RNA extraction was done using commercially available kits (ORIonX Total RNA Isolation Kit) and c-DNA was synthesised from the extracted total RNA using PrimeScript™ 1st strand cDNA Synthesis Kit (TaKaRa) as per the manufacturer's protocol. Then, RT-nPCR, was done employing published primers[16] targeting the *E2* gene for the outer reaction (F - 5′-AGRCCAGACTGGTGGCCNTAYGA-3′ and R - 5′-TTYACCACTTCTGTTCTCA-3′) and the PCR product of the outer reaction as the template for the inner reaction. Here, we used inner primers targeting 271 bp of the *E2* gene (F - 5′-TCRWCAACCAAYGAGATAGGG-3′ and R - 5′-CACAGYCCRAAYCCRAAGTCATC-3′) and corresponding PCR conditions (Table 3, 4).

Sequencing of the amplicons was done at Genespec Pvt. Ltd., Kochi, Kakkanad, to confirm the identity of the viruses. Sequence and alignment of PCV2 was done using Clustal W programme and phylogenetic analyses were carried out by neighbour-joining method using Mega 11 software. Tissue samples were subjected to bacteriological isolation and identification employing standard methods[7]. Formalin fixed paraffin embedded (FFPE) sections of 5 µm thickness were subjected to routine haematoxylin and eosin staining technique[17].

RESULTS

The detailed post-mortem examination revealed pale conjunctival mucous membrane, petechial to ecchymotic skin haemorrhages and erythematous skin lesions over the snout, ear pinnae, all the four limbs, scrotum, ventral abdominal area, inner thigh region and perineal area (Fig. 1a). The lungs of the affected animals were non-collapsed and emphysematous. Congestion, cranio-ventral pulmonary consolidation, multifocal petechial to purpural haemorrhages and marbling were the other lung lesions noticed (Fig. 1b). Endocardial petechial haemorrhages,

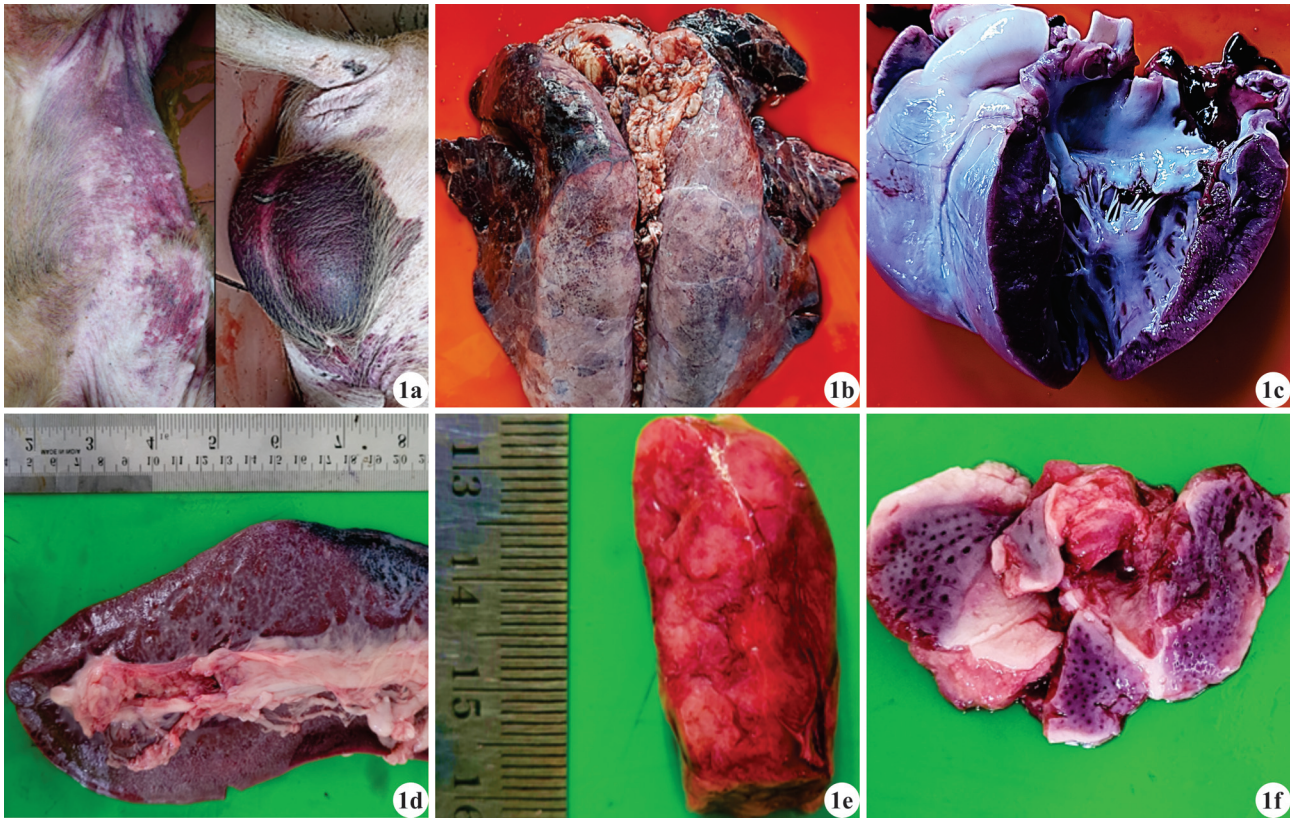

Fig. 1. Gross pathological changes: **1a.** Erythema and petechial to ecchymotic haemorrhages in the skin of the ventral abdomen and scrotum. **1b.** Lungs: Severe congestion, haemorrhages and cranio-ventral consolidation. **1c.** Heart: Endocardial haemorrhages & right ventricular hypertrophy. **1d.** Spleen: Moderate congestion and wedge-shaped infarcts on the lateral margin of spleen. **1e.** Lymph node: Enlarged lymph node with severe congestion and haemorrhages. **1f.** Tonsil: Severe and diffuse congestion.

ventricular hypertrophy and hydropericardium were also observed (Fig. 1c). Moderately congested liver with pale patches, severely congested kidneys and congested spleen with focal splenic infarction were the other features noticed (Fig. 1d). The gastric mucosa was severely congested with focal ulcers and diphtheritic membrane formation and catarrhal exudate were evident in the intestine. Severely congested, haemorrhagic and enlarged lymph nodes and tonsils were also characteristic (Fig. 1e, 1f).

Histopathological examination of the organs revealed severe extensive congestion and haemorrhages, moderate emphysema, formation of vascular and fibrin thrombi, mild degenerative changes with desquamation of bronchiolar epithelial cells and broncho-interstitial pneumonia in the lungs (Fig. 2a). In the heart, mild degenerative and necrotic changes, infiltration of mononuclear inflammatory cells, thrombus formation and focal congested areas were noticed (Fig. 2b). Microthrombi formation, multifocal congestion and haemorrhages in the epidermal region of the skin were noted. In testes, thrombi formation, interstitial glandular haemorrhages, multifocal congestion, inflammation and degenerative changes, including the detachment of germinal epithelial cells from the basement membrane were observed (Fig. 2c). The liver showed moderate sinusoidal congestion and mild haemorrhages, thrombus formation, bile duct hyperplasia, degenerative and necrotic changes like vacuolations in hepatocytes and dilatation of the central vein and infiltration of mononuclear inflammatory cells. The kidney was presented with interstitial nephritis with infiltrating mononuclear cells, multifocal congestion, thrombus formation, fluid filled eosinophilic areas and severe degenerative and necrotic changes mainly in the renal tubules (Fig. 2d). In spleen and lymph nodes vascular changes like congestion, haemorrhages, thrombi formation and lymphoid depletion also observed. Similarly, lymphoid depletion, histiocytic replacement, giant cell formation, thrombus formation, abscessation and multifocal congestion of the tonsils of the soft palate were observed (Fig. 2e, 2f).

The molecular confirmation of PCV2, CSFV and *Pasteurella* spp. were done using PCR and RT-nPCR and got 481 bp amplicons for PCV2, amplicons with 560 bp size for *Pasteurella* spp. and a 271 bp sized amplified product for CSFV (Fig. 3). The FASTA sequences of the PCR products that were obtained after sequencing were further blasted to confirm the identity of viruses. The

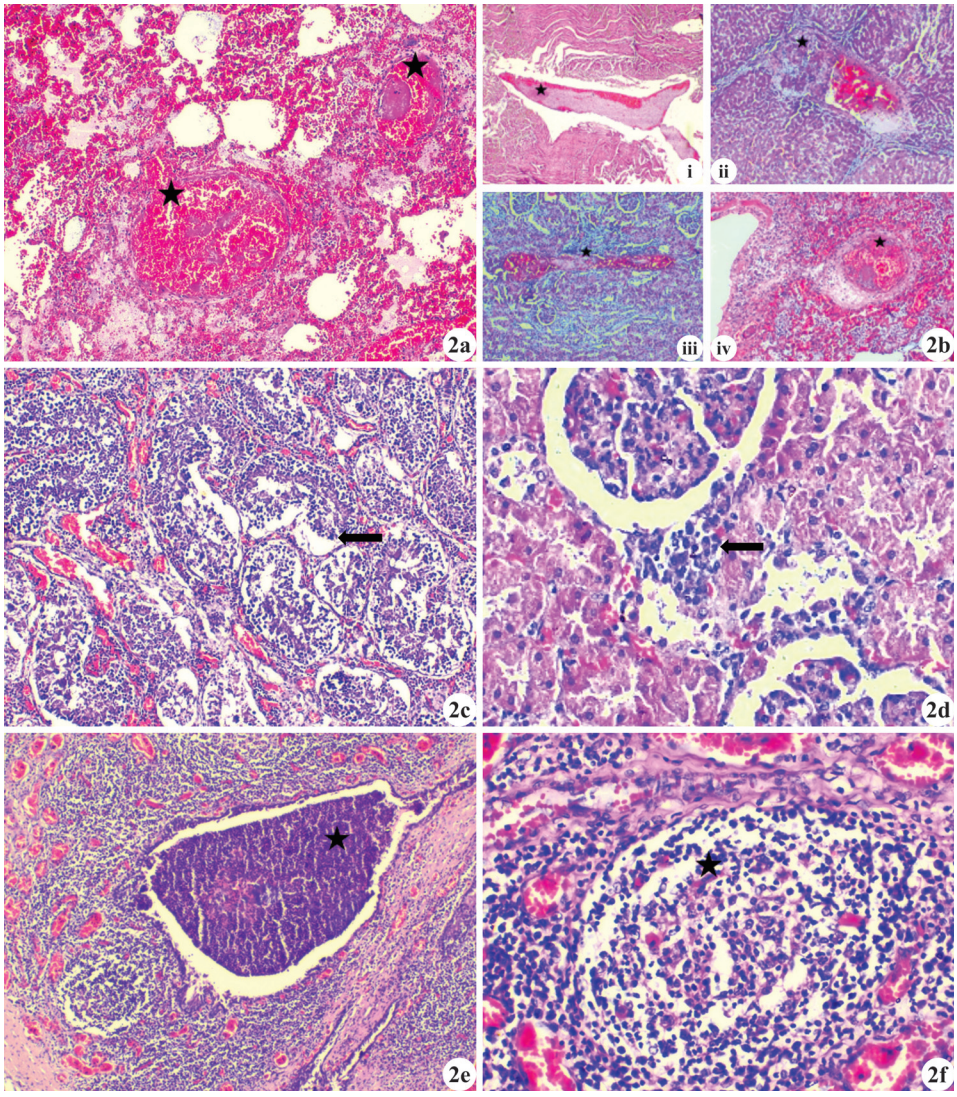

Fig. 2. Histopathological changes in different organs: **2a.** Lungs: Severe and extensive haemorrhages, thrombus formation (★), moderate pulmonary oedema and infiltration of inflammatory cells in the bronchiolar lumen and interstitial space (H&E x100). **2b.** Thrombus formation in different organs including (i) heart, (ii) liver, (iii) kidney and (iv) spleen (★) (H&E x100). **2c.** Testes: Multifocal interstitial congestion and detachment of germinal epithelial cells from the basement membrane (Arrow) (H&E x100). **2d.** Kidney: Infiltration of inflammatory cells in the interstitial areas (H&E x400). **2e.** Tonsil: Multifocal vascular congestion and abscess formation (★) (H&E x100). **2f.** Tonsil: Lymphoid depletion and histiocytic replacement within the lymphoid follicle (★) (H&E x400).

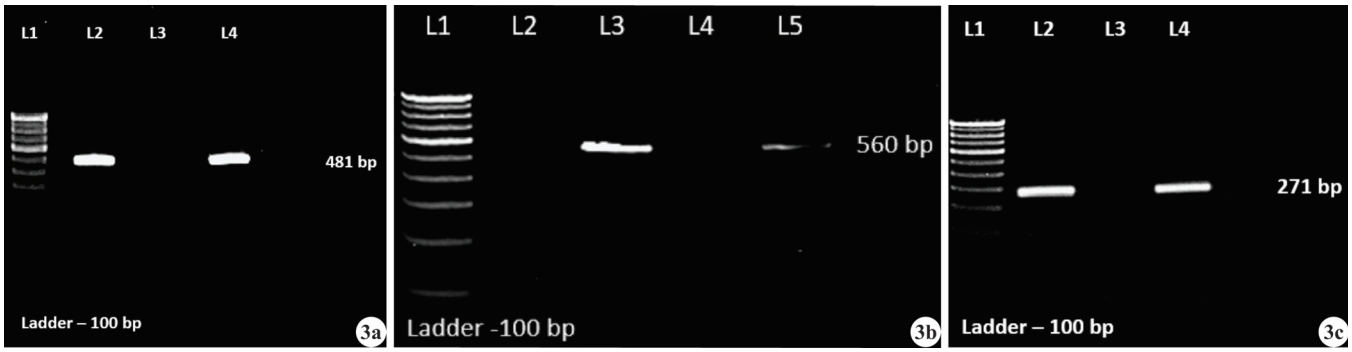

Fig. 3. Molecular detection of viruses and bacteria. **3a.** Agarose gel electrophoresis showing PCR product of PCV2. L1 - Ladder, L2 - Positive control, L3 - Negative control, L4 - Positive PCR product (481 bp) for PCV2. **3b.** Agarose gel electrophoresis showing PCR product. L1 - Ladder, L3 - Positive control, L4 - Negative control, L5 - Positive PCR product (560 bp) for *Pasteurella* spp. **3c.** Agarose gel electrophoresis showing PCR product of CSFV. L1 - Ladder, L2 - Positive control, L3 - Negative control, L4 - Positive PCR product (271 bp) for CSFV.

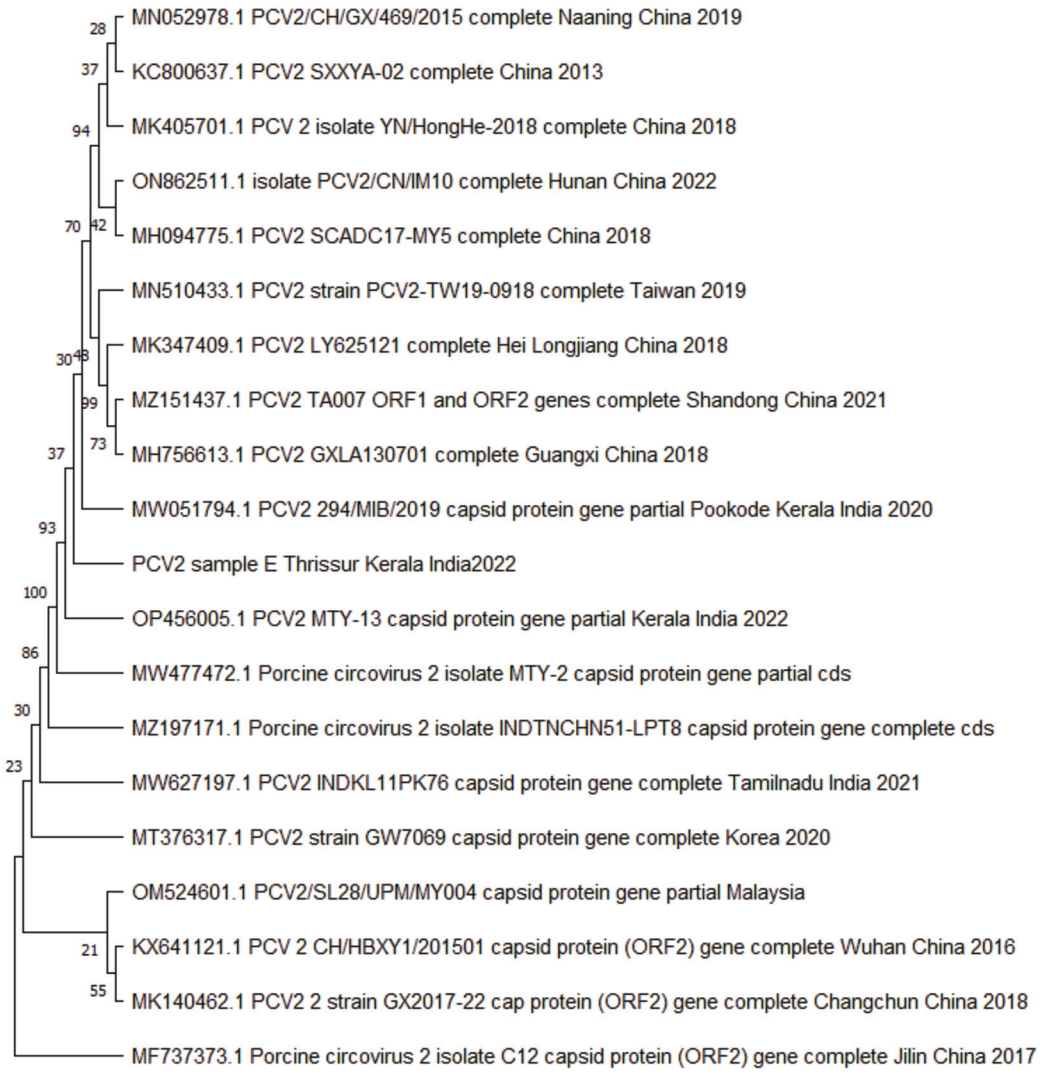

Fig. 4. Phylogenetic tree based on the analysis of 481 bp nucleotide of ORF-2 gene of PCV-2 isolates from India and in other countries.

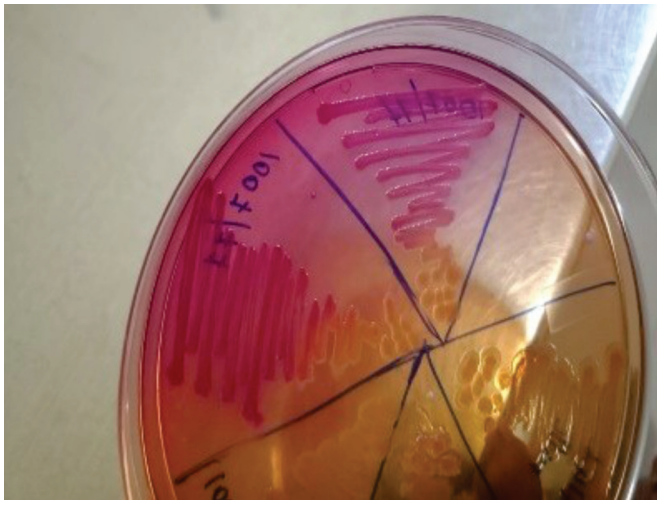

Fig. 5. Mac Conkey agar culture plate showing pink colonies suggestive of *E. coli*.

PCV2 isolate obtained in the present case was found to be more related to earlier sequences from Kerala, especially PCV2 MTY-13 isolate (OP456005.1) (Fig. 4). Microscopic examination of the blood smear showed the presence of short rods and bipolar organisms. Tissue samples of lungs, heart, liver and spleen cultured on Mac Conkey agar, revealed lactose-fermenting pink colonies (Fig. 5), which were identified as *E. coli* based on staining and biochemical tests.

DISCUSSION

Respiratory and enteric disease conditions being the most leading causes of morbidity and mortality in the swine population are often associated with various factors, including nutritional problems, poor management practices, adverse environmental conditions and infectious and non-infectious aetiologies. Among these, the contribution of viral and bacterial

synergistic infections is found to be an important factor for the economic losses in the swine industry.

In this study, various clinical signs showed by infected animals, including diarrhoea, icterus, respiratory distress and fever were in parallel with the earlier findings of PMWS and CSF cases[13,18,19]. The main gross lesions, like skin erythema, congestion and haemorrhages in the ear pinnae, all four limbs, scrotum, ventral-abdominal area, inner thigh region and perineal area and visceral organs like the lungs, heart, kidney, liver, spleen, lymph nodes, tonsils, stomach and lungs were similar to the findings of previous studies and such lesions might be due to the vascular endothelial damage elicited by the combined action of PCV2 and CSFV[20,21]. Other lesions like non-collapsed and emphysematous lungs with cranio-ventral pulmonary consolidation, hydropericardium, catarrhal enteritis and splenic infarction were in accordance with the results of earlier research studies[10,21]. Vascular changes, infiltration of mononuclear inflammatory cells and varying degrees of degenerative and necrotic changes in different visceral organs noticed during microscopic examination of this case were also in agreement with the findings of certain researchers[7,10]. Broncho-interstitial pneumonia which had occurred as a consequence of bacterial synergism was another feature noted, which was consistent with earlier findings[10,22]. According to previous reports, lymphoid depletion and histiocytic replacement observed in spleen, lymph node, tonsil and thymus were some of the consistent features observed in PMWS-affected piglets[7,10,11,23]. The decline of B and T lymphocytes by viral or cytokine mediated apoptosis of infected lymphocytes in lymphoid organs and loss of germinal centres of lymphoid follicles accounted for immune suppression and occurrence of synergistic infections[9,24,25]. In this study, thrombus formation was a marked lesion in organs like the lungs, heart, spleen, lymph node, tonsil, kidney, skin and testes, which might be due to the vascular damage caused by CSFV or PCV2 infection. PCV2 can cause endothelial damage, develop a prothrombotic stage and cause associated vascular lesions[26]. Similarly, CSFV also has tropism for vascular endothelial cells and can cause cellular damage, necrosis of blood capillaries and extensive microthrombi formation, which could result in disseminated intravascular coagulation[27]. Phylogenetic analysis of PCV2 revealed more similarity towards earlier Kerala sequences and the gross and histopathological lesions also were comparable to the lesions of those previous cases[28].

Mixed infections with different types of viruses and bacteria, as noted in the current study, were also reported earlier, wherein, a combined infection of PCV2, PPV, CSFV and multidrug-resistant *E. coli* had been described[7,29]. Based on the results obtained, the current case study concluded that co-infections with viruses and bacteria could increase the complexity of the disease condition and severity of lesions. In this case, the occurrence of synergistic infections was facilitated by the immunosuppressive condition generated by PCV2. Concurrent viral infections with subsequent emergence of secondary bacterial infections and their synergistic multisystemic pathogenicity could have contributed abundantly to the increased severity of the clinical presentation in the present case.

ACKNOWLEDGEMENTS

The authors are grateful to the Dean, College of Veterinary and Animal Sciences, Mannuthy for providing necessary facilities to carry out this research work.

REFERENCES

1. Kennedy S, Moffett D, McNeilly F, Meehan B, Ellis J, Krakowka S and Allan GM. 2000. Reproduction of lesions of postweaning multisystemic wasting syndrome by infection of conventional pigs with porcine circovirus type 2 alone or in combination with porcine parvovirus. *J Comp Pathol* **122:** 9-24.
2. Pallares FJ, Halbur PG, Opriessnig T, Sorden SD, Villar D, Janke BH, Yaeger MJ, Larson DJ, Schwartz KJ, Yoon KJ and Hoffman LJ. 2002. Porcine circovirus type 2 (PCV2) coinfections in US field cases of postweaning multisystemic wasting syndrome (PMWS). *J Vet Diagn Invest* **14:** 515-519.
3. Rovira A, Balasch M, Segales J, Garcia L, Plana-Duran J, Rosell C, Ellerbrok H, Mankertz A and Domingo M. 2002. Experimental inoculation of conventional pigs with porcine reproductive and respiratory syndrome virus and porcine circovirus 2. *J Virol* **76:** 3232-3239.
4. Opriessnig T, Madson DM, Schalk S, Brockmeier S, Shen HG, Beach NM, Meng XJ, Baker RB, Zanella EL and Halbur PG. 2011. Porcine circovirus type 2 (PCV2) vaccination is effective in reducing disease and PCV2 shedding in semen of boars concurrently infected with PCV2 and Mycoplasma hyopneumoniae. *Theriogenology* **76:** 351-360.
5. Takada-Iwao A, Nakanishi M, Souma J, Chikata S, Okuda Y, Imai Y and Sato S. 2011. Porcine circovirus type 2 potentiates morbidity of *Salmonella enterica* serovar Choleraesuis in Cesarean-derived, colostrum-deprived pigs. *Vet Microbiol* **154:** 104-112.
6. Wang Q, Zhou H, Fan H and Wang. 2020. Coinfection with porcine circovirus type 2 (PCV2) and Streptococcus suis serotype 2 (SS2) enhances the survival of SS2 in swine tracheal epithelial cells by decreasing reactive oxygen species production. *Infect Immun* **88:** 10-1128.
7. Das T, Sethi M, John JK, Tomar N, Chavan AS, Pathak M and Saikumar G. 2022. Pathology of PMWS Associated with Classical Swine Fever Virus, Porcine Parvo Virus and Multidrug Resistant Enteric Escherichia coli Infections in an Organized Swine Farm, Rajasthan, India. *Indian J Anim Res* **1:** 1-7.
8. Du S, Xu F, Lin Y, Wang Y, Zhang Y, Su K, Li T, Li H and Song Q. 2022. Detection of Porcine Circovirus Type 2a and Pasteurella spp. Capsular Serotype D in Growing Pigs Suffering from Respiratory Disease. *Vet Sci* **9:** 528.
9. Meng XJ. 2013. Porcine circovirus type 2 (PCV2): pathogenesis and interaction with the immune system. *Annu Rev Anim Biosci* **1:** 43-64.
10. Segalés J. 2012. Porcine circovirus type 2 (PCV2) infections:

clinical signs, pathology and laboratory diagnosis. *Virus Res* **164:** 10-19.
11. Keerthana J, Abraham MJ, Krithiga K and Priya PM. 2019. Studies on naturally infected cases of post weaning multi systemic wasting syndrome (PMWS) in piglets. *Pharm Innov* **8:** 485-488.
12. Tong W, Zheng H, Li GX, Gao F, Shan TL, Zhou YJ, Yu H, Jiang YF, Yu LX, Li LW and Kong N. 2020. Recombinant pseudorabies virus expressing E2 of classical swine fever virus (CSFV) protects against both virulent pseudorabies virus and CSFV. *Antivir Res* **173:** p.104652.
13. Fairbrother JM, Nadeau É and Gyles CL. 2005. Escherichia coli in postweaning diarrhea in pigs: an update on bacterial types, pathogenesis and prevention strategies. *Anim Health Res Rev* **6:** 17-39.
14. Ellis J, Krakowka S, Lairmore M, Haines D, Bratanich A, Clark E, Allan G, Konoby C, Hassard L, Meehan B and Martin K. 1999. Reproduction of lesions of postweaning multisystemic wasting syndrome in gnotobiotic piglets. *J Vet Diagn Invest* **11:** 3-14.
15. Korczak B, Christensen H, Emler S, Frey J and Kuhnert P. 2004. Phylogeny of the family Pasteurellaceae based on rpoB sequences. *Int J Syst Evol* **54:** 1393-1399.
16. Barman NN, Gupta RS, Bora DP, Kataria RS, Tiwari AK and Roychoudhury P. 2010. Molecular characterization of classical swine fever virus involved in the outbreak in Mizoram. *Indian J Virol* **21:** 76-81.
17. Suvarna K, Layton C and Bancroft JD. 2018. *Bancroft's Theory* and *Practice of Histological Techniques*. 8th Ed. Elsevier Health Sciences, Churchill, 584p.
18. Rosell C, Segalés J, Plana-Duran J, Balasch M, Rodríguez-Arrioja GM, Kennedy S, Allan GM, McNeilly F, Latimer KS and Domingo M. 1999. Pathological, immunohistochemical and in-situ hybridization studies of natural cases of postweaning multisystemic wasting syndrome (PMWS) in pigs. *J Comp Pathol* **120:** 59-78.
19. Petrov A, Blohm U, Beer M, Pietschmann J and Blome S. 2014. Comparative analyses of host responses upon infection with moderately virulent classical swine fever virus in domestic pigs and wild boar. *Virol J* **11:** 1-6.
20. Carman S, McEwn B, DeLay J, van Druemel T, Lusis P, Cai H and Fairles J. 2006. Porcine circovirus-2 associated disease in swine in Ontario (2004 to 2005). *Can Vet J* **47:** 761-762.
21. Blome S, Staubach C, Henke J, Carlson J and Beer M. 2017. Classical swine fever an updated review. *Viruses* **9:** 86.
22. Morin M, Girard C, El Azhary Y, Fajardo R, Drolet R and Lagacé A. 1990. Severe proliferative and necrotizing pneumonia in pigs: A newly recognized disease. *Can Vet J* **31:** 837-839.
23. Chianini F, Majó N, Segalés J, Domínguez J and Domingo M. 2003. Immunohistochemical characterisation of PCV2 associate lesions in lymphoid and non-lymphoid tissues of pigs with natural postweaning multisystemic wasting syndrome (PMWS). *Vet Immunol Immunopathol* **94:** 63-75.
24. Shibahara T, Sato K, Ishikawa Y and Kadota K. 2000. Porcine circovirus induces B lymphocyte depletion in pigs with wasting disease syndrome. *J Vet Med Sci* **62:** 1125-1131.
25. Yu S, Opriessnig T, Kitikoon P, Nilubol D, Halbur PG and Thacker E. 2007. Porcine circovirus type 2 (PCV2) distribution and replication in tissues and immune cells in early infected pigs. *Vet Immunol Immunopathol* **115:** 261-272.
26. Marks FS, Reck Jr J, Almeida LL, Berger M, Corrêa AM, Driemeier D, Barcellos DE, Guimarães JA, Termignoni C and Canal CW. 2010. Porcine circovirus 2 (PCV2) induces a procoagulant state in naturally infected swine and in cultured endothelial cells. *Vet Microbiol* **141:** 22-30.
27. Calderón NL, Paasch LH and Bouda J. 1997. Haematological and histological bone marrow findings in experimental classical swine fever. *Acta Vet Brno* **66:** 171-176.
28. Jessil J. 2021. Pathological evaluation of central nervous and reproductive system of porcine circovirus-2 infected pigs. *MVSc thesis*, Kerala Veterinary and Animal Sciences University, Pookode, 58p.
29. Opriessnig T and Halbur PG. 2012. Concurrent infections are important for expression of porcine circovirus associated disease. *Virus Res* **164:** 20-32.

Indian J. Vet. Pathol., 48(2) : 123-131, 2024: DOI: 10.5958/0973-970X.2024.00022.8

RESEARCH ARTICLE

Concurrent occurrence of wet form of feline infectious peritonitis (FIP) and feline parvovirus (FPV) infection in a cat

K.A. Reshma, S.S. Devi*, C. Divya, R. Anoopraj, Sankar Surya[1], K.S. Prasanna, I.S. Sajitha, R. Bharathi and C. Udhayakumar

[1]Department of Veterinary Microbiology, College of Veterinary and Animal Sciences, Mannuthy, Thrissur-680 651, Kerala, Department of Veterinary Pathology, College of Veterinary and Animal Sciences, Mannuthy, Kerala Veterinary and Animal Sciences University, Pookode, Wayanad-680 656, Kerala, India

Address for Correspondence

S.S. Devi, Assistant Professor, Department of Veterinary Pathology, College of Veterinary and Animal Sciences, Mannuthy, Kerala Veterinary and Animal Sciences University, Pookode, Wayanad-680 656, Kerala, India, E-mail: deviss@kvasu.ac.in

Received: 9.10.2023; Accepted: 4.11.2023

ABSTRACT

The present study conducted in the Department of Veterinary Pathology, College of Veterinary and Animal Sciences, Mannuthy aimed at screening parvo, rota and coronaviral infections in cat carcasses with lesions of gastroenteritis. Among the 30 cases examined, 23 turned out to be positive for parvoviral infection, of which, a single case of combined infection with coronavirus was observed. The present case describes a concurrent occurrence of wet form of FIP, FPV and *Escherichia coli* (*E. coli*) infection in a one-year-old male Persian cat with clinical signs of distended abdomen, anorexia, lethargy, respiratory distress, diarrhoea and pyrexia. A detailed post-mortem examination revealed the presence of about 50mL of moderately cloudy fluid in the peritoneum and thorax with congested liver, spleen, kidneys and catarrhal gastroenteritis. The positive reaction to Rivalta test indicated wet form of FIP and further confirmed by reverse transcriptase polymerase chain reaction (RT-PCR) for feline coronavirus (FCoV) by targeting *M* gene. The case was screened for Feline parvovirus (FPV), rotavirus and *E. coli* employing conventional PCR targeting *VP2* gene, *VP6* gene and *FimC* gene respectively, and found positive for parvovirus and *E. coli* infections as well. Sequencing was done to confirm the identity of FPV followed by phylogenetic analysis to determine the relationship with previously submitted sequences of *VP2* gene. Histopathology showed infiltration of inflammatory cells in lungs, hepatic congestion, renal desquamation and enteritis. Immunohistochemical analysis of corona and parvoviral antigen revealed the localization of the viruses in intestine, mesenteric lymph nodes, spleen, liver and thymus. The present case study established the concurrent occurrence of various feline enteric viruses with bacterial co-infection emphasising the requisite of routine screening for multiple infections so as to aid in modified therapeutic and preventive strategies.

Keywords: *E. coli,* FCoV, FPV, immunohistochemical analysis, PCR, Rivalta test, RT-PCR, wet form-FIP

INTRODUCTION

In India, viral infections continue to be the predominant cause of canine and feline gastroenteritis despite routine vaccinations. The three most frequent viral gastrointestinal pathogens are parvo, rota and corona viruses. The prevalence of mixed infections with various enteric virus combinations, bacterial and helminthic co-infections exacerbates the severity of the disease by accelerating intestinal cell turnover and, in turn, viral replication, have also been discovered. Here, the pathology of a case with concurrent infection of FCoV, FPV and *E. coli* in a Persian cat is described.

The members of *Coronaviridae* can infect a number of hosts and lead to various diseases including infectious bronchitis (IB) in poultry, FIP in cats, gastroenteritis in dogs and Covid-19 in humans. The feline coronavirus (FCoV) belongs to group 1 coronaviruses in the family *Coronaviridae* of order *Nidovirales* with enteric canine coronavirus and porcine transmissible gastroenteritis virus as the other main members. These viruses are large, spherical, enveloped, positive sense single stranded RNA viruses. There are two different biotypes of FCoV: the feline enteric coronavirus (FECV) and the feline infectious peritonitis virus (FIPV). The FIPV causes FIP, a deadly and systemic illness, while FECV causes subclinical infections but are highly infectious with a morbidity rate close to 100%[1]. The FCoV infection is very frequent in cats and around 40% of the domestic cat population has been reported to be infected[2]. The majority of FCoV-infected cats are healthy or exhibit only a mild to moderate enteritis; nevertheless, some develop FIP, a condition that is more prevalent in young cats and multi-cat environments. Stress is a risk factor for the development of the disease in up to 12% of FCoV-infected cats[3]. Feline infectious peritonitis is an immune mediated significant sporadic disease and is typically fatal, the biology of which is still little understood and prevention

How to cite this article : Reshma, K.A., Devi, S.S., Divya, C., Anoopraj, R., Surya, S., Prasanna, K.S., Sajitha, I.S., Bharathi, R. and Udhayakumar, C. 2024. Concurrent occurrence of wet form of feline infectious peritonitis (FIP) and feline parvovirus (FPV) infection in a cat. Indian J. Vet. Pathol., 48(2) : 123-131.

Table 1. Primers used for PCR and RT-PCR.

Virus	Target gene	Primer sequence 5′-3′ direction	Position of the genome	Product size	Reference
FCoV	m-RNA *M* gene	(F) 5′-TAATGCCATACACGAACCAGCT-3′ (22)	26440-26461	279 bp	10
		(R) 5′-GTGCTAGATTTGTCTTCGGACACC-3′ (25)	60-83		
Rotavirus	*VP6* gene	(F) 5′-GACGGVGCRACTACATGGT-3′	750-769	379 bp	11
		(R) 5′-GTCCAATTCATNCCTGGTGG-3′	920-939		
FPV	*VP2* gene	(F) 5′-CAT TGG GCT TAC CAC CAT TT-3′ (20-mer)	3136-3155	160 bp	12
		(R) 5′-CCA ACC TCA GCT GGT CTC AT-3′ (20-mer)	3276-3295		
E.coli	*FimC* gene	(F) 5′-GGGTAGAAAATGCCGATGGTG-3′	215-235	477 bp	13
		(R) 5′-CGTCATTTTGGGGGTAAGTGC-3′	671-691		

Table 2. PCR conditions for amplification of FCoV (m-RNA *M* gene).

Steps		Temperature	Time
Initial denaturation		94°C	5 min
35 cycles	Denaturation	94°C	1 min
	Annealing	61°C	1 min
	Extension	72°C	2 min
Final extension		72°C	5 min

Table 3. PCR conditions for amplification of Rotavirus (*VP6* gene).

Steps		Temperature	Time
Initial denaturation		94°C	5 min
35 cycles	Denaturation	94°C	1 min
	Annealing	61°C	1 min
	Extension	72°C	2 min
Final extension		72°C	5 min

Table 4. PCR conditions for amplification of FPV (*VP2* gene).

Steps		Temperature	Time
Initial denaturation		94°C	3 min
30 cycles	Denaturation	94°C	30 sec
	Annealing	52°C	1 min
	Extension	72°C	30 sec
Final extension		72°C	5 min

Table 5. PCR conditions for amplification of *E.coli* (*FimC* gene).

Steps		Temperature	Time
Initial denaturation		94°C	5 min
35 cycles	Denaturation	94°C	1 min
	Annealing	59°C	1 min
	Extension	72°C	2 min
Final extension		72°C	5 min

is challenging. It affects both domesticated and wild felids around the world[4].

Laboratory testing of the fluid, particularly Rivalta's test, should be done on cats with an effusion as a primary test for FIP. The RT-PCR and IHC on post-mortem or laparotomy tissue samples could aid in the further confirmation of FIP[5]. Cats with FIP exhibit high levels of FCoV RNA in organs that show inflammatory alterations. The organs with the highest viral load include the spleen, mesenteric lymph nodes and omentum; hence, RT-PCR analysis would be yielding the most reliable results when done with these tissues[6]. Immunohistochemistry remains the gold standard diagnostic tool of FCoV when applied to histopathologically aberrant tissue samples[5].

Feline parvoviral infection is characterized by a severe gastroenteritis, fatal especially in kittens, with intestinal villi degradation and a consequent reduction in nutrient absorption[7]. The secondary infections to FPV by other viruses, bacteria and helminths are caused by immunosuppression brought on by a dramatic drop in white blood cell count. It has also been reported that lesions with combined FCoV and FPV infection with other bacterial and helminthic secondary infections could enhance the severity of diseases, thus highlighting the requisite of routine and thorough monitoring for multiple infections with improved therapeutic and prophylactic strategies in feline veterinary medicine.

MATERIALS AND METHODS

A one-year-old male Persian cat presented to the Department of Veterinary Pathology, College of Veterinary and Animal Sciences, Mannuthy for post-mortem examination formed the material for the study. For PCR, pooled tissue samples from visceral organs exhibiting gross lesions (intestine, mesenteric lymph node, liver, spleen and thymus) were collected and stored at -80°C until extraction of nucleic acid; and in 10% neutral buffered formalin (NBF) solution for immunohistochemistry and histopathological studies.

Rivalta test

Rivalta test is a simple, economical method to differ-entiate between transudate and exudate usually done in effusions to predict FIP in cats. In a test tube filled with 7 to 8 mL of distilled water, one drop of glacial acetic acid (8%) was added, mixed thoroughly and a drop of effusion collected in a sterile syringe was layered on the surface by a dropper. The interpretation can be made as positive if the drop retains its shape and floats down slowly to the bottom (jelly fish like).

Histopathology and Immunohistochemistry

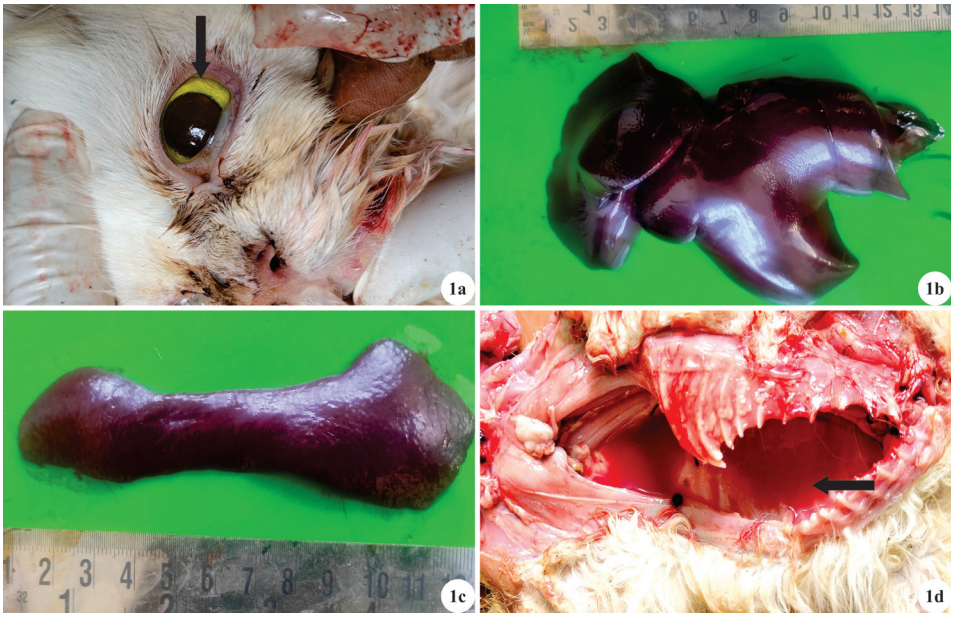

Fig. 1. Gross pathology of concurrent infection by FIP and FPV in one year old male cat. **a.** Sclera showing severe icteric changes. **b.** Enlarged liver showing diffuse congestion. **c.** Splenomegaly with severe congestion. **d.** Intrathoracic and intraperitoneal effusion.

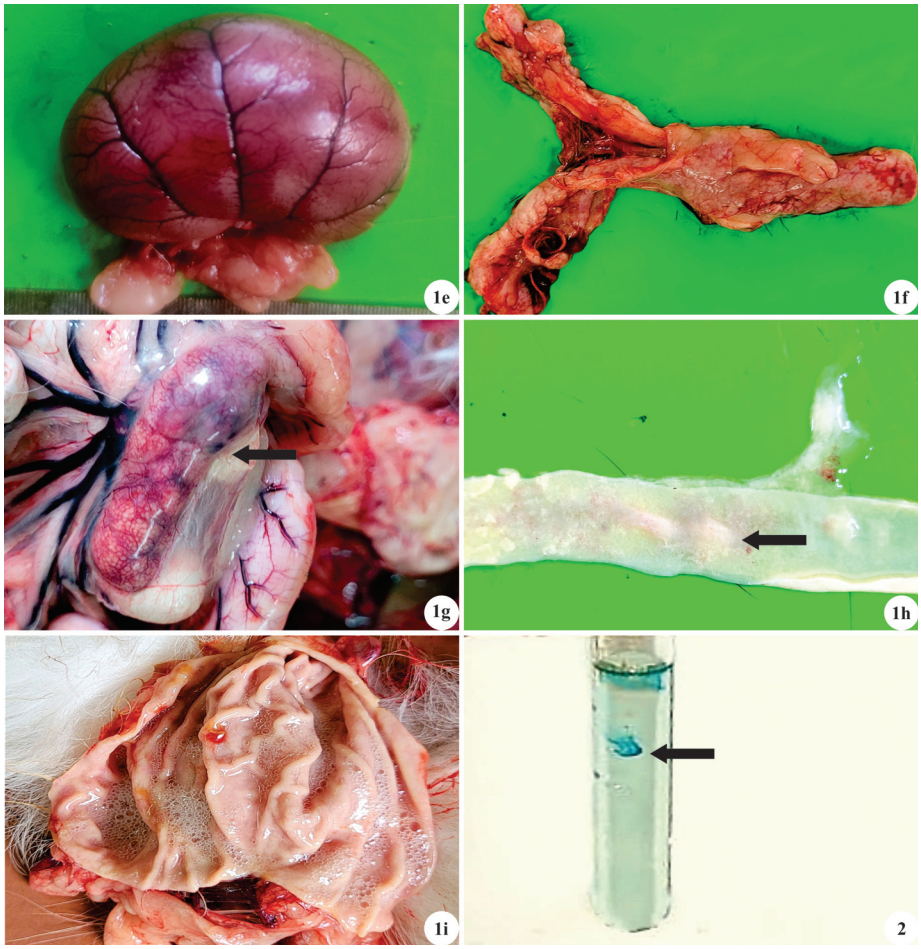

Fig. 1. Gross pathology of concurrent infection by FIP and FPV in a one year old male cat. **e.** Kidneys showing engorged blood vessels. **f.** Moderately congested pancreas. **g.** Mesenteric lymph nodes were enlarged and congested. **h.** Intestine showing watery contents mixed with mucous. **i.** Stomach with watery contents; **Fig. 2.** Figure showing positive result for Rivalta test done on the intrathoracic and intraperitoneal effusion.

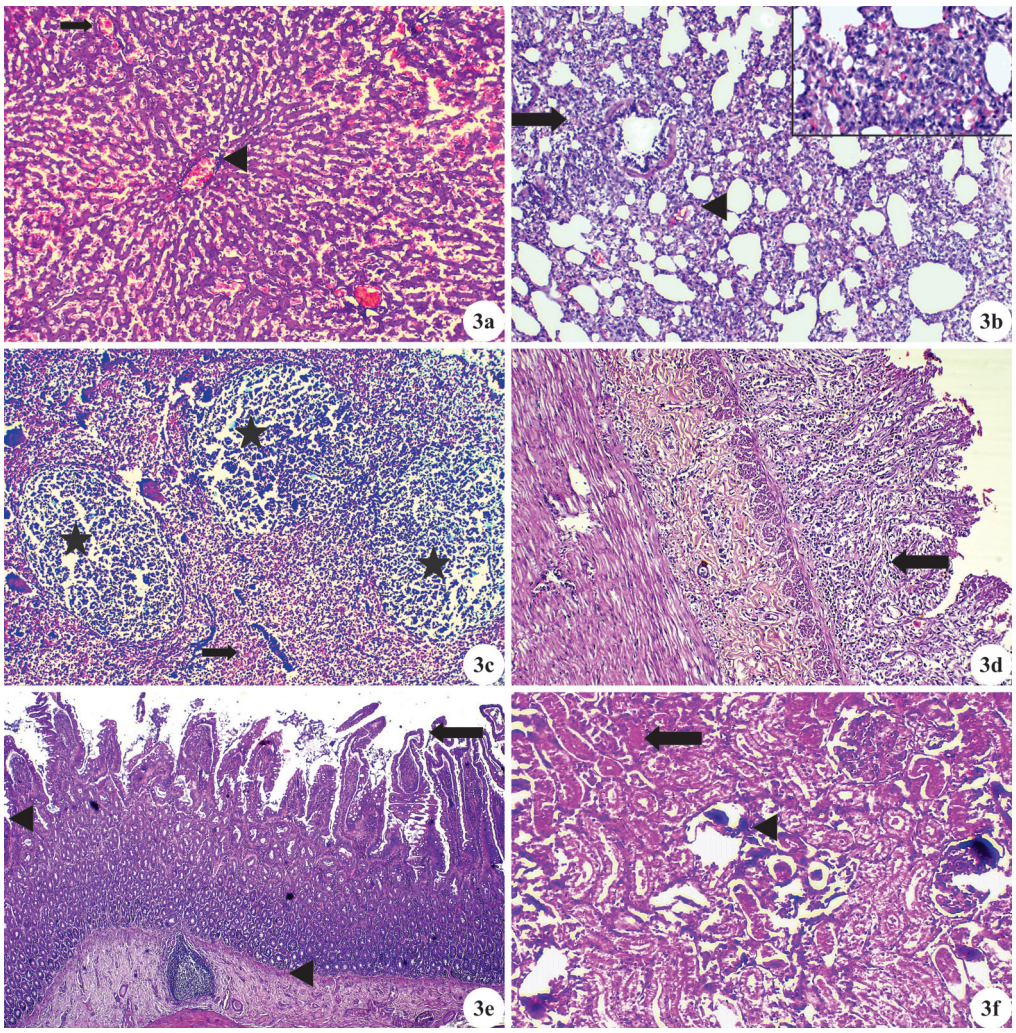

Fig. 3. Histopathology of concurrent infection by FIP and FPV in a one year old male cat. **a.** Liver showing severe congestion in sinusoids (arrow) and central vein (arrowhead) (H&E x100). **b.** Lungs showing thickened alveolar wall, severe mononuclear cell infiltrations (arrow) and haemorrhages (arrowhead) (H&E x100), inset: (H&E x400). **c.** Mesenteric lymph nodes showing lymphoid depletion (asterisk) and haemorrhages (arrow) (H&E x100). **d.** Intestine showing denudation of villi (arrowhead), fusion and stunting of villi, denudation of the necrosed cryptgl and epithelium (arrow), congestion and haemorrhages in the submucosa (H&E x40). **e.** Intestine showing severe submucosal lymphoid depletion (arrowhead) and disruption of villi tips (arrow) (H&E x100). **f.** Kidney showing severe tubular necrosis (arrow) and glomerular atrophy (arrowhead), dilation of Bowman's space and mild infiltration of mononuclear cells in the interstitium (H&E x100).

Formalin fixed paraffin embedded (FFPE) sections of 5 µm thickness were subjected to routine haematoxylin and eosin staining technique[8]. Localization of corona and parvoviruses in the FFPE tissue sections was studied by immunohistochemistry as per standard technique[9]. The primary antibodies used were polyclonal anti coronaviral antibody procured from R&D Systems in the dilution of 1:200 and polyclonal anti parvoviral antibody procured from Santa Cruz Biotechnology in the dilution of 1:1000 and secondary antibody from, Quartett Germany.

Table 6. Optimized concentrations of PCR reagents.

Components	FCoV Volume (µl)	Rotavirus Volume (µl)	FPV Volume (µl)	*E.coli* Volume (µl)
Nuclease free water	1.75	1.75	2.0	2.0
Forward primer (10 pM/µl)	1.0	1.0	1.0	1.0
Reverse primer (10 pM/µl)	1.0	1.0	1.0	1.0
Master mix	6.25	6.25	5	5
cDNA/DNA sample	3.0	3.0	1.0	1.0
Total	12.5	12.5	10	10

Polymerase chain reaction

The pooled tissue samples were screened for FCoV and rotavirus by RT-PCR targeting 295 bp fragment of the *M* gene[10] and 379 bp fragment of the *VP6* gene[11] respectively, for which the RNA was extracted using

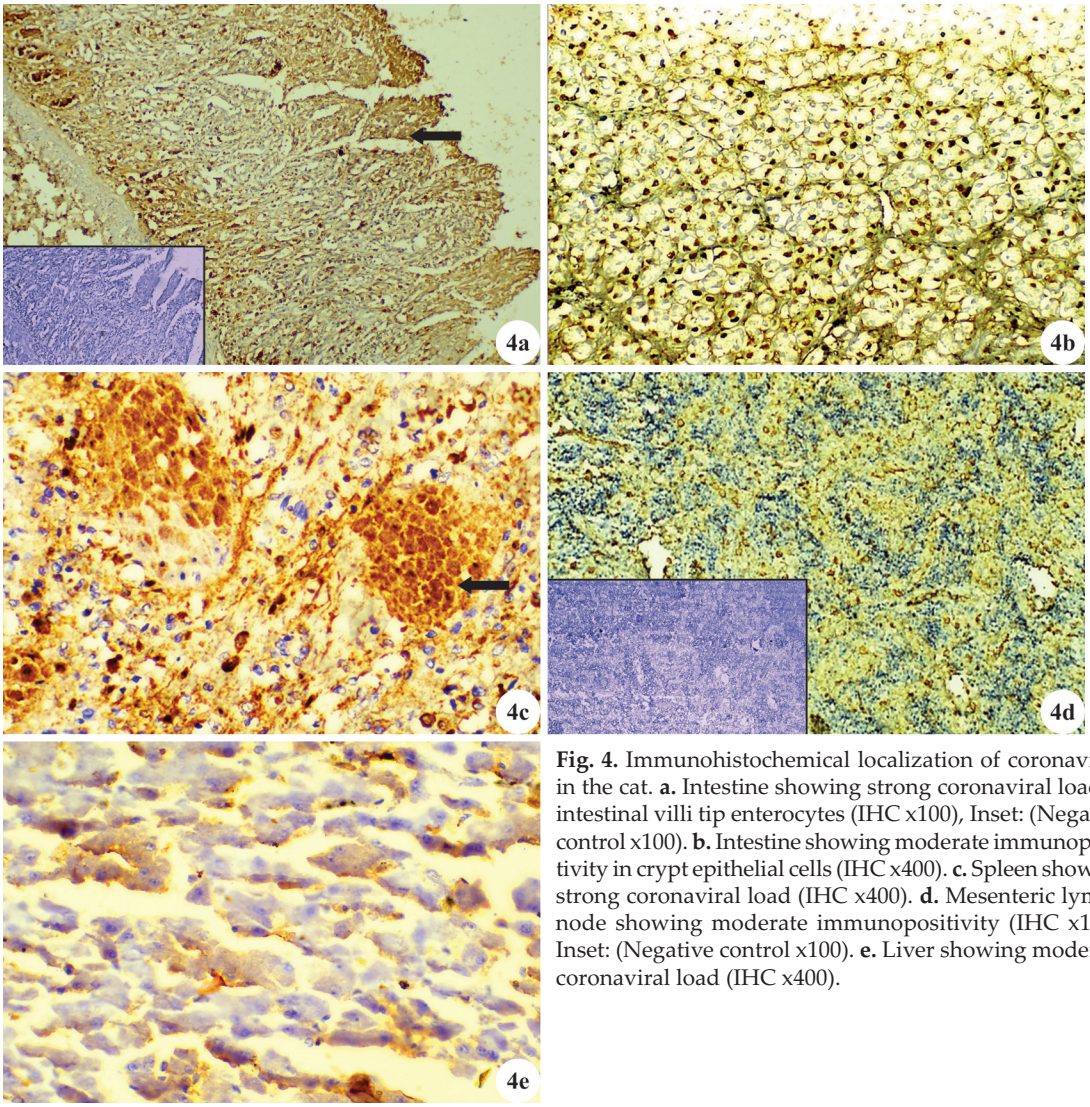

Fig. 4. Immunohistochemical localization of coronavirus in the cat. **a.** Intestine showing strong coronaviral load in intestinal villi tip enterocytes (IHC x100), Inset: (Negative control x100). **b.** Intestine showing moderate immunopositivity in crypt epithelial cells (IHC x400). **c.** Spleen showing strong coronaviral load (IHC x400). **d.** Mesenteric lymph node showing moderate immunopositivity (IHC x100), Inset: (Negative control x100). **e.** Liver showing moderate coronaviral load (IHC x400).

a commercially available total RNA isolation kit (QIA GEN), as per the manufacturer's instructions. The cDNA was synthesised from the extracted total RNA using PrimeScript™ 1st strand cDNA Synthesis Kit (TaKaRa) as per the manufacturer's protocol. After synthesis, cDNA was stored at -80^{O}C until further use.Further, the sample was screened for FPV targeting 160 bp fragment of *VP2* gene[12] and for *E. coli* targeting 477 bp fragment of *FimC* gene[13] by PCR. Extraction of DNA from the pooled tissue samples was made using DNeasy Blood & Tissue Kit (QIAGEN) as per the manufacturer's protocol. The RT-PCR for FCoV and Rotavirus and PCR for FPV and *E. coli*, were done using published primers (Table 1). Appropriate PCR conditions (Table 2-5) and optimised concentrations of PCR reagents followed are as given in Table 6.

The PCR products were detected by electrophoresis in 1.5% agarose gel. Sample revealing a 295 bp fragment was considered positive for coronavirus, a 160 bp fragment for parvovirus and a 477 bp fragment for *E. coli*. Sequencing of the amplicons was done at Eurofins Genomics India Pvt. Ltd., Karnataka, India so as to confirm the identity of the viruses and the sequence of the FPV was aligned using Clustal W and phylogenetic analysis was carried out by neighbour-joining method using Mega 11 software.

RESULTS AND DISCUSSION

The animal presented for necropsy was a one-year-old male Persian cat with a clinical history of distended abdomen, anorexia, lethargy, weight loss, diarrhoea, respiratory distress and pyrexia. Male cats as well as young cats under the age of two were reported to be particularly susceptible to FIP[14] with non-specific clinical signs like anorexia, lethargy, weight loss, pyrexia, along with ocular and neurological symptoms including gait abnormalities or improper mentation[15]. Tachypnoea with a fast, shallow breathing pattern and respiratory distress

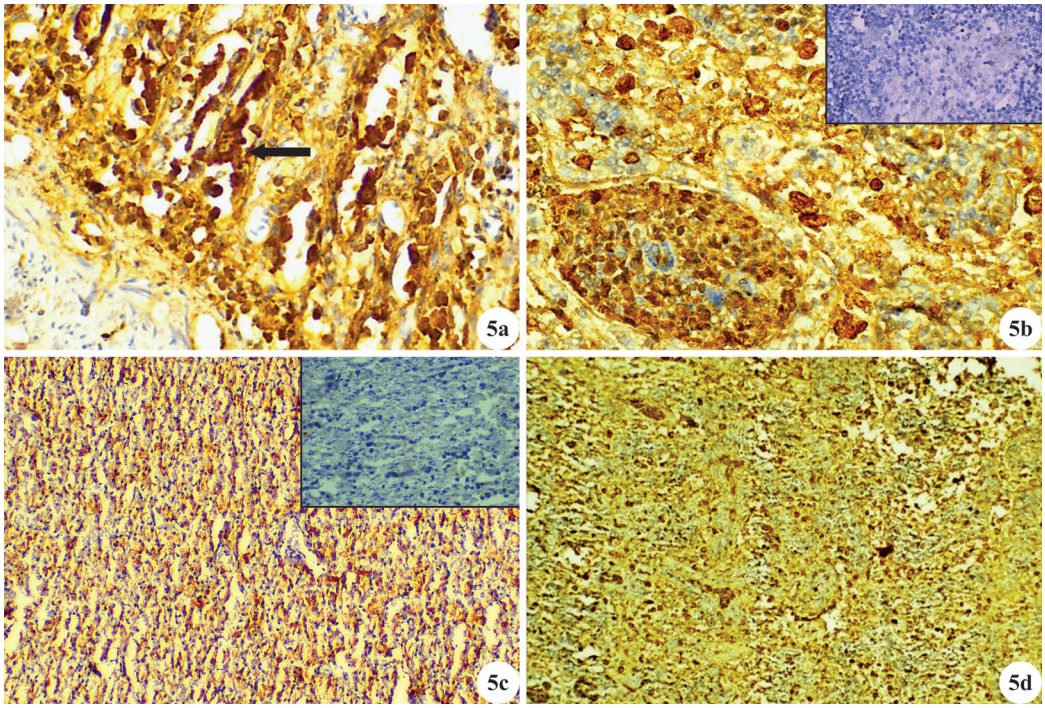

Fig. 5. Immunohistochemical localization of parvovirus in the cat. **a.** Intestine showing strong parvoviral load in crypt epithelial cells (IHC x400). **b.** Spleen showing strong immunopositivity for parvoviral antigen (IHC x400), Inset: (Negative control x100). **c.** Liver showing strong immunopositivity for parvoviral antigen (IHC x100), Inset: (Negative control x100). **d.** Mesenteric lymph node showing strong immunopositivity for parvoviral antigen (IHC x40).

could also result from pleural effusion in FIP[16].

Upon detailed necropsy, the presence of about 50 mL of moderately cloudy effusion in the abdominal and thoracic cavity (Fig. 1d) with sclera showing severe icteric changes (Fig. 1a), enlarged liver showing diffuse congestion (Fig. 1b), splenomegaly with severe congestion (Fig. 1c), engorged blood vessels in kidneys (Fig. 1e), moderately congested pancreas (Fig. 1f), enlarged and congested mesenteric lymph nodes (Fig. 1g) and catarrhal enteritis (Fig. 1h) with watery intestinal and gastric contents (Fig. 1i) were noticed. The microscopic examination of heart blood smear and impression smears of lungs and liver revealed the presence of numerous cocci, short rods and bipolar organisms indicating multiple bacterial secondary infections. Haemorrhagic enteritis, hepatic necrosis, enlarged spleen and mesenteric lymph nodes strewn with haemorrhages were the frequent gross alterations reported in FPV[17]. The most extensive lymphadenomegaly in FIP was reported to be observed in the mesenteric lymph nodes[18].

The Rivalta test done in the peritoneal and thoracic effusion gave positive result as shown in Fig. 2. The Rivalta test, which was initially designed to distinguish between transudate and exudate, would be most likely positive in FIP as a result of higher levels of protein and inflammatory mediators in a fluid[19]. The Rivalta test should be recommended as a part of the diagnostic routine for any cat with an effusion as it is an inexpensive, quick test that can be easily done on effusions in clinical practice. It has strong sensitivity for the diagnosis of FIP (91%-100%) and 66-81 per cent specificity for excluding FIP[20].

Histopathological analysis revealed severe congestion in sinusoids and central vein (Fig. 3a), severe congestion in spleen, thickening of alveolar wall due to severe mononuclear cell infiltration into the interstitium, congestion of alveolar capillaries and haemorrhages in lungs (Fig. 3b), moderate congestion in pancreas, oedema and haemorrhages in mesenteric lymph nodes (Fig. 3c), denudation of intestinal villi, fusion and stunting of villi, denudation of the necrotic crypt gland epithelium into the lumen, congestion and haemorrhages in the submucosa (Fig. 3d) with submucosal lymphoid depletion in intestine (Fig. 3e) and severe glomerular atrophy and tubular necrosis, dilation of Bowman's space and mild infiltration of mononuclear cells in kidneys (Fig. 3f). The above histological outcomes were in corroboration with the findings of previous researchers[21-22]. The FPV usually causes a widespread systemic infection. The virus requires quickly proliferating cells to establish infection and hence causes damage to tissues with the highest rate of mitotic activity during the S phase of the cell cycle. Hence, intestinal mucosal crypts (intestinal glands), lymphoid tissue and bone marrow are the most commonly invaded organs[17].

Fig. 6a. Molecular detection of FCoV showing 295 bp PCR amplified product of *M gene* of FCoV. L1: Ladder-100 bp, L2-L6: Negative samples and L7: Positive sample.

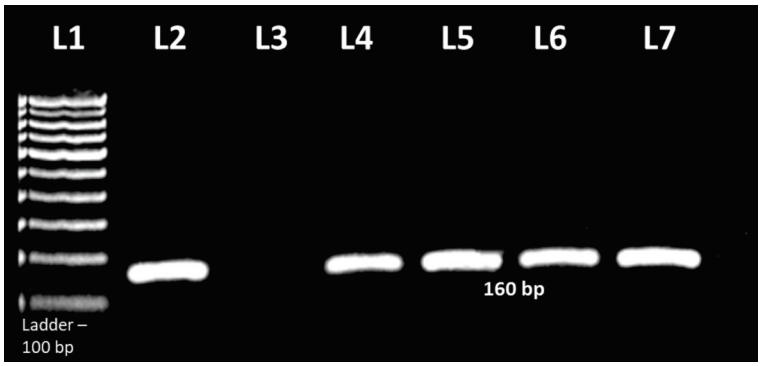

Fig. 6b. Molecular detection of FPV showing 160 bp PCR amplified product of *VP2 gene* of FPV. L1: Ladder-100 bp, L2: Positive control, L3: Negative control and L4-L7: Positive.

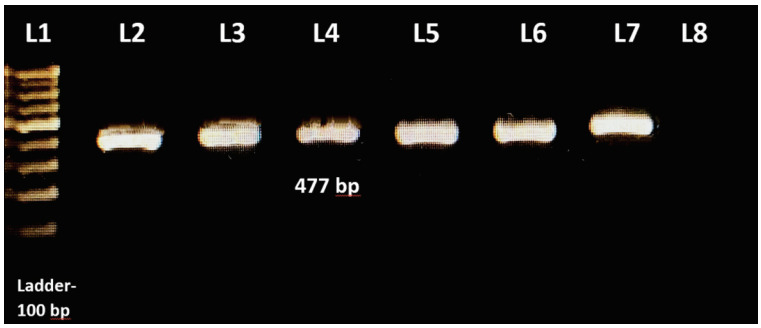

Fig. 6c. Molecular detection of *E. coli* showing 477 bp PCR amplified product of *FimC gene* of *E.coli* with L1: Ladder-100 bp, L2-L7: Positive samples and L8: Negative control.

Immunohistochemical localization study of coronavirus revealed strong viral load in intestinal villi tip enterocytes (Fig. 4a) and spleen (Fig. 4c), moderate viral load in crypt epithelial cells of intestine (Fig. 4b), mesenteric lymph nodes (Fig. 4d) and liver (Fig. 4e). Immunohistochemical analysis of parvovirus showed localization in intestine with strong viral load in the crypt and denuded epithelial cells (Fig. 5a), along with strong signals from spleen (Fig. 5b), liver (Fig. 5c), thymus and mesenteric lymph nodes (Fig. 5d). The parvovirus requires cellular DNA polymerase enzyme for replication[23], so it infects more rapidly dividing cells of the intestine and bone marrow; as a result, more immunostaining was observed from the crypt epithelium than villi tip enterocytes. The FCoV primarily affects mature cells[24], so mature intestinal villi tip epithelial cells showed more viral load than rapidly multiplying crypt epithelium. It has been reported that immunohistochemistry (IHC) show an excellent sensitivity of 97-100% and specificity of up to 100% for demonstration of FCoV antigen in recognizable histopathological tissue lesions from cats with FIP[25]. The results of the present study reinstate IHC for detection of FCoV antigen as the gold standard test for the diagnosis of FIP.

The case was confirmed as combined FCoV, FPV and *E. coli* infections by molecular techniques including RT-PCR and PCR[10,12,13]. The 295 bp PCR amplified product of *M* gene of FCoV is shown in the Fig. 6a, the 160 bp PCR amplified product of *VP2* gene of FPV is shown in the Fig. 6b and the 477 bp PCR amplified product of *FimC* gene of *E. coli* is shown in the Fig. 6c. The FASTA sequences that were obtained after sequencing the PCR products were further blasted to confirm the identity of viruses. The FPV isolate obtained in the present case was found to be more related to earlier submitted sequences from Australia, Kerala and China, especially MW285760.1 isolate from Kerala (Fig. 6d-e). The most common

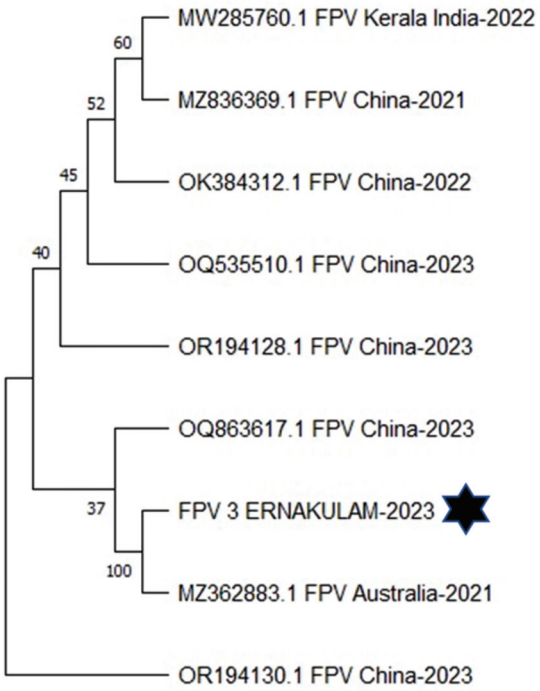

Fig. 6d. Phylogenetic Tree of 160 bp fragment of *VP2 gene* of FPV isolate showing close relation with sequences from Australia, Kerala and China.

Description	Scientific Name	Max Score	Total Score	Query Cover	E value	Per. Ident	Acc. Len	Accession
Feline panleukopenia virus isolate PSY01-2 capsid protein VP2 gene, complete cds	Feline panleukop...	163	240	21%	5e-35	96.08%	1755	OR260993.1
Feline panleukopenia virus isolate FPV/2022/77 VP2 protein (VP2) gene, complete cds	Feline panleukop...	163	163	15%	5e-35	96.08%	1755	OR399567.1
Feline panleukopenia virus isolate FPV/2022/42 VP2 protein (VP2) gene, complete cds	Feline panleukop...	163	163	15%	5e-35	96.08%	1755	OR399563.1
Feline parvovirus isolate HY nonstructural protein 1 (NS1) and structural protein 2 (VP2) genes, complete cds	Feline parvovirus	163	163	15%	5e-35	96.08%	5176	OR257446.2
Feline parvovirus isolate WH 1 nonstructural protein 1 (NS1) and structural protein 2 (VP2) genes, complete cds	Feline parvovirus	163	240	21%	5e-35	96.08%	5123	OR257444.1
Feline panleukopenia virus strain CH/YCYH/2021, complete genome	Feline panleukop...	163	240	21%	5e-35	96.08%	4888	OR227624.1
Protoparvovirus carnivoran1 isolate SRB-Jackal 101/2023 capsid protein (VP2) gene, partial cds	Protoparvovirus ...	163	240	21%	5e-35	96.08%	680	OR236706.1
Protoparvovirus carnivoran1 isolate SRB-Jackal 56/2022 capsid protein (VP2) gene, partial cds	Protoparvovirus ...	163	240	21%	5e-35	96.08%	680	OR236705.1
Protoparvovirus carnivoran1 isolate SRB-Jackal 49/2022 capsid protein (VP2) gene, partial cds	Protoparvovirus ...	163	240	21%	5e-35	96.08%	680	OR236704.1
Feline parvovirus isolate AHWH52 VP2 protein gene, complete cds	Feline parvovirus	163	163	15%	5e-35	96.08%	1755	OR211675.1
Feline parvovirus strain NTU/C148/2020, complete genome	Feline parvovirus	163	234	21%	5e-35	96.08%	4903	OR198066.1
Feline panleukopenia virus strain 18DIAPD52063/2 VP2 gene, complete cds	Feline panleukop...	163	240	21%	5e-35	96.08%	2433	MZ508522.1
Feline parvovirus isolate JS2201 VP2 gene, complete cds	Feline parvovirus	163	163	15%	5e-35	96.08%	1755	OQ868568.1
Feline parvovirus isolate HN2101 VP2 gene, complete cds	Feline parvovirus	163	163	15%	5e-35	96.08%	1755	OQ868566.1
Feline parvovirus isolate JS2002 VP2 gene, complete cds	Feline parvovirus	163	163	15%	5e-35	96.08%	1755	OQ868565.1
Feline parvovirus isolate AH2012 VP2 gene, complete cds	Feline parvovirus	163	163	15%	5e-35	96.08%	1755	OQ868564.1
Feline parvovirus isolate AH2010 VP2 gene, complete cds	Feline parvovirus	163	163	15%	5e-35	96.08%	1755	OQ868563.1
Feline parvovirus isolate JS2001 VP2 gene, complete cds	Feline parvovirus	163	163	15%	5e-35	96.08%	1755	OQ868562.1
Feline parvovirus isolate AH2011 VP2 gene, complete cds	Feline parvovirus	163	240	21%	5e-35	96.08%	1755	OQ868561.1
Feline parvovirus isolate AH2009 VP2 gene, complete cds	Feline parvovirus	163	163	15%	5e-35	96.08%	1755	OQ868560.1
Feline parvovirus isolate AH2007 VP2 gene, complete cds	Feline parvovirus	163	163	15%	5e-35	96.08%	1755	OQ868559.1
Feline parvovirus isolate AH2004 VP2 gene, complete cds	Feline parvovirus	163	163	15%	5e-35	96.08%	1755	OQ868557.1
Feline parvovirus isolate AH2003 VP2 gene, complete cds	Feline parvovirus	163	163	15%	5e-35	96.08%	1755	OQ868556.1
Feline parvovirus isolate AH2002 VP2 gene, complete cds	Feline parvovirus	163	163	15%	5e-35	96.08%	1755	OQ868555.1
Feline parvovirus isolate AH2001 VP2 gene, complete cds	Feline parvovirus	163	163	15%	5e-35	96.08%	1755	OQ868554.1
Feline parvovirus isolate AH1904 VP2 gene, complete cds	Feline parvovirus	163	163	15%	5e-35	96.08%	1755	OQ868553.1
Feline parvovirus isolate AH1902 VP2 gene, complete cds	Feline parvovirus	163	163	15%	5e-35	96.08%	1755	OQ868551.1
Feline parvovirus isolate AH1901 VP2 gene, complete cds	Feline parvovirus	163	163	15%	5e-35	96.08%	1755	OQ868550.1
Feline parvovirus isolate HB2002 VP2 gene, complete cds	Feline parvovirus	163	163	15%	5e-35	96.08%	1755	OQ868549.1

Fig. 6e. Figure showing the blast analysis results of the FPV isolate.

method for detecting coronavirus RNA is RT-PCR as the viral isolation is not clinically practical in all the cases[26]. The significant pathogenic event in FIP is the infection of monocytes and macrophages, where the mutant virus develops a novel tropism and replicates at high titres. A correlation between the detection of FCoV mRNA in blood samples by RT-PCR targeting mRNA of *M* gene of FCoV and the onset of FIP has also been proposed[10], there by establishing the significance of molecular tools for the detection of the virus. Similarly, molecular detection of *E. coli* by PCR has become a widely-used technique because it is quick and consistent with high sensitivity and specificity[27].

CONCLUSION

In conclusion, a confirmatory diagnosis of wet form of FIP with a combined infection of FPV was made based on the collective outcomes of the history and clinical signs coupled with the gross and histopathological lesions, immunohistochemical findings and PCR results. The viral infections combined with other secondary bacterial infections aggravated the severity of the lesions, pointing to the necessity of routine screening for mixed infection as a mandate in feline veterinary practice. The FIP is typically fatal in cats with no specific cure and only supportive care can be offered to the affected animals. As the infection spreads through faeco-oral route, avoiding sharing of the litter box, keeping the litter box as clean as possible, and reducing stress could be the successful approaches in abating the occurrence of FIP.

ACKNOWLEDGEMENTS

The authors are grateful to the Dean, College of Veterinary and Animal Sciences, Mannuthy for providing necessary facilities to carry out this research work.

REFERENCES

1. Licitra BN, Millet JK, Regan AD, Hamilton BS, Rinaldi VD, Duhamel GE and Whittaker GR. 2013. Mutation in spike protein cleavage site and pathogenesis of feline coronavirus. *Emerg Infect Dis* **19:** 1066.
2. Stranieri A, Probo M, Pisu MC, Fioletti A, Meazzi S, Gelain ME, Bonsembiante F, Lauzi S and Paltrinieri S. 2020. Preliminary investigation on feline coronavirus presence in the reproductive tract of the tom cat as a potential route of viral transmission. *J Feline Med Surg* **22:** 178-185.
3. Addie D, Belák S, Boucraut-Baralon C, Egberink H, Frymus T, Gruffydd-Jones T, Hartmann K, Hosie MJ, Lloret A, Lutz H and Marsilio F. 2009. Feline infectious peritonitis. ABCD guidelines on prevention and management. *J Feline Med Surg*

11: 594-604.
4. Horzinek MC and Osterhaus ADME. 1979. Feline infectious peritonitis: a worldwide serosurvey. *Am J Vet Res* **40:** 1487-1492.
5. Felten S and Hartmann K. 2019. Diagnosis of feline infectious peritonitis: a review of the current literature. *Viruses* **11:** 1068.
6. Pedersen NC, Eckstrand C, Liu H, Leutenegger C and Murphy B. 2015. Levels of feline infectious peritonitis virus in blood, effusions, and various tissues and the role of lymphopenia in disease outcome following experimental infection. *Vet Microbiol* **175:** 157-166.
7. Gelberg HB. 2017. Alimentary system and the peritoneum, omentum, mesentery, and peritoneal cavity. *Pathologic Basis Vet Dis* 324p.
8. Suvarna K, Layton C and Bancroft JD. 2018. *Bancroft's Theory* and *Practice of Histological Techniques*. (8th Ed.). Elsevier Health Sciences, Churchill, 584p.
9. Ramos-Vara JA. 2005. Technical aspects of immunohistochemistry. *Vet Pathol* **42:** 405-426.
10. Simons FA, Vennema H, Rofina JE, Pol JM, Horzinek MC, Rottier PJ and Egberink HF. 2005. A mRNA PCR for the diagnosis of feline infectious peritonitis. *J Virol Methods* **124:** 111-116.
11. Ortega AF, Martinez-Castaneda JS, Bautista-Gomez LG, Munoz RF and Hernandez IQ. 2017. Identification of co-infection by rotavirus and parvovirus in dogs with gastroenteritis in Mexico. *Braz J Microbiol* **48:** 769-773.
12. Nandi S, Chidri S and Kumar M. 2009. Molecular characterization and phylogenetic analysis of a canine parvovirus isolate in India. *Vet Med* **54:** 483-490.
13. Janben T, Schwarz C, Preikschat P, Voss M, Philipp HC and Wieler LH. 2001. Virulence-associated genes in avian pathogenic Escherichia coli (APEC) isolated from internal organs of poultry having died from colibacillosis. *Int J Med Microbiol* **291:** 371-378.
14. Riemer F, Kuehner KA, Ritz S, Sauter-Louis C and Hartmann K. 2016. Clinical and laboratory features of cats with feline infectious peritonitis-a retrospective study of 231 confirmed cases (2000-2010). *J Feline Med Surg* **18:** 348-356.
15. Pedersen NC. 2009. A review of feline infectious peritonitis virus infection: 1963-2008. *J Feline Med Surg* **11:** 225-258.
16. Sykes JE. 2014. Feline coronavirus infection. *Canine Feline Inf Dis* 195p.
17. Decaro N, Buonavoglia D, Desario C, Amorisco F, Colaianni ML, Parisi A, Terio V, Elia G, Lucente MS, Cavalli A and Martella V. 2010. Characterization of canine parvovirus strains isolated from cats with feline panleukopenia. *Res Vet Sci* **89:** 275-278.
18. Krentz D, Zwicklbauer K, Felten S, Bergmann M, Dorsch R, Hofmann-Lehmann R, Meli ML, Spiri AM, von Both U, Alberer M and Honl A. 2022. Clinical Follow-Up and Postmortem Findings in a Cat That Was Cured of Feline Infectious Peritonitis with an Oral Antiviral Drug Containing GS-441524. *Viruses* **14:** 2040.
19. Berti-Bock G, Vial F, Premuda L and Rulliere R. 1979. Exudates, transudates and the Rivalta reaction (1895). Current status and historical premises. *Minerva Med* **70:** 3573-3580.
20. Felten S and Hartmann K. 2019. Diagnosis of feline infectious peritonitis: a review of the current literature. *Viruses* **11:** 1068.
21. Meurs KM, Fox PR, Magnon AL, Liu SK and Towbin JA. 2000. Molecular screening by polymerase chain reaction detects panleukopenia virus DNA in formalin-fixed hearts from cats with idiopathic cardiomyopathy and myocarditis. *Cardiovasc Pathol* **9:** 119-126.
22. Bayati HAA and Akaby SRA. 2017. Study of Histopathological changes associated with Feline Pan Leukopenia Virus infection in naturally infected cats. *J Edu College Wasit University* **1:** 511-520.
23. Stancu A, Ghise A, Pentea M, Pasca S, Carpinisan L, Petcu M, Degi J, Berceanu-Vaduva DM, Velimirovici DE, Romeo C and Tulcan C. 2020. Immunohistochemical Diagnosis Method in Parvovirus. *Rev de Chim* **1:** 491-496.
24. Stranieri A, Scavone D, Paltrinieri S, Giordano A, Bonsembiante F, Ferro S, Gelain ME, Meazzi S and Lauzi S. 2020. Concordance between histology, immunohistochemistry, and RT-PCR in the diagnosis of feline infectious peritonitis. *Pathog* **9:** 852.
25. Tammer R, Evensen O, Lutz H and Reinacher M. 1995. Immunohistological demonstration of feline infectious peritonitis virus antigen in paraffin-embedded tissues using feline ascites or murine monoclonal antibodies. *Vet Immunol Immunopathol* **49:** 177-182.
26. Veir JK and Lappin MR. 2010. Molecular diagnostic assays for infectious diseases in cats. *Vet Clin Small Anim Pract* **40:** 1189-1200.
27. Bellin T, Pulz M, Matussek A, Hempen HG and Gunzer F. 2001. Rapid detection of enterohemorrhagic Escherichia coli by real-time PCR with fluorescent hybridization probes. *J Clin Microbiol* **39:** 370-374.

Indian J. Vet. Pathol., 48(2) : 132-142, 2024: DOI: 10.5958/0973-970X.2024.00023.4

RESEARCH ARTICLE

Amelioration of lipopolysaccharide induced acute lung injury using chlorogenic acid and baicalein in mice: Clinicopathological study

Mandeep Kaur, Nittin Dev Singh*, Geeta Devi Leishangthem and Harmanjit Singh Banga
Department of Veterinary Pathology, College of Veterinary Science, Guru Angad Dev Veterinary and Animal Sciences University, Ludhiana, Punjab, India

Address for Correspondence
Nittin Dev Singh, Professor, Department of Veterinary Pathology, College of Veterinary Science, Guru Angad Dev Veterinary and Animal Sciences University, Ludhiana, Punjab, India, E-mail: drndsingh@gmail.com

Received: 19.9.2023; Accepted: 24.11.2023

ABSTRACT

Lung injury is the most significant cause of morbidity and mortality in humans as well as animals without current effective treatment plan. Lipopolysaccharide (LPS) is pro-inflammatory glycolipid component of cell wall of gram-negative bacteria which lead cause to acute lung injury (ALI). Most prevalent polyphenols in the human diet are chlorogenic acid (CGA), which have a number of biological functions viz anti-bacterial, anti-oxidant and anti-carcinogenic properties. Baicalein (BAC) is a phenolic flavonoid which has been reported to have anti-inflammatory properties. The study aimed to investigate the combined ameliorative effect of CGA and BAC on LPS induced ALI in murine model.Albino mice were divided into five groups. Seven days prior to instillation of LPS, treatment group mice were administered with CGA and BAC at three different dosages (0.1, 1 and 10 mg/kg body weight) intra-peritoneally. After 24 hours, mice of each group were sacrificed. Samples collected were blood, lungs and BALF. Hb, TLC, DLC estimation (blood); wet to dry weight ratio estimation, histopathology (lungs) and cytology, total protein estimation (BALF) were done. Different doses of CGA and BAC @ 0.1, 1 and 10 mg/kg body weight were studied for ameliorative effect, of which 10 mg/kg body weight was found to be having potential ameliorative effect. CGA and BAC is a rate limiting factors in inflammation and prevents inflammation by reducing the recruitment of neutrophils. Lung injury was amended by CGA and BAC as evident by histopathology in a synergistic manner.

Keywords: Acute lung injury, baicalein, chlorogenic acid, lipopolysaccharide, mice

INTRODUCTION

Acute lung injury (ALI) is the first stage of acute respiratory distress syndrome (ARDS), which is marked by increased pulmonary vascular permeability, tissue fluid exudation, inflammatory cell accumulation and gaseous exchange dysfunction. Being the front line of defense neutrophils infiltrate the lungs leading to inflammation and damage to alveolar epithelium thus resulting in lung injury[1]. Acute lung injury (ALI) is an injury to the alveolar epithelial cells and vascular endothelial cells caused by a various causes resulting in acute hypoxic respiratory failure[2]. Acute lung injury can lead to sepsis if not controlled, hence, this condition needs to be treated immediately[3].

Despite recent advancements, the specific pathophysiology of lung damage is still unknown. Innovative treatments are needed to enhance the clinical outcomes because the currently available treatments *viz.* antibiotics, steroids etc. have severe adverse side effects that can disrupt other vital body systems[4].

Lipopolysaccharide (LPS) often known as endotoxin, is an important pro-inflammatory glycolipid component of the cell wall of gram-negative bacteria which is one of the leading causes that lead to acute lung injury as reported[1]. The clinical aspects of human and animal ALI are mimicked by LPS-induced ALI in mice, which is a frequently used animal model[3].

Despite substantial advances in understanding the pathophysiology of ALI and current therapeutic options, acute lung injury continues to have a significant fatality rate[4]. Furthermore, present medicinal medications are ineffective and have several adverse effects such as antibiotic resistance, immunosuppression etc. Antibiotic overuse in animals causes antimicrobial resistance (AMR) not only in animals but also in humans, as these antibiotics enter the food chain and cause AMR in humans as well as animals[4].

How to cite this article : Kaur, M., Singh, N.D., Leishangthem, G.D. and Banga, H.S. 2024. Amelioration of lipopolysaccharide induced acute lung injury using chlorogenic acid and baicalein in mice: Clinicopathological study. Indian J. Vet. Pathol., 48(2) : 132-142.

One of the most prevalent polyphenols in the human diet is chlorogenic acid (CGA), which is generated through esterification of caffeic and quinic acids. CGA appears to have a number of biological functions viz anti-bacterial, anti-oxidant and anti-carcinogenic properties according to findings from *in vivo* and *in vitro* investigations[5].

Baicalein (BAC) is a phenolic flavonoid derived from the root of

the *Scutellaria baicalensis* Georgi plant (Lamiaceae family). Baicalein, which has been utilised as a Traditional Chinese medication for numerous inflammatory disorders has been reported to have anti-inflammatory properties[6] and has been reported to be effective in bacterial and viral infections of the respiratory and gastrointestinal tracts as well as cardiovascular disease and inflammation[7].

The present study investigated the combined ameliorative effect of chlorogenic acid and baicalein on lipopolysaccharide induced acute lung injury in murine model.

MATERIALS AND METHODS

Experimental design

The Institutional Animal Ethics Committee (IAEC) of GADVASU, Ludhiana, approved the animal experiment with memo number. IAEC/2021/180-200 dated 13-08-2021. Healthy albino mice (n=30, 4-6 weeks age), were obtained from Disease free small animal house, Central Research Institute (CRI), Kasauli, Himachal Pradesh, India and housed in the small animal house of GADVASU. All mice received humane care. After the acclimatization period of 7 days, the animals were weighed again and 30 male albino mice were divided into five experimental groups with 6 animals each and named according to the challenge and treatment: SHAM/CONTROL, LPS (LPS @ 2 mg/kg bw intratracheal), LPS/CGA/BAC/0.1 (LPS (2 mg/kg bw I/T)/treated with chlorogenic acid @ 0.1 mg/kg + baicalein @ 0.1 mg/kg bw ip) LPS/CGA/BAC/1 (LPS (2 mg/kg bw I/T)/treated with chlorogenic acid @ 1 mg/kg + baicalein @ 1 mg/kg bw ip), LPS/CGA/BAC/10 (LPS (2 mg/kg bw I/T)/treated with chlorogenic acid @ 10 mg/kg + baicalein @ 10 mg/kg bw ip). Mice received a single intratracheal instillation of 50 µl PBS saline containing LPS (2 mg/kg body wt). For experiment, seven days prior to LPS instillation the mice were treated with chlorogenic acid and baicalein intraperitoneally. Mice were sacrificed after 24 hours of LPS instillation by Ketamine (Neon Laboratories Ltd, Mumbai, India) and Xylazine (Indian Immunological Ltd, Hyderabad, Telangana, India) overdose in order to study the LPS-induced acute lung injury in mice and its amelioration with chlorogenic acid (Sigma chemicals) and baicalein (Sigma chemicals). Basically, it was a pre-treatment study. Table 1 shows the experimental design as well as the dose schedule.

Collection of blood and bronchoalveolar lavage fluid (BALF)

At the time of sacrifice, blood was withdrawn from each animal by cardiac puncture and collected in vials containing EDTA @ 1 mg/ml. The hematological estimations, such as hemoglobin concentration (Hb), total leucocyte count (TLC) and differential leukocyte count (DLC) were conducted. BAL was performed in left lungs three times through a tracheal cannula with 0.7 mL of PBS in each animal as described earlier[8]. A tracheal cannula attached to a 1ml syringe was used. Each animal's lavage cells were collected and centrifuged at 1000 rpm for 3 minutes at 4^{O}C. Using a haemocytometer, the total cell count was measured, cell differentiation was assessed for 500 cells and cell pellets were resuspended in fresh PBS before being cytospun onto glass slides and stained with Leishman's stain.

Wet to Dry Lung Weight Ratio

After sacrificing the animals, the lobe of right lung was taken and weight was measured immediately after its excision (wet weight). Then they were dried at 60°C for 72 hours, and weighed again. The wet dry (W/D) lung weight ratio was calculated as an indicator of pulmonary oedema[9].

Estimation of protein and cytokines in bronchoalveolar lavage fluid

Protein in BALF was estimated by using commercially available BCA Protein Assay Kit (Thermo Scientific,USA) as per the manufacturer's protocol.

Histopathological studies

Small representative sections of lungs (about 0.5 mm thickness) from sacrificed animals were taken and preserved in 10% neutral buffered formalin after a

Table 1. Experimental designs and dosage.

Groups	Treatment (1 week)	Number of animals
Gp-I Sham/Control group	Vehicle only	6
Gp-II LPS/Vehicle group	LPS @ 2 mg/kg bw intratracheal	6
Gp-III LPS/CGA/BAC/0.1	LPS (2 mg/kg bw I/T)/treated with pre-treatment *chlorogenic acid* @ 0.1 mg/kg + *baicalein* @ 0.1 mg/kg bw ip	6
Gp-IV LPS/CGA/BAC/1	LPS (2 mg/kg bw I/T)/treated with *chlorogenic acid* @ 1 mg/kg + *baicalein* @ 1 mg/kg bw ip	6
Gp-V LPS/CGA/BAC/10	LPS (2 mg/kg bw I/T)/treated with *chlorogenic acid* @ 10 mg/kg + *baicalein* @ 10 mg/kg bw ip	6

thorough gross examination. Tissues were sliced into narrower slices after adequate fixing for 3-4 days (1.2 mm thickness). The tissues were washed under running water for 7-8 hours, then dehydrated in ethyl alcohol in ascending grades, clarified in benzene, and embedded in paraffin wax. The hand-operated microtome was used to prepare the paraffin blocks and cut the sections at a thickness of 4-5 mm. The paraffin-embedded sections were then mounted on microscope slides and subjected to a series of steps that included deparaffinization in xylene, rehydration in descending grades of ethyl alcohol to running water and colouring with pone or other stains to highlight various cellular and intracellular components.

Routine Haematoxylin and Eosin (H&E) staining

The Haematoxylin and Eosin stain was mostly utilised, which involved staining the nucleus with haematoxylin, which produces a blue colour and then counterstaining with an aqueous or alcoholic solution of eosin, which produces various hues of red, pink, and orange in eosinophilic structures[10].

Lung Injury Assessment

To assess the severity of the lung injury, a semi-quantitative histological index was used. Five sections were randomly selected from each group of mice and five fields were examined per section. The lung histopathological changes were scored on a scale of 0-5 according to the degree of congestion, lung oedema, inflammatory cells infiltration and haemorrhage in lung tissues. Scores of 0 meant that there was no damage to the lung tissues; 1, moderate damage; 2, intermediate damage; 3, widespread damage; and 4, severe damage. The mean ± standard error of the mean (SEM) of the scores were calculated for the lungs of the normal air controls and the overall score of hyperoxia-induced ALI was created based on the sum of all scores[11].

$$\text{Score (x)} = \frac{(20xA) + (14xB) + (7xC) + (7xD) + (2xE)}{\text{Number of field x } 100}$$

Statistical Methods

Data generated from various experiments were presented as Mean ± SE. All the grouped data was evaluated using SPSS/10.0 software. One way analysis of variance (ANOVA) was used to detect differences among groups and the means were compared by LSD post hoc test and a value of $P \leq 0.05$ was taken as significant.

RESULTS

Chlorogenic acid and baicalein attenuated lipopolysaccharide induced hematological alterations

In the present study, the mean value of Hb of LPS group mice (12.00 ± 0.35 g/dl) was significantly decreased as compared to control group (15 ± 0.62 g/dl) and CGA/BAC treated groups. (Table 3 and Fig. 1) However, the mean values of Hb level of CGA and BAC treated groups LPS/CGA/BAC/0.1 (13.86 ± 0.25 g/dl), LPS/CGA/BAC/1 (14.13 ± 0.53 g/dl) and LPS/CGA/BAC/10 (14.26 ± 0.48 g/dl) showed significant increased as compared to LPS group.

Table 2. Parameter and scores to assess lung injury.

S.No.	Parameter	Score Per Field		
		0	1	2
A.	Neutrophils in the alveolar space	None	1-5	>5
B.	Neutrophils in the interstitial space	None	1-5	>5
C.	Hyaline membrane	None	1	>1
D.	Proteinaceous debris filling the air spaces	None	1	>1
E.	Alveolar septal thickening	<2X	2X-4X	>4X

Alteration in Total Leukocyte Count (TLC) and Differential Leukocyte Count (DLC)

The mean TLC values of mice are presented in Table 3 and Fig. 2. The mean TLC value was increased in LPS treated group ($5.05 \pm 0.49 \times 10^3/\mu l$) as compared to control ($4.09 \pm 0.27 \times 10^3$) and CGA/BAC treated groups. Mean TLC value of CGA/BAC treated groups LPS/CGA/BAC/0.1 ($4.59 \pm 0.33 \times 10^3/\mu l$), LPS/CGA/BAC/1 ($4.06 \pm 0.25 \times 10^3/\mu l$), LPS/CGA/BAC/10 ($3.80 \pm 0.36 \times 10^3 \mu l$). LPS/CGA/BAC/10 were near normal and showed significant difference as compared to LPS group.

Additionally, the mean value of difference leukocyte counts namely for mononuclear cells and neutrophils in mice of each five groups, (control, LPS, LPS/CGA/BAC/0.1, LPS/CGA/BAC/1 and LPS/CGA/BAC/10) did not differ significantly from each other. All the mean values of DLC in all the groups were comparable to normal DLC range. The mean DLC values of all groups is presented (Fig. 3 and Fig. 4).

Effect of CGA/BAC on LPS induced pulmonary oedema

Wet-to-dry lung weight ratio

The ratio of wet to dry (W/D) lung weights was calculated as a marker of pulmonary oedema. In the present study, the mean wet/dry (W/D) lung weight ratio of LPS treated mice (6.59 ± 0.93) was significantly higher than the control group (2.83 ± 0.28) and other CGA and BAC treated groups. The treatment groups LPS/CGA/BAC/0.1 (4.74 ± 0.07), LPS/CGA/BAC/1 (4.42 ± 0.14) and LPS/CGA/BAC/10 (3.55 ± 0.12) was significantly less as compared to LPS. This indicated that CGA/BAC led to a dose dependent improvement in the wet/dry (W/D) lung weight ratio and thus, attenuated LPS induced lung oedema. Mean values of wet-to-dry lung weight ratio are presented in Table 4 and Fig. 5.

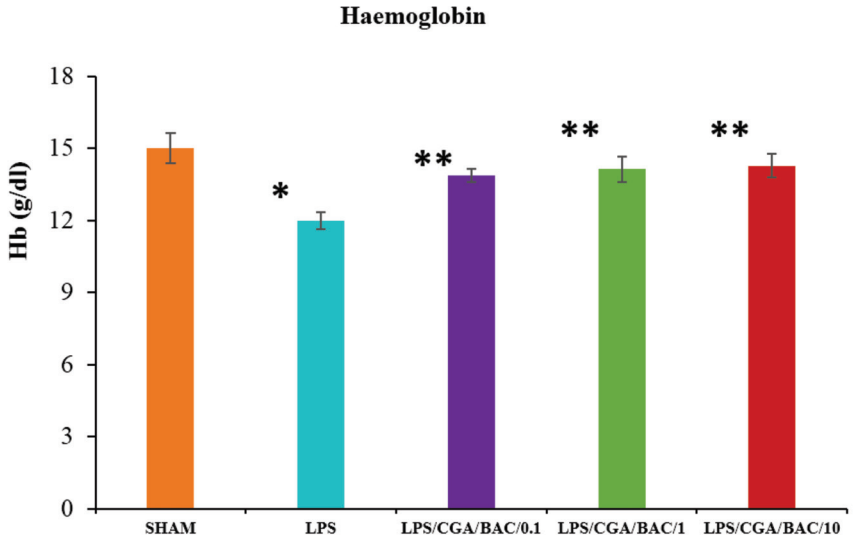

The data are Mean ± SE of six mice for each group. *P<0.05 vs SHAM group. **P<0.05 vs treatment group (LPS/CGA/BAC @ 0.1, 1, 10 mg/kg). **Fig. 1.** Haemoglobin level in different groups.

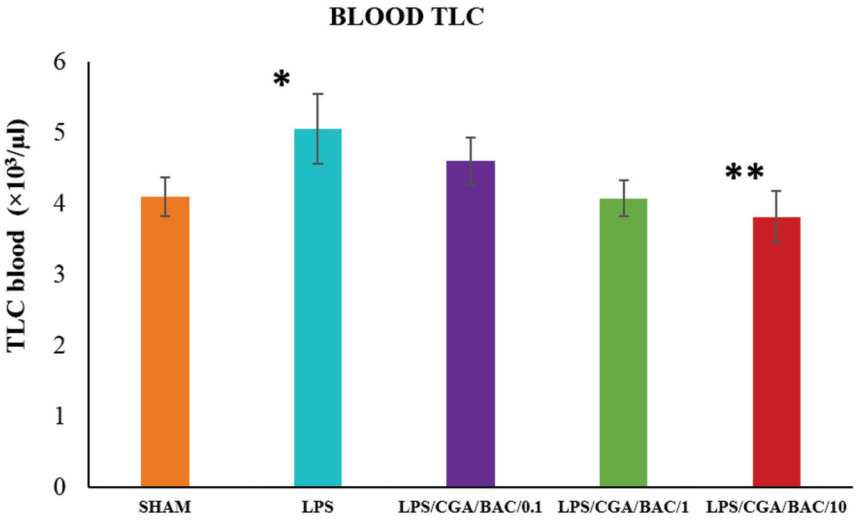

Fig. 2. Total leukocyte concentration (Blood) in different groups.

Table 3. Haemoglobin, TLC and DLC of different groups.

Groups	Hb (g/dL) (Mean ± SE)	TLC (×10³/µl) (Mean ± SE)	Neutrophils	Mononuclear Cells
Gp-I Sham/Control group	15.00 ± 0.62	4.09 ± 0.27	28.33 ± 2.02	71.66 ± 2.02
Gp-II LPS/Vehicle group	12.00 ± 0.35*	5.05 ± 0.49*	43.00 ± 2.86*	57.0 ± 2.86*
Gp-III LPS/CGA/BAC/0.1	13.86 ± 0.25**	4.59 ± 0.33	34.33 ± 3.77**	65.66 ± 3.77**
Gp-IV LPS/CGA/BAC/1	14.13 ± 0.53**	4.06 ± 0.25	32.33 ± 0.95**	67.66 ± 0.95**
Gp-V LPS/CGA/BAC/10	14.26 ± 0.48**	3.80 ± 0.36**	29.33 ± 2.71**	70.66 ± 2.71**

The data are Mean ± SE of six mice for each group.

Protein concentration in bronchoalveolar lavage fluid (BALF)

The values for the mean protein concentration in the BALF of the five mice groups are listed in Table 5 and shown in Fig. 6. The amount of total protein in BALF was calculated in order to estimate vascular permeability. The total protein concentration in BALF of LPS treated mice (962.83 ± 25.17µg/ml) was significantly (p<0.05) higher as compared to that of control (177.83 ± 9.75µg/ml) group and treatment groups. However, LPS/CGA/BAC/0.1 (671.16 ± 31.03), LPS/CGA/BAC/1 (446.00 ± 17.89) and LPS/CGA/BAC/10 (262.33 ± 15.98) showed

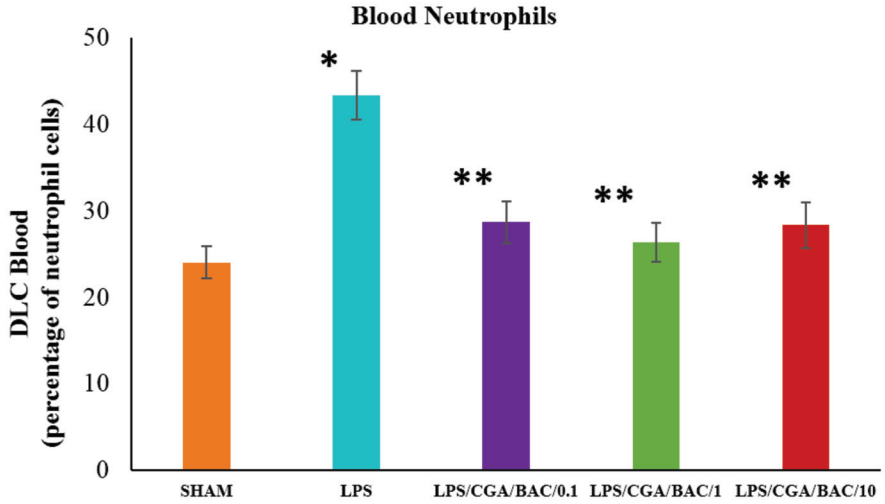

Fig. 3. Differential leukocyte count in Blood (Neutrophils) of different groups.

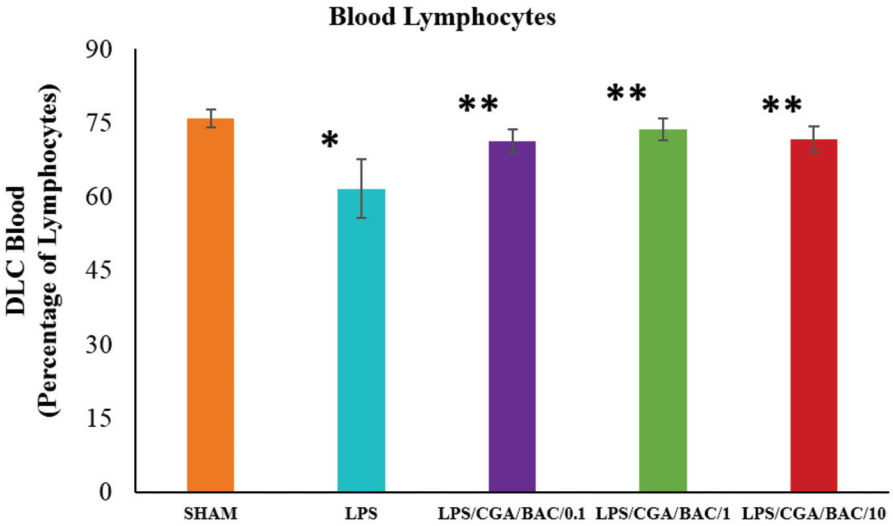

Fig. 4. Differential leukocyte count in Blood (Mononuclear cells) of different groups.

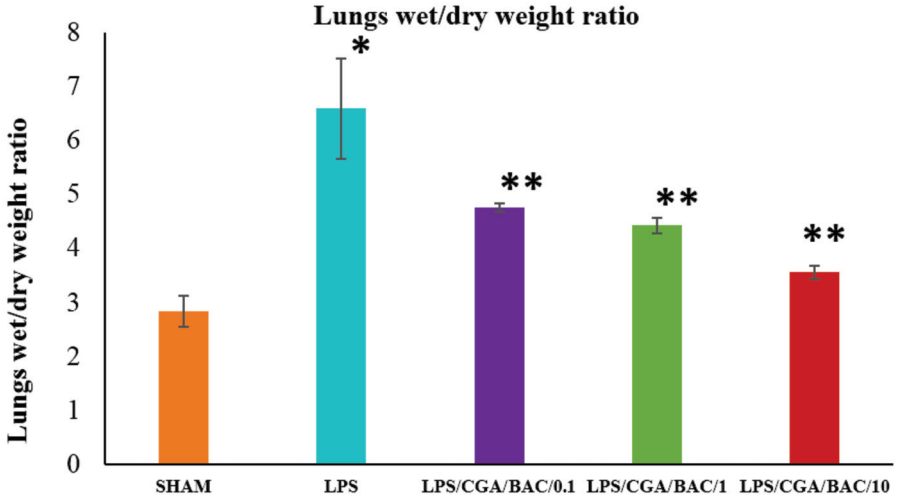

Fig. 5. Wet to dry lung weight ratio in different groups.

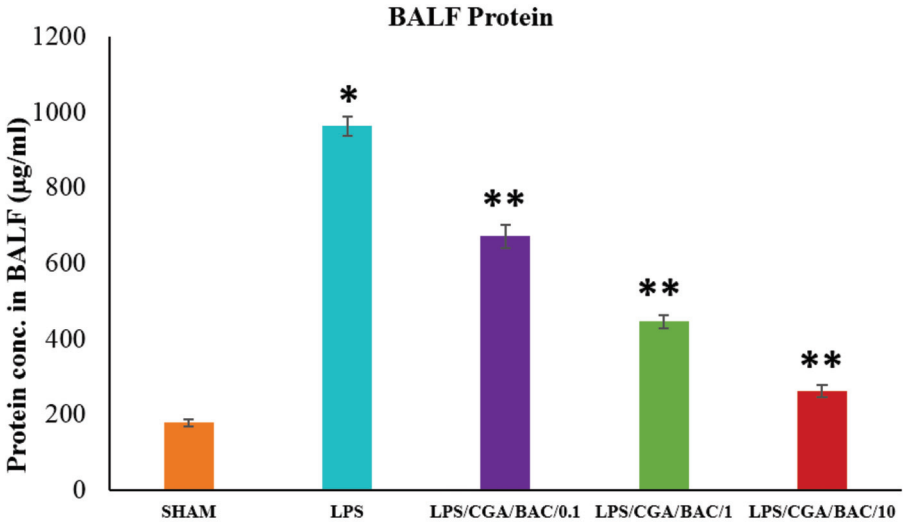

Fig. 6. Protein concentration in BALF of different groups.

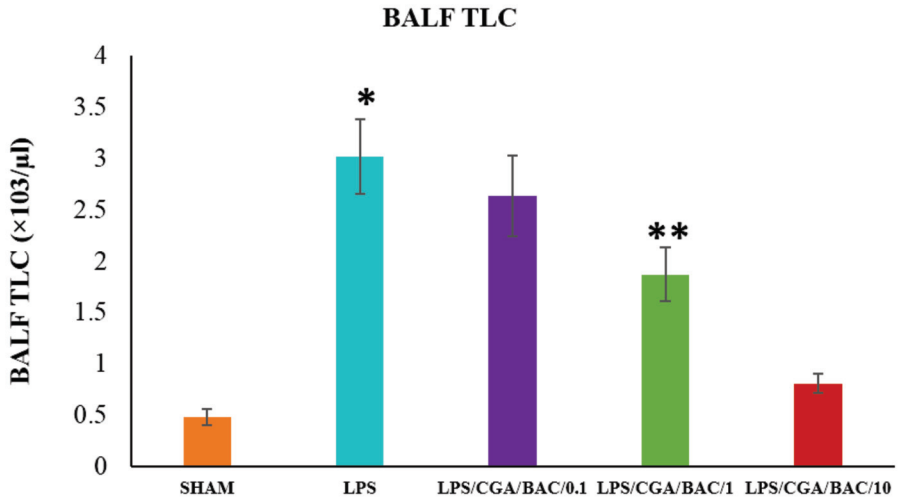

Fig. 7. TLC in BALF of different groups.

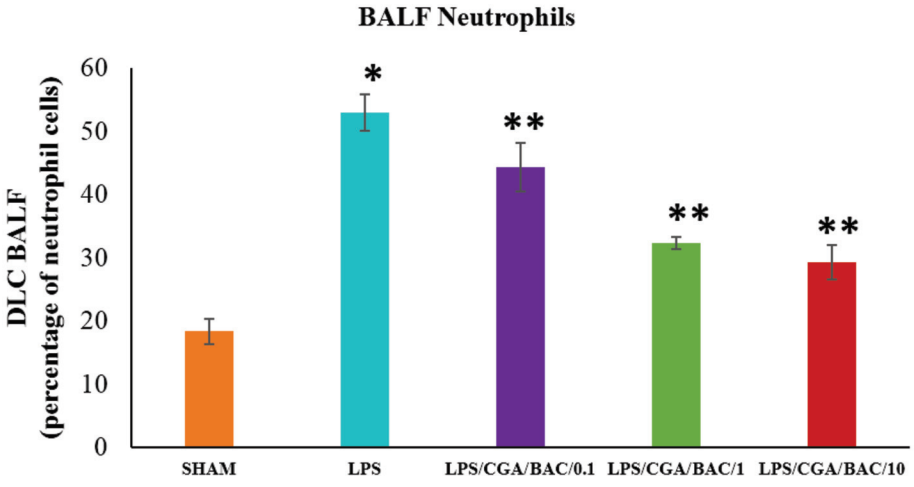

Fig. 8. Neutrophil count in BALF of different groups.

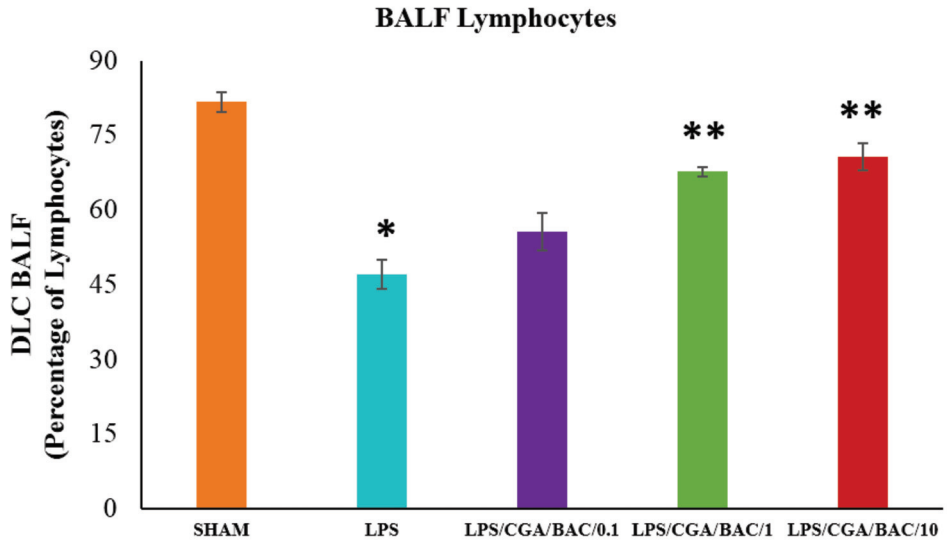

Fig. 9. Mononuclear cell count in BALF of different groups.

significant reduction in total protein concentration as compared to that of LPS group. The improvement was also observed in LPS/CGA/ BAC/1 and LPS/ CGA/BAC/0.1 groups but the decrease in protein was significant in highest dose (10 mg/kg) group. Hence, this showed that CGA and BAC at maximum dose was able to control vascular permeability in lungs.

Bronchoalveolar lavage fluid (BALF) cell count

Alteration in Total Leukocyte Count (TLC) and Differential Leukocyte Count (DLC) in bronchoalveolar lavage fluid (BALF)

Mean values of TLC are presented in Table 6 and Fig. 7 There was significant increase in the mean value of TLC in BALF of LPS (53 ± 2.86) as compared to control (18.33 ± 2.02). In contrast, TLC count of LPS/CGA/BAC/1 (32.33 ± 0.95) and LPS/CGA/BAC/10 (29.33 ± 2.71) group showed marked reduction in the total numbers of inflammatory cells as compared to LPS/CGA/BAC/0.1 (44.33 ± 3.77). However, there was no significant difference in LPS/CGA/BAC/0.1 (2.63 ± 0.38). This proved the anti-inflammatory action of CGA and BAC.

Table 4. Wet-to-dry lung weight ratio in different groups.

Groups	W/D Ratio (Mean ± SE)
Gp-I Sham/Control group	2.83 ± 0.28
Gp-II LPS/Vehicle group	6.59 ± 0.93*
Gp-III LPS/CGA/BAC/0.1	4.74 ± 0.07**
Gp-IV LPS/CGA/BAC/1	4.42 ± 0.14**
Gp-V LPS/CGA/BAC/10	3.55 ± 0.12**

Additionally, Table 6 and Fig. 8 and 9 display the average differential leukocyte counts (DLC) in BALF of various animal groups at various time intervals. When compared to the control group in the current investigation, the majority of the cells found in the BALF belonged to the LPS group.

Effect of chlorogenic acid and baicalein on LPS induced histopathological changes

In contrast to the LPS group, which showed infiltration of inflammatory cells, primarily neutrophils, in alveolar, perivascular and peribronchiolar areas (Fig. 11, 12), which indicated acute phase of inflammation during lung injury, histopathological analysis of the lung section from the control group revealed normal architecture (Fig. 10). These aforementioned alterations were decreased by CGA/BAC and due to their anti-inflammatory and antioxidant properties, the LPS/CGA/BAC/10 group (Fig. 15) showed a decreased infiltration of inflammatory cells in alveolar, perivascular and peribronchiolar locations. LPS/CGA/BAC/0.1 and LPS/CGA/BAC/1 groups shown in (Fig. 13) and (Fig. 14) respectively.

Histopathological scoring

Using an OLYMPUS BX61 microscope, histopathological alterations were captured on camera. Different histopathological parameters of lung injury and their scoring pattern is given in Table 7 and Fig. 16.

The histopathological score was shown to be considerably higher in LPS group mice (0.75 ± 0.01) than in the control (0.05 ± 0.00) group. However, CGA and BAC treated groups LPS/CGA/BAC/0.1 (0.62 ± 0.02), LPS/CGA/BAC/1 (0.55 ± 0.01) and LPS/CGA/BAC/10 (0.43 ± 0.02) showed reduction in histopathological scores but this was significant in middle and highest dose group. The histopathological findings and the ensuing scoring indicated that CGA and BAC were able to ameliorate the acute

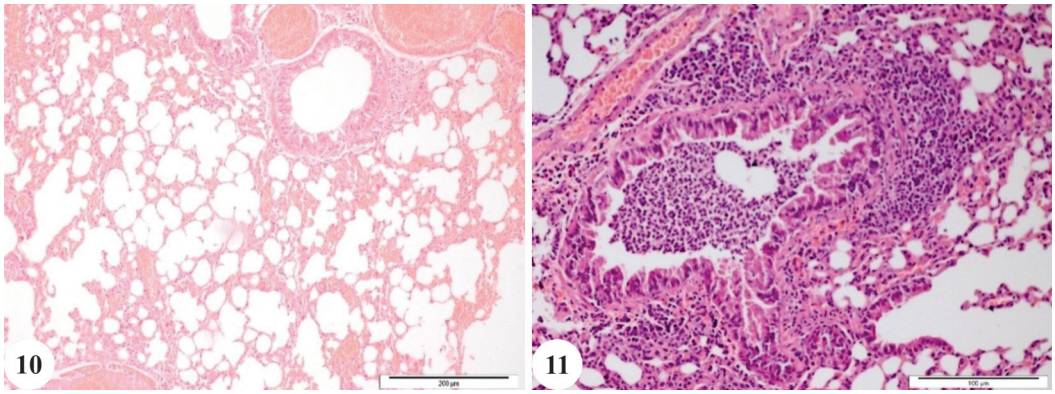

Fig. 10. SHAM/Control: Lung: Normal architecture showing normal histology of bronchiole and normal inter-alveolar septa (H&E X10, Bar = 200 μm); **Fig. 11.** LPS: Lungs: Showing infiltration of neutrophils in bronchial and peribronchial area and thickening of alveolar septa (H&E X20, Bar = 100 μm).

lung injury induced by LPS.

DISCUSSION

Alteration in haemoglobin concentration

One of the polyphenols is chlorogenic acid (CGA), which is present in large quantities in many plant foods like coffee beans and apples. CGA is an interesting substance since it possesses anti-inflammatory, anti-cancer, and anti-oxidant qualities. *In vitro*, CGA inhibits the synthesis of proinflammatory cytokines. *In vivo* research has shown that CGA can prevent tissue damage and inflammation in rheumatoid arthritis, hepatitis, and colitis[12].

Baicalein's antioxidant and anti-inflammatory properties contribute to its protective therapeutic ability. According to our research, baicalein prevents severe lung damage brought on by lipopolysaccharide by boosting antioxidant defences and drastically lowering inflammatory cells and mediators through the Nrf2-mediated HO-1 signalling pathway. This may be the possible reason of improvement of Hb levels in chlorogenic acid and baicalein treated groups[13].

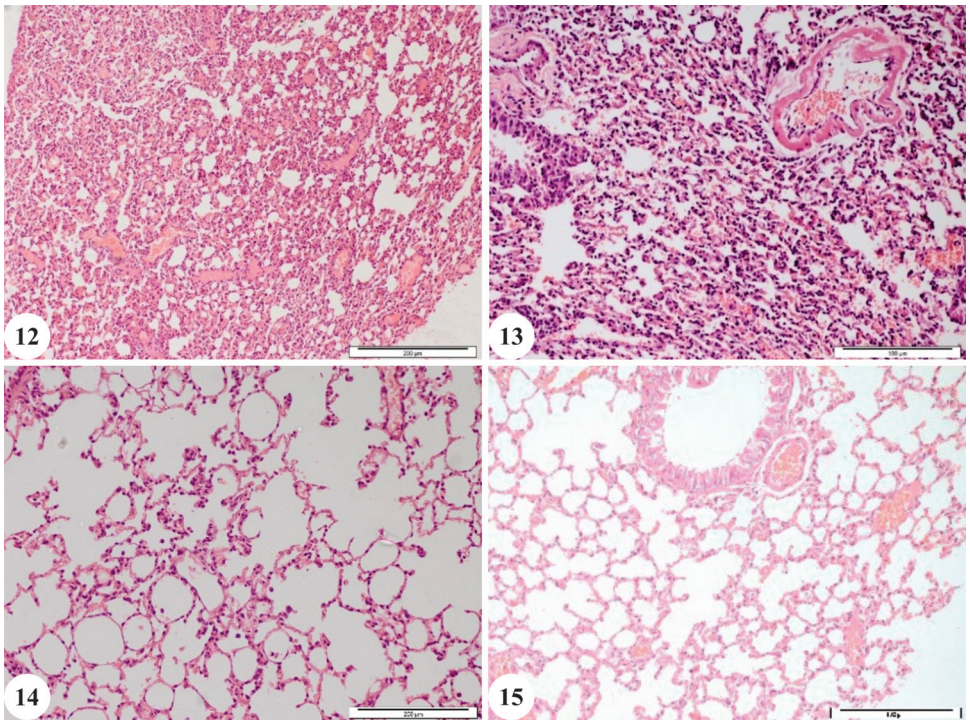

Fig. 12. LPS: Lung: Showing infiltration of neutrophils in alveolar, perivascular and peribronchiolar areas (H&E X10, Bar = 200 μm); **Fig. 13.** LPS/CGA/BAC/0.1: Lung: CGA/BAC treatment showed decreased infiltration of PMN cells wrt LPS (H&E X20, Bar = 100 μm); **Fig. 14.** LPS/CGA/BAC/1: Lung: CGA/BAC treatment moderately reduced the inflammation as evident by decreased neutrophil infiltration (H&E X10, Bar = 200 μm); **Fig. 15.** LPS/CGA/BAC/10: Lung: CGA/BAC treatment significantly reduced inflammation as is evident by near normal architecture and bronchi (H&E X20, Bar = 100 μm).

Table 5. Protein concentration in broncho alveolar lavage fluid (BALF) of different groups.

Groups	Protein concentration in BALF (µg/ml) (Mean ± SE)
Gp-I Sham/Control	177.83 ± 9.75
Gp-II LPS/Vehicle	962.83 ± 25.17*
Gp-III LPS/CGA/BAC/0.1	671.16 ± 31.03**
Gp-IV LPS/CGA/BAC/1	446.00 ± 17.89**
Gp-V LPS/CGA/BAC/10	262.33 ± 15.98**

Data expressed as Mean ± SE and Significant at p≤0.05, *Vs SHAM, **Vs LPS

In the present study, the level of Haemoglobin was also improved in chlorogenic acid and baicalein groups suggesting synergistic effect of both drugs.

Alteration in Total Leukocyte Count (TLC) and Differential Leukocyte Count (DLC)

The value of DLC did not show significant differences in the present study which might be due to the fact that in LPS induced acute lung injury, there is intense inflammatory process in the lungs and this inflammation is mostly limited to the lung with very low levels of inflammatory mediators in the systemic circulation[14].

In the present study, the level of TLC and DLC including number of neutrophils and lymphocytes were also improved in LPS/CGA/BAC/10 as compared to LPS group suggesting synergistic effect of both chlorogenic acid and baicalein.

Protein concentration in bronchoalveolar lavage fluid (BALF)

Lung alveolar-capillary membrane is composed of alveolar capillary barrier. This barrier is composed of microvascular endothelium, interstitium, and alveolar epithelium[15]. Acute respiratory distress syndrome (ARDS) and acute lung injury both have cellular characteristics that are primarily caused by damage to the alveolar epithelium and microvascular endothelium. This damage results in the loss of the integrity of the alveolar capillary membrane and increased vascular permeability, which allows protein-rich oedema fluid to swell up into the air spaces[16].

Chlorogenic acid (CGA), also known as 5-O-caffeoylquinic acid (5-CQA), is one of the most frequent and highly beneficial polyphenolic compounds in the human diet. It is known that AMPK is involved in a number of activities, including oxidative stress, autophagy, apoptosis, and angiogenesis[17]. It has been proposed that CGA modifies the SIRT1/AMPK/PPARGC1A signalling pathway to restore mitochondrial activity in human endothelial cells. Therefore, activation of AMPK by CGA may also open up the downstream signalling pathways, leading to effects including those that combat oxidative stress, prevent apoptosis preserve mitochondrial function, and have anti-inflammatory properties[18].

The production of inflammatory cytokines positively correlates with mitochondrial dysfunction at each corresponding baicalein concentration. Baicalein reduces mitochondrial abnormalities through regulating the expression of the protein Drp1, according to further mRNA analysis. These reprogrammed mitochondria stop reactive oxygen species (ROS) generation after the LPS instillation, which suppresses the transcription of inflammatory cytokines that depend on NF-kB[19].

In the present study, as described chlorogenic acid and baicalein @ 10 mg/kg body weight reduced the vascular permeability and pulmonary oedema, thus ameliorating the damage caused by LPS in the lung injury.

Alteration in Total Leukocyte Count (TLC) and Differential Leukocyte Count (DLC) in bronchoalveolar lavage fluid (BALF)

The current study used the total leucocyte count (TLC) and differential leucocyte count (DLC) in bronchoalveolar lavage (BAL) fluid to evaluate the lung damage induced by LPS. LPS administration to mice resulted in an increase in neutrophils in their BALF, demonstrating that LPS triggered an acute inflammatory response that resulted in ALI and was characterised by the neutrophils infiltration in the lung tissue[20]. According to several earlier studies, LPS is primarily responsible for the acute inflammatory response and LPS-induced ALI is linked to an increase in the inflammatory cells, such as neutrophils in the BALF as a first line of defence[21].

In the present study, chlorogenic acid and baicalein @ 10 mg/kg body weight has led to reduction in total cell count of BALF indicating anti-inflammatory effect and thus ameliorating LPS induced ALI.

Effect of chlorogenic acid and baicalein on LPS induced histopathological changes

According to the lung damage score system developed by which provides scores ranging from 0 to 5, significant and consistent lesions in lung sections of various groups were classified[22]. Pulmonary morphological changes were assessed by this lung injury scoring scale showed reduction of the score in LPS/CGA/BAC treated group when compared to that of LPS group. These findings conclude that CGA and BAC showed anti-inflammatory action on LPS induced lung injury.

Similar to the LPS group, interstitial and alveolar neutrophilic

Table 6. Cell count in BALF of different groups.

Groups	TLC (×10³/µl) (Mean ± SE)	DLC Neutrophil	DLC Mononuclear Cells
Gp-I Sham/Control group	18.33 ± 2.02	24.0 ± 1.86	81.66 ± 2.02
Gp-II LPS/Vehicle group	53 ± 2.86*	43.33 ± 2.76*	47 ± 2.86*
Gp-III LPS/CGA/BAC/0.1	44.33 ± 3.77	28.66 ± 2.40**	55.66 ± 3.77
Gp-IV LPS/CGA/BAC/1	32.33 ± 0.95**	26.33 ± 2.21**	67.66 ± 0.95**
Gp-V LPS/CGA/BAC/10	29.33 ± 2.71	28.33 ± 2.65**	70.66 ± 2.71**

including capillaries wall hyperaemia and significant neutrophil infiltration surrounding the pulmonary veins. Treatment with baicalin reduced the severity of APEC induced lung damage. The histopathological alterations were decreased in chlorogenic acid and baicalein @ 0.1, 1 and 10 mg/kg treated groups as compared to LPS group.

Histopathological scoring

The degree of lung injury was assessed using a semi-quantitative histology approach. Five sections were randomly selected from each group of mice and five fields were examined in each section. The degree of congestion, lung oedema, infiltration of inflammatory cell and haemorrhage in lung tissues were used to assess the lung histological changes on a scale of 0-5. Scores of 0 indicated no lung tissue damage, 1, 2, 3, or 4 indicated mild, moderate, extensive, or severe damage, respectively. The mean and standard error of the mean (SEM) of the scores were calculated based on the sum of all scores[11].

Neutrophils in the interstitial space (A), neutrophils in alveolar space (B), the number of hyaline membranes (C), the number of proteinaceous debris (D) and the extent of thickening of the alveolar septum (E) were all used to grade the severity of lung injury on a scale of 0 to 2[24]. The final injury score was estimated by using formula:

$$\text{Score (x)} = \frac{(20xA) + (14xB) + (7xC) + (7xD) + (2xE)}{\text{Number of field x 100}}$$

infiltration was seen indicating an early onset of the inflammatory process upon lung damage. Increased MPO activity and an increase in neutrophil count in animal BALF which may be related to free radicals produced by LPS further supported this. It's possible that reactive oxygen species are mostly to blame for the cellular damage that results from ALI[23].

H&E staining was done to evaluate the protective impact of baicalin on lung histological alterations. The findings demonstrated that the lung tissues of control group showed no changes or nearly normal. However, the lung tissues of the APEC treatment group showed clearly damaged lung tissues,

Table 7. Lung injury score of different groups.

Groups	Lung Injury Score
Gp-I Sham/Control group	0.05 ± 0.00
Gp-II LPS/Vehicle group	0.75 ± 0.01*
Gp-III LPS/CGA/BAC/0.1	0.62 ± 0.02**
Gp-IV LPS/CGA/BAC/1	0.55 ± 0.01**
Gp-V LPS/CGA/BAC/10	0.43 ± 0.02**

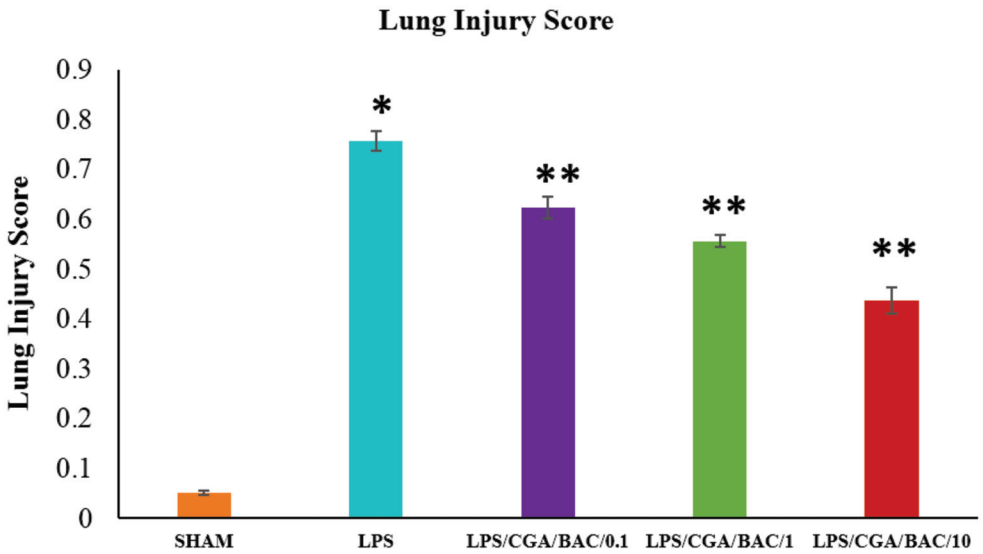

Fig. 16. Lung injury score of different groups.

CONCLUSIONS

Chlorogenic acid and baicalein @ 10 mg/kg body weight was found to be having potential ameliorative effect. Lung injury was ameliorated by chlorogenic acid and baicalein as was evidenced by histopathology. Both chlorogenic acid and baicalein are rate limiting factors in inflammation and prevented inflammation by reducing the recruitment of neutrophils. Chlorogenic acid and baicalein showed synergistic effect in ameliorating the ALI induced by LPS.

ACKNOWLEDGMENT

The authors are thankful to SERB, New Delhi, India for providing financial support.

REFERENCES

1. Lei J, Wei Y, Song P, Li Y, Zhang T, Fen Q and Xu G. 2018. Cordycepin inhibits LPS-induced acute lung injury by inhibiting inflammation and oxidative stress. *Eur J Pharmacol* **818:** 110-114.
2. Burnham EL. 2008. Circulating progenitors in lung injury: a novel therapy for acute respiratory distress syndrome. *ASA* **108:** 354-356.
3. Zhu DZ, Wang YT, Zhuo YL, Zhu KJ, Wang XZ and Liu AJ. 2020. Fucoidan inhibits LPS-induced acute lung injury in mice through regulating GSK-3β-Nrf2 signaling pathway. *Arch Pharm Res* **43:** 646-654.
4. Aidara-Kane A. 2012. Containment of antimicrobial resistance due to use of antimicrobial agents in animals intended for food: WHO perspective. *Rev Sci Tech* **31:** 277-287.
5. Kono Y, Kashine S, Yoneyama T, Sakamoto Y, Matsui Y and Shibata H. 1998. Iron chelation by chlorogenic acid as a natural antioxidant. *Biosci Biotechnol Biochem* **62:** 22-27.
6. Tsai CL, Lin YC, Wang HM and Chou TC. 2014. Baicalein, an active component of Scutellariabaicalensis, protects against lipopolysaccharide-induced acute lung injury in rats. *J Ethnopharmacol* **153:** 197-206.
7. Shang X, He X, He X, Li M, Zhang R, Fan P and Jia Z. 2010. The genus Scutellaria an ethnopharmacological and phytochemical review. *J Ethnopharmacol* **128:** 279-313.
8. Song JA, Yang HS, Lee J, Kwon S, Jung KJ, Heo JD and Lee K. 2010. Standardization of bronchoalveolar lavage method based on suction frequency number and lavage fraction number using rats. *Toxicol Res* **26:** 203-208.
9. Matsuyama H, Amaya F, Hashimoto S, Ueno H, Beppu S, Mizuta M and Hashimoto S. 2008. Acute lung inflammation and ventilator-induced lung injury caused by ATP via the P2Y receptors: an experimental study. *Respir Res* **9:** 1-13.
10. Kiernan JA. 1999. Histological and histochemical methods: theory and practice. *Shock* **12:** 479.
11. Tian Y, Li H, Qiu T, Dai J, Zhang Y, Chen J and Cai H. 2019. Loss of PTEN induces lung fibrosis via alveolar epithelial cell senescence depending on NF-κB activation. *Aging Cell* **18:** e12858.
12. Ohkawara T, Takeda H and Nishihira J. 2017. Protective effect of chlorogenic acid on the inflammatory damage of pancreas and lung in mice with l-arginine-induced pancreatitis. *Life Sci* **190:** 91-96.
13. Meng X, Kawahara KI, Matsushita K, Nawa Y, Shrestha B, Kikuchi K and Maruyama I. 2009. Attenuation of LPS-induced iNOS expression by 1, 5-anhydro-D-fructose. *Biochem Biophys Res Commun* **387:** 42-46.
14. Pugin J, Verghese G, Widmer MC and Matthay MA. 1999. The alveolar space is the site of intense inflammatory and profibrotic reactions in the early phase of acute respiratory distress syndrome. *Crit Care Med* **27:** 304-312.
15. Elizabeth RJ and Matthay MA. 2010. Acute Lung Injury: Epidemiology, Pathogenesis, and Treatment. *J Aerosol Med Pulm Drug Deliv* **23:** 243-252.
16. Ware LB and Matthay MA. 2000. The acute respiratory distress syndrome. *N Engl J Med* **342:** 1334-1349.
17. Jiang C, Zhong R, Zhang J, Wang X, Ding G, Xiao W and Ma S. 2019. Reduning injection ameliorates paraquat-induced acute lung injury by regulating AMPK/MAPK/NF-κB signaling. *J Cell Biochem* **120:** 12713-12723.
18. Tsai CL, Lin YC, Wang HM and Chou TC. 2014. Baicalein, an active component of *Scutellaria baicalensis*, protects against lipopolysaccharide-induced acute lung injury in rats. *J Ethnopharmacol* **153:** 197-206.
19. Lu H, Tian Z, Cui Y, Liu Z and Ma X. 2020. Chlorogenic acid: A comprehensive review of the dietary sources, processing effects, bioavailability, beneficial properties, mechanisms of action, and future directions. *Comp Rev Food Sci Food Saf* **19:** 3130-3158.
20. Chang HY, Chen YC, Lin JG, Lin IH, Huang HF, Yeh CC and Huang GJ. 2018. Asatone prevents acute lung injury by reducing expressions of NF-κB, MAPK and inflammatory cytokines. *Am J Chinese Med* **46:** 651-671.
21. Abdelmageed ME, El-Awady MS and Suddek GM. 2016. Apocynin ameliorates endotoxin-induced acute lung injury in rats. *International Immunopharmacology* **30:** 163-170.
22. Matute-Bello G, Frevert CW and Martin TR. 2008. Animal models of acute lung injury. *Am J Physiol Lung Cell Mol Physiol* **295:** L379-L399.
23. Pittet JF, Mackersie RC, Martin TR and Matthay MA. 1997. Biological markers of acute lung injury: prognostic and pathogenetic significance. *Am J Respir Crit Care Med* **155:** 1187-1205.
24. Patel BV, Wilson MR and Takata M. 2012. Resolution of acute lung injury and inflammation: a translational mouse model. *Eur Respir J* **39:** 1162-1170.

Indian J. Vet. Pathol., 48(2) : 143-158, 2024: DOI: 10.5958/0973-970X.2024.00024.0

RESEARCH ARTICLE

Antioxidant role of chlorogenic acid and baicalein in lipopolysaccharide induced acute lung injury in mice

Mandeep Kaur, Nittin Dev Singh*, Geeta Devi Leishangthem and Harmanjit Singh Banga
Department of Veterinary Pathology, College of Veterinary Science, Guru Angad Dev Veterinary and Animal Sciences University, Ludhiana, Punjab, India

Address for Correspondence
Nittin Dev Singh, Professor, Department of Veterinary Pathology, College of Veterinary Science, Guru Angad Dev Veterinary and Animal Sciences University, Ludhiana, Punjab, India, E-mail: drndsingh@gmail.com

Received: 27.9.2023; Accepted: 21.11.2023

ABSTRACT

Without an adequate current therapeutic plan, lung injury is the leading cause of morbidity and mortality in both humans and animals. Acute lung injury (ALI) is mostly caused by lipopolysaccharide (LPS), which is a pro-inflammatory glycolipid component of cell wall of gram-negative bacteria. Chlorogenic acid (CGA) is frequent polyphenol in the human diet with multiple of biological qualities including anti-bacterial, anti-oxidant and anti-carcinogenic capabilities. Baicalein (BAC) is a phenolic flavonoid with anti-inflammatory properties. Thus, the important objective of this study is to investigate the combined amelioratory effect of CGA and BAC on LPS induced ALI Albino mice were divided into five groups named as SHAM/CONTROL, LPS (2 mg/kg body weight), LPS/CGA/BAC/0.1, LPS/CGA/BAC/1 and LPS/CGA/BAC/10 and treatment group mice received intraperitoneal doses of CGA and BAC at three different concentrations (0.1, 1 and 10 mg/kg) seven days prior to the instillation of LPS. In this one-week pre-treatment experiment, mice from each group were scarified after 24 hours. Lungs and BALF were collected. The various biochemical assays (MPO, LPO, NO, SOD and CAT activity), cytokine estimation (TNF-α and IL-6) and immunostaining (i-NOS, Nitrotyrosine and caspase-3) for estimation of inflammation and oxidative stress. CGA and BAC alleviated oxidative stress and inflammation by reducing the production of the inflammatory cytokines. Thus, BAC and CGA had a synergistic effect.

Keywords: Acute lung injury, baicalein, chlorogenic acid, lipopolysaccharide, mice

INTRODUTION

To keep up with other technologically advanced nations, our nation is in need of industrialization. Although extensive industrialization has increased the global economy but it has also seriously harmed the environment. Five significant issues of today's world include pollution, water scarcity, deforestation, climate change and population growth. All of these variables are having a detrimental effect on both human and animal health since they introduce several toxic and harmful chemicals into the air, we breath. Lungs may suffer the most serious damage from prolonged exposure to pollutants by inhalation, which can cause a variety of acute and chronic respiratory conditions that might eventually result in respiratory failure.

Acute lung injury is more severe form of acute respiratory distress syndrome (ARDS) on the basis of their time of course[1]. The acute lung injury may be caused due to direct and indirect causes. Direct causes include - pneumonia, aspiration of gastric content, lung transplant etc. Indirect causes- sepsis, severe trauma, shock, multiple organ failure etc[2].

Lipopolysaccharide (LPS) is a pro-inflammatory glycolipid component of cell wall of gram-negative bacteria. LPS is closely linked to ARDS and lung damage. LPS causes apoptosis and the release of cytokines in type II alveolar epithelial cells. ALI with neutrophil emigration caused by LPS instillation intratracheally in mice[3].

Chlorogenic acid (CGA) is produced by esterification of caffeic and quinic acids which is one of the most common dietary polyphenols in humans. According to results from both in vivo and in vitro studies, CGA seems to have a variety of biological roles, including anti-bacterial, anti-oxidant and anti-carcinogenic effects[4]. In addition to having anti-inflammatory effects, CGA also suppresses the generation of cytokines and has antipyretic, analgesic and antifungal effects[5].

During course of advancement in treatment strategies, the use of antibiotic has tremendously increased. All these therapeutic management strategies provide temporary effect and marginal safety with plenty of adverse effects like antibiotic resistance, immunosuppression etc. To avoid such adverse effects on health, there is an urgent need to develop a novel strategy for the

How to cite this article : Kaur, M., Singh, N.D., Leishangthem, G.D. and Banga, H.S. 2024. Antioxidant role of chlorogenic acid and baicalein in lipopolysaccharide induced acute lung injury in mice. Indian J. Vet. Pathol., 48(2) : 143-158.

treatment of not only ALI but also for other inflammatory conditions.

The sole and singular method when it comes to treatment that has little to no adverse effects is the usage of herbal remedies. A plant or component of a plant that is used for its flavour, aroma or medicinal qualities is known as herb. Herbal remedies are used by people to attempt and keep or boost their immunity. Therefore, focusing on the potential sites of inflammatory processes may result in novel ALI preventative and therapeutic approaches. *Scutellariabaicalensis Georgi*, a member of the Lamiaceae family of plants, produces baicalein (BAC) which is a phenolic flavonoid and is present in its roots. *Scutellariabaicalensis Georgi* is used to make Huang Qin which is one of the famous traditional Chinese medicines. Baicalein used to treat many inflammatory conditions because of its anti-inflammatory properties[6]. It has also been shown to be effective against inflammation, cardiovascular disease, respiratory problems and intestinal viral and bacterial infections[7]. The current goal is to study the ameliorative role of CGA and BAC in LPS induced ALI in mice.

MATERIALS AND METHODS

The proposed research project was carried out at the Department of Veterinary Pathology, College of Veterinary Science, Guru Angad Dev Veterinary and Animal Sciences University (GADVASU), Ludhiana and was titled "Antioxidant role of chlorogenic acid and baicalein in lipopolysaccharide induced acute lung injury in mice." The Institutional Animal Ethics Committee (IAEC) of GADVASU, Ludhiana, approved the animal experiment with memo number IAEC/2021/180-200 dated 13-08-2021.

Procurement of experimental animals

The healthy albino mice of about 4-6 week of age (n=30) were procured from Central Research Institute (CRI), Kasauli (HP).

Maintenance of experiment animals

The mice were kept in separate laboratory cages and fed standard laboratory animal feed for mice from Ashirwad feeds in Chandigarh. The mice were fed and given water on an *ad libitum* basis.

Research Methodology and Experimental Design Animal

The animals were weighed again after a seven-day acclimation period. 30 albino mice were randomly divided into five experimental groups, each containing six albino mice in order to achieve roughly comparable initial mean group body weights in each group and the groups were named after the inoculation/treatment/dose. Mice received a single intra-tracheal instillation of PBS containing lipopolysaccharide @ 2 mg/kg bw (Sigma chemicals) in a volume of 50µl of PBS.

For experiment, seven days prior to LPS instillation the mice were treated with chlorogenic acid and baicalein intraperitoneally. In this one-week experiment, mice were sacrificed after 24 hours of LPS instillation by Ketamine (Neon Laboratories Ltd, Mumbai, India) and Xylazine (Indian Immunological Ltd, Hyderabad, Telangana, India) overdose in order to study the LPS-induced acute lung injury in mice and its amelioration with chlorogenic acid (Sigma chemicals) and baicalein (Sigma chemicals). Basically, it was a pre-treatment study.

Estimation of Myeloperoxidase (MPO) activity

MPO activity in lungs tissue was assessed using o-dianisidine method and procedure is explained as below:

1. Preparation of Hexadecyl-Trimethyl-Ammonium Bromide (HTAB) buffer. This tissue lysis buffer was freshly prepared by dissolving 0.5g of HTAB in 100ml of phosphate buffer (PH-6).
2. The frozen lungs tissues samples (10mg) weighed and homogenized in the Eppendorf tube containing 200µl of HTAB lysis buffer at $4^{O}C$. The supernatant was collected and proceeded for MPO activity assay.
3. Preparation of 1% Hydrogen Peroxide: this electron donor solution was freshly prepared by dissolving 20µl of 30% H_2O_2 in 580µl of distilled water.

Table 1. Experimental designs and dosage.

Groups	Treatment (1 week)	Number of animals
Gp-I Sham/Control group	Vehicle only	6
Gp-II LPS/Vehicle group	LPS @ 2 mg/kg bw intratracheal	6
Gp-III LPS/CGA/BAC/0.1	LPS (2 mg/kg bw I/T)/treated with pre-treatment *chlorogenic acid* @ 0.1 mg/kg + *baicalein* @ 0.1 mg/kg bw ip	6
Gp-IV LPS/CGA/BAC/1	LPS (2 mg/kg bw I/T)/treated with *chlorogenic acid* @ 1 mg/kg + *baicalein* @ 1 mg/kg bw ip	6
Gp-V LPS/CGA/BAC/10	LPS (2 mg/kg bw I/T)/treated with *chlorogenic acid* @ 10 mg/kg + *baicalein* @ 10 mg/kg bw ip	6

4. Preparation of Dianisidine substrate: Dianisidine substrate was freshly prepared. For 10 tissue samples, 10 mg 0-Dianisidine dihydrochloride (Sigma) was dissolved in solution (45 ml distilled water + 5 ml potassium phosphate buffer), mixed and stored at room temperature.
5. On a pre-chilled 96 well ELISA plate, supernatant tissue homogenates (10µl) were loaded to each of three well (triplicate). For blank, 10µl of HTAB lysis buffer was used instead of tissue supernatant.
6. In each well, 200µl of active dianisidine substrate (10 ml Dianisidine substrate supplemented with 10µl of 1% H_2O_2) was added to each sample well. Immediately, optical density (absorbance A450) was measured at 450 nm using spectrometer every 30 seconds for 5 minutes at 37^{O}C.
7. MPO activity was estimated taking average of the triplicate results for different time points, finding the difference in absorbance [ΔA450 (t30-t0)] from time 0s to 30s and the difference [ΔA450 (t60-t30)] from time 30s to 60s and went upto 5minutes time point. Then, average of these differences ΔA450s were taken to produce the final Δ450 change.
8. MPO Activity was calculated as: MPO activity = A450 ÷ 0.5 ÷ 0.0113 ÷ 0.05 [where 0.0113 is MPO constant; 0.5 is for time intervals (30 seconds, or 0.5 minutes), and 0.05 is dilution factor of sample: HTAB lysis buffer (10mg of tissue per 200µl)]. The MPO activity was expressed as U/g tissue.

Oxidative stress related biochemical parameters

A Double Beam UV-VIS spectrophotometer was used to calculate several oxidative stress-related biochemical parameters in the lungs of mice. 100 mg of fresh lung tissue was homogenised in 1:10 volumes of ice-cold PBS (pH-7.4). The homogenates were centrifuged at 10,000 rpm for 10 minutes. The supernatants obtained were used to calculate the following:

Lipid peroxidation (LPO)

Lipid peroxidation in tissue homogenate was performed by the method described below:

Principle

Malondialdehyde (MDA), an end product of lipid peroxidation reacts with thiobarbituric acid (TBA) and yields a pink coloured complex exhibiting an absorption maximum at 532 nm.

Procedure

To 1 ml of 10% tissue homogenate, 1 ml of 40 mM hydrogen peroxide and 0.1ml of sodium azide were added in the test tube and incubated at 37^{O}C for 1 hour. After incubation, the total volume was made to 4 ml with PBS in each tube and 2 ml of ice chilled trichloroacetic acid (TCA) was added to stop the reaction. The tubes were centrifuged at 3000 rpm for 15 minutes. To 4 ml of supernatant, 1 ml of TBA was added and tubes were kept in boiling water bath for 15 minutes. Finally, the optical density was measured for 15 minutes. Finally, the optical density at 532 nm against a blank (no H_2O_2 was added) after cooling the contents of tubes to room temperature. The blank was prepared using 1ml of PBS. For tissues the amount of LPO was expressed as nanomoles of MDA produced/g protein of tissue. The absorbance was measured at 535 nm and expressed as nanomoles of MDA formed per g of wet tissue.

LPO (nm MDA gm^{-1}) =

$$\frac{\text{OD of test}}{\text{EC}} \times \frac{\text{Total volume of reaction mixture}}{\text{Amount of sample taken}} \times 10^9 \times \text{DF} \times \text{time of incubation}$$

Where OD: Optical Density; EC: Extinction Coefficient (1.56/M/cm)

Nitric Oxide (NO)

Nitrite (NO_2^-), a stable oxidation product of NO, was analysed using 10% dilution by the Griess reagent (0.1% N- (1-naphthyl) ethylenediamine dihydrochloride (NEED) and 1% sulphanilamide) as described in the following method[8].

Procedure

150 µl aliquot of 10% tissue homogenate/sodium citrate ($NaNO_2$) standard was incubated with 75µl of 1.0% sulphanilamide solution for 5-10 minutes at room temperature, protected from light and, 1% sulphanilamide solution was added with gentle mixing each time in the wells of a 96 well microplate, in triplicate. After 10 minutes of incubation, the absorbance was measured at 545 nm against a blank containing no biological sample. Concentration of nitrite (µM/L) was calculated from standard curve and results were expressed as nanomoles of nitrite released into the medium per gram wet tissues.

Concentration of nitrite =

$$\frac{\text{Concentration derived from standard curve (µmoles/L)} \times \text{DF}}{\text{(nm/g wet tissue)}}$$

Where DF - Dilution Factor

Estimation of catalase

Catalase is an enzyme found in almost all living organisms doing aerobics respiration and protects the cell from oxidative damage by ROS. It catalyses the decomposition of hydrogen peroxide to water and oxygen.

$$2\,H_2O_2 \rightarrow 2\,H_2O + O_2$$

Procedure

The sample was incubated in 1.0 ml substrate (hydrogen peroxide (65 mmol/ml) in sodium-potassium phosphate buffer (60 mmol/l, pH 7.4) at 37°C for three

minutes. The reaction was stopped with ammonium molybdate. Absorbance of was read at 374 nm against the blank[9].

Superoxide dismutase (SOD)

The activity of superoxide dismutase (SOD) of 10% tissue supernatant was determined using the method described below[10]. Pyragallol auto-oxidation generates superoxide and SOD from tissue sample inhibits the superoxide dependent reduction of the tetrazolium dye MTT [3-(4-5 dimethyl thiazol 2-xl) 2,5 diphenyl tetrazolium bromide], to formazan, which was measured at 570 nm (Multiskan Go ELISA reader, Thermoscientific).

Procedure

Three cuvettes designated as sample, control and blank were taken. To each cuvette 0.65 ml of PBS followed by 30 µl of MTT were added. To test cuvette 10 µl of tissue homogenate was added. After that 75 µl of pyragallol was added to all three cuvettes and incubated for 5 minutes at room temperature. After incubation 0.75 ml of DMSO were added to stop the reaction. Finally, 10 µl of tissue homogenate was added to control cuvette.

The absorbance was read at 570 nm against blank containing distilled water.

Collection of Bronchoalveolar lavage fluid (BALF)

Mice were euthanized, then their lungs were split into left and right lungs and BALF was collected[11]. Lavage was performed three times with a tracheal cannula attached to a 1 ml syringe (0.7 ml PBS for the left lung). Each animal's lavage cells were collected and centrifuged at 1000 rpm for 3 minutes at 4^{O}C. Using a haemocytometer, the total cell count was measured and cell pellets were resuspended in fresh PBS before being cytospun onto glass slides and stained with Leishman's stain. The remaining supernatant was collected and stored at -80^{O}C for TNF-α and IL-6 measurement.

Estimation of cytokine

Tumour necrosis factor alpha (TNF-α) and interleu-kin-6 (IL-6) in BALF in lung homogenates were estimated using commercially available kits.

Tumour necrosis factor alpha (TNF-α)

It is a potent multifunctional cytokine which can exert regulatory and cytotoxic effects on a wide range of normal lymphoid, non-lymphoid cells and tumour cells. 100 µl of standards and samples were added into each well of the plate (Mouse TNF-α ELISA Kit, Krishgen Biosystems). Six 2-fold serial dilutions of the 2000 pg/ml top standard were done within plate. Hence, concentration of standard was 2000 pg/ml, 1000 pg/ml, 500 pg/ml, 250 pg/ml, 125 pg/ml, 62.5 pg/ml and 31.3 pg/ml. plate was sealed and incubated for 2 hours at room temperature. Plate was aspirated and washed 4 times with wash buffer (1X), then residual buffer was blotted by tapping plate upside down on the absorbent paper. After that 100 µl of diluted detection antibody was added to each well and incubated for 1 hour at room temperature. Plate was washed 4 times with wash buffer (1X). 100 µl of diluted Streptavidin-HRP was added to each well; plate was sealed and incubated for 30 minutes at room temperature. Plate was again washed 4 times with wash buffer (1X). To minimize the background in the final wash, wells were soaked in wash buffer for 30 seconds to 1 minutes for each wash. 100µl of tetramethylbenzidine (TMB) substrate solution was added and incubated in the dark for 15 minutes. Positive wells turned bluish in colour. Stop solution @100 µl was added in each well to stop reaction. After this step positive wells turned yellow from blue. The absorbance was read at 450 nm (infinite M200, NanoQuat Autoanalyzer).

Interleukin-6 (IL-6)

IL-6 is a pleiotropic cytokine and functions as a proinflammatory factor as well as a profibrotic factor in lung injury[12]. For assessment of IL-6, 100µl of standards and samples were added into each well of the plate (Mouse IL-6 ELISA Kit, KRISHGEN Biosystems). Two-fold serial dilutions of the 1000 pg/ml top standard were done within plate. Hence, concentration of standard was 1000 pg/ml, 500 pg/ml, 250 pg/ml, 125 pg/ml, 62.5 pg/ml, 31.3 pg/ml and 15.63 pg/ml. Plate was sealed and incubated for 2 hours at room temperature. Plate was aspirated and washed 4 times with wash buffer (1X), then residual buffer was blotted by tapping plate upside down on absorbent paper. After that 100 µl of diluted detection antibody was added to each well and incubated for 1 hour at room temperature. Plate was washed 4 times with wash buffer (1X). 100 µl of diluted Streptavidin-HRP was added to each well, plate was sealed and incubated for 30 minutes at room temperature. Plate was again washed 4 times with wash buffer (1X). To minimize the background in the final wash, wells were soaked in wash buffer for 30 seconds to 1 minutes for each wash. 100 µl of tetramethylbenzidine (TMB) substrate solution was added and incubated in the dark for 15 minutes. Positive wells turned bluish in colour. Stop solution @ 100 µl was added in each well to stop reaction. After this step positive wells turned yellow from blue. The absorbance was read at 450 nm (infinite M200, NanoQuat Autoanalyzer).

Immunohistochemistry (IHC)

The sections were cut at 4-5 thickness with the manually powered microtome after the paraffin blocks were prepared.

Table 2. Different types of primary antibodies used and their dilutions.

S.No.	Name of Primary Antibody	Name of Company	Dilutions
1.	i-NOS	Abcam	1:250
2.	Caspase-3	Abcam	1:250
3.	Nitrotyrosine	Abcam	1:250

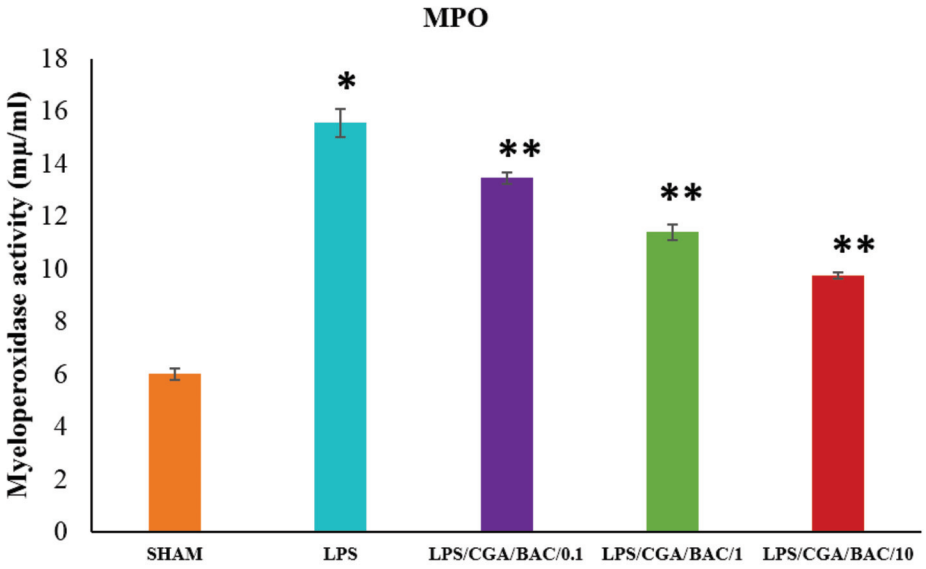

The data are expressed as Mean ± SE of six mice for each group. *P<0.05 (vs control group) **P<0.05 (vs LPS group). **Fig. 1.** Myeloperoxidase (MPO) activity in lung homogenates of different groups.

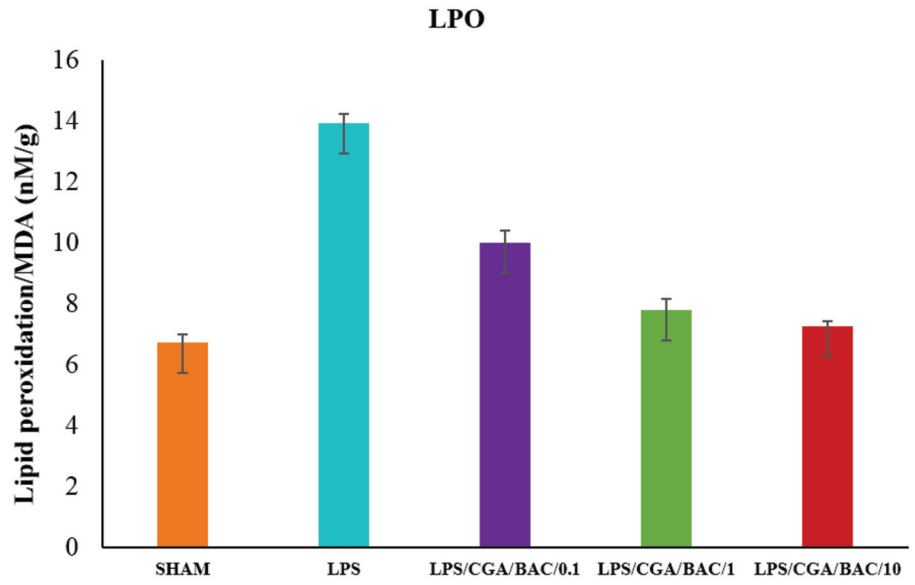

Fig. 2. Lipid peroxidation level in lung homogenates of different groups.

Table 3. Myeloperoxidase activity in different groups.

Groups	MPO (Unit/mg of tissue)
Gp-I Sham/Control group	6.00 ± 0.22
Gp-II LPS/Vehicle group	15.55 ± 0.53*
Gp-III LPS/CGA/BAC/0.1	13.45 ± 0.22**
Gp-IV LPS/CGA/BAC/1	11.38 ± 0.30**
Gp-V LPS/CGA/BAC/10	9.73 ± 0.10**

The paraffin embedded sections were then glued to poly-L-lysine coated microscope slides in duplicate and deparaffinized with two changes of xylene for 5 minutes each, rehydrated with descending grades of ethyl alcohol (3 minutes each) and washed in distilled water.

The slides were cleaned in deionized water and placed in a microwave-safe plastic staining jar with antigen retrieval solution citrate buffer (10mM citrate, 0.05% Tween twenty, pH-6.0) for 2 minutes, 80 minutes and 7 minutes respectively. The slides were allowed to cool to room temperature after retrieval. For 5 minutes, the slides were washed in PBS + Tween twenty. After then, the tissue sections were ringed with a hydrophobic pen (BioGenex Laboratories Inc., San Ramon, California, USA).

The activity of non-specific proteins was blocked by using

normal horse serum (Vector, ImmunoPRESS reagent kit, Burlingame, CA, USA) for 30 minutes at room temperature in a humidified chamber. As negative control, sections were incubated with horse serum instead of primary antibody. Thereafter, the sections with positive control were incubated overnight with re-constituted primary antibody with proper dilutions at 4^{O}C in a humidified chamber. Next day the sections were given three washings with PBS for 5 minutes each, followed by quenching of endogenous peroxidase activity by dipping the tissue sections in 3% H_2O_2 in PBS for 10 minutes at room temperature in a humidified chamber and after that tissue sections were washed two times with PBS for 5 minutes each. It was then followed by 30 minutes incubation of slides with horseradish peroxidase conjugated polyclonal secondary antibody (Vector, ImmunoPRESS reagent peroxidase kit, Burlingame, USA) to primary antibody and these slides were subsequently rinsed twice in PBS for five minutes each. The antigen antibody reaction was visualized by using freshly prepared 3, 3-diaminobenzidine (DAB) solution (Vector, Immpact peroxidase substrate kit, Burlingame, CA, USA) under microscope. Sections were later on washed with distilled water for 5 minutes and counterstained with Gill's haematoxylin (Merck, Germany) for 30 seconds and washed in running tap water for 5 minutes. Finally, the slides were dehydrated in ascending grades of alcohol, cleared in xylene, mounted with DPX and examined under microscope (BX 61, Olympus Corporation and Japan).

Statistical analyses

Data generated from various experiments were presented as Mean ± SE. All the grouped data was evaluated using SPSS/10.0 software one-way analysis of variance (ANOVA) was used to detect differences among groups and the means were compared by Dunnett post hoc test and a value of $P \leq 0.05$ was taken as significant.

RESULTS

Effect of chlorogenic acid and baicalein on LPS induced pulmonary inflammatory cells infiltration

Myeloperoxidase (MPO) activity

Measuring myeloperoxidase (MPO) activity in lung homogenates were done in order to estimate the amount of pulmonary inflammatory cell infiltration. The enzyme activity of myeloperoxidase (MPO) was measured in units per mg of tissue (U MPO/mg). The amount of enzyme required to break down one micromole of peroxide per minute at 25^{O}C was designated as one unit of MPO. MPO activity was used to monitor the buildup of polymorphonuclear leukocytes (PMNL). Table 3 and Fig. 1 indicate the mean MPO activity value for each group.

The mean values of MPO activity in lung homogenates of sacrificed animals were significantly higher in LPS group (15.55 ± 0.53 U/mg of tissue) as compared to control (6.00 ± 0.22 U/mg of tissue) group. However, LPS/CGA/BAC/0.1 (13.45 ± 0.22U/mg of tissue), LPS/CGA/BAC/1 (11.38 ± 0.30 U/mg of tissue) and LPS/CGA/BAC/10 (9.73 ± 0.10 U/mg of tissue) groups showed reduction in the MPO activity, but maximum significant decrease was observed in two highest dose groups i.e., LPS/CGA/BAC/1 and LPS/CGA/BAC/10. All these findings suggested that LPS/CGA/BAC/10 mg/kg body weight was able to limit the inflammatory cells infiltration especially neutrophils in lungs.

Effect of chlorogenic acid and baicalein on LPS induced oxidative/nitrosative stress

Effect of chlorogenic acid and baicalein on LPS induced Lipid peroxidation (LPO)

Malondial dehyde levels (nM MDA/g), a marker of lipid peroxidation, were measured in lung homogenates from various groups and are shown in Table 4 and Fig. 2 as an indicative of oxidative stress.

The lung MDA level of LPS group increased to (13.92 ± 0.29 nM/g) in comparison to control (6.74 ± 0.24 nM/g) group. The levels of MDA in LPS/CGA/BAC/0.1 (10.01 ± 0.39 nM/g), LPS/CGA/BAC/1 (7.81 ± 0.36 nM/g) and LPS/CGA/BAC/10 (7.27 ± 0.16 nM/g) groups were lowered as compared to LPS group. The level of MDA was decreased significantly in middle and highest dose i.e., LPS/CGA/BAC/1 (7.81 ± 0.36 nM/g) and LPS/CGA/BAC/10 (7.27 ± 0.16 nM/g) respectively. This showed that CGA and BAC reduces the increased level of LPO by LPS, hence its antioxidant action.

Effect of chlorogenic acid and baicalein on LPS induced Nitric oxide (NO)

Table 5 and Fig. 3 showed the NO levels in different treatment groups. Using the Griess reagent, the nitrite content in lung homogenates of killed animals was determined as a measure of NO production and it was shown to be considerably higher in LPS group mice (2.94 ± 0.07 nM/mg of protein) than in the control (0.64 ± 0.13 nM/mg of protein) group. However, CGA and BAC treated groups LPS/CGA/BAC/0.1 (2.39 ± 0.17 nM/mg of protein), LPS/CGA/BAC/1 (2.11 ± 0.12 nM/mg of protein) and LPS/CGA/BAC/10 (1.76 ± 0.05 nM/mg of protein) showed reduction in NO level but this was significant in middle and highest dose group. This indicated the anti-inflammatory and anti-oxidant effect of CGA and BAC.

Effect of chlorogenic acid and baicalein on LPS induced Catalase (CAT) and Superoxide dismutase (SOD)

Table 3 and Fig. 4 (SOD) and 5 (CAT) provide information on the concentration of various antioxidant enzymes in the lung homogenate. Reactive oxygen and reactive nitrogen species that are generated during lung inflammation are scavenged by antioxidant enzymes. So, the activities of various antioxidant enzymes were

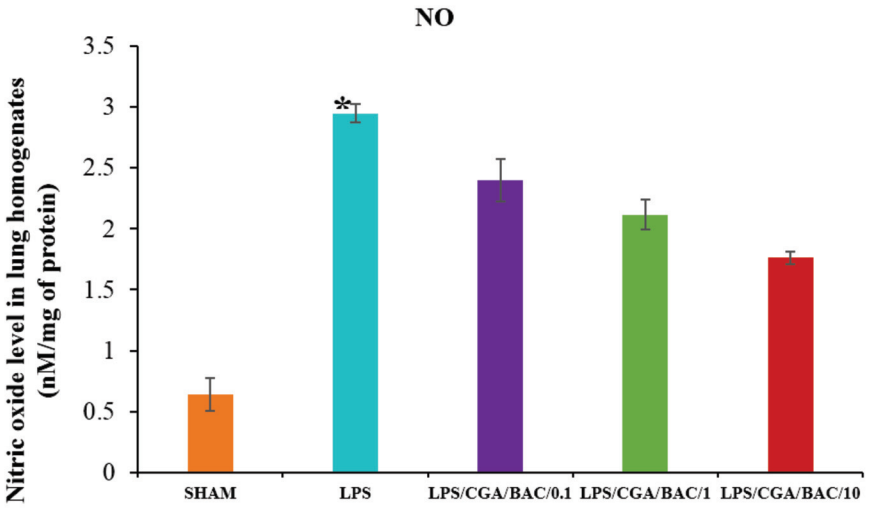

Fig. 3. NO level in lung homogenates of different groups.

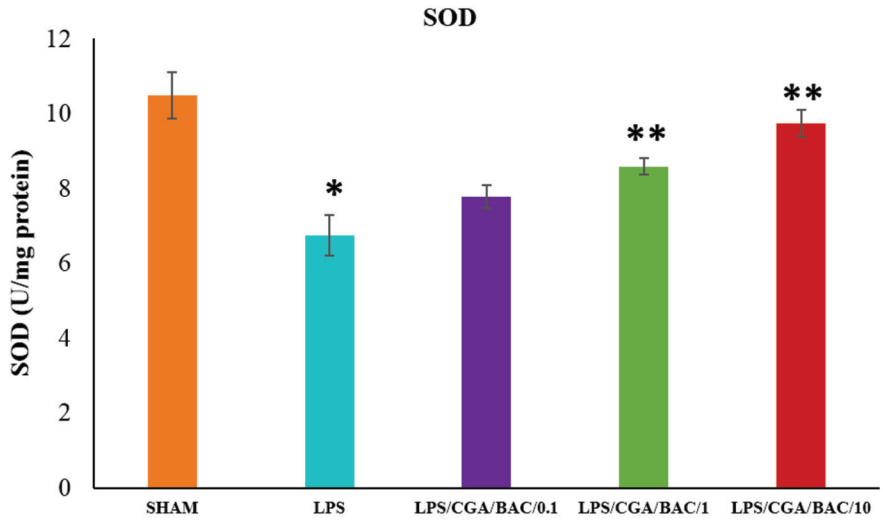

Fig. 4. SOD level in lung homogenates of different groups.

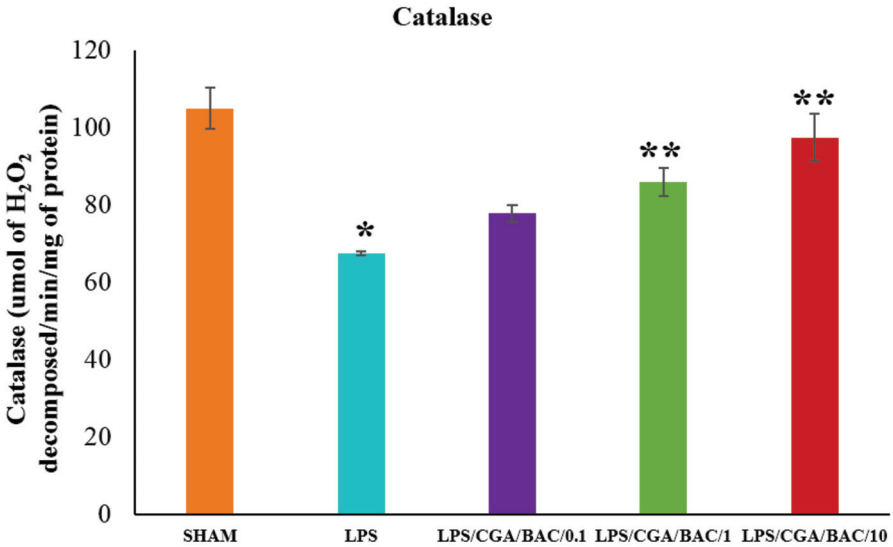

Fig. 5. Catalase level in lung homogenates of different groups.

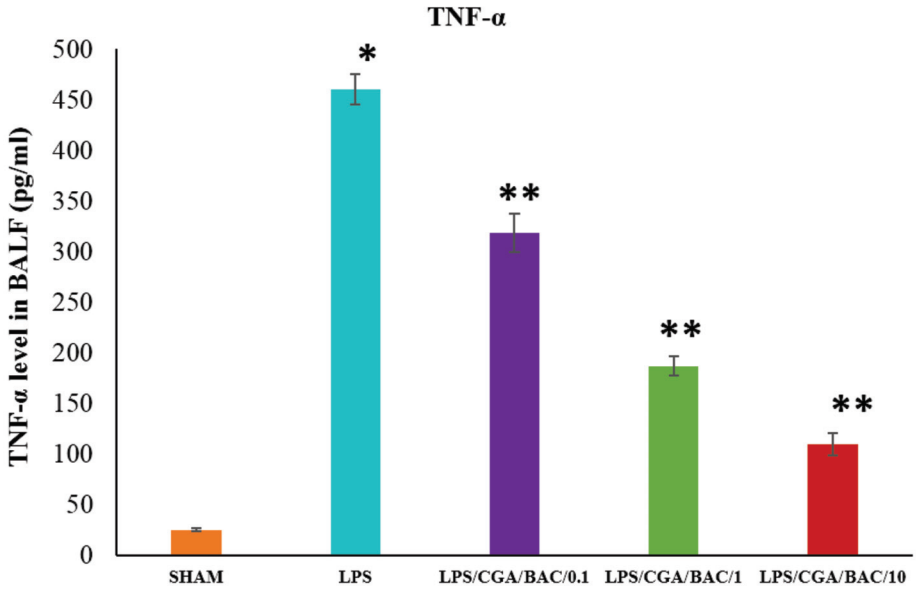

Fig. 6. TNF-α level in BALF of different groups.

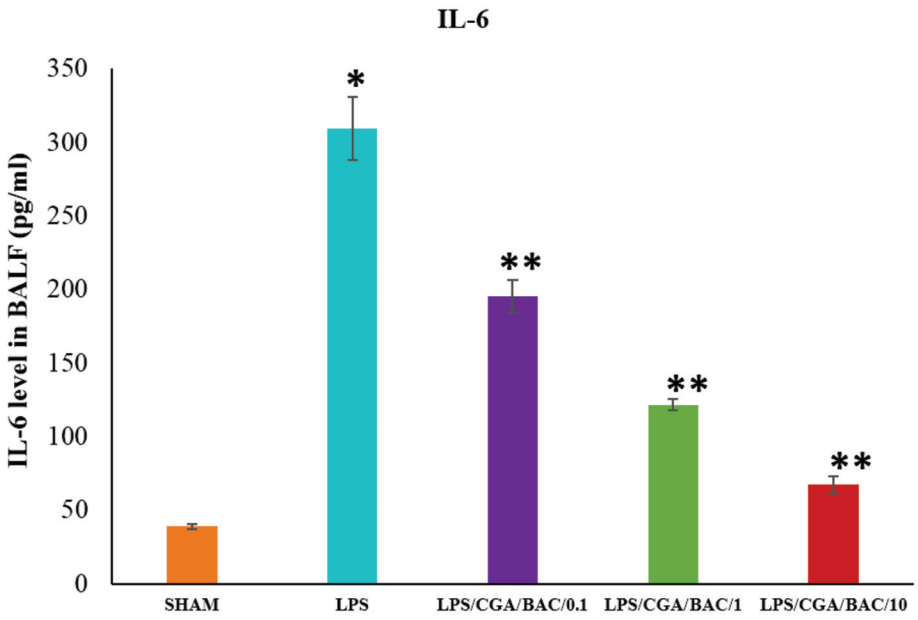

Fig. 7. IL-6 level in BALF of different groups.

examined.

The catalase (CAT) activity in lung homogenates was significantly decreased in LPS group (67.42 ± 0.55 nM/mg of protein) than in the control (104.90 ± 5.36 nM/mg of protein) group. However, CGA and BAC treated groups LPS/CGA/ BAC/0.1 (77.74 ± 2.20 nM/mg of protein), LPS/CGA/BAC/1 (85.82 ± 3.63 nM/mg of protein) and LPS/CGA/BAC/10 (97.41 ± 6.13 nM/mg of protein) showed dose dependant increase in catalase (CAT) activity as compared to LPS group.

The superoxide dismutase (SOD) activity in lung homogenates was significantly decreased in LPS group (6.74 ± 0.53 nM/mg of protein) than in the control (10.49 ± 0.61 nM/mg of protein) group. However, CGA and BAC treated groups LPS/CGA/BAC/0.1 (7.77 ± 0.30 nM/mg of protein), LPS/CGA/BAC/1 (8.58 ± 0.22 nM/mg of protein) and LPS/CGA/BAC/10 (9.74 ± 0.36 nM/mg of protein) showed dose dependant increase in superoxide dismutase (SOD) activity as compared to LPS group.

Effect of chlorogenic acid and baicalein on LPS induced inflammatory cytokines

Effect of chlorogenic acid and baicalein on Levels of TNF-α and IL-6 in BALF

In LPS group (460.57 ± 14.68 pg/mg), there was

Table 4. LPO level in lung homogenates of different groups.

Groups	MDA (nM/g) (Mean ± SE)
Gp-I Sham/Control group	6.74 ± 0.24
Gp-II LPS/Vehicle group	13.92 ± 0.29*
Gp-III LPS/CGA/BAC/0.1	10.01 ± 0.39
Gp-IV LPS/CGA/BAC/1	7.81 ± 0.36**
Gp-V LPS/CGA/BAC/10	7.27 ± 0.16**

Table 5. NO level in lung homogenates of different groups.

Groups	NO (nm/mg of protein) (Mean ± SE)
Gp-I Sham/Control group	0.64 ± 0.13
Gp-II LPS/Vehicle group	2.94 ± 0.07*
Gp-III LPS/CGA/BAC/0.1	2.39 ± 0.17
Gp-IV LPS/CGA/BAC/1	2.11 ± 0.12**
Gp-V LPS/CGA/BAC/10	1.76 ± 0.05**

increase in the level of TNF-α with respect to control (25.48 ± 1.86 pg/mg) group. However, there was significant decline in the level of TNF-α in LPS/CGA/BAC/10 group (109.74 ± 10.76 pg/mg) as compared to LPS group. LPS/CGA/BAC/0.1 (318.65 ± 19.10 pg/mg), LPS/CGA/ BAC/1 (187.06 ± 9.63 pg/mg) groups also showed decreased level of TNF-α as compared to LPS group.

Further in case of IL-6 levels, there was massive increase in its level to (309.16 ± 21.55 pg/mg) in LPS group as compared to control (38.78 ± 1.68 pg/mg). This was diminished significantly in LPS/CGA/BAC/10 (67.14 ± 5.57 pg/mg). Dose dependent reduction in IL-6 level was also seen in LPS/CGA/BAC/0.1 (195.15 ± 11.21 pg/mg) and LPS/CGA/BAC/1(121.61 ± 3.88 pg/mg) groups. These findings suggested that CGA and BAC were able to decelerate the increasing pro-inflammatory cytokines in lungs induced by LPS. Both the levels of TNF-α and IL-6 are shown in Table 7; Fig. 6 and 7 respectively.

Effect of chlorogenic acid and baicalein on i-NOS expression in LPS induced nitrosative stress

The primary antibody against i-NOS was used in the current investigation to conduct an immunohistochemistry analysis. LPS group (Fig. 9, 10) showed enhanced expression of iNOS in the cells as compared to control (Fig. 8) which corroborated with our findings pertaining to oxidative stress parameters which proved that oxidative stress played a pivotal role in ALI.

The dose dependant improvement was seen in the lung injury as chlorogenic acid and baicalein ameliorated acute lung injury induced by LPS and iNOS immunopositive cells also were less in higher dose group i.e., LPS/CGA/BAC/10 group which is also in consonant with oxidative stress parameters (Fig. 11).

Effect of chlorogenic acid and baicalein on immunohistochemical expression of caspase-3 in LPS induced apoptosis.

The primary antibody against caspase-3 was used in the current investigation to conduct an immunohistochemistry analysis. Caspase-3 plays an important role in ALI as caspase-3 is an indicator of oxidative stress. Apoptosis was also one of the contributing factors for causing damage to lungs in ALI as quite significant number of alveolar epithelial cells showed immunopositivity for caspase-3 (Fig. 13, 14) as compared to control (Fig. 12). ALI induced by LPS was ameliorated by chlorogenic acid and baicalein and it helped in preventing lung damage by reducing apoptosis (Fig. 15).

Effect of chlorogenic acid and baicalein on Nitrotyrosine (NT) expression in LPS induced oxidative stress

The primary antibody against Nitrotyrosine was used in the current investigation to conduct an immunohistochemistry analysis. The LPS group (Fig. 17, 18) showed high expression of Nitrotyrosine suggesting oxidative stress induced injury to the lung parenchyma as compared to control (Fig. 16). The dose dependant improvement in ALI was evident and the highest dose group showed remarketed ameliorative properties as there was very less expression of Nitrotyrosine in the highest dose group i.e., LPS/CGA/BAC/10 group (Fig. 19).

DISCUSSION

Effect of chlorogenic acid and baicalein on LPS induced pulmonary inflammatory cells infiltration

Myeloperoxidase (MPO) activity

Myeloperoxidase (MPO), an enzyme primarily found in neutrophil primary granules, was found to be more active in the lungs of mice treated with LPS in this study, indicating that endotoxin is to blame for neutrophil-mediated tissue injury. Increased MPO levels also suggested that neutrophils had infiltrated the lung parenchyma or alveolar spaces[13].

Polymorphonuclear neutrophil (PMN) migration into bronchoalveolar lavage fluid and an increase in pulmonary MPO activity caused by LPS were both reduced by CGA. The sequestration of pulmonary microvascular blood flow and subsequent neutrophil tissue infiltration are pathologic indicators of ALI. PMNs cause an increase in neutral protease activity, such as myeloperoxidase (MPO) and lysozyme activities and they also produce a variety of oxygen metabolites, which causes the alveolar matrix to degrade and is linked to the emergence of

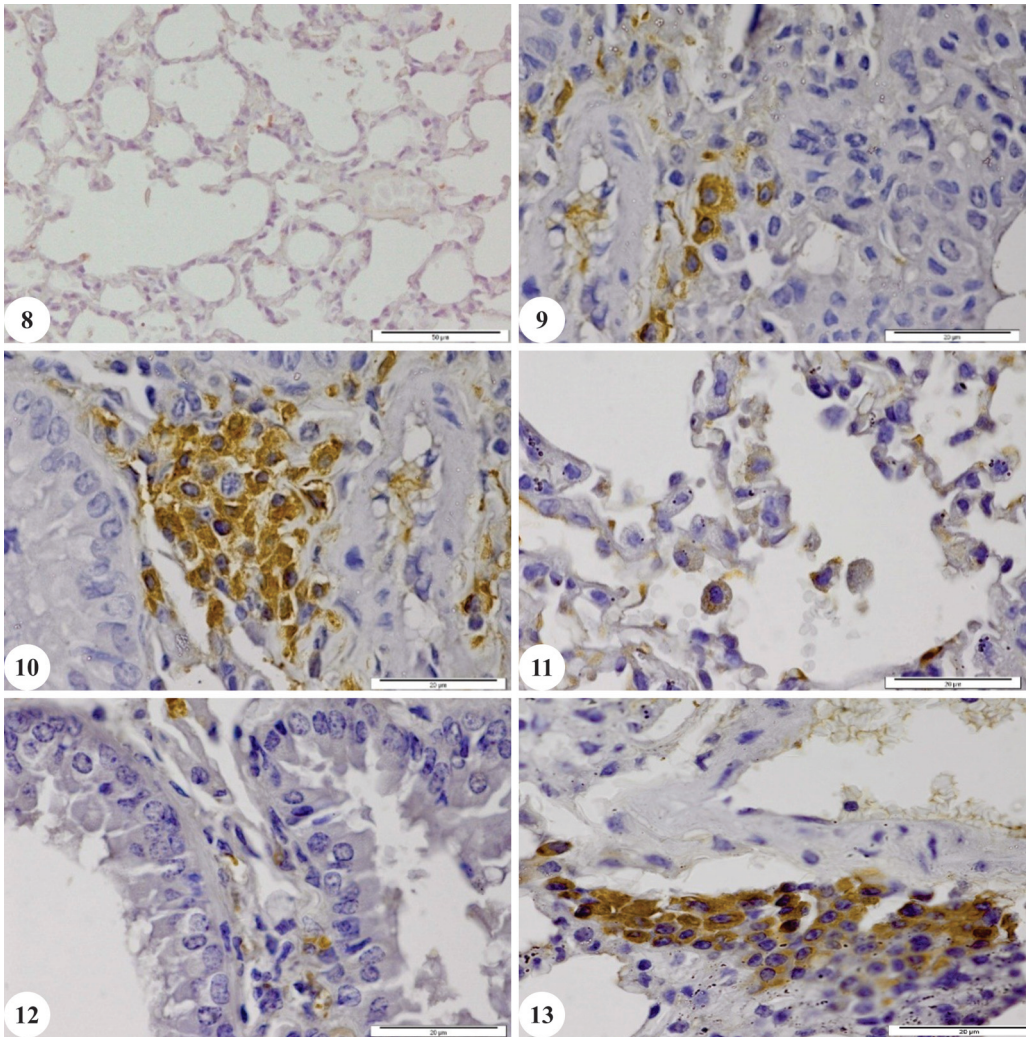

Fig. 8. SHAM/Control: Lung: Showing normal architecture with no expression of iNOS in bronchial epithelial cells (IHC X40, Bar = 50 μm); **Fig. 9.** LPS: Lung parenchymal cells showed increased expression of iNOS (IHC X40, Bar = 50 μm); **Fig. 10.** LPS: Lung parenchymal cells showing enhanced immunopositivity of iNOS (IHC X100, Bar = 20 μm); **Fig. 11.** LPS/CGA/BAC/10: CGA/BAC treatment showed mild expression of iNOS in lungs (IHC X100, Bar = 20 μm); **Fig. 12.** SHAM/Control: Lung: Bronchial epithelial cells showing no expression of caspase-3 (IHC X100, Bar = 20 μm); **Fig. 13.** LPS: Lung: Markedly more immunopositive cells for caspase 3 suggesting apoptosis (IHC X100, Bar = 20 μm).

Table 6. Antioxidant enzymes (CAT and SOD) level in lung homogenate of different groups.

Groups	Catalase (μmol of H_2O_2 decomposed/ min/mg of protein)	SOD (U/mg protein)
Gp-I Sham/Control group	104.90 ± 5.36	10.49 ± 0.61
Gp-II LPS/Vehicle group	67.42 ± 0.55*	6.74 ± 0.53*
Gp-III LPS/CGA/BAC/0.1	77.74 ± 2.20	7.77 ± 0.30
Gp-IV LPS/CGA/BAC/1	85.82 ± 3.63**	8.58 ± 0.22**
Gp-V LPS/CGA/BAC/10	97.41 ± 6.13**	9.74 ± 0.36**

a number of pulmonary diseases[14].

MPO activity was found to be markedly increased in LPS-induced mice compared to control tissues. In mice with LPS-induced ALI, baicalein significantly decreased the infiltration of total cells, neutrophils, macrophages and lymphocytes in BALF and suppressed MPO activity in lung tissues. MPO activity is a direct indicator of neutrophil accumulation and a prooxidant enzyme, revealed lung inflammation and cell damage in ALI[15].

MPO is a heme-containing enzyme that catalyzes the oxidation of halide ions to hypohalous acid under the control of hydrogen peroxidase. The lysosomal protein MPO, which is highly expressed in neutrophils, participates in the antimicrobial effects due to neutrophil stimulation.

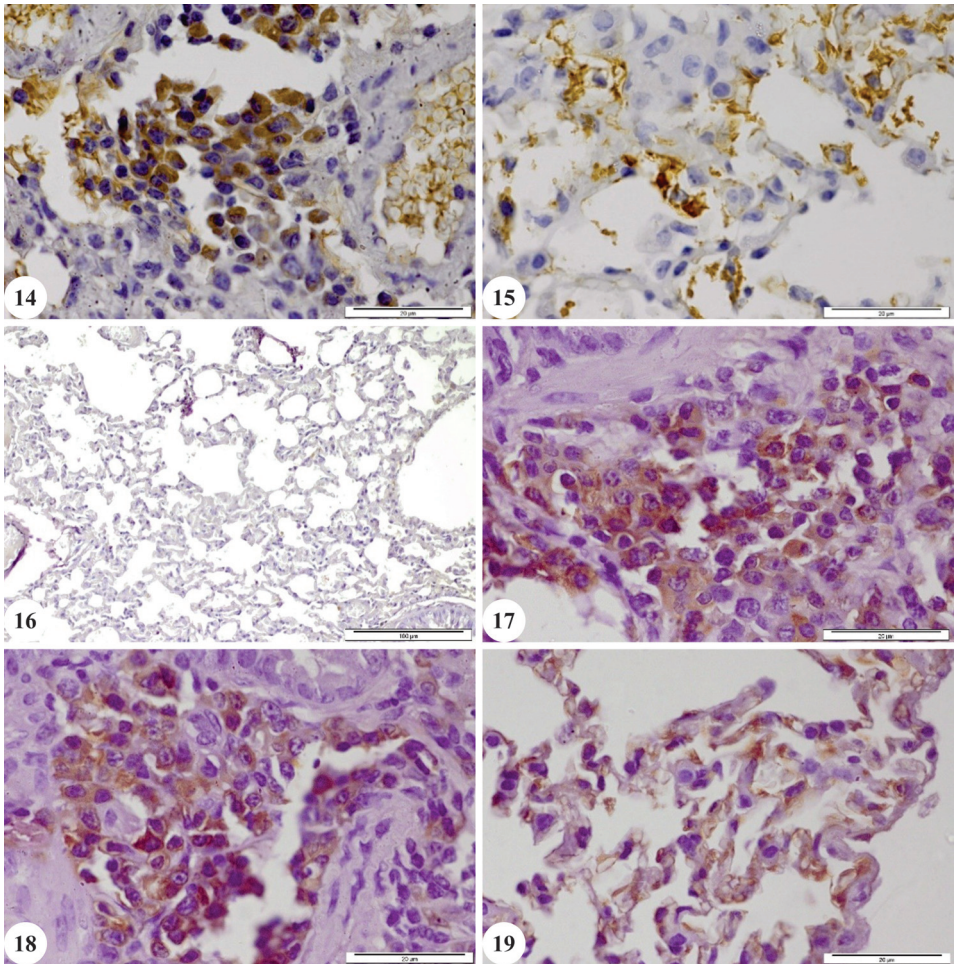

Fig. 14. LPS: Lung: Enhanced expression of caspase-3 in the lumg parenchyma (IHC X100, Bar = 20 μm); **Fig. 15.** LPS/CGA/BAC/10: Lung: Ameliorated the apoptosis induced lung damage as very few cells showed caspase 3 expression w.r.t. LPS treated group (IHC X100, Bar = 20 μm); **Fig. 16.** SHAM/Control: Lung: Showing normal architecture with no expression of NT (IHC X100, Bar = 100 μm); **Fig. 17.** LPS: Lung: NT immunopositive cells in the lung parenchyma (IHC X20, Bar = 20 μm); **Fig. 18.** LPS: Lung: Cytoplasm of alveolar macrophages and neutrophils showed increased expression of NT (IHC X100, Bar = 20 μm); **Fig. 19.** LPS/CGA/BAC/10: Lung: Amelioration was evident by reduced number of alveolar epithelial cells expressing NT (IHC X100, Bar = 20 μm).

Table 7. TNF-α and IL-6 level in BALF of different groups.

Groups	IL-6 (pg/mg)	TNF-α (pg/mg)
Gp-I Sham/Control group	38.78 ± 1.68	25.48 ± 1.86
Gp-II LPS/Vehicle group	309.16 ± 21.55*	460.57 ± 14.68*
Gp-III LPS/CGA/BAC/0.1	195.15 ± 11.21**	318.65 ± 19.10**
Gp-IV LPS/CGA/BAC/1	121.61 ± 3.88**	187.06 ± 9.63**
Gp-V LPS/CGA/BAC/10	67.14 ± 5.57**	109.74 ± 10.76**

Chlorogenic acid and baicalein reduced the activity of myeloperoxidase in dose a dependent manner @ 0.1, 1 and 10 mg/kg, suggesting that they both prevented infiltration of inflammatory cells. Hence, chlorogenic acid and baicalein showing synergistic effect.

Effect of chlorogenic acid and baicalein on LPS induced oxidative/nitrosative stress

Effect of chlorogenic acid and baicalein on LPS induced Lipid peroxidation (LPO)

Oxidative stress, which is defined as an increase in reactive oxygen species (ROS) and reactive nitrogen species (RNS), has the biggest role in the emergence of ALI[16,17]. There are a number of mechanisms by which these ROS and RNS can harm lung cells, including: (1) DNA oxidation leading to strand breaks and point mutations; (2) lipid peroxidation produces vasoactive and pro-inflammatory molecules; (3) protein oxidation altering protein activity; and (4) increased expression of pro-inflammatory genes due to altered nuclear factor kappa beta (NF-kB)[18]. An irritant, resident leukocytes and circulating oxidant enzymes are possible sources for the formation of such ROS[19].

Furthermore, the inhibitory effects of BAC on LPS-induced pro-inflammatory inducible cyclooxygenase-2 expression, nitric

oxide synthase (i-NOS) and tumour necrosis factor (TNF) formation *in vitro* and *in vivo* have been reported to be mediated by blocking nuclear factor-kappa B (NF-kB) activation, which is important for modulating several inflammatory gene expressions[20].

Free radicals play a role in the process of LPO. The primary byproduct of LPO is Malondialdehyde (MPO) which is a marker of lipid peroxidation. MPO has the property of cross-linking cellular macromolecules like protein or DNA and causes extensive cellular damage. A substantial rise in MDA is typically indicative of LPO damage. It claimed that CGA boosted endogenous antioxidant enzymes and helped in fending off oxidative stress[21].

The anti-inflammatory action of BAC in endotoxemia rats has been linked to an increase in HO-1 expression, according to new research[22]. These data imply that BAC could be used as therapeutic agent against inflammatory disorders caused by LPS.

The present study also concluded that chlorogenic acid and baicalein ameliorate the harmful effect of LPS on ALI due to its antioxidant effect.

Effect of chlorogenic acid and baicalein on LPS induced Nitric oxide (NO)

Alveolar macrophages in the lungs produce nitric oxide (NO), an essential mediator for maintaining the host defence response. However, excessive NO production by alveolar macrophages as a result of iNOS overexpression in alveolar macrophages is linked to severe acute lung inflammation[23]. Due to its interaction with the toll-like receptor (TLR-4) and activation of transcriptional factors like (NF-kβ) nuclear factor-kappa beta, LPS might have caused excessive NO production in the current investigation. This enhanced the amount of NO produced by the alveolar macrophages in the LPS group[24].

In primary microglia activated by LPS, CGA dramatically reduced NO generation and TNF-α release. Additionally, CGA inhibited transcriptional factor (NF-kβ), translocation and the phosphorylation and degradation of inhibitory kappa B-alpha (IkBα) induced by LPS[25] which might have been the reason of ameliorative activity of chlorogenic acid in the present investigation.

Baicalein dramatically decreased the BALF's protein concentration levels and total cell count. In LPS-stimulated RAW 264.7 cells, water extract of *S. baicalensis* (WSB) prevented the protein expression of inducible NO synthase (i-NOS), cyclooxygenase-2 (COX-2), phosphorylation of IB-protein, and MAPKs. LPS-induced lung damage was also prevented. This might the reason of decreasing NO-related inflammatory pathway inhibition in the present study[26].

The present study also indicated that chlorogenic acid and baicalein ameliorate the harmful effect of LPS on ALI due to its antioxidant effect as LPS/CGA/BAC/10 group showed decreased NO level as compared to LPS group.

Effect of chlorogenic acid and baicalein on LPS induced Catalase (CAT) and superoxide dismutase (SOD)

In the present study the activity of antioxidant enzymes like Catalase (CAT) and superoxide dismutase (SOD) in the LPS treated group was significantly decreased as compared to control group. The activity in the CGA and BAC treated group did, however improved in a dose-dependent way and the increase was significant at the highest dose, LPS/CGA/BAC/10. This proved how effective chlorogenic acid and baicalein are as antioxidants.

The activated PMNs operate as a mediator for the tissue damage caused by oxidative stress brought on by reactive oxygen species like superoxide radicles, hydroxyl radicals and hypochlorous acid that are formed during oxidative burst and degranulation of PMN[27]. However, several antioxidant enzymes like catalase (CAT) and superoxide dismutase (SOD) can minimise the tissue damage caused by oxidative radicals. By reducing hydrogen peroxide, these antioxidant enzymes including CAT and SOD guard the lung against oxidative stress[28]. In contrast, the increased formation of reactive oxygen species (ROS) in LPS-induced tissue injury disturbs the equilibrium between ROS and antioxidant enzyme activity. Lipid peroxidation and decreased antioxidant enzyme activity are both to blame for the accelerated tissue damage in ALI[29].

Baicalein and chlorogenic acid has been shown to reduce oxidative stress and inflammation by activating the nuclear erythroid factor 2-mediated heme oxygenase-1 signalling pathway, which has been shown to protect against LPS induced acute lung injury which might be the case in the present study too. It is reasonable to suppose that baicalein's capacity to protect against lipopolysaccharide-induced lung injury depends in part on maintaining a balance between oxidative and antioxidative stress[30].

As discussed earlier, chlorogenic acid and baicalein reduced LPS induced MDA content and in turn reduces the lipid peroxidation which ultimately might have reduced production of ROS and increased antioxidant enzyme activity. By altering the levels of anti-oxidant enzymes, it might be postulated that chlorogenic acid and baicalein was able to reduce the extent of lung injury caused by LPS by acting as an antioxidant agent by maintaining or improving the activity of antioxidant enzymes.

Effect of chlorogenic acid and baicalein on LPS induced inflammatory cytokines

Effect of chlorogenic acid and baicalein on Levels of TNF-α and IL-6 in BALF

In this investigation, LPS was found to activate alveolar macrophages and PMN, which in turn produced proinflammatory cytokines and demonstrated a significant capacity to produce ROS, including superoxide anion, hydrogen peroxide and hydroxyl radicals[31]. Additionally, LPS can decrease metal ions like iron, which breaks down hydrogen peroxide into the most reactive and harmful chemical species - the hydroxyl radical[32].

LPS is believed to induce neutrophil and macrophage infiltration, which in turn causes an increase in the production of pro-inflammatory cytokines like TNF-α and IL-6 in the lungs[33]. TNF-α (tumour necrosis factor) is a typical pro-inflammatory mediator that has the ability to cause a substantial inflammatory response, including the activation of leukocytes and endothelial cells, leukocyte adherence to endothelium and increased vascular permeability[34]. Increased formation of ROS by a variety of phagocytic cells such as neutrophils and macrophages and decreased GSH activity, an antioxidant enzyme, are two effects that may result from overexpression of TNF-α[35,36].

Numerous inflammatory and chemotactic cytokines are known to be produced in response to LPS. The cytokines TNF-α and IL-6 are known to play a role in the inflammation associated with acute lung damage[37,38]. These cytokines start increase and sustain the inflammatory response in acute lung damage, together with other proinflammatory substances.

TNF-α, which is mostly produced by monocytes and macrophages, can trigger an inflammatory cascade, harm vascular endothelial cells and prompt the production of other biological factors including IL-6 by alveolar epithelial cells. In this work, we discovered that after exposure to LPS, BALF levels of TNF-α and IL-6 clearly.

Additionally, oxidative stress triggers inflammation and TNF-α and IL-6 are important inflammatory mediators that are controlled by NF-κβ activation. As already discussed, LPS-induced NF-κβ activity was reduced by chlorogenic acid and baicalein, which may have resulted in decreased expression of VCAM (vascular adhesion molecule) and ICAM (intracellular adhesion molecule), which in turn may have resulted in decreased leukocyte infiltration and its activity. This might reduce activation of leukocytes like macrophages as it decreased generation of TNF-α because macrophage activation is crucial for the inflammatory process[39]. The data mentioned above suggested that baicalein and chlorogenic acid have anti-inflammatory properties because they decreased TNF-α production. The anti-inflammatory activity of chlorogenic acid and baicalein reduced levels of proinflammatory cytokines mainly IL-6 and TNF-α production.

Effect of chlorogenic acid and baicalein on i-NOS expression in LPS induced nitrosative stress

Nitric oxide (NO) plays a key role in the development of ALI in the same way that pro-inflammatory cytokines and ROS do. Nitric oxide (NO), which is generated by a group of hemoproteins known as nitric oxide synthatase (NOS) is the second messenger[40]. The formation of the third type of isoform, known as i-NOS, by various inflammatory cells in the lung when normal lungs are exposed to various inflammatory cytokines induced by LPS or any other noxious stimulus is harmful[41] and may be responsible for additional tissue damage by producing peroxynitrite, a potent oxidative species[42]. The general mechanism by which i-NOS causes tissue damage is oxidation of sulfhydryl groups, DNA cleavage, lipid peroxidation, inhibition of mitochondrial respiration, inactivation of a1-proteinase inhibitor, alteration of pulmonary surfactant and inhibition of ion transport in the epithelial cells which are the characteristics of ALI[43-45]. The fact that LPS produced more i-NOS when compared to the control group in the current study suggests that LPS is to blame for the excessive nitric oxide generation that plays a significant role in tissue damage and acute lung injury through the aforementioned mechanism.

NO overproduction and iNOS expression are both strongly stimulated by LPS. Higher pulmonary iNOS expression and increased NO production are linked to ALI in both people and animal models. LPS promotes the production of iNOS in a variety of pulmonary cell types, including neutrophils, macrophages, bronchial epithelial and smooth muscle cells in the pulmonary artery in LPS-induced ALI. LPS substantially stimulates iNOS expression as well as NO overproduction. In both human and animal models higher pulmonary iNOS expression and increased NO production are associated with ALI. In LPS-induced ALI, LPS increases iNOS synthesis in a range of pulmonary cell types, including neutrophils, macrophages, bronchial epithelia, and smooth muscle cells in the pulmonary artery. Nitric oxide (NO) release in response to an LPS challenge was blocked by CGA because it significantly reduced the activity of inducible nitric oxide synthase (i-NOS) in lung tissues. These findings showed that CGA was very successful at preventing ALI and might be used as a therapeutic drug in the future to treat ALI.

Baicalein significantly reduced the enhanced i-NOS cascade and superoxide production in lungs induced with LPS. Based on the findings of this investigation, it was concluded that the protective effect of Baicalein in LPS-induced ALI may include reduction of i-NOS

and ROS-mediated activities. In the present study there was reduced expression of i-NOS in a group which has treated with maximum dose of chlorogenic acid and baicalein which may be due to antioxidant property of the chlorogenic acid and baicalein.

Effect of chlorogenic acid and baicalein on immunohistochemical expression of caspase-3 in LPS induced apoptosis

LPS may induce endothelial and epithelial cells to undergo apoptosis, which results in disseminated alveolar damage, a sign of ALI[46]. Increased levels of several pro-inflammatory cytokines (TNF-α) which is a key mediator for activating the extrinsic pathway of the apoptotic cascade, were caused by LPS[47]. As was previously noted, LPS was responsible for the development of oxidative stress which may damage mitochondria and activate the intrinsic route of apoptosis[48]. As a result, in the current investigation, caspase-3 expression was higher in the LPS group compared to the control group. LPS may be responsible for activating both apoptosis pathways and any of the activated routes may be responsible for activating caspase-3. According to reports, the Fas/Fas ligand system which is a component of the extrinsic pathway and belongs to the TNF family may also activate different initiator caspases such as caspase-8 and caspase-9 before activating caspase-3 which may cause apoptosis in alveolar and endothelial cells in cases of ALI or ARDS[49]. All of these initiator caspase activation events, such as those involving caspase-8, caspase-9 and effector caspase-3, may have been influenced by the expression of pro and anti-apoptotic proteins, such as Bcl-2[50] and Bax[51]. Bcl-2 and Bax proportions are balanced under normal circumstances, but in ALI, the LPS may have upset this equilibrium, which could account for the increased production of caspase-3.

Key apoptotic mediators caspase-3 and caspase-9 are triggered by both the mitochondrial apoptotic and death receptor pathways. Antioxidant and anti-inflammatory activities of chlorogenic acid (CGA) have been demonstrated[52].

Chlorogenic acid and baicalein treated groups showed significant decrease in the number of apoptotic cells, as detected by decreased immune-positive caspase-3 cell than in a dose dependant manner. Based on these results, it may be concluded that chlorogenic acid and baicalein treated groups reduced apoptosis in ALI.

Effect of chlorogenic acid and baicalein on Nitrotyrosine (NT) expression in LPS induced oxidative stress

As seen in the current work, the overproduction of ROS is currently thought to be another significant mediator influencing the development of lung damage in response to LPS. It is noteworthy that the reaction between NO and $O2^-$ can quickly produce peroxynitrite ($ONOO^-$), a more cytotoxic substance that causes serious harm to cells and tissues. The *in vivo* data demonstrated that Baicalein significantly reduced the elevated i-NOS/NO cascade, $O2^-$ formation and Nitrotyrosine expression, a marker of peroxynitrite, in the lungs induced by LPS[53].

When the peroxynitrite interacts with protein residues, it produces nitrotyrosine in a variety of inflammatory cells including macrophages and lung vascular endothelial cells which damages the tissue[54].

By preventing an excessive amount of ROS from being produced, CGA and BAC minimise oxidative stress and increase nitric oxide bioavailability and leads to the attenuation of LPS induced ALI. In the present study there was reduced expression of Nitrotyrosine in a group which has treated with maximum dose of chlorogenic acid and baicalein which may be due to antioxidant property of the chlorogenic acid and baicalein.

Baicalein significantly reduced the enhanced $O2^-$ production and nitrotyrosine expression, a marker of peroxynitrite, in lungs induced with LPS. Based on the findings of this investigation, it was concluded that the protective effect of Baicalein in LPS-induced ALI may include reduction of ROS-mediated activities. The present study there was reduced expression of Nitrotyrosine in a group which has treated with maximum dose of chlorogenic acid and baicalein which may be due to antioxidant property of the chlorogenic acid and baicalein.

CONCLUSIONS

Chlorogenic acid and baicalein @ 10 mg/kg body weight was found to be having potential ameliorative effect. Lung injury was ameliorated by chlorogenic acid and baicalein as was evidenced by levels of MPO activity, oxidative stress parameters, proinflammatory cytokines, apoptosis and immunohistochemistry. Thus, Chlorogenic acid and baicalein ameliorated LPS induced ALI through attenuation of inflammation, oxidative stress and apoptosis of alveolar epithelial and endothelial cells.

ACKNOWLEDGEMENT

The authors are thankful to SERB, New Delhi, India for providing financial support.

REFERENCES

1. Matthay MA, Ware LB and Zimmerman GA. 2012. The acute respiratory distress syndrome. *J Clin Investig* **122:** 2731-2740.
2. Ware LB and Matthay MA. 2000. The acute respiratory distress syndrome. *New Engl J Med* **342:** 1334-1349.
3. Ogata-Suetsugu S, Yanagihara T, Hamada N, Ikeda-Harada C, Yokoyama T, Suzuki K and Nakanishi Y. 2017. Amphiregulin suppresses epithelial cell apoptosis in lipopolysaccharide-induced lung injury in mice. *Biochem Biophys Res Commun* **484:** 422-428.

4. Kono Y, Kashine S, Yoneyama T, Sakamoto Y, Matsui Y and Shibata H. 1998. Iron chelation by chlorogenic acid as a natural antioxidant. *Biosci Biotechnol Biochem* **62:** 22-27.
5. Dos Santos MD, Almeida MC, Lopes NP and De Souza GEP. 2006. Evaluation of the anti-inflammatory, analgesic and antipyretic activities of the natural polyphenol chlorogenic acid. *Biol Pharm Bull* **29:** 2236-2240.
6. Tsai CL, Lin YC, Wang HM and Chou TC. 2014. Baicalein, an active component of *Scutellaria baicalensis*, protects against lipopolysaccharide-induced acute lung injury in rats. *J Ethnopharmacol* **153:** 197-206.
7. Huang XT, Liu W, Zhou Y, Ha CX, Zhou Y, Zhan CY and Tang SY. 2019. Dihydroartemisinin attenuates lipopolysaccharide-induced acute lung injury in mice by suppressing NF-κB signaling in an Nrf2-dependent manner. *Int J Mol Med* **44:** 2213-2222.
8. Sastry KVH, Moudgal RP, Mohan J, Tyagi JS and Rao G. 2002. Spectrophotometric determination of serum nitrite and nitrate by copper-cadmium alloy. *Anal Biochem* **306:** 79-82.
9. Hadwan MH and Abed HN. 2016. Data supporting the spectrophotometric method for the estimation of catalase activity. *Data Br* **6:** 194-199.
10. Madesh M and Balasubramanian KA. 1998. Microtiter plate assay for superoxide dismutase using MTT reduction by superoxide. *Indian J Biochem Biophys* **35:** 184-188.
11. Song JA, Yang HS, Lee J, Kwon S, Jung KJ, Heo JD and Lee K. 2010. Standardization of bronchoalveolar lavage method based on suction frequency number and lavage fraction number using rats. *Toxicol Res* **26:** 203-208.
12. Saito K, Tanaka N, Ikari J, Suzuki M, Anazawan R, Abe M and Tatsumi K. 2019. Comprehensive lipid profiling of bleomycin-induced lung injury. *J Appl Toxicol* **39:** 658-671.
13. Klebanoff SJ. 2005. Myeloperoxidase: friend and foe. *J Leukoc Biol* **77:** 598-625.
14. Zang CB. 2010. Mechanism of liver and lung injury in septic mice. *Acad J Second Mil Med* **15:** 616-619.
15. Zhang L, Yang L, Xie X, Zheng H, Zheng H, Zhang L and Li F. 2021. Baicalin Magnesium Salt Attenuates Lipopolysaccharide-Induced Acute Lung Injury via Inhibiting of TLR4/NF-κB Signaling Pathway. *J Immunol Res*.
16. Ward PA. 2010. Oxidative stress: acute and progressive lung injury. *Ann NY Acad Sci* **1203:** 53-59.
17. Shah NR, Iqbal MB, Barlow A and Bayliss J. 2011. Severe physical exertion, oxidative stress, and acute lung injury. *Clin J Sport Med* **21:** 537-538.
18. Fialkow L, Chan CK, Rotin D, Grinstein S and Downey GP. 1994. Activation of the mitogen-activated protein kinase signaling pathway in neutrophils. Role of oxidants. *J Biol Chem* **269:** 31234-31242.
19. Brigham KL. 1986. Role of free radicals in lung injury.*Chest* **89:** 859-863.
20. Wu YL, Lian LH, Wan Y and Nan JX. 2010. Baicalein inhibits nuclear factor-κB and apoptosis via c-FLIP and MAPK in D-GalN/LPS induced acute liver failure in murine models. *Chembiol Interact* **188:** 526-534.
21. Wang JM, Chen RX, Zhang LL, Ding NN, Liu C, Cui Y and Cheng YX. 2018. In vivo protective effects of chlorogenic acid against triptolide-induced hepatotoxicity and its mechanism. *Pharm Biol* **56:** 626-631.
22. Lee YM, Cheng PY, Chim LS, Kung CW, Ka SM, Chung MT and Sheu JR. 2011. Baicalein, an active component of *Scutellariabaicalensisgeorgi*, improves cardiac contractile function in endotoxaemic rats via induction of heme oxygenase-1 and suppression of inflammatory responses. *J Ethnopharmacol* **135:** 179-185.
23. Farley KS, Wang LF, Razavi HM, Law C, Rohan M, McCormack DG and Mehta S. 2006. Effects of macrophage inducible nitric oxide synthase in murine septic lung injury. *Am J Physiol Lung Cell Mol Physiol* **290:** L1164-L1172.
24. Arias-Salvatierra D, Silbergeld EK, Acosta-Saavedra LC and Calderon-Aranda ES. 2011. Role of nitric oxide produced by iNOS through NF-κB pathway in migration of cerebellar granule neurons induced by lipopolysaccharide. *Cell Signal* **23:** 425-435.
25. Shen W, Qi R, Zhang J, Wang Z, Wang H, Hu C and Lu D. 2012. Chlorogenic acid inhibits LPS-induced microglial activation and improves survival of dopaminergic neurons. *Brain Res Bull* **88:** 487-494.
26. Chen JJ, Huang CC, Chang HY, Li PY, Liang YC, Deng JS and Huang GJ. 2017. *Scutellariabaicalensis* ameliorates acute lung injury by suppressing inflammation in vitro and in vivo. *Am J Chinese Med* **45:** 137-157.
27. Grommes J and Soehnlein O. 2011. Contribution of neutrophils to acute lung injury. *Mol Med* **17:** 293-307.
28. Pryor WA and Stone K. 1993. Oxidants in cigarette smoke radicals, hydrogen peroxide, peroxynitrate, and peroxynitrite A. *Ann NY Acad Sci* **686:** 12-27.
29. Juránek I, Bezek S. 2005. Controversy of free radical hypothesis: reactive oxygen species-cause or consequence of tissue injury. *Gen Physiol Biophys* **24:** 263.
30. Zhang X, Huang H, Yang T, Ye Y, Shan J, Yin Z and Luo L. 2010. Chlorogenic acid protects mice against lipopolysaccharide-induced acute lung injury. *Injury* **41:** 746-752.
31. Yeh CH, Yang JJ, Yang ML, Li YC and Kuan YH. 2014. Rutin decreases lipopolysaccharide-induced acute lung injury via inhibition of oxidative stress and the MAPK-NF-κB pathway. *Free Radic Biol Med* **69:** 249-257.
32. Kalyanaraman B, Morehouse KM and Mason RP. 1991. An electron paramagnetic resonance study of the interactions between the adriamycin semiquinone, hydrogen peroxide, iron-chelators, and radical scavengers. *Arch Biochem Biophys* **286:** 164-170.
33. Chang HY, Chen YC, Lin JG, Lin IH, Huang HF, Yeh CC and Huang GJ. 2018. Asatone prevents acute lung injury by reducing expressions of NF-κB, MAPK and inflammatory cytokines. *Am J Chinese Med* **46:** 651-671.
34. Carvalho-Tavares J, Hickey MJ, Hutchison J, Michaud J, Sutcliffe IT and Kubes P. 2000. A role for platelets and endothelial selectins in tumor necrosis factor-α-induced leukocyte recruitment in the brain microvasculature. *Circ Res* **87:** 1141-1148.
35. Ferro TJ, Hocking DC and Johnson ARNOLD. 1993. Tumor necrosis factor-alpha alters pulmonary vasoreactivity via neutrophil-derived oxidants. *Am J Physiol Lung Cell Mol Physiol* **265:** L462-L471.
36. Glosli H, Tronstad KJ, Wergedal H, Müller F, Svardal A, Aukrust P and Prydz H. 2002. Human TNF-α in transgenic mice induces differential changes in redox status and glutathione-regulating enzymes. *FASEB J* **16:** 1450-1452.
37. Bradley PP, Priebat DA, Christensen RD and Rothstein G. 1982. Measurement of cutaneous inflammation: estimation of neutrophil content with an enzyme marker. *J Invest Dermatol* **78:** 206-209.
38. Bhatia M and Moochhala S. 2004. Role of inflammatory mediators in the pathophysiology of acute respiratory distress syndrome. *J Pathol: J Path Soc* **202:** 145-156.
39. Medzhitov R and Janeway CA. 1997. Innate immunity: the virtues of a nonclonal system of recognition. *Cell* **91:** 295-298.
40. Knowles RG and Moncada S. 1994. Nitric oxide synthases in mammals. *Biochem J* **298:** 249.

41. GuoFH, De Raeve HR, Rice TW, Stuehr DJ, Thunnissen FB and Erzurum SC. 1995. Continuous nitric oxide synthesis by inducible nitric oxide synthase in normal human airway epithelium *in vivo*. *Proc Natl Acad Sci* **92:** 7809-7813.
42. Beckman JS and Koppenol WH. 1996. Nitric oxide, superoxide, and peroxynitrite: the good, the bad, and ugly. *AJ Physiol Cell Physiol* **271:** C1424-C1437.
43. Moreno JJ and Pryor WA. 1992. Inactivation of alpha 1-proteinase inhibitor by peroxynitrite. *Chem Res Toxicol* **5:** 425-431.
44. Cassina A and Radi R. 1996. Differential inhibitory action of nitric oxide and peroxynitrite on mitochondrial electron transport. *Arch Biochem Biophys* **328:** 309-316.
45. Rubbo H, Radi R, Trujillo M, Telleri R, Kalyanaraman B, Barnes S and Freeman BA. 1994. Nitric oxide regulation of superoxide and peroxynitrite-dependent lipid peroxidation. Formation of novel nitrogen-containing oxidized lipid derivatives. *J Biol Chem* **269:** 26066-26075.
46. Guinee Jr D, Fleming M, Hayashi T, Woodward M, Zhang J, Walls J and Travis W. 1996. Association of p53 and WAF1 expression with apoptosis in diffuse alveolar damage. *Am J Pathol* **149:** 531.
47. Nair P, Lu M, Petersen S and Ashkenazi A. 2014. Apoptosis initiation through the cell-extrinsic pathway. *Methenzymol* (Vol. 544)**:** 99-128. In Press.
48. Radogna F, Cristofanon S, Paternoster L, D'Alessio M, De Nicola M, Cerella C and Ghibelli L. 2008. Melatonin antagonizes the intrinsic pathway of apoptosis via mitochondrial targeting of Bcl-2. *J Pineal Res* **44:** 316-325.
49. Matute-Bello G, Liles WC, Steinberg KP, Kiener PA, Mongovin S, Chi EY and Martin TR. 1999. Soluble Fas ligand induces epithelial cell apoptosis in humans with acute lung injury (ARDS). *J Immun* **163:** 2217-2225.
50. Nihal M, Ahmad N, Mukhtar H and Wood GS. 2005. Anti-proliferative and proapoptotic effects of (−) epigallocatechin-3-gallate on human melanoma: Possible implications for the chemoprevention of melanoma. *Int J Cancer* **114:** 513-521.
51. Oltval ZN, Milliman CL and Korsmeyer SJ. 1993. Bcl-2 heterodimerizes in vivo with a conserved homolog, Bax that accelerates programed cell death. *Cell* **74:** 609-619.
52. Qu S, Dai C, Hao Z, Tang Q, Wang H, Wang J and Zhao H. 2020. Chlorogenic acid prevents vancomycin-induced nephrotoxicity without compromising vancomycin antibacterial properties. *Phytother Res* **34:** 3189-3199.
53. Park WY, Goodman RB, Steinberg KP, Ruzinski JT, Radella F, Park DR and Martin TR. 2001. Cytokine balance in the lungs of patients with acute respiratory distress syndrome. *Am J Respir Crit Care Med* **164:** 1896-1903.
54. Wizemann TM, Gardner CR, Laskin JD, Quinones S, Durham SK, Goller NL and Laskin DL. 1994. Production of nitric oxide and peroxynitrite in the lung during acute endotoxemia. *J Leukoc Biol* **56:** 759-768.

Indian J. Vet. Pathol., 48(2) : 159-168, 2024: DOI: 10.5958/0973-970X.2024.00025.7

RESEARCH ARTICLE

Fipronil toxicity induced hemato-biochemical alterations in male Wistar albino rats and its alleviation with pomegranate peel extract *(Punica granatum)*

P. Nakul, K. Sujatha[1*], A. Anand Kumar and S. Vijayalakshmi[2]

[1]Centre for Continuing Veterinary Education and Communication, [2]Department of Veterinary Microbiology, Department of Veterinary Pathology, College of Veterinary Science, Tirupati-517 502, Sri Venkateswara Veterinary University, Andhra Pradesh, India

Address for Correspondence

K. Sujatha, Coordinator, Centre for Continuing Veterinary Education and Communication, Department of Veterinary Pathology, College of Veterinary Science, Tirupati-517 502, Sri Venkateswara Veterinary University, Andhra Pradesh, India, E-mail: karamalasujatha@gmail.com

Received: 30.10.2023; Accepted: 5.12.2023

ABSTRACT

The present study was carried out to investigate the ameliorative effect of pomegranate peel extract (*Punica granatum*) against haemato-biochemical alterations induced by fipronil in male Wistar albino rats. A total of 24 male Wistar albino rats were randomly divided into four groups with six rats in each group. Fipronil was gavaged orally at a dose rate of 10 mg/kg body weight to group II rats for a period of 6 weeks using distilled water as vehicle. *Punica granatum* peel extract at a dose rate of 200 mg/kg body weight along with fipronil was administered to group IV rats to study the ameliorative effect. Group I and group III served as vehicle control and *Punica granatum* control respectively. The results of hematological parameters showed significant ($P<0.05$) reduction in total erythrocyte count (TEC), Haemoglobin (Hb), Packed Cell Volume (PCV), Total Leukocyte Count (TLC) and percent lymphocyte count in fipronil treated rats. Compared to control group,serum biochemical markers like aspartate aminotransferase (AST), alanine aminotransferase (ALT), blood urea nitrogen (BUN), serum creatinine were significantly ($P<0.05$) increased and serum total protein (TP), serum albumin and globulin levels were significantly ($P<0.05$) decreased in fipronil treated rats. Meanwhile, significant improvement in the hematological and biochemical parameters were observed in *Punica granatum* ameliorated rats (Group IV) which proved that *Punica granatum* has a protective effect against fipronil induced haemato-biochemical alterations in rats.

Keywords: Biochemical alterations, fipronil, fipronil toxicity, hematological alterations, *Punica granatum,* wistar rats

INTRODUCTION

The agricultural community has been impelled to a large extend for using broad-spectrum insecticides to enhance the crop yield and to decrease the post-harvest losses due to the increasing surge of insect pests. However, the toxic potential imparted by these insecticides in different livestock is on discussion among the scientific community[1]. Indiscriminate and inappropriate use of pesticides have led to environmental contamination globally with adverse effects on non-target organisms including humans[2]. At the same time, insects also developed resistance towards old generation insecticides like organophosphate, organochlorine, carbamates and pyrethroid compounds. Thus, use of a new class of insecticides with lesser field application and broad-spectrum activity shall be a better alternative[3].

Fipronil is one among the "new generation" broad spectrum phenyl pyrazole insecticide, which is widely used in veterinary, households, topical pet care products and agricultural practices to control ticks, fleas and other pests[4]. Fipronil induce oxidative damage in tissues including haemopoietic organs by altering the cell membrane permeability and by generating excess free radicals[5]. It mainly targets the brain and induces neurotoxicity in insects and mammals by inhibiting GABAA-gated chloride ion channels in the central nervous system[6]. Along with this, recent studies suggested that, fipronil develops toxic effects on other non-neuronal sites like liver, kidney, thyroid and reproductive organs[7]. Toxic impairment in these organs results in changes in biochemical status of organs. Hence, evaluating the haematologic and biochemical profile of animals shall help to understand the extent of damage induced by insecticides in different organs.

Use of an ameliorating agent with high antioxidant potential, less side effects and better compatibility shall be a better solution to mitigate the complications caused by insecticides. Pomegranate (*Punica*

How to cite this article : Nakul, P., Sujatha, K., Kumar, A.A. and Vijayalakshmi, S. 2024. Fipronil toxicity induced hemato-biochemical alterations in male Wistar albino rats and its alleviation with pomegranate peel extract *(Punica granatum)*. Indian J. Vet. Pathol., 48(2) : 159-168.

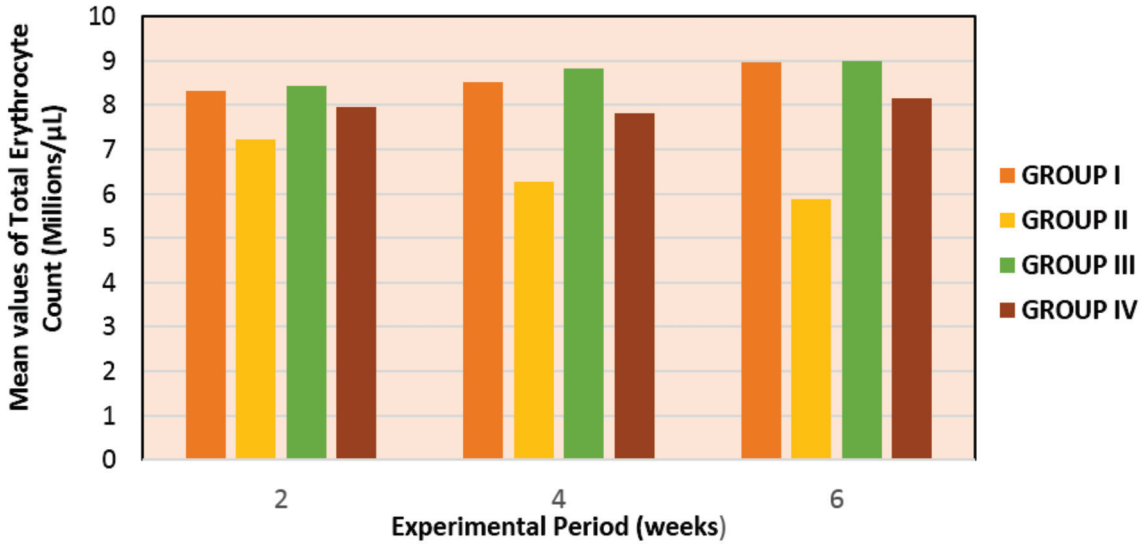

Fig. 1. Mean values of Total Erythrocyte Count (millions/µl) in rats of different experimental groups.

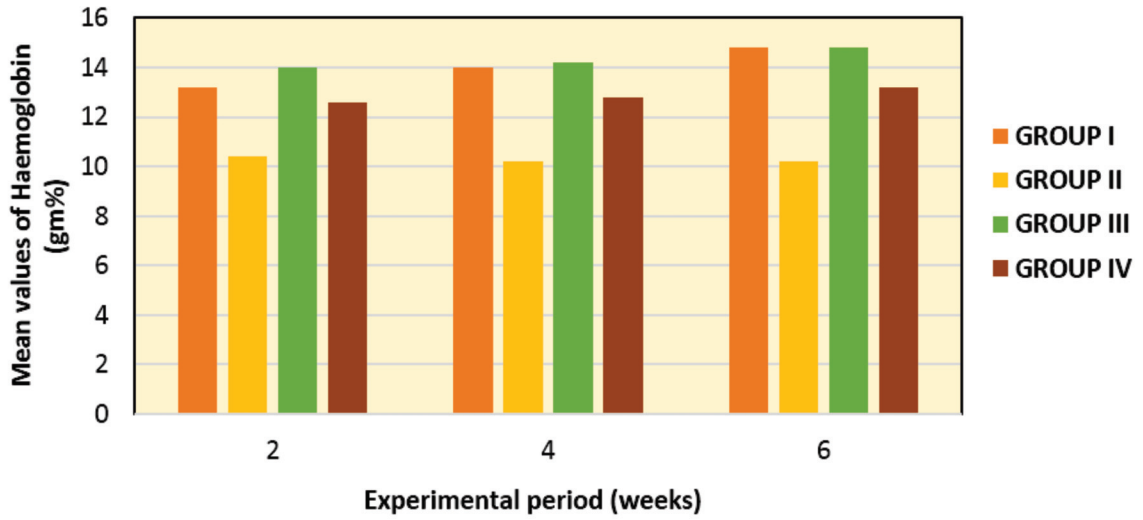

Fig. 2. Mean values of Hemoglobin (gm%) in rats of different experimental groups.

granatum) is one among them with enriched polyphenolic compounds, which has been widely used in traditional medicine due to its antioxidant[8], anti-inflammatory[9] and antibacterial[10] properties in human and animal studies. Pomegranate fruit and peelis rich in bioactive compounds, including phenolic compounds (ellagic acid), flavonoids (catechins and quercetin), and anthocyanidin (cyanidin), ferulic acids, ellagitannins which were responsible for antioxidant property[11].

Even though, much research work has been conducted to investigate the hematobiochemical changes induced by conventional group of pesticides, research on fipronil which is a new class of insecticide is limited. Hence, the present investigation was carried out to study the various haemato-biochemical alterations induced by fipronil and its amelioration with *Punica granatum* peel extract in Wistar rats.

MATERIALS AND METHODS

Procurement of experimental animals, fipronil and *Punica granatum* peel extract

Wistar albino rats with body weight of around 120 grams were procured from Sri Venkateshwara Enterprises, Bangalore. After two weeks of acclimatization, the rats were grouped and housed in standard polypropylene rat cages (three rats in one cage) during the experiment. They were maintained at 25^{O}C ± 1^{O}C and a 12:12 hour interval light / dark cycle throughout the experimental period of 6 weeks by taking necessary precautions, providing laboratory animal feed and water *ad libitum* and adhering to standard laboratory hygienic conditions. The approval of the institutional animal ethical committee was obtained

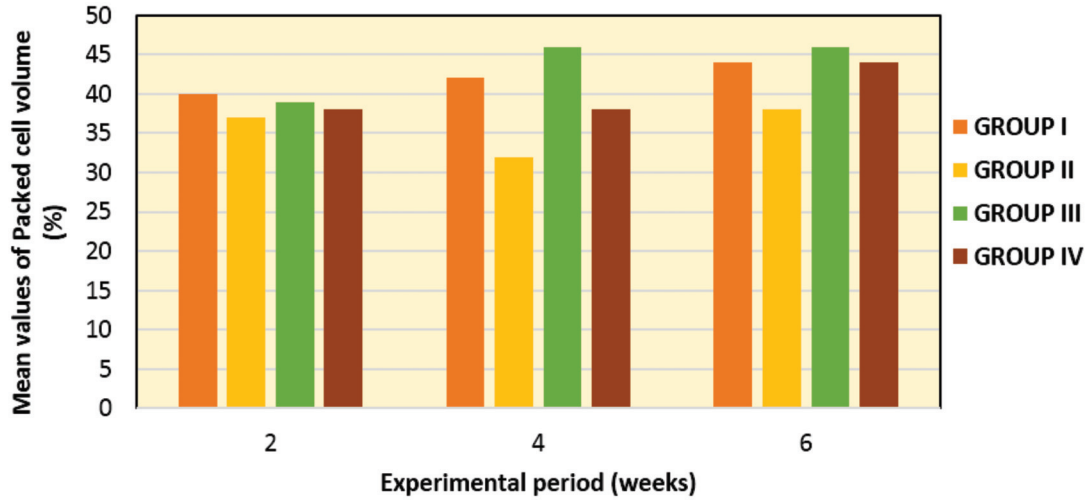

Fig. 3. Mean values of Packed cell volume (%) in rats of different experimental groups.

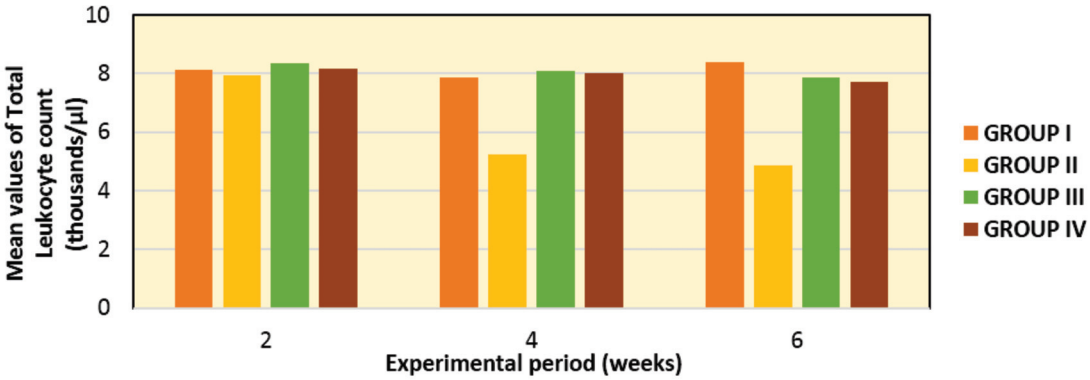

Fig. 4. Mean values of Total Leukocyte Count (thousands/µl) in rats of different experimental groups.

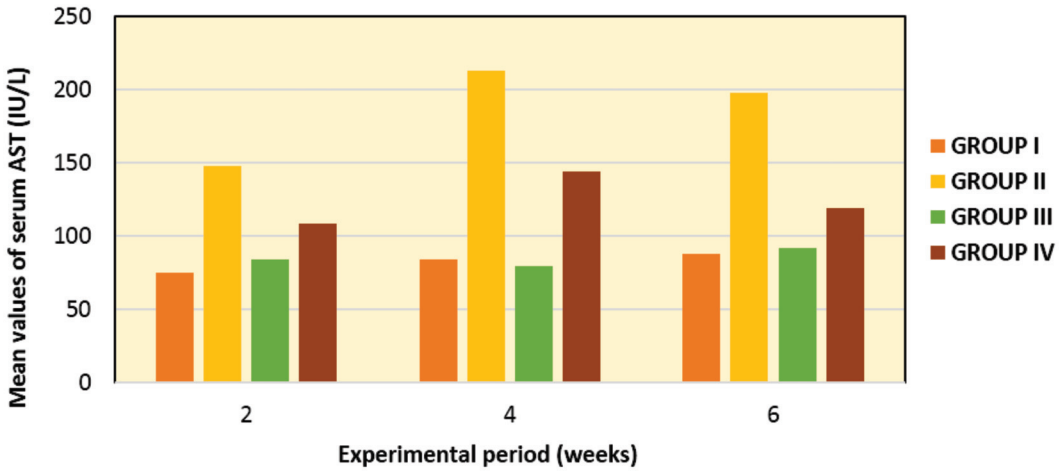

Fig. 5. Mean values of serum AST (IU/L) in rats of different experimental groups.

prior to the commencement of the experiment. The fipronil (Batch No. FIP92B5266, Technical grade) was procured from Gharda Chemicals Ltd. Mumbai with 99% purity. The *Punica granatum* (Pomegranate) peel extract product (Dadim LC23030077) was procured from Chemiloids Life Science Pvt. Ltd. Vijayawada, Andhra Pradesh.

Study design

A total of 24 healthy young male Wistar albino rats were randomly divided into four groups, containing 6 animals each. Fipronil and *Punica granatum* peel extract were administered orally for 6 weeks. Rats in Group I

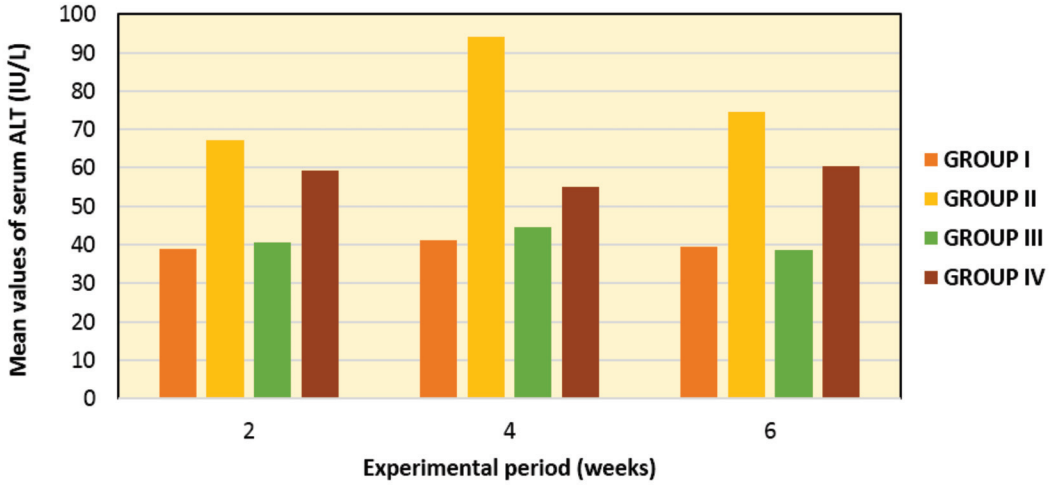

Fig. 6. Mean values of serum ALT (IU/L) in rats of different experimental groups.

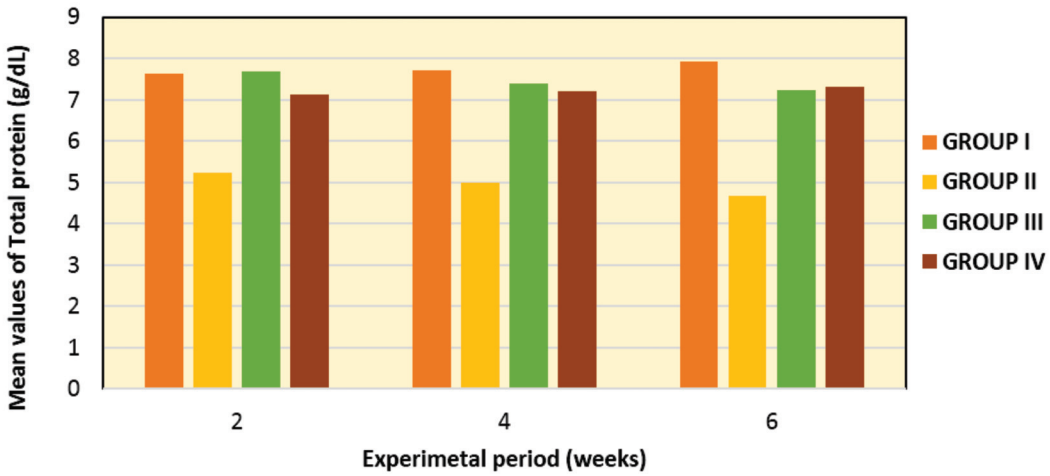

Fig. 7. Mean values of serum Total Protein (g/dL) in rats of different groups.

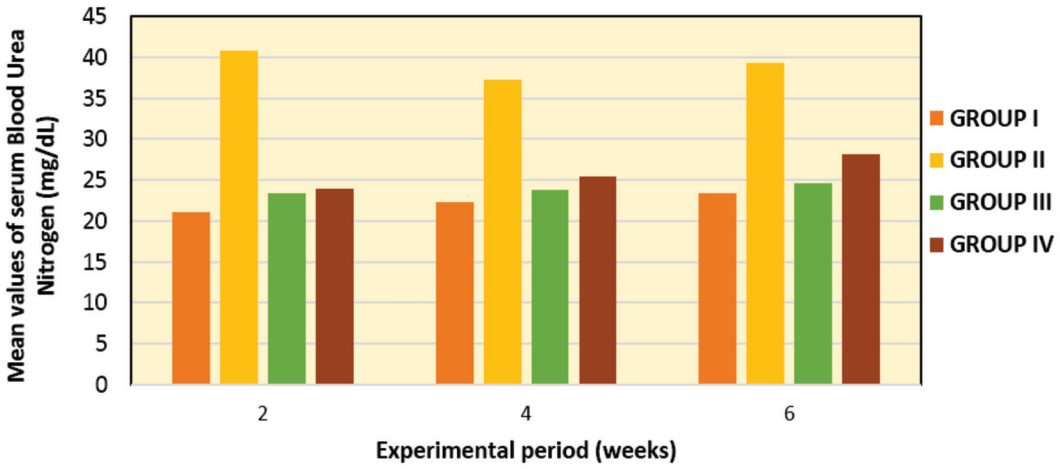

Fig. 8. Mean values of Serum Blood Urea Nitrogen (mg/dL) in rats of different experimental groups.

served as vehicle control and were given feed and water *adlibitum*. Rats in Group II were given fipronil in distilled waterorally at a dose rate of 10 mg/kg b. wt. for a period of 6 weeks using distilled water as vehicle. Rats in Group III were treated *Punica granatum* peel extract orally at a dose rate of 200 mg/kg b. wt. and Group IV rats were treated with fipronil along with *Punica granatum* peel at the dose rates of 10 mg/kg and 200 mg/kg b. wt. respectively.

Pooled blood and serum samples were collected at fortnight interval from all groups for hematological and biochemical studies. All rats were maintained for 6 weeks and sacrificed at the end of the research study (45th day).

Haematology

Pooled blood samples were collected in EDTA vials at fortnight intervals from all the groups for hematological studies such as Total Leucocyte Count (TLC), Total Erythrocyte Count (TEC) by dilution method[12], Haemoglobin by Sahli's method[13] and Packed Cell Volume (PCV) by Micro haematocrit method[12]. The blood smears were directly prepared and stained by Field's stain for Differential Leucocyte Count (DLC) by Battlement method[12].

Biochemical profiles

Blood was collected from all groups at fortnight intervals directly into a serum vials and allowed to clot. The serum was separated after being centrifuged at 4000 rpm for 20 minutes, stored at -20°C and thereafter used for the estimation of ALT, AST, BUN, creatinine, total protein, and albumin by using Auto span semiautomatic biochemical analyzer with commercially available ERBA biochemical kits.

Statistical analysis

By performing one-way ANOVA, the results were statistically analysed[14].

RESULTS

Total Erythrocyte Count (TEC)

The mean TEC values were 8.59, 6.45, 8.74, and 7.97 (millions/µl) in Group I to IV respectively, and are given in Table 1 and Figure 1. There was a significant ($p<0.05$) decrease in mean TEC values in fipronil treated rats (group II) when compared to the control rats (group I). *Punica granatum* ameliorated rats (group IV) showed a statistically significant improvement in mean TEC values when compared to the fipronil treated rats (group II). At the same time there was no significant difference between the *Punica granatum* treated rats (group III) when compared to control (group I).

Haemoglobin (Hb)

The mean Hb concentration were 14, 10.26, 14.33, and 12.86 (g%) in Group I to IV respectively, and are shown in Table 2 and Figure 2**.** A significant ($P< 0.05$) decrease was recorded in mean Hb concentration in fipronil treated rats (group II) compared to the control rats (group I). *Punica granatum* ameliorated rats (group IV) showed a statistically significant improvement in mean Hb concentration when compared to the fipronil treated rats (group II).

Packed Cell Volume (PCV)

The mean values of PCV were 42, 33.33, 43.6, and 40 (%) in Group I to IV respectively, and depicted in Table 3 and Figure 3. There was a significant ($P< 0.05$) decrease in mean PCV values in fipronil treated rats (group II) when compared to the control rats (group I). *Punica granatum* ameliorated rats (group IV) showed a statistically significant improvement in mean PCV values when compared to the fipronil treated rats (group II).

Total Leukocyte Count (TLC)

The mean TLC values in Group I to IV were 8.12, 6.68, 8.10, and 7.95 (Thousands/µl) respectively and given in Table 4 and Figure 4. There was a significant ($P< 0.05$) decrease in mean TLC values in fipronil treated rats (group II) when compared to the control rats (group I). A nonsignificant improvement in TLC values of ameliorated (group IV) rats was observed when compared to fipronil treated rats (group II).

Percent Neutrophil Count

The mean percent neutrophil count values were 19, 23.66, 17.33, and 18.66 (%) in Group I to IV respectively, and given in Table 5. There was a significant ($P<0.05$)

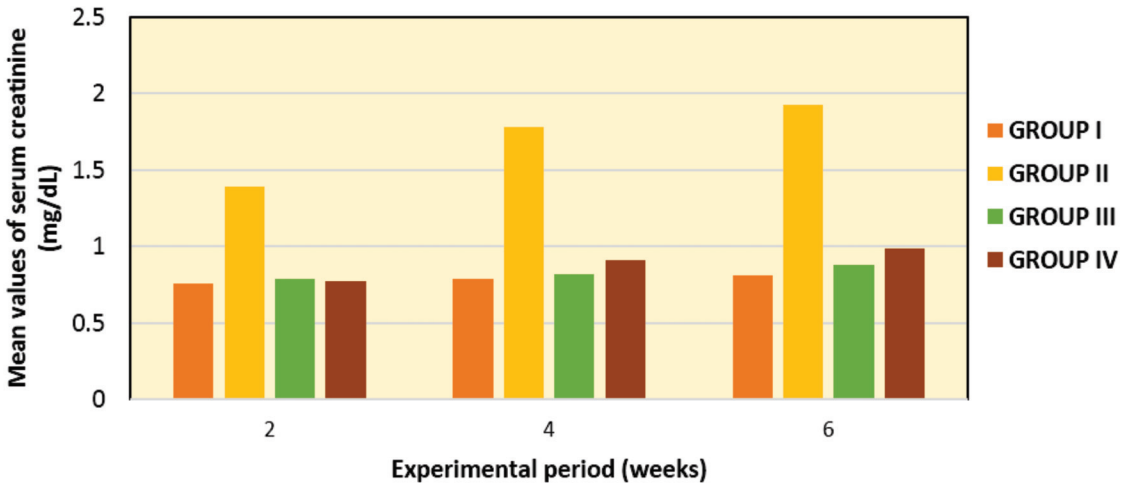

Fig. 9. Mean values of Serum Creatinine (mg/dL) in rats of different experimental groups.

Table 1. Mean values of Total Erythrocyte Count (millions/µl) in rats of different experimental groups.

Experimental Period (Weeks)	GROUP I	GROUP II	GROUP III	GROUP IV
2	8.31	7.21	8.43	7.94
4	8.52	6.26	8.82	7.82
6	8.96	5.88	8.99	8.16
Mean ± SE	8.59 ± 0.19^{a}	6.45 ± 0.39^{b}	8.74 ± 0.16^{a}	7.97 ± 0.09^{a}

Mean values with different superscripts differ significantly (P < 0.05), ANOVA, SE - Standard error

Table 2. Mean values of Haemoglobin (gm%) in rats of different experimental groups.

Experimental Period (Weeks)	GROUP I	GROUP II	GROUP III	GROUP IV
2	13.2	10.4	14	12.6
4	14	10.2	14.2	12.8
6	14.8	10.2	14.8	13.2
Mean ± SE	14 ± 0.46^{a}	10.26 ± 0.06^{c}	14.33 ± 0.24^{a}	12.86 ± 0.17^{b}

Mean values with different superscripts differ significantly (P < 0.05), ANOVA, SE - Standard error

Table 3. Mean values of Packed cell volume (%) in rats of different experimental groups.

Experimental Period (Weeks)	GROUP I	GROUP II	GROUP III	GROUP IV
2	40	37	39	38
4	42	32	46	38
6	44	31	46	44
Mean ± SE	42 ± 1.15^{a}	33.33 ± 1.85^{b}	43.6 ± 2.33^{a}	40 ± 2^{a}

Mean values with different superscripts differ significantly (P < 0.05), ANOVA, SE - Standard error

Table 4. Mean values of Total Leukocyte Count (thousands/µl) in rats of different experimental groups.

Experimental Period (Weeks)	GROUP I	GROUP II	GROUP III	GROUP IV
2	8.12	7.95	8.35	8.15
4	7.85	5.25	8.10	8.00
6	8.40	4.85	7.85	7.72
Mean ± SE	8.12 ± 0.15^{a}	6.68 ± 0.97^{b}	8.10 ± 0.14^{a}	7.95 ± 0.12^{a}

Mean values with different superscripts differ significantly (P < 0.05), ANOVA, SE - Standard error

Table 5. Mean values of Neutrophil Count (%) in rats of different experimental groups.

Experimental Period (Weeks)	GROUP I	GROUP II	GROUP III	GROUP IV
2	18	22	18	20
4	20	24	17	19
6	19	25	17	17
Mean ± SE	19 ± 0.57^{b}	23.66 ± 0.88^{a}	17.33 ± 0.33^{b}	18.66 ± 0.88^{b}

Mean values with different superscripts differ significantly (P < 0.05), ANOVA, SE - Standard error

increase in the percent neutrophil count in fipronil treated group (Group II) rats compared to the control group (Group I). A significant (P<0.05) reduction in percent neutrophil count was noticed in *Punica granatum* ameliorated rats (Group IV) compared to fipronil treated rats (Group II).

Percent Lymphocyte Count (PLC)

The mean percent lymphocyte count values were 79, 74.33, 80.33, and 78.33 in Group I to IV respectively, and given in Table 6. There was a significant (P<0.05) reduction in the percent lymphocyte count in fipronil treated group (Group II) compared to the control group (Group I). A significant improvement was noticed in PLC values in Group IV compared to fipronil treated rats (Group II).

No significant difference was noticed in various hematological parameters like TEC, Hb, PCV, TLC, percent neutrophil count and percent lymphocyte count among *Punica granatum* treated rats (Group III) when compared to the control (Group I).

Biochemical profile

Aspartate Aminotransferase (AST)

The mean AST values in Group I to IV were 82.49, 186.30, 85.16, and 123.89 (IU/L) respectively, and are given in Table 7 and Figure 5. In comparison to control rats (Group I), fipronil treated rats (group II) showed a statistically significant (P< 0.05) increase in mean AST levels. No significant difference was noticed in the values of *Punica granatum* treated rats (Group III) compared to control rats (Group I). Meanwhile, serum AST values in Punica granatum ameliorated rats (group IV) were significantly decreased when compared to the fipronil treated rats (group II).

Alanine Aminotransferase (ALT)

The mean ALT values in Group I to IV were 39.78, 78.67, 41.27, and 58.21(IU/L) respectively, and are given in Table 8 and Figure 6. There was a significant (P< 0.05) increase in mean ALT levels in fipronil treated rats (group II) when compared to the control rats (group I). A significant decrease in mean serum ALT values was noticed in *Punica granatum* ameliorated rats (group IV) when compared to the fipronil treated rats (group II). No significant difference was noticed in the values of

Table 6. Mean values of Lymphocyte Count (%) in rats of different experimental groups.

Experimental Period (Weeks)	GROUP I	GROUP II	GROUP III	GROUP IV
2	80	76	81	78
4	78	73	80	76
6	79	74	80	81
Mean ± SE	79 ± 0.57[a]	74.33 ± 0.88[b]	80.33 ± 0.33[a]	78.33 ± 1.45[a]

Mean values with different superscripts differ significantly (P < 0.05), ANOVA, SE - Standard error

Table 7. Mean serum AST values (IU/L) in rats of different experimental groups.

Experimental Period (Weeks)	GROUP I	GROUP II	GROUP III	GROUP IV
2	75.19	147.49	84.21	108.12
4	84.16	213.31	79.63	144.26
6	88.14	198.12	91.64	119.30
Mean ± SE	82.49 ± 3.82[c]	186.30 ± 19.89[a]	85.16 ± 3.49[c]	123.89 ± 10.68[b]

Mean values with different superscripts differ significantly (P < 0.05), ANOVA, SE - Standard error

Table 8. Mean serum ALT values (IU/L) in rats of different experimental groups.

Experimental Period (Weeks)	GROUP I	GROUP II	GROUP III	GROUP IV
2	38.76	67.20	40.47	59.30
4	41.13	94.22	44.64	54.91
6	39.46	74.60	38.65	60.43
Mean ± SE	39.78 ± 0.7[c]	78.67 ± 8.06[a]	41.27 ± 1.77[c]	58.21 ± 1.68[b]

Mean values with different superscripts differ significantly (P < 0.05), ANOVA, SE - Standard error

Table 9. Mean values of serum Total Protein (g/dL) in rats of different experimental groups.

Experimental Period (Weeks)	GROUP I	GROUP II	GROUP III	GROUP IV
2	7.63	5.24	7.68	7.12
4	7.71	4.98	7.40	7.19
6	7.92	4.67	7.24	7.32
Mean ± SE	7.75 ± 0.08[a]	4.96 ± 0.16[c]	7.44 ± 0.12[ab]	7.21 ± 0.05[b]

Mean values with different superscripts differ significantly (P < 0.05), ANOVA, SE - Standard error

Table 10. Mean values of serum Albumin (g/dL) in rats of different experimental groups.

Experimental Period (Weeks)	GROUP I	GROUP II	GROUP III	GROUP IV
2	4.39	3.42	4.25	4.05
4	4.38	2.99	4.19	4.38
6	4.55	2.79	4.60	4.41
Mean ± SE	4.44 ± 0.05[a]	3.06 ± 0.18[b]	4.34 ± 0.12[a]	4.28 ± 0.11[a]

Mean values with different superscripts differ significantly (P < 0.05), ANOVA, SE - Standard error

Punica granatum treated rats (Group III) compared to control rats (Group I).

Serum Total Protein

The mean TSP values in Group I, II, III, and IV were 7.75, 4.96, 7.44, and 7.21 (g/dL) respectively, and are given in Table 9 and Figure 7. There was a significant (P<0.05) decrease in total protein value in fipronil treated rats (Group II) compared to control rats (Group I). No significant difference was noticed in the values of *Punica granatum* treated rats (Group III) compared to control rats (Group I). At the same time, a significant improvement was noticed in *Punica granatum* ameliorated rats (Group IV) compared to fipronil treated rats (Group II).

Serum Albumin

The mean albumin values in Group I to IV were 4.44, 3.06, 4.34, and 4.28 (g/dL) respectively, and are given in Table 10. There was a significant (P<0.05) difference in serum albumin values in control rats (Group I) and fipronil treated rats (Group IV). No significant difference was noticed in the values of *Punica granatum* treated rats (Group IV) compared to control rats (Group I). Meanwhile, significant improvement was noticed in *Punica granatum* ameliorated rats (Group IV) compared to fipronil treated rats (Group II).

Serum Globulin

The mean serum globulin values in Group I to IV were 3.31, 1.89, 3.09, and 2.93 (g/dL) respectively and depicted in Table 11. Statistically, a significant (P<0.05) decrease in mean serum globulin levels in fipronil treated rats (Group II) was observed when compared to the control rats (Group I). No significant difference was noticed in the values of *Punica granatum* treated rats (Group III) compared to control rats (Group I).

Serum Blood Urea Nitrogen (mg/dL)

A significant (P<0.05) increase in mean serum BUN values was recorded in fipronil treated rats (Group II) compared to control rats (Group I). The mean serum blood urea nitrogen values in Group I to IV were 22.26, 39.12, 23.93, and 25.83 respectively and given in Table 12 and Figure 8. No significant difference was noticed in the values of *Punica granatum* treated rats

Table 11. Mean values of serum Globulin (g/dL) in rats of different experimental groups.

Experimental Period (Weeks)	GROUP I	GROUP II	GROUP III	GROUP IV
2	3.24	1.82	3.43	3.07
4	3.33	1.99	3.21	2.81
6	3.37	1.88	2.64	2.91
Mean ± SE	3.31 ± 0.03^{a}	1.89 ± 0.49^{b}	3.09 ± 0.23^{a}	2.93 ± 0.07^{a}

Mean values with different superscripts differ significantly (P < 0.05), ANOVA, SE - Standard error

Table 12. Mean values of Serum Blood Urea Nitrogen (mg/dL) in rats of different experimental groups.

Experimental Period (Weeks)	GROUP I	GROUP II	GROUP III	GROUP IV
2	21.08	40.83	23.41	23.96
4	22.25	37.25	23.77	25.44
6	23.45	39.28	24.62	28.10
Mean ± SE	22.26 ± 0.68^{c}	39.12 ± 1.03^{a}	23.93 ± 0.35^{bc}	25.83 ± 1.21^{b}

Mean values with different superscripts differ significantly (P < 0.05), ANOVA, SE - Standard error

Table 13. Mean values of Serum Creatinine (mg/dL) in rats of different experimental groups.

Experimental Period (Weeks)	GROUP I	GROUP II	GROUP III	GROUP IV
2	0.76	1.39	0.79	0.77
4	0.79	1.78	0.82	0.91
6	0.81	1.93	0.88	0.99
Mean ± SE	0.78 ± 0.01^{b}	1.7 ± 0.16^{a}	0.83 ± 0.02^{b}	0.89 ± 0.06^{b}

Mean values with different superscripts differ significantly (P < 0.05), ANOVA, SE - Standard error

(Group III) compared to control rats (Group I). A nonsignificant improvement was noticed in Group IV rats as compared to Group II rats.

Serum Creatinine (mg/dL)

The mean serum creatinine values in Group I to IV were 0.78, 1.7, 0.83, and 0.89 (mg/dL) respectively and presented in Table 13 and Figure 9. A significant (P<0.05) increase in the serum creatinine values was recorded in fipronil treated rats (Group II) compared to control rats. A nonsignificant improvement was observed in Group IV rats as compared to Group II rats. No significant difference was noticed in values of *Punica granatum* treated rats (Group III) and ameliorated rats (Group IV) compared to control rats (Group I).

DISCUSSION

Data obtained from the present study indicated significant decrease in TEC, Hb, and PCV values in fipronil treated rats (Group II) when compared to the corresponding control group (Group I). This was in accordance with the findings of previous authors[15]. The reduction in Hb value is mainly due to decreased rate of haemoglobin synthesis or an increased rate of destruction of hemoglobin. Normally, body utilises iron either from dietary sources or from stored ferritin. In experimental rats, reduced feed intake along with a lack of additional iron supplementation may result in decreased production of haemoglobin[16]. Decreased PCV and TEC values in fipronil treated rats might be due to the adverse effect of fipronil on haemopoietic tissue thereby demolishing the erythropoietic mechanism[17]. Excess production of free radicals by fipronil results in increased rate of erythrocyte destruction which also results in impairment in hematological parameters[18].

Significant leukopenia along with lymphocytopenia and neutrophilia was observed in fipronil treated rats (Group II) when compared to corresponding control rats (Group I). These findings were in agreement with findings of[12] who observed sudden elevation followed by a sudden decline in WBC count in fipronil-treated rats in dose dose-dependent manner. The leukopenia might be due to lymphocytolysis associated with fipronil toxicity in lymphoid organs like lymph nodes and spleen as observed microscopically in the present study. Decreased lymphocyte counts are also indicative of immunosuppressive effects of fipronil in animals.

Punica granatum ameliorated rats (Group IV) showed significant improvement in the various haematological parameters like Hb, PCV, TEC, Total leucocyte, and lymphocyte count when compared to fipronil treated rats (Group II). This was in accordance with the observations of earlier author[19]. This might be due to immunomodulatory effects[20] and antioxidant property[21] of pomegranate peel extract which helps to scavenge the free radicals which damage haemopoietic cells.

Evaluation of biochemical parameters revealed significant increase (P<0.05) in mean aspartate aminotransferase (AST) and alanine aminotransferase (ALT) levels in fipronil treated rats (Group II) when compared to control rats (Group I). These findings were in accordance with the findings of authors[22]. AST and ALT are the major hepatic enzymes that are responsible for the biosynthesis of essential macromolecules and detoxification[23] and are hence considered to be the specific indicators of hepatic damage[24]. Elevated levels of AST, and ALT might be due to the

hepatic damage induced by fipronil which in turn alters the permeability of the liver membrane[25]. Exact molecular mechanism behind hepatic damage and elevated serum liver enzymes is that, fipronil initially undergoes biotransformation to fipronil sulfone in liver, which then binds to mitochondrial membrane and alter electron transport chain[26]. Impaired mitochondrial membrane potential and electron transport chain results in decreased ATP production, reduced cell viability of hepatocytes and excess release of Ca^{2+} into cytoplasm[27]. Increased cytosolic Ca^{2+} activates proteases, phospholipases and ion dependant endonucleases production. It will disrupt the cytoskeleton - plasma membrane interaction and destabilise lipid bilayer configuration. Loss of membrane integrity of hepatocytes ultimately results in leakage of mitochondrial enzyme (AST) and cytoplasmic enzyme (ALT) into blood[28].

Mean serum total protein, albumin, and globulin values were significantly ($P< 0.05$) decreased in fipronil treated rats (Group II) when compared to control rats (Group I) and the results. Decrease in serum total protein, albumin, and globulin levels in experimental rats might be due to decreased production of serum proteins in liver due to hepatocellular injury induced by fipronil. Molecular mechanism remains the same as explained.

Significant reduction in serum AST and ALT values and increased serum TP, albumin, and globulin values were observed in *Punica granatum* ameliorated rats (group IV) compared to fipronil treated rats (Group II). It might be due to the hepatoprotective action of various polyphenolic compounds like ellagic acids and anthocyanins present in pomegranate peel extract[30].

A significant increase in the serum creatinine and BUN values was observed in fipronil treated rats (Group II) when compared to control rats (Group I). Similar observations were reported by previous authors[31,32]. Normally, creatine phosphate present in the muscle undergoes metabolic breakdown to produce creatinine. Similarly, urea is produced as a major nitrogenous end-product of amino acid and protein metabolism. Both of them were filtered and eliminated from blood through glomeruli. But, when there is any renal impairment, these enzyme levels get elevated in blood. Fipronil increases NADPH oxidase (NOXs) levels and superoxide levels in mitochondrial membrane of renal epithelium. It will further increase the ROS signalling in the cells and produces excess free radicals. Generated free radical binds to plasma membrane and in turn generates more lipid peroxidase by autocatalytic process. Increased lipid peroxidase and ROS may alter the structural configurations of proteins and lipids of renal tissue which results in complete distortion in renal architecture. Altered glomerular structure subsequently results in decreased glomerular filtration and elimination of urea and creatinine from the body, thereby causing the elevation of these enzymes in the blood[33].

Significant ($P<0.05$) decrease in serum creatinine and BUN levels were observed in *Punica granatum* ameliorated rats (group IV) compared to control rats (group I). It might be due to the nephroprotective property of pomegranate peel extract as reported by authors[34] in rats.

CONCLUSION

Results of the present investigation ascertain that fipronil causes alterations in various haemato-biochemical indices in rats and co-administration of *Punica granatum* peel extract along with fipronil have protective effects on different haemato-biochemical alterations. So, supplementation of herbal agents like *Punica granatum* peel extract could be an alternative method to mitigate the hemotoxic effects and biochemical alterations induced by fipronil.

ACKNOWLEDGMENTS

The authors are thankful to the Sri Venkateswara Veterinary University, Tirupati for providing various facilities to carry out the present research work.

REFERENCES

1. Eisenstein M. 2015. Pesticides: Seeking answers amid a toxic debate. *Nature* **521:** 52-55.
2. David M and Kartheek RM. 2015. Malathion acute toxicity in tadpoles of Duttaphrynus melanostictus, morphological and behavioural study. *The J Bas Appl Zool* **72:** 1-7.
3. Tingle CC, Rother JA, Dewhurst CF, Lauer S and King WJ. 2003. Fipronil: environmental fate, ecotoxicology, and human health concerns. *Rev Environ Contam Toxicol* **176:** 1-66.
4. Badgujar PC, Pawar NN, Chandratre GA, Telang AG and Sharma AK. 2015. Fipronil induced oxidative stress in kidney and brain of mice: protective effect of vitamin E and vitamin C. *Pestic Biochem Physi* **118:** 10-18.
5. Romero A, Ramos E, Ares I, Castellano V, Martínez M, Martínez-Larrañaga MR, Anadón A and Martínez MA. 2016. Fipronil sulfone induced higher cytotoxicity than fipronil in SH-SY5Y cells: protection by antioxidants. *Toxicol Lett* **252:** 42-49.
6. Gunasekara AS, Truong T, Goh KS, Spurlock F and Tjeerdema RS. 2007. Environmental fate and toxicology of fipronil. *J Pest Sci* **32:** 189-199.
7. Khan S, Jan MH, Kumar D and Telang AG. 2015. Firpronil induced spermotoxicity is associated with oxidative stress, DNA damage and apoptosis in male rats. *Pestic Biochem Physiol* **124:** 8-14.
8. Singh R, Chidambara Murthy K and Jayaprakasha G. 2002. Studies on the antioxidant activity of pomegranate (Punica granatum) peel and seed extracts using in vitro models. *J Agric Food Chem* **50:** 81-6.
9. Lansky EP and Newman RA. 2007. Punica granatum (Pomegranate) and its potential for prevention and treatment of inflammation and cancer. *J Ethnopharmcol* **109:** 177-206.
10. Naz S, Siddiqi R, Ahmad S, Rasool S and Sayeed S. 2007.

Antibacterial activity directed isolation of compounds from Punica granatum. *J Food Sci* **72:** M341-5.
11. Dkhil MA. 2013. Anti-coccidial, anthelmintic and antioxidant activities of pomegranate (Punica granatum) peel extract. *Parasitol Res* **112:** 2639-2646.
12. Jain NC. 1986. Schalms Veterinary Hematology - Lea and Febiger Philadelphia II edition.
13. Coles EH. 1986. Veterinary clinical pathology. WB Saunders Company, Philadelphia, USA, pp. 445-446.
14. Snedecor WG and Cochran GW. 1967. Statistical Methods, 6th Edition, Oxford and IBH Publishing Company, New Delhi. 258-268.
15. Kartheek RM and David M. 2017. Modulations in haematological aspects of Wistar rats exposed to sublethal doses of fipronil under subchronic duration. *J Pharm Chem Biol Sci* **5:** 187-194.
16. Moss J and Hathway E. 1964. *J Biochem* **91:** 383-93.
17. Mehra BL, Sharma P, Kaushik U and Joshi SC. 2014. Effect of Fytolan on Haematology and Serum Parameters of Male Albino Rats. *Int J Pharma Res Health Sci* **2:** 332-338.
18. Wang X, Xu Y, Wang F, Tang L, Liu Z, Li H and Liu S. 2006. Aging related changes of microglia and astrocytes in hypothalamus after intraperitoneal injection of hypertonic salinein rats. *Huaz Univ Sci Technol Med Sci* **26:** 231-234.
19. Abdul-Zahra MT and Jwad SM. 2020. The Effect of Alcoholic Extract of Pomegranate Peel on the level of Erythropoietin and some of the Blood Properties in Albino Male Rats treated with Erythromycin. *International J Psychosocial Rehabilit* **24:** 6350-6361.
20. Labsi M, Khelifi L, Mezioug D, Soufli I and Touil-Boukoffa C. 2016. Antihydatic and immunomodulatory effects of Punica granatum peel aqueous extract in a murine model of echinococcosis. *Asian Pacific J Tropmedi* **9:** 211-220.
21. Chidambara Murthy KN, Jayaprakasha GK and Singh RP. 2002. Studies on antioxidant activity of pomegranate (Punica granatum) peel extract using in vivo models. *Journal of Agricultural Food Chem* **50:** 4791-4795.
22. Mossa ATH, Swelam ES and Mohafrash SMM. 2015. Sub-chronic exposure to fipronil induced oxidative stress, biochemical and histopathological changes in the liver and kidney of male albino rats. *Toxicol Rep* **2:** 775-784.
23. Altenburger R, Boedeker W, Faust M and Grimme LH. 1996. *Food Chem Toxicol* **34:** 1155-1157.
24. Klaassen CD and Eaton DL. 1991. Principles of toxicology. In: Amdur MO, Doull J, Klaassen CD (eds) Toxicology, 4th edn. McGraw Hill, New York, p. 12.
25. Plaa GL and Hewitt WR. 1982. Detection and evaluation of chemically induced liver injury. In: Hayes W (ed) Principles and Methods of Toxicology. Raven Press, New York, p. 407.
26. Caboni P, Sammelson RE and Casida JE. 2003. Phenylpyrazole insecticide photochemistry, metabolism, and GABAergic action: ethiprole compared with fipronil. *J Agric Food Chem* **51:** 7055-7061.
27. Tavares MA, Palma IDF, Medeiros HC, Guelfi M, Santana AT and Mingatto FE. 2015. Comparative effects of fipronil and its metabolites sulfone and desulfinyl on the isolated rat liver mitochondria. *Environ Toxicol Pharmacol* **40:** 206-214.
28. Nicotera P, Leist M and Ferrando-Mey E. 1986. The formation of plasma membrane blebs in hepatocytes exposed to agents that increase cytosolic Ca2+ is mediated by the activation of a nonlysosomal proteolytic system. *FEBS Lett* **209:** 139-144.
29. Goel A, Dani V and Dhawan D. 2005. *J Chem Biol Interact* **156:** 131-140.
30. Ahmad Nadia & Tahir and Mohammad & Lone Khalid. 2016. Amelioration of acetaminophen induced hepatotoxicity by methanolic extract of pomegranate peels in rats. *J Pakistan Medi Assoc* **66:** 859-863.
31. Yadav D, Dewangan G, Rajput N, Waskel N, Dhakar R and Chaudhary K. 2020. Ameliorating effect of curcumin against fipronil induced subacute toxicity in rats. *J Pharmacognosy and Phytochem* **9:** 1518-1520.
32. Abou-Zeid SM, Tahoun EA and AbuBakr HO. 2021. Ameliorative effects of jojoba oil on fipronil-induced hepatorenal-and neuro-toxicity: the antioxidant status and apoptotic markers expression in rats. *Environ Sci and Pollu Res* **28:** 25959-25971.
33. Walmsley RN and White GH. 1994. A Guide to Diagnostic Clinical Chemistry, 3rd edn. Blackwell Scientific Publication, London.
34. Ahmad MM and Ali SE. 2010. Protective effect of pomegranate peel ethanol extract against ferric nitrilotriacetate induced renal oxidative damage in rats. *J Cell Mol Biol* **7 & 8:** 35-43.

Indian J. Vet. Pathol., 48(2) : 169-175, 2024: DOI: 10.5958/0973-970X.2024.00026.3

RESEARCH ARTICLE

Nephropathy associated with bacterial diseases in broiler chicken in Kashmir Valley

Mehvish Rafiq, Pankaj Goswami[1], Mehreen Yaqub, Majid Shafi, Shayaib Ahmad Kamil and Showkat Ahmad Shah*

[1]Division of Veterinary Pathology, R.S. Pura, SKUAST-J, Division of Veterinary Pathology, Faculty of Veterinary Science & Animal Husbandry, Shuhama-190 006, Sher-Kashmir University of Agriculture Science and Technology, Kashmir

Address for Correspondence

Showkat Ahmad Shah, Assistant Professor, Division of Veterinary Pathology, Faculty of Veterinary Science & Animal Husbandry, Shuhama-190 006, Sher-Kashmir University of Agriculture Science and Technology, Kashmir, E-mail: vetshowkat@gmail.com

Received: 25.10.2023; Accepted: 1.12.2023

ABSTRACT

Bacterial nephritis of poultry is responsible for considerable mortality and production losses worldwide, it is the most neglected area in avian pathology. The present study was aimed to elucidate the renal pathology of broiler birds associated with bacterial disease conditions in the temperate climate of Kashmir valley. The research comprised of thorough examination of necropsied birds belonging to different poultry farms of Kashmir valley. A total of 112 cases out of 320 were associated with bacterial disease. The incidence of nephropathy was recorded in 26.8% colibacillosis and 8.1% salmonellosis cases. Tissue samples of affected kidneys were cultured on different microbial agar plates and isolates were confirmed by special culture and biochemical tests. The isolated microorganism included *Escherchia coli* (76.7%), *Salmonella* spp, (7.8%) and *Proteus* spp, (16.1%). The gross changes in the kidneys associated with bacterial nephritis revealed moderate to severe infection characterised by congestion, enlargement, paleness of parenchyma, along with dilated ureters. The histological lesions were characterized by hypertrophy of epithelial cells of renal tubules with pale cytoplasm, congestion of capillaries in both renal glomeruli and intertubular space with hypercellularity of glomeruli and interstitial oedema. In addition, there was atrophy of renal corpuscles affected with bacterial infection by *E. coli* and Salmonella. The present study recorded a high percentage of the *E.coli* isolates (76.7%) in kidneys, confirming the importance of this bacterium for inducing the lesions in kidneys of broilers.

Keywords: Broiler, *Escherchia coli*, kidney, nephropathy

INTRODUCTION

Avian kidneys comprise 1 to 2.6% of body weight and are considered to be important organs just like in mammals[1,2]. These are paired and located in depressions in the pelvis bone in the abdominal cavity with three distinct lobes[1,3]. In both avian and mammals kidneys carry out diverse metabolic and excretory functions such as removal of metabolic waste and toxic products in the form of urine, regulation of blood pressure and blood volume and conservation of fluids and electrolytes. These functions of the kidney are affected by a number of specific diseases and disorders that include gout, urolithiasis, infectious bursal disease, infectious bronchitis, avian nephritis, aspergillosis, and bacterial nephritis. Bacterial nephritis occurs when bacteria enter the kidney secondary to systemic disease through the renal arteries or the renal portal system[4,5]. A wide range of bacteria has been reported to cause bacterial nephritis including *Enterobacteriaceae*, *Pasteurella* spp., *Pseudomonas* spp., *Streptococcus* spp., and *Staphylococcus* spp.[6,7,8]. *Erysipelothrix rhusiopathiae* has also been reported in quail and chicken causing renal lesions[8,9].

How to cite this article : Rafiq, M., Goswami, P., Yaqub, M., Shafi, M., Kamil, S.A. and Shah, S.A. 2024. Nephropathy associated with bacterial diseases in broiler chicken in Kashmir Valley. Indian J. Vet. Pathol., 48(2) : 169-175.

MATERIALS AND METHODS

Sampling and Occurrence

In order to study the occurrence of nephropathies, poultry carcasses from various poultry farms of Kashmir valley as well as University farms were brought for disease diagnosis to the Division of Veterinary Pathology, FVSc & AH, SKUAST-K. The investigation included the collection of history from the farmer, data on mortality patterns, post-mortem examinations, pathogen isolation/identification and histopathology.

Pathogen isolation/identification

Bacterial isolation

Kidney samples from selected cases were collected and processed for isolation of commonly occurring bacteria of *Enterobacteriaceae* family.

Isolation and characterisation of *Enterobacteriaceae*

For bacteriological examination, kidney tissues were collected following sterile precautions immediately after opening the abdominal cavity and the *Enterobacteriaceae* family was isolated according to standard

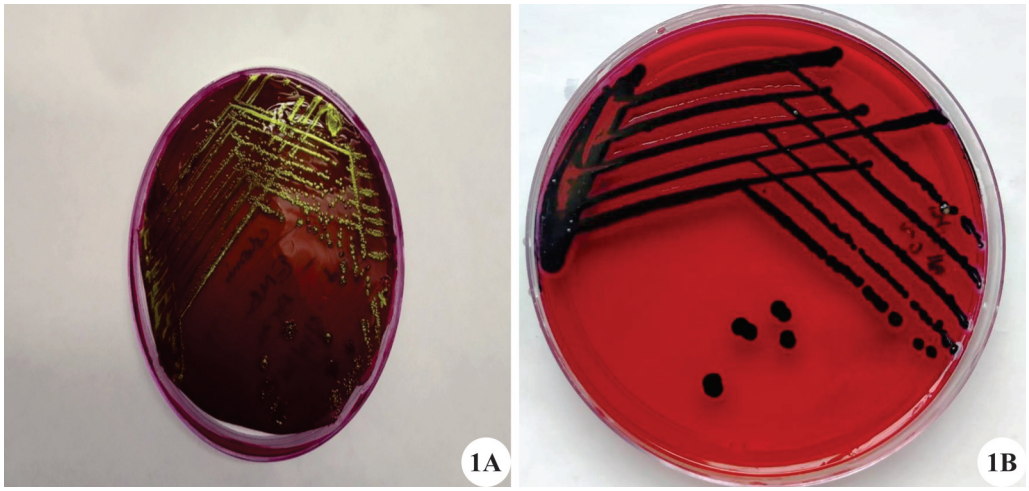

Fig. 1A. Characteristic metallic sheen of *E. coli* on EMB agar plate. **B.** Characteristic red colonies with black centre of *Salmonella* spp on XLD agar.

methods[10]. Primary cultures were evaluated by visual examination of morphology of the bacterial colonies and sub-cultured for further examination. The identification of the isolated colonies was confirmed using standard bacteriological and biochemical procedures as described by[11,12].

Pathological studies

Gross pathology

The birds were subjected to thorough postmortem examination. The kidneys were thoroughly examined for gross lesions in the identified diseases such as change in colour, consistency, size, distribution and type of lesions.

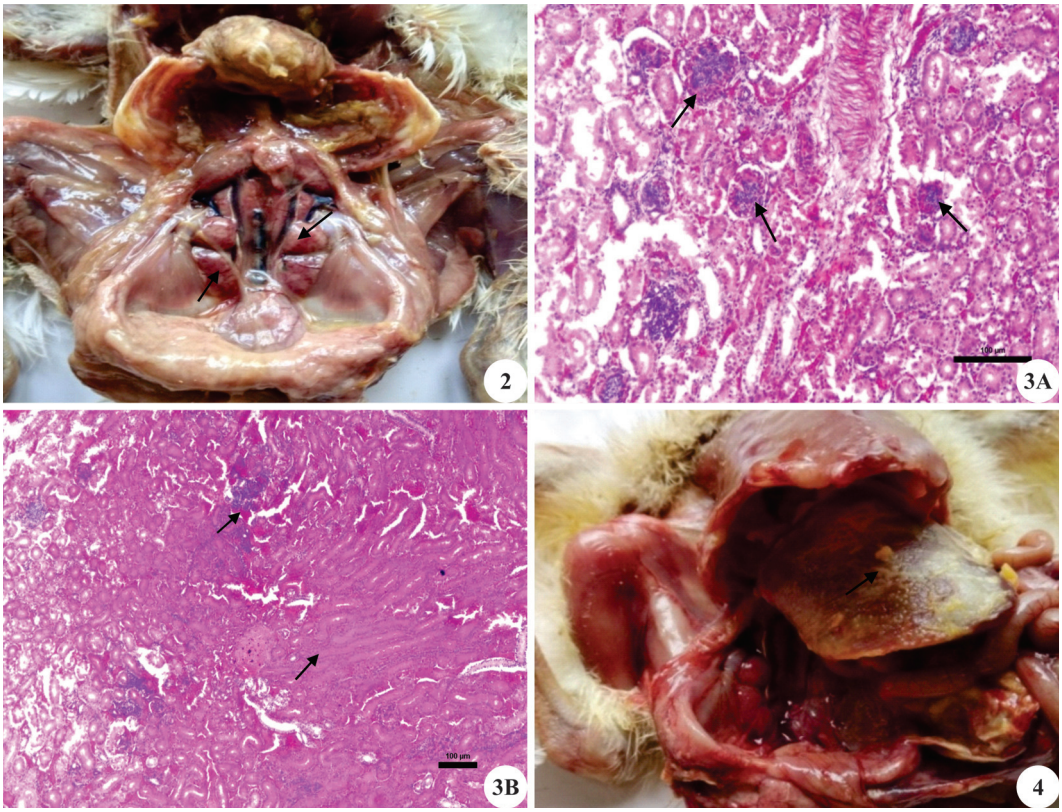

Fig. 2. Broiler chicken affected with colibacillosis showing necrotic foci and pinpoint haemorrhages on the surface of swollen kidney; **Fig. 3A.** Section of kidney from colibacillosis affected chicken revealing hypertrophy of epithelial cells of renal tubules with pale cytoplasm and atrophy of renal corpuscles (H&E). **B.** Section of kidney from colibacillosis affected chicken revealing oedema and heterophilic infiltration at corticomedullary junction (H&E); **Fig. 4.** Broiler chicken affected with severe colibacillosis showing massive fibrin deposition with formation of lumps on liver parenchyma.

The associated gross abnormalities in the other organs were also recorded.

Histopathology

Representative tissue samples from kidneys and other affected organs were collected in 10% neutral buffered formalin for fixation. The tissue samples were processed for routine paraffin embedding technique and 5 micron thin tissue sections were cut and stained with Haris' Haematoxylin and Eosin[13].

RESULTS

The isolation and identification for bacteria belonging to the *Enterobacteriaceae* family was done as per standard protocol. A total of 112 birds showing kidney lesions suspected for bacterial nephritis encountered at post-mortem examination were subjected for isolation and identification of bacteria. Pooled tissue samples from all lobes of kidneys were initially placed in nutrient broth as well as in buffered peptone water and kept at 37^{O}C overnight. For isolation of *E.coli,* inoculums from nutrient broth were streaked on McConkey agar plates, and kept for 24 hours at 37^{O}C. Similarly for isolation of *Salmonella spp.* samples enriched in buffered peptone water were directly inoculated in tetrathionate broth for overnight incubation.

Growth on selective media

The rose pink colonies that were identified as Gram-negative rods were inoculated on eosin methylene blue (EMB) agar plates. On EMB the *E. coli* isolates showed typical metallic sheen (Fig. 1A).

The inoculum from tetrathionate broth was cultured on xylose deoxycholate (XLD); presence of red colonies with black centers provided confirmation for *Salmonella* Spp. (Fig. 1B).

Biochemical characterization

Further the identification of the isolated colonies was performed using standard bacteriological and biochemical procedures. *Proteus* spp. bacteria were identified from the Salmonella enriched media by urease test.

Bacteriological and biochemical test results showed 76.7% (86) of isolates were *E. coli,* 7.8% (8) isolates were *Salmonella* spp and 21.6% (18) isolate was of *Proteus* spp. There was no mixed infection of bacteria that has been identified.

Pathomorphological studies

Colibacillosis

Avian colibacillosis was recorded in 86 cases showing generalised septicaemia and other characteristic post-mortem changes. The gross and histopathological lesions recorded in various visceral organs along with appreciable kidney lesions are described below.

Kidney

Gross pathology

The gross lesions were observed in different lobes of kidneys and severity was categorized. In severe cases, kidneys were swollen, pale in colour with dilated ureters. Some of the cases also revealed presence of necrotic foci and pin point haemorrhages on the surface of kidney besides enlargement (Fig. 2). In less severe cases moderate enlargement of kidney parenchyma, oedema and congestion were noticed.

Histopathology

The histopathological examination of affected kidneys included atrophy of renal corpuscles, in addition there was hypertrophy of epithelial cells of renal tubules with pale cytoplasm, (Fig. 3A). Corticomedullary junction showed heterophilic infiltration within tubular as well as intertubular area, oedema and haemorrhages (Fig. 3B).

Liver

Gross pathology

Postmortem findings revealed perihepatitis with

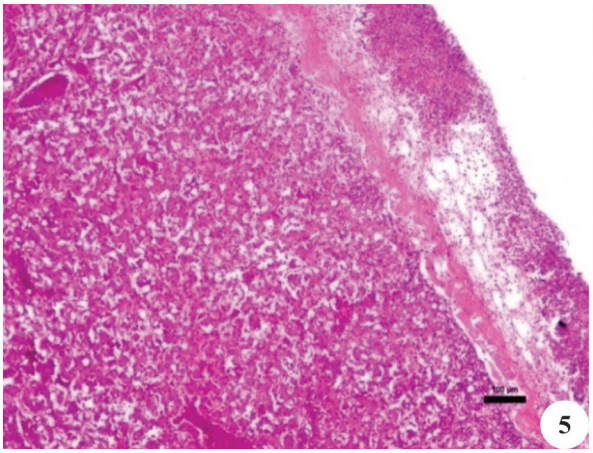

Fig. 5. Section of liver from colibacillosis affected chicken revealing fibrinous perihepatitis and degeneration of hepatocytes (H&E); **Fig. 6.** Broiler chicken affected with colibacillosis showing fibrinous pericarditis.

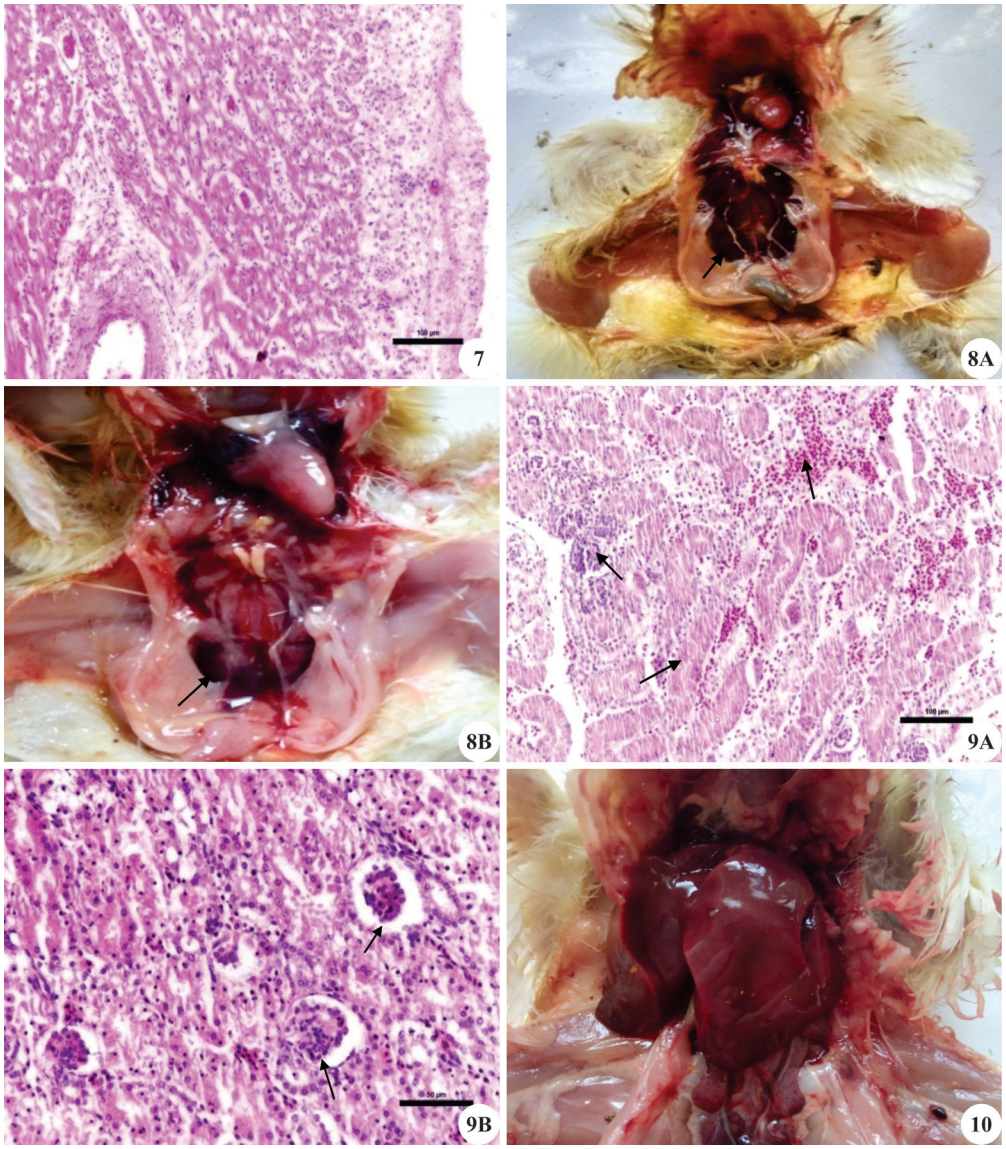

Fig. 7. Section of heart from colibacillosis affected chicken revealing thickening of pericardium along with fibrinous exudates and myocardial infiltration (H&E); **Fig. 8A.** Broiler chicken affected with Salmonellosis showing atrophied kidneys and urate deposition in ureters. **B.** Broiler chicken affected with salmonellosis showing haemorrhages on surface of kidney and right distal division of kidney depressed in renal fossa with whitish fluid material in dilated ureters; **Fig. 9A.** Section of kidney from salmonellosis affected chicken revealing homogenous pinkish cellular material in lumen of renal tubules along with haemorrhage and leukocytic infiltration (H&E). **B.** Section of kidney from salmonellosis affected chicken revealing increase in bowman's space with glomerular changes (H&E); **Fig. 10.** Broiler chicken affected with salmonellosis showing marked enlargement with bronze discolouration of liver.

formation of white yellowish fibrin covering over liver. In advanced cases of *E.coli* infection massive fibrin deposition covered the whole liver giving characteristic "bread and butter" appearance (Fig. 4). In some cases the liver showed severe haemorrhages and focal areas of necrosis.

Histopathology

Microscopically, there was degeneration of hepatocytes along with fibrinous perihepatitis and thickening of liver capsule (Fig. 5). In severe cases, marked congestion as well as marked infiltration of heterophils in hepatic parenchyma with loss of hepatocytes was seen.

Heart

Gross pathology

In severe outbreaks, the heart was covered with a thick layer of fibrin and revealed congestion and pinpoint haemorrhages in most of the cases (Fig. 6).

Histopathology

In general there was fibrinous pericarditis along with myocardial infiltration (Fig. 7).

Salmonellosis

Nephropathy was also encountered in salmonellosis cases. Salmonella organism was isolated from kidney

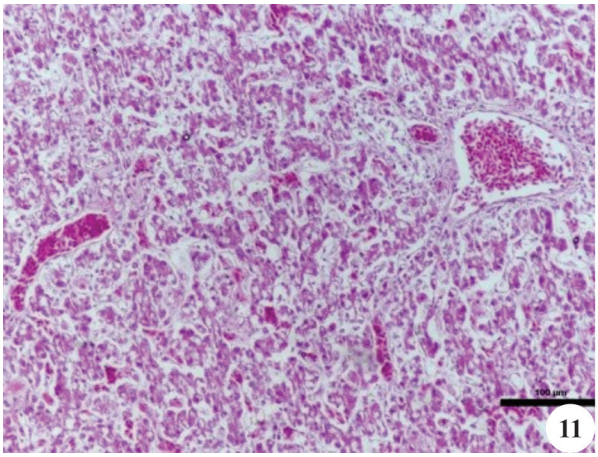

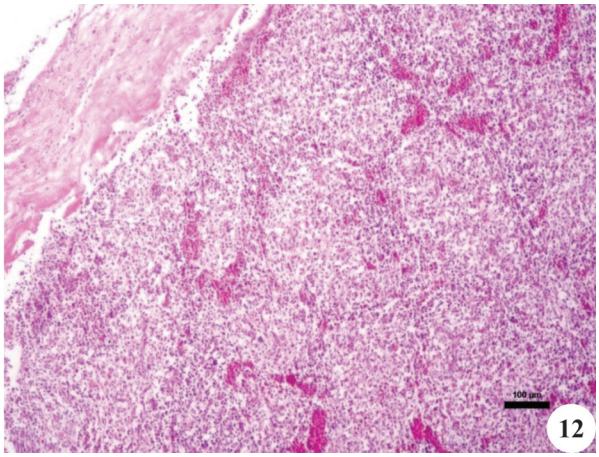

Fig. 11. Section of liver from salmonellosis affected chicken revealing haemorrhages along with necrosis of hepatocytes and vacuolar degeneration (H&E); **Fig. 12.** Section of spleen from salmonellosis affected chicken revealing congestion along with spleenic necrosis and heterophilic infiltration (H&E).

tissue in 8 cases suspected for salmonellosis. The gross and histopathological lesions are described below.

Kidney

Gross pathology

In Salmonella positive cases, the kidney showed marked congestion and enlargement. In certain cases nephrosis was seen in atrophic kidneys with urate deposition in distended ureters (Fig. 8A). Haemorrhages with the right distal lobe of kidneys depressed in renal fossa were seen with whitish fluid materials in dilated ureters (Fig. 8B).

Histopathology

Lesions in kidneys were characterized by cortical congestion. Renal tubules showed homogenous pinkish cellular material in lumen and haemorrhages (Fig. 9A). Increased Bowman's space with glomerular changes revealing necrosis, disruption and in few cases mild glomerulitis was other evident feature (Fig. 9B). Interstitial nephritis and deposition of urate crystals with marked congestion and haemorrhages along with tubular nephritis with necrotic heterophils mixed with mononuclear cells was also observed.

Liver

Gross pathology

Liver showed marked enlargement, bronze discolouration with mahogany colour appeared as metallic sheen on surface parenchyma (Fig. 10).

Histopathology

The liver revealed vascular congestion, vacuolar degenerative changes and diffuse hepatic necrosis (Fig. 11). Fatty changes in hepatocytes and focal infiltration of both heterophils and mononuclear cells was seen in some cases. Degenerated erythrocytes along with macrophages in and around periportal vessels were also noticed.

Spleen

Gross pathology

Spleen was enlarged and congested in all positive cases of Salmonella affection.

Histopathology

Microscopically, spleen showed loss of the germinal centre of follicles and marked necrotic changes of lymphocytes. In most of the cases, besides congestion of spleen, there was diffused splenic necrosis and cells were replaced by leukocytes and reticuloendothelial cells (Fig. 12).

DISCUSSION

Bacteria are pathogenic living organisms but; not all the bacteria are detrimental to poultry health. In fact, many bacteria are beneficial and necessary for processes such as food digestion and manufacturing of some dairy products. The present investigation recorded a considerable percent (112/320; 35%) of nephropathy associated with bacterial diseases. The results of bacteriological and biochemical tests showed that 76.7% (86) of isolates were *E.coli*, 16.1% (18) isolates were *Proteus* spp. and 7.8% (8) isolates were *Salmonella* spp. The isolation results of the present study revealed high percentage of *E.coli* which agree with results mentioned by[14,15], the high percentage of the *E.coli* isolates (76.7%), confirmed the importance of this bacteria for inducing the lesions in kidneys of broiler chicks which is identical to the earlier results[6]. A wide range of bacteria has been reported to cause bacterial nephritis including *Enterobacteriaceae, Pasteurella* spp., *Pseudomonas* spp., *Streptococcus* spp., and *Staphylococcus* spp. in layer birds[6-8]. However, the present report recorded *Enterobacteriaceae* family only in the broiler birds of Kashmir valley. The absence of lymph nodes and the presence of renal and hepatic portal systems in birds increase the risk of systemic or gastrointestinal microbes affecting the

kidney. The gross changes in the kidney associated with bacterial nephritis revealed moderate to severe infection characterized by congestion, enlargement, paleness of parenchyma, along with dilated ureters. In some cases kidneys were found depressed in renal fossa showing atrophy of the organ. Enlargement of the kidneys has been reported in a number of common infectious diseases ascribed with viral and bacterial infection[6,16,17]. Generally lesions in the kidney varied from congestion, oedema and in severe cases presence of pinpoint haemorrhages on its surface. Similar changes were also observed in earlier studies[18] whereas other reports suggested that there were no appreciable changes in kidneys in colibacillosis affected chicken[19].

The histopathological examination of the affected kidney included atrophy of renal corpuscles; in addition there was hypertrophy of epithelial cells of renal tubules with pale cytoplasm affected with bacterial infection by *E. coli* and *Salmonella*. The results of histopathological examination of the current study are identical with those mentioned by[6,15]. The histological changes in the kidney with bacterial infection also consisted of inflammatory changes like accumulation of heterophils, focal areas of mononuclear cell infiltration and hypercellularity of glomeruli. The observations were in concurrence with earlier researchers[20], who also observed kidneys revealing marked congestion and interstitial oedema along with infiltration of mononuclear cells in colibacillosis. However, report of[19] indicated that *E. coli* infected birds fed with ocharatoxin A did not reveal appreciable changes in kidneys, bursa and thymus. Degeneration, necrosis, desquamation of epithelial cells of tubular epithelium was also observed by previous workers in renal infections[6]. The colibacillosis in poultry evolves as a systemic infection (perihepatitis, pericarditis, and septicaemia) due to the invasive abilities of the *E. coli* strains[21], hence, can infect and cause damage to the both kidneys and impair its functions[14].

CONCLUSION

In conclusion, post-mortem findings have revealed the presence of kidney lesions in broiler chicken due to bacteria. In the present study, *E.coli* was recorded in most cases with appreciable kidney lesion and generalised septicaemia. Pathological lesions in the kidneys are marked but often overlooked in routine post-mortem examination of various diseases. Therefore, therapeutic and preventive regimens may be planned to combat the kidney lesions. The further studies on renal pathology of the birds respective to specific causes in experimental birds need to be explored.

ACKNOWLEDGEMENT

The authors gratefully acknowledge the pain staking co-operation and invaluable support rendered by all staff members of the Division of Veterinary Pathology, FVSc & AH, Shuhama.

REFERENCES

1. Lumeij JT. 2000. Pathophysiology, diagnosis and treatment of renal disorders in birds of prey. In: Lumeij JT, Remple JD, Redig PT, Lierz M, Cooper JE (eds) Raptor Biomedicine III. Lake Worth, FL, Zoological Education Network, Inc, USA, pp. 169-178.
2. Rupley AE. 1997. Manual of Avian Practice. WB Saunders Co. Philadelphia, USA.
3. Frazier DL, Jones MP and Orosz SE. 1995. Pharmacokinetic considerations of the renal system in birds: part I. Anatomic and physiologic principles of allometric scaling. *J Avian Med Surg* **9:** 92-103.
4. Phalen DN, Ambrus S and Graham DL. 1990. The avian urinary system: form, function, diseases. In: The Proceedings of Association of Avian Veterinarians Annual Conference. Boca Raton (FL): Association of Avian Veterinarians, pp. 44-57.
5. Speer BL. 1997. Diseases of the urogenital system. In: Altman RB, Clubb S, Dorrestein GM, Quesenberry K. (eds). Avian Medicine and Surgery. WB Saunders, Philadelphia, USA pp. 625-644.
6. Ameen NA, Aref ED, Al-Obaidi RM and Raoof HH. 2015. Isolation and identification of bacteria from kidney lesions in broilers in Sulaimania province. *Assiut Vet Med J* **61:** 8-11.
7. Lierz M. 2003. Avian renal disease: pathogenesis, diagnosis, and therapy. *Vet Clin North Am: Exotic Am Pract* **6:** 29-55.
8. Schmidt RE, Reavill DR and Phalen DN. 2003. Urinary system. In: Pathology of Pet and Aviary Birds. Iowa State Press, Ames (IA), pp. 95-107.
9. Mutalib A, Keirs R and Austin F. 1995. Erysipelas in quail and suspected erysipeloid in processing plant employees. *Avian Dis* **39:** 191-193.
10. Quiun PJ, Markey BK, Carter ME, Donnelly WJ and Leonard FC. 2002. Veterinary Microbiology and Microbial Diseases. Blackwell Publishing Company, USA.
11. Barrow GI and Feltham RKA. 1993. Cowan and Steel's Manual for the Identification of Medical Bacteria, (3rd Edn), Cambridge University Press, Cambridge, pp. 352.
12. Carter GR and Cole JR. 1990. Diagnostic Procedures in Veterinary Bacteriology and Mycology, (5th Edn) Academic press, Inc. Diego, California.
13. Luna LG. 1968. Manual of Histologic Staining Method of Armed Forces Institute of Pathology, (3rd Edn), Mc Graw Hill Book Company, New York, pp. 87-88.
14. Al-Hiyali HM, Al-Kabbi HT and Abdulkarim S. 2005. Isolation of four types of bacteria that cause kidney damage in broiler chickens. *The Iraqi J Vet Med* **29:** 33-42.
15. Sokker SM, Mohammad MA and Atwia M. 1998. Experimental induction of renal lesion in chickens. *Berl Tierärztl Wschr* **111:** 161-163.
16. Franca M, Woolcock PR, Yu M, Jackwood MW and Shivaprasad HL. 2011. Nephritis associated with infectious bronchitis virus Cal99 variant in game chickens. *Avian Dis* **55:** 422-428.
17. Wilson FD, Wills RW, Senties-Cues CG, Maslin WR, Stayer PA and Magee DL. 2010. High incidence of glomerulonephritis associated with inclusion body hepatitis in broiler chickens: routine histopathology and histomorphometric studies. *Avian Dis* **54:** 975-980.
18. Gangane GR, Kulkarni GB and Yeotikar PV. 2006. Studies on

experimental colibacillosis in chicks. *Indian Vet J* **83:** 118-119.
19. Kumar A, Jindal N, Shukla CL, Asrani RK, Ledoux DR and Rottinghaus GE. 2004. Pathological changes in broiler chickens fed ochratoxin A and inoculated with Escherichia coli. *Avian Pathol* **33:** 413-417.
20. Baliarsingh SK, Rao AG and Mishra PR. 1993. Pathology of experimental colibacillosis in chicks. *Indian Vet J* **70:** 808-812.
21. Dho-Moulin M and Fairbrother JM. 1999. Avian pathogenic Escherichia coli (APEC). *Vet Res* **30:** 299-316.

Indian J. Vet. Pathol., 48(2) : 176-180, 2024: DOI: 10.5958/0973-970X.2024.00035.5

RESEARCH ARTICLE

Serological profiling of foot and mouth disease virus nonstructural protein antibodies in susceptible wild or captive ruminants in India

M. Rout*, M. Karikalan[1], V. Manjunatha[2], N. Sahoo[3], N.S. Nair[4], J.K. Mohapatra, B.B. Dash, A.K. Sharma[1] and R.P. Singh

ICAR-National Institute on Foot and Mouth Disease, International Centre for Foot and Mouth Disease, Bhubaneswar -752 050, [1]Centre for Wildlife Conservation Management and Disease Surveillance, Indian Veterinary Research Institute, Izatnagar-243 122, Bareilly, Uttar Pradesh, [2]Wild Animal Disease Diagnostic Laboratory, Institute of Animal Health and Veterinary Biologicals, Bannerghatta Biological Park, Bannerghatta, Bengaluru-560 083, Karnataka, India, [3]Department of Epidemiology and Preventive Medicine, Centre for Wildlife Health, College of Veterinary Science and Animal Husbandry, Orissa University of Agriculture and Technology, Bhubaneswar-751 003, Odisha, [4]AICRP on FMD Collaborating Unit, Palode, Thiruvananthapuram-695 562, Kerala, India

Address for Correspondence

M. Rout, Scientist, ICAR-National Institute on Foot and Mouth Disease, International Centre for Foot and Mouth Disease, Bhubaneswar-752 050, India, E-mail: drmrout@gmail.com

Received: 21.10.2023; Accepted: 15.11.2023

ABSTRACT

There is dearth of surveillance reports elucidating the role of wild/captive ruminants in FMD epidemiology in India. The study was conducted on serum samples collected from wild/captive ruminants in India during 2015-2016. Serum samples from 20 spotted deer, 6 sambar deer, 6 thamin or brow-antlered deer, 3 hog deer, 1 barking deer, 3 bison, 1 gaur, 1 giraffe, 5 four-horned antelopes, 6 nilgai, 2 mithun or gayal, 28 blackbucks (Indian antelopes) and 1 white buck from various states were collected and subjected to competitive 3ABC nonstructural protein (NSP) ELISA using commercial kit PrioCHECK® FMDV NS to detect NSP-antibodies. Finally, 5 (25%) spotted deer, 1 (16.66%) sambar deer, 1 (33.33%) bison, 4 (80%) four- horned antelopes, 2 (33.33%) nilgai and 7 (25%) blackbucks were found positive for NSP-antibodies indicating their previous exposure to FMDV. The serum samples were subjected to in-house liquid phase blocking ELISA to assess the protective antibody against FMDV serotypes O, A and Asia 1, where none was found to have protective antibody (log_{10} titre of ≥1.8) against all three serotype strains in the vaccine. As FMD is highly infectious, necessary control measures including prophylactic vaccination should be put into practice in order to protect these rare wildlife species in the country.

Keywords: Antelope, bison, blackbuck, deer, FMD, gaur, mithun, nilgai, NSP antibody

INTRODUCTION

Several economically important livestock diseases are considered to be maintained by wildlife hosts. Pathogen transmission between species either at wild-domestic interface or within wildlife species has still been a rarely studied entity. Foot-and-mouth disease (FMD), an economically devastating disease of artiodactyls and over 70 different wild animal species, is greatly feared all around the world[1]. The devastating consequences of FMD have been exemplified through estimates of the cost of outbreaks in different countries e.g., $1.6 billion in 1997 in Taiwan[2], $14 billion in the United States[3], more than $15 billion in the United Kingdom in 2001[4] and $1.5-10 billion in Australia. The farm-level economic loss due to FMD in cattle and buffaloes in severe incidence scenario, India might lose USD 3.2 billion/year[5]. FMD is caused by a virus of the *Aphthovirus* genus within the *Picornaviridae* family that is highly contagious[6]. In wildlife species, the FMD pathogenesis varies from an inapparent to a rare acutely lethal infection, making the diagnosis difficult[7,8]. The transmission dynamics of FMD in India is driven by many factors due to socio-economic variables, where susceptible wild and/or domestic ruminants help spreading the disease. Although wildlife species have been suggested as having contributed to FMD dynamics in several outbreaks[9], their actual role was reported to be of only limited significance[1,7]. This might have been an additional factor besides the restrictive conditions and regulations for sampling materials from wildlife species, for which substantial studies have not been undertaken in India despite having a vast number and variety of wildlife species maintained at its different biological parks, zoos or biosphere reserves and forests. In order to produce an overall baseline serological picture, this study on serological profiling for FMDV infection-specific nonstructural protein (NSP) antibodies was planned in different susceptible captive/free-ranging ruminants from National Parks and faunal reserves of

How to cite this article : Rout, M., Karikalan, M., Manjunatha, V., Sahoo, N., Nair, N.S., Mohapatra, J.K., Dash, B.B., Sharma, A.K. and Singh, R.P. 2024. Serological profiling of foot and mouth disease virus nonstructural protein antibodies in susceptible wild or captive ruminants in India. Indian J. Vet. Pathol., 48(2) : 176-180.

various states of India sampled between 2015 and 2016. Such serological study can indicate the level of FMDV activity or circulation in the wild ruminants in the country. Government of India has taken a comprehensive step towards FMD control targeting 100% vaccination in cattle and buffaloes by the year 2025. This study becomes increasingly important for effective disease control and virus maintenance in non-primary hosts.

MATERIALS AND METHODS

Study populations and sampling

Serum samples were sourced from total 83 susceptible captive/wild ungulates/ruminants of different species (within family *Cervidae*, *Bovidae* and *Giraffidae*) including 20 spotted deer/cheetal/axis deer (*Axis axis* in the family *Cervidae*), 6 sambar deer (*Cervus unicolor or Rusa unicolor* in the family *Cervidae*), 6 thamin deer/Eld's deer/brow-antlered deer (*Panolia eldii* or *Rucervus eldii* in the family *Cervidae*), 3 hog deer (*Hyelaphus porcinus* or *Cervus porcinus* in the family *Cervidae*), 1 barking deer (*Muntiacus muntjak* in the family *Cervidae*), 3 bison (*Bison bison* in the family *Bovidae*), 1 gaur (*Bos gaurus* in the family *Bovidae*), 1 giraffe (*Giraffa camelopardalis* in the family *Giraffidae*), 5 four-horned antelope/chousingha (*Tetracerus quadricornis* in the family *Bovidae*), 6 nilgai/ blue bull (*Boselaphus tragocamelus* in the family *Bovidae*), 2 mithun/gayal (*Bos frontalis* in the family *Bovidae*), 28 blackbuck/Indian antelope (*Antilope cervicapra* in the family *Bovidae*) and 1 white buck (*Antilope cervicapra* in the family *Bovidae*) from different Zoological Parks and wildlife reserves across various states of India were collected with due permission from the competent wildlife authorities (MoEF and wildlife authority of the concerned state) between 2015 and 2016. Some serum samples collected from such animals during routine health check-up by the zoo veterinarians were also shared with us for FMD surveillance. Sera were kept cool or frozen in cool box and were transported to the laboratory for processing where they were stored at -40°C in the laboratory awaiting analysis.

Detection of FMDV non-structural protein antibodies (NSP-Abs)

NSP-Ab in case of FMD is considered to be indicative of virus exposure in FMD-susceptible hosts. The serum samples were screened for antibodies against the highly conserved NSP 3ABC of FMDV using commercially available ELISA kit PrioCHECK FMDV NS [Prionics AG, Switzerland or Prionics Lelystad B.V., The Netherlands (currently owned by Thermo Fisher Scientific, Inc.)] according to the manufacturer's instructions and as previously reported[10,11]. The kit is based on the principle of blocking ELISA with baculovirus-expressed 3ABC polypeptide[10]. The frozen serum samples were serially arranged and allowed to thaw at 25°C of the laboratory as per the plate layout indicated in the instruction manual. The ELISA test plates of the kit contain the FMDV 3ABC protein captured by the coated anti-3ABC monoclonal antibody (mAb). A second mAb labeled with an enzyme/ conjugate (mAb-HRPO) that generates a color signal is then added. The reaction between the FMDV-NS antigen and the mAb-HRPO conjugate is blocked by the antibodies directed against the NSP present in the serum sample. Consequently, a positive sample develops no color when chromogen (TMB) substrate is dispensed following incubation at room temperature (22±3°C). Finally, the color development is stopped by the stop solution and the optical densities (ODs) of plates are read at a wavelength of 450 nm. The ODs of all samples including the controls are calculated and expressed as percent inhibition (PI) as follows:

$$PI = 100 - [(OD_{450} \text{ of test sample}) / (\text{mean OD of negative controls})] \times 100$$

PI value of <50% was considered negative, while PI of ≥50% was classed as positive to indicate the presence of anti-NSP antibodies in the tested animal indicative of recent exposure to FMDV (within the previous 6 to 12 months)[12,13]. More specifically, a PI value of ≥50% but <70% was considered a weak positive result and PI value of ≥70% was considered a strong positive result[10].

Titration of FMDV structural protein antibodies (SP-Abs)

In order to correlate the non-vaccination status of the sampled animals against FMD as informed by the veterinarians of wildlife units, the serum samples were subjected to liquid phase blocking (LPB) ELISA to assess the level of protective antibody against FMDV serotypes O, A and Asia 1. For this, two-fold dilution (from 1:16 to 1:128) of serum samples were tested against all three component vaccine strains using the in-house LPB ELISA kit (DFMD, Mukteswar) as per the procedure described earlier[14]. The results were expressed as percentage reactivity for each serum dilution as follows:

$$\text{Percentage reactivity} = (OD_{\text{mean of each test serum dilution}} / OD_{\text{mean of antigen control}}) \times 100$$

The antibody titres were expressed as logarithm of reciprocal of serum dilutions giving 50% of the absorbance recorded in the antigen control wells. The samples showing $\log_{10}$ titre of ≥1.8 were considered as having sufficient protective antibody[15].

RESULTS AND DISCUSSION

The NSP serological assay could be able to detect 5 (25%) spotted deer, 1 (16.66%) sambar deer, 1 (33.33%) bison, 4 (80%) four-horned antelope, 2 (33.33%) nilgai and 7 (25%) blackbucks to be positive for FMDV infection-specific Abs indicating their previous exposure to FMDV

Table 1. Details of serum samples from wildlife species tested and number found positive.

Wildlife species	No. of sera tested	No. found positive for NSP antibodies	% positive
Spotted deer/cheetal/axis deer *(Axis axis)*	20	5	25 %
Sambar deer *(Cervus unicolor or Rusa unicolor)*	6	1	16.66 %
Thamin deer/Eld's deer/brow-antlered deer *(Panolia eldii or Rucervus eldii)*	6	0	0 %
Hog deer *(Hyelaphus porcinus or Cervus porcinus)*	3	0	0 %
Barking deer *(Muntiacus muntjak)*	1	0	0 %
Bison *(Bison bison)*	3	1	33.33 %
Gaur *(Bos gaurus)*	1	0	0 %
Giraffe *(Giraffa camelopardalis)*	1	0	0 %
Four-horned antelope/Chousingha *(Tetracerus quadricornis)*	5	4	80 %
Nilgai/Blue bull *(Boselaphus tragocamelus)*	6	2	33.33 %
Mithun/Gayal *(Bos frontalis)*	2	0	0 %
Blackbuck/Indian antelope *(Antilope cervicapra)*	28	7	25 %
White buck *(Antilope cervicapra)*	1	0	0 %
Total	83	20	24.09 %

(Table 1). The sampled animals in the national parks/ reserves were not vaccinated against FMD during the preceding years of sampling. Based on the findings, such sero-reactors could be indicative of either FMDV infection with possible active FMDV circulation (OIE 2023) or their exposure to the virus. None of the sampled animals tested in LPB ELISA were found to have protective antibody (log_{10} titre of ≥1.8) against all three serotype strains indicating the lack of protective antibody against FMDV. The same kit PrioCHECK FMDV NS was used to detect serum antibodies to FMDV 3ABC in red deer (*Cervus elaphus elaphus*)[16], in livestock and wildlife species in Uganda[17], while researchers[18] have performed the serological profile of FMD in wildlife populations of West and Central Africa with special reference to *Syncerus caffer* subspecies with NSP positivity in 17.8% non-buffalo wildlife samples. Presence of FMDV antibodies in several wildlife species has been documented in different countries in eastern and southern regions of the African continent[19,20]. The seroprevalence of FMD in susceptible wild ungulates in Israel during 2000 and 2005-2013 was estimated using NSP ELISA[21]. The detection of such antibodies to FMDV NSP is often used to confirm a history of active infection.

The PrioCHECK FMDV NS kit is reported to have a high sensitivity and specificity compared with others[22,23]. The test is assumed to have sensitivity of 97.2% and specificity of 98.1%[22,24]. The specificity of the kit for bovine sera was reported as 98.1%[22], while the sensitivity in non-vaccinated, experimentally infected bovines could approach 100%. Researchers[19] have reported the sensitivity and specificity estimates of 87.7% and 87.3%, respectively for African buffalo (*Syncerus caffer*). In addition, antibodies to 3ABC protein are considered to be the reliable indicator of infection/exposure regardless of vaccination status and of the serotype of FMDV[10,25]. It is independent of serotype and may be used to detect exposure in vaccinated as well as infected animals. In addition, as a blocking ELISA, it is species-independent and a test of choice for samples from a range of susceptible wildlife species circumventing the need for species-specific conjugate. In view of this, the overall prevalence of FMDV antibodies in wildlife population to the tune of 24.09% as found in the present study is a strong indicator of virus circulation in different wildlife species at different parts of the country.

In India, researchers[26] at ICAR-Directorate of Foot and Mouth Disease not only reported FMDV serotype O on clinical samples derived from affected Indian gaur, chital deer, nilgai, black buck, spotted deer, bison, sambar deer using antigen detection ELISA and RT-multiplex PCR, but also the VP1 region-based phylogenetic analysis of the recovered virus indicated the involvement of both O/ME-SA/Ind2001 and PanAsia lineage of serotype O in the outbreaks. Earlier workers[27] reported FMDV serotype O in captive nilgai at S.V. Zoologcal Park, Andhra Pradesh. The same serotype was also isolated and identified from the affected cattle surrounding the zoo during the same time period indicating the virus exchange between species. In India FMD has been reported in free-living wildlife[28] and well known in captive ruminants[29-31]. Some reports in other countries indicate FMD in cervids such as reindeer, moose and deer, including white tailed deer[8,32-34]. Sometimes wild ruminants may infect domestic species at the interface area or *vice versa* where the probability of intermixing appears to be more. Even the best maintained fences cannot restrain the movements of all wild animals[35,36] resulting in outbreaks of infectious

diseases in neighboring livestock, including FMD[37]. Roe deer (*Capreolus capreolus*) in the United Kingdom has been reported to be likely involved in an epizootic by infecting both cattle and sheep[38].

Animals infected with FMDV produce antibodies to structural and non-structural proteins[39]. Antibodies to FMDV NSPs are used to monitor for FMDV infection or virus circulation[40]. In addition, it should be noted that wildlife usually avoids livestock and human contacts (i.e., at watering points or locations with key forage resources) in a space-time fashion unless habituated. As FMD requires a relatively close contact setting for interspecies transmission, the FMD interface between wildlife and livestock should, therefore, not be seen as a direct physical interaction but as an indirect contact (i.e., through soil, forage and water contaminated by bodily discharge of infected animals), which might be regarded as the most likely factor to be associated with the risk of FMDV transmission from domestic to wildlife species and vice-versa.

Logically, though domestic livestock and wildlife can spread the disease to each other, in some endemic countries, wild ungulates have been shown to harbor and spread FMDV to livestock despite vaccination and control efforts. Some reports are of opinion that FMDV infrequently spills over from domestic animals into wildlife populations, while wildlife such as gazelles and deer have not proven capable of maintaining FMDV independently of livestock. Meanwhile, transmission of FMDV to livestock by persistently infected wild ungulates has been debated for years. The present study reports the FMD serological profile derived from susceptible captive/wild ruminant populations in different states of India indicating FMDV circulation within wildlife ecosystems. In India, wildlife species have earlier been reported for FMD and the clinical samples have been tested positive for FMDV as highlighted before. In addition, further studies in collaboration with wildlife authorities are warranted to collect more number of serum samples to demonstrate FMDV infection-specific antibodies as well as clinical samples during the face of outbreak in order to enable the genome characterization of FMDV lineages circulating within wild animal species to confirm if FMDV serotypes normally present in domestic livestock are really matching with such wildlife species.

In conclusion, the study could gather serological evidence of FMDV activity in wild/captive species like spotted deer, sambar deer, bison, four- horned antelopes, nilgai and blackbucks indicating their previous exposure to FMDV. None of the animals were further found to have protective antibody against all three serotype strains indicating the lack of protective antibody against FMDV. The susceptible wild/captive FMD-susceptible species should be vaccinated with a suitable vaccine with appropriate dose, a researchable area in the sphere of FMD vaccinology, so as to build a strong immunity against FMD.

ACKNOWLEDGEMENTS

This research study was supported by ICAR. We would like to thank zoo veterinarians for their support. We thank the MoEF, PCCFs/CWLWs of different states for according permission for the sampling.

REFERENCES

1. Weaver GV, Domenech J, Thierman AR and Karesh WB. 2013. Foot and mouth disease: a look from the wild side. *J Wildlife Dis* **49:** 759-785.
2. Yang PC, Chu RM, Chung WB and Sung HT. 1999. Epidemiological characteristics and financial costs of the 1997 foot-and-mouth disease epidemic in Taiwan. *Vet Rec* **145:** 731-734.
3. Paarlberg PL, Lee JG and Seitzinger AH. 2002. Potential revenue impact of an outbreak of foot-and-mouth disease in the United States. *J Am Vet Med Assoc* **220:** 988-992.
4. Kao RR. 2003. The impact of local heterogeneity on alternative control strategies for foot-and-mouth disease. *Proc Biol Sci* **270:** 2557-2564.
5. Govindaraj G, Ganesh Kumar B, Krishnamohan A, Hegde R, Kumar N, Prabhakaran K, Wadhwan VM, Kakker N, Lokhande T, Sharma K, Kanani A, Limaye Natchimuthu K, Ananth PN, De AK, Khan TA, Misri J, Dash BB, Pattnaik B and Rahman H. 2021. Foot and Mouth Disease (FMD) incidence in cattle and buffaloes and its associated farm-level economic costs in endemic India. *Prev Vet Med* **190:** 105318.
6. Haydon DT, Woolhouse MEJ and Kitching RP. 1997. An analysis of foot-and-mouth-disease epidemics in the UK. *IMA J Math Appl Med Biol* **14:** 1-9.
7. Thomson GR, Vosloo W and Bastos AD. 2003. Foot and mouth disease in wildlife. *Virus Res* **91:** 145-161.
8. Arzt J, Baxt B, Grubman MJ, Jackson T, Juleff N, Rhyan J, Rieder E, Waters R and Rodriguez LL. 2011. The pathogenesis of foot-and-mouth disease II: viral pathways in swine, small ruminants, and wildlife; myotropism, chronic syndromes, and molecular virus-host interactions. *Transbound Emerg Dis* **58:** 305-326.
9. Valdazo-Gonzalez B, Polihronova L, Alexandrov T, Normann P, Knowles NJ, Hammond JM, Georgiev GK, Özyörük F, Sumption KJ, Belsham GJ and King DP. 2012. Reconstruction of the transmission history of RNA virus outbreaks using full genome sequences: Foot-and-mouth disease virus in Bulgaria in 2011. *PLoS One* **7:** e49650.
10. Sorensen KJ, Madsen KG, Madsen ES, Salt JS, Nqindi J and Mackay DKJ. 1998. Differentiation of infection from vaccination in foot-and-mouth disease by the detection of antibodies to the non-structural proteins 3D, 3AB and 3ABC in ELISA using antigens expressed in baculovirus. *Arch Virol* **143:** 1461-1476.
11. Sorensen KJ, de Stricker K, Dyrting KC, Grazioli S and Haas B. 2005. Differentiation of foot-and-mouth disease virus infected animals from vaccinated animals using a blocking ELISA based on baculovirus expressed FMDV 3ABC antigen and a 3ABC monoclonal antibody. *Arch Virol* **150:** 805-814.
12. De Diego M, Brocchi E, Mackay D and De Simone F. 1997. The nonstructural polyprotein 3ABC of foot-and-mouth disease virus as a diagnostic antigen in ELISA to differentiate infected from vaccinated cattle. *Arch Virol* **142:** 2021-2033.

13. Brocchi E, De Diego MI, Berlinzani A, Gamba D and De Simone F. 1998. Diagnostic potential of Mab-based ELISAs for antibodies to nonstructural proteins of foot-and-mouth disease virus to differentiate infection from vaccination. *Vet Q* **20:** S20-S24.
14. Ranabijuli S, Mohapatra JK, Pandey LK, Rout M, Sanyal A, Dash BB, Sarangi LN, Panda HK and Pattnaik B. 2010. Serological evidence of foot and mouth disease infection in randomly surveyed goat population of Orissa, India. *Transbound Emerg Dis* **57:** 448-454.
15. Sharma GK, Mahajan S, Matura R, Subramaniam S, Mohapatra JK and Pattnaik B. 2015. Quantitative single dilution liquid phase blocking ELISA for sero-monitoring of foot-and-mouth disease in India. *Biologicals* **43:** 158-164.
16. Kittelberger R, Nfon C, Swekla K, Zhang Z, Hole K, Bittner H, Salo T, Goolia M, Embury-Hyatt C, Bueno R, Hannah M, Swainsbury R, O'Sullivan C, Spence R, Clough R, McFadden A, Rawdon T and Alexandersen S. 2017. Foot-and-Mouth Disease in Red Deer - Experimental infection and test methods performance. *Transbound Emerg Dis* **64:** 213-225.
17. Ayebazibwe C, Mwiine FN, Balinda SN, Tjørnehøj K and Alexandersen S. 2012. Application of the Ceditest® FMDV type O and FMDV-NS enzyme-linked immunosorbent assays for detection of antibodies against Foot-and-mouth disease virus in selected livestock and wildlife species in Uganda. *J Vet Diagn Invest* **24:** 270-276.
18. Di Nardo A, Libeau G, Chardonnet B, Chardonnet P, Kock RA, Parekh K, Hamblin P, Li Y, Parida S and Sumption KJ. 2015. Serological profile of foot-and-mouth disease in wildlife populations of West and Central Africa with special reference to *Syncerus caffer* subspecies. *Vet Res* **46:** 77.
19. Bronsvoort BM, Parida S, Handel I, McFarland S, Fleming L, Hamblin P and Kock R. 2008. Serological survey for foot-and-mouth disease virus in wildlife in eastern Africa and estimation of test parameters of a nonstructural protein enzyme linked immunosorbent assay for buffalo. *Clin Vac Immunol* **15:** 1003-1011.
20. Vosloo W, Thompson PN, Botha B, Bengis RG and Thomson GR. 2009. Longitudinal study to investigate the role of impala (*Aepyceros melampus*) in foot-and-mouth disease maintenance in the Kruger National Park, South Africa. *Transbound Emerg Dis* **56:** 18-30.
21. Elnekave E, King R, van Maanen K, Shilo H, Gelman B, Storm N and Klement E. 2016. Seroprevalence of foot-and-mouth disease in susceptible wildlife in Israel. *Front Vet Sci* **3:** 32.
22. Brocchi E, Bergmann IE, Dekker A, Paton DJ, Sammin DJ, Greiner M, Grazioli S, De Simone F, Yadin H, Haas B, Bulut N, Malirat V, Neitzert E, Goris N, Parida S, Sorensen K and De Clercq K. 2006. Comparative evaluation of six ELISAs for the detection of antibodies to the non-structural proteins of foot-and-mouth disease virus. *Vaccine* **24:** 6966-6979.
23. Engel B, Buist W, Orsel K, Dekker A, de Clercq K, Grazioli S and van Roermund H. 2008. A Bayesian evaluation of six diagnostic tests for foot-and-mouth disease for vaccinated and non-vaccinated cattle. *Prev Vet Med* **86:** 124-138.
24. Paton DJ, de Clercq K and Greiner M. 2006. Application of nonstructural protein antibody tests in substantiating freedom from foot-and-mouth disease virus infection after emergency vaccination of cattle. *Vaccine* **24:** 6503-6512.
25. Sun T, Lu P and Wang X. 2004. Localization of infection-related epitopes on the non-structural protein 3ABC of foot-and-mouth disease virus and the application of tandem epitopes. *J Virol Meth* **119:** 79-86.
26. Rout M, Subramaniam S, Das B, Mohapatra JK, Dash BB, Sanyal A and Pattnaik B. 2017. Foot-and-mouth disease in wildlife population of India. *Indian J Anim Res* **51:** 344-346.
27. Sujatha K and Srilatha Ch. 2007. A note on an outbreak of foot-and-mouth disease in captive nilgai *Boselaphus tragocamelus*. *Zoos' Print J* **22:** 2733.
28. Sinha SK. 1976. Wildlife losses due to disease in Indian wild animals. *Cheetal* **17:** 25-38.
29. Paikne DL, Dhoke PR and Ahmed SS. 1976. An outbreak of acute form of foot-and-mouth disease in nilgai. *Haryana Vet J* **15:** 100-103.
30. Ahuja KL, Pramod S, Kumar A, Sharma R and Kharole MV. 1985. FMD in nilgai and deer in Haryana. International Conference on Wildlife Diseases, Uppsala, Sweden.
31. Singh B and Gupta PP. 1988. Causes of mortality in zoo animals. All India Zoo Veterinarian Seminar, Chandigarh, 2 and 3 December 2003, Pp. 54-58.
32. Haigh JC, Mackintosh C and Griffin F. 2002. Viral, parasitic and prion diseases of farmed deer and bison. *Rev Sci Tech* **21:** 219-248.
33. Dunbar MR, Johnson SR, Rhyan JC and McCollum M. 2009. Use of infrared thermography to detect thermographic changes in mule deer (*Odocoileus hemionus*) experimentally infected with foot-and-mouth disease. *J Zoo Wildl Med* **40:** 296-301.
34. Moniwa M, Embury-Hyatt C, Zhang Z, Hole K, Clavijo A, Copps J and Alexandersen S. 2012. Experimental foot-and-mouth disease virus infection in white tailed deer. *J Comp Pathol* **147:** 330-342.
35. Sutmoller P, Thomson GR, Hargreaves SK, Foggin C and Anderson E. 2000. The foot-and-mouth disease posed by African buffalo within wildlife conservancies to cattle industry of Zimbabwe. *Prev Vet Med* **44:** 43-60.
36. Dion E, VanSchalkwyk L and Lambin EF. 2011. The landscape epidemiology of foot-and-mouth disease in South Africa: A spatially explicit multi-agent simulation. *Ecol Model* **222:** 2059-2072.
37. Hargreaves SK, Foggin CM, Anderson EC, Bastos ADS, Thomson GR, Ferris NP and Knowles NJ. 2004. An investigation into the source and spread of foot and mouth disease virus from a wildlife conservancy in Zimbabwe. *Rev Sci Tech* **23:** 783-790.
38. Gibbs EPJ, Herniman KAJ, Lawman MJP and Sellers RF. 1975. Foot-and-mouth disease in British deer: transmission of virus to cattle, sheep and deer. *Vet Rec* **96:** 558-563.
39. Robiolo B, Seki C, Fondevilla N, Grigera P, Scodeller E, Periolo O, Torre JL and Mattion N. 2006. Analysis of the immune response to FMDV structural and non-structural proteins in cattle in Argentina by the combined use of liquid phase and 3ABC-ELISA tests. *Vaccine* **24:** 997-1008.
40. OIE. 2023. Foot and Mouth Disease (Infection with Foot and Mouth Disease Virus). Manual of Diagnostic Tests and Vaccines for Terrestrial Animals, 12th Edn, Chapter 3.1.8., World Organization for Animal Health, Paris, France. Pp. 11-17.

Indian J. Vet. Pathol., 48(2) : 181-184, 2024: DOI: 10.5958/0973-970X.2024.00027.X

SHORT COMMUNICATION

A rare case of pulmonary paragonimiasis and spirocercosis in a Chippiparai dog

K. Thilagavathi*, J. Selvaraj, N. Babu Prasath, P.C. Prabu and R. Jyothi Priya
Department of Veterinary Pathology, Veterinary College and Research Institute, Tamil Nadu Veterinary and Animal Sciences University, Orathanadu, Thanjavur-614 625, Tamil Nadu, India

Address for Correspondence
K. Thilagavathi, Assistant Professor, Department of Veterinary Pathology, Veterinary College and Research Institute, Tamil Nadu Veterinary and Animal Sciences University, Orathanadu, Thanjavur-614 625, Tamil Nadu, India, E-mail: thilagapatho@gmail.com

Received: 8.9.2023; Accepted: 10.11.2023

ABSTRACT

A one-year-old male Chippiparai dog was submitted for necropsy to the Department of Veterinary pathology, Veterinary College and Research institute, Orathanadu. During necropsy, the gross lesions were observed and required tissue samples were collected for histopathology. Fluke and worms were collected for parasitological identification. Grossly, right lung showed a grey patch and on cut section showed the presence of cavity containing two conical flukes. Oesophageal lumen contained spiral worm near the nodule and on section of nodule contained blood mixed exudate. Based on the morphology, the fluke was identified as *Paragonimus* sp and worm was identified as *Spirocerca lupi*. Histopathologically, lung revealed the presence of eggs of *Paragonimus* sp, chronic bronchitis, immature eggs, mature eggs with miracidium, and giant cell. Based on the gross lesions, morphology and histopathology, the very rare case of combined infection of pulmonary paragonimiasis and spirocercosis in a chippiparai dog is documented.

Keywords: Chippiparai dog, Paragonimiasis, Spirocercosis

How to cite this article : Thilagavathi, K., Selvaraj, J., Prasath, N.B., Prabu, P.C. and Priya, R.J. 2024. A rare case of pulmonary paragonimiasis and spirocercosis in a Chippiparai dog. Indian J. Vet. Pathol., 48(2) : 181-184.

Paragonimosis is a parasitic disease caused by trematodes of the genus Paragonimus and is an important food-borne endemic zoonosis worldwide. Adult trematodes reside in the lungs of definitive hosts (humans and various wild and domestic animals, including dogs)[1,2]. Dogs and cats, as more likely definitive hosts, generally play a greater role than humans in the Paragonimus life cycle[1]. In veterinary medicine, *Paragonimus* spp., *Paragonimus westermani* and *Paragonimus kellicotti*, are of particular interest[3]. *P. westermani* is the best-known species in Asia; *P. kellicotti* occurs in North America. In addition, in Japan, *P. miyazakii* is another important species responsible for human and animal paragonimosis[1,2,5]. The life cycle of Paragonimus is typical of trematodes but involves two intermediate hosts. The river water snail act as a first intermediate host and fresh water crabs or crayfishes act as a second intermediate hosts[6]. Humans, many wild felids and canids including domestic dogs and cats are definitive hosts and get infections by ingesting second intermediate hosts (fresh water crabs and Crayfishes) containing metacercaria[7].

The life cycle of *P. westermani*: In the definitive host (dogs, cat, wild animals, humans), the adult trematode exists in the bronchioles of lungs and produce eggs. Eggs are shed into the external environment via sputum and faeces. Eggs develop into miracidia in water and penetrate the melania snail the first intermediate host. Miracidia inside the snail go through several developmental stages like sporocysts, rediae and develop as cercariae, which are shed into water and seek the second intermediate hosts (crabs and crayfishes), in which the cercariae encyst as metacercariae in the musculature or other organs[8]. When the definitive hosts ingest a raw or undercooked or even inadequately cured, dried, pickled or salted infected crustacean host, the metacercariae excyst in the small intestine (especially in the duodenum), migrate through the intestine wall and reach the abdominal cavity in 3 to 6 hours[9]. They enter and remain in the abdominal wall for several days before migration through or around the diaphragm to the pleural cavity and lungs, finally arriving at the vicinity of the bronchioles, where they develop into the adult worms. Time from infection to oviposition is 65-90 days[10].

Spirocercosis is a disease caused by the nematode *Spirocerca lupi* which has a variety of clinical presentations. *S. lupi* is found worldwide especially in tropical and subtropical regions. This nematode has been found in many species, but affects mostly carnivores, especially Canidae[11]. The lifecycle of *S. lupi* involves intermediate and paratenic hosts. The adult worms are found coiled within nodules in the oesophageal wall. *S. lupi* eggs containing larvae (L1) are passed from the oesophagus through the gastrointestinal tract and into the faeces or may be shed in the vomitus. A variety of species of

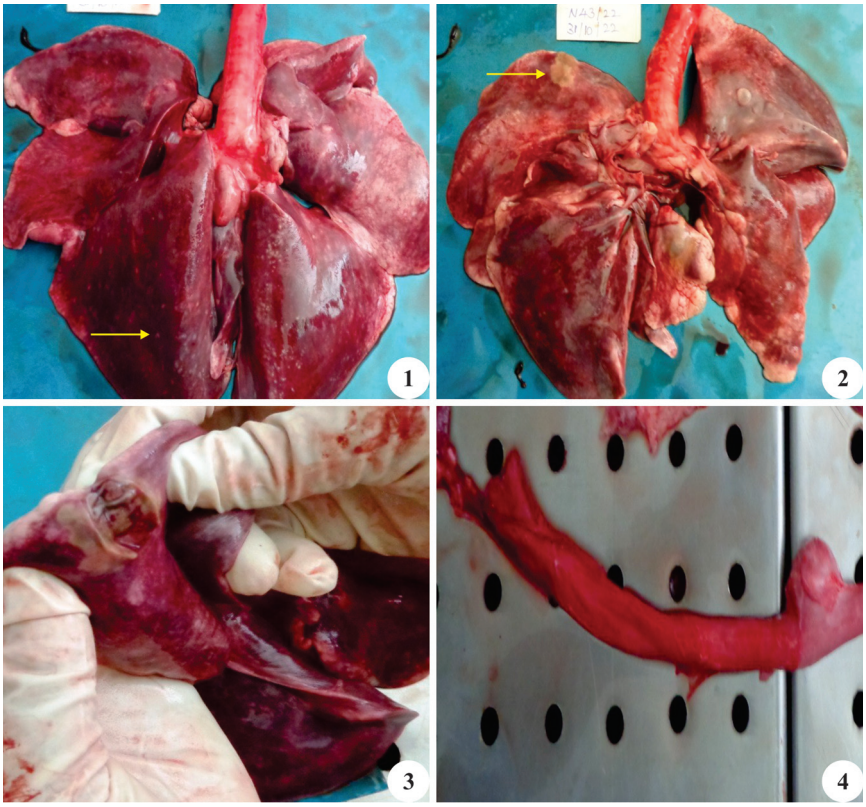

Fig. 1. Lungs showing dark reddish, firm and scattered white foci (yellow arrow); **Fig. 2.** Lung showing gray patches and few cysts (yellow arrow); **Fig. 3.** Lung cut section showing the presence of fluke; **Fig. 4.** Oesophageal serosa revealed nodule of 2 cm diameter attached to the wall; **Fig. 5.** Oesophageal lumen contains spiral worm near the nodule.

coprophagous beetles act as intermediate hosts. Eggs are ingested by the intermediate host and the larvae encyst within the tissues and develop to infective larvae (L3). The beetle is ingested by the final host (dog) or a paratenic host. The final host becomes infected by ingesting either the infected beetle or paratenic host. The L3 excyst in the stomach and penetrate the gastric mucosa, evidenced by petechial haemorrhages and erosions on the mucosa[12]. Larvae migrate within the walls of the gastric and gastroepiploic arteries and reach the caudal thoracic aorta via the coeliac artery where they mature to L4[12]. After their final moult, they migrate as immature adults, from the caudal thoracic aorta to the caudal oesophagus and live in nodules in the submucosa and adventitia of the oesophagus[13].

A one-year-old male Chippiparai dog was submitted for necropsy to the Department of Veterinary Pathology, Veterinary College and Research institute, Orathanadu. During necropsy, the gross lesions were recorded and required tissue samples for histopathology were collected and fixed in 10% formalin. Fluke and worms were collected in normal saline for parasitological identification. The tissues were routinely processed, sectioned and stained with Haematoxylin and Eosin (H&E) stain.

Grossly, the lungs revealed dark reddish, firm and scattered white foci with few cysts (Fig. 1). Middle lobe on right lung showed grey patches of 0.7-1 cm diameter (Fig. 2). On cut section, the grey area showed the presence of cavity containing two conical flukes (Fig. 3). Oesophageal serosa revealed nodule of 2 cm diameter attached to the wall (Fig. 4). Oesophageal lumen contained a spiral worm

near the opening of nodule which on section revealed blood mixed exudate (Fig. 5). Fluke and worm were sent to the Department of Parasitology. Based on the morphology, the fluke was identified as *Paragonimus sp* and worm was identified as *Spirocerca lupi.*

Histopathologically, lung revealed the presence of huge number of eggs of *Paragonimus sp* with cellular infiltration around it (Figs. 6, 7). Additionally chronic bronchitis with infiltration of mononuclear cells was also observed (Fig. 8). Few areas of lung showed the presence of immature egg and miracidium without egg shell (Figs. 9, 10) and multinucleated giant cells around the miracidium (Fig. 11).

On cut section of gray area of lung, cavity containing flukes were seen in accordance with recent report[14] who identified fluke in royal Bengal tiger. Oesophageal serosa revealed nodule attached to wall and the lumen contained spiral worm near the nodule opening and were in agreement with earlier report[15]. Microscopically, the lung revealed huge number of eggs of *Paragonimus* sp was similar to earlier reports[16-19]. Giant cells observed in the lung was in accordance with recent report[16] who observed inflammatory cells along with giant cell in ectopic paragonimus infection in lymph node of dog and was also similar to another report[19] who observed similar lesions in wild carnivores. In the lungs, flukes usually occur in pairs

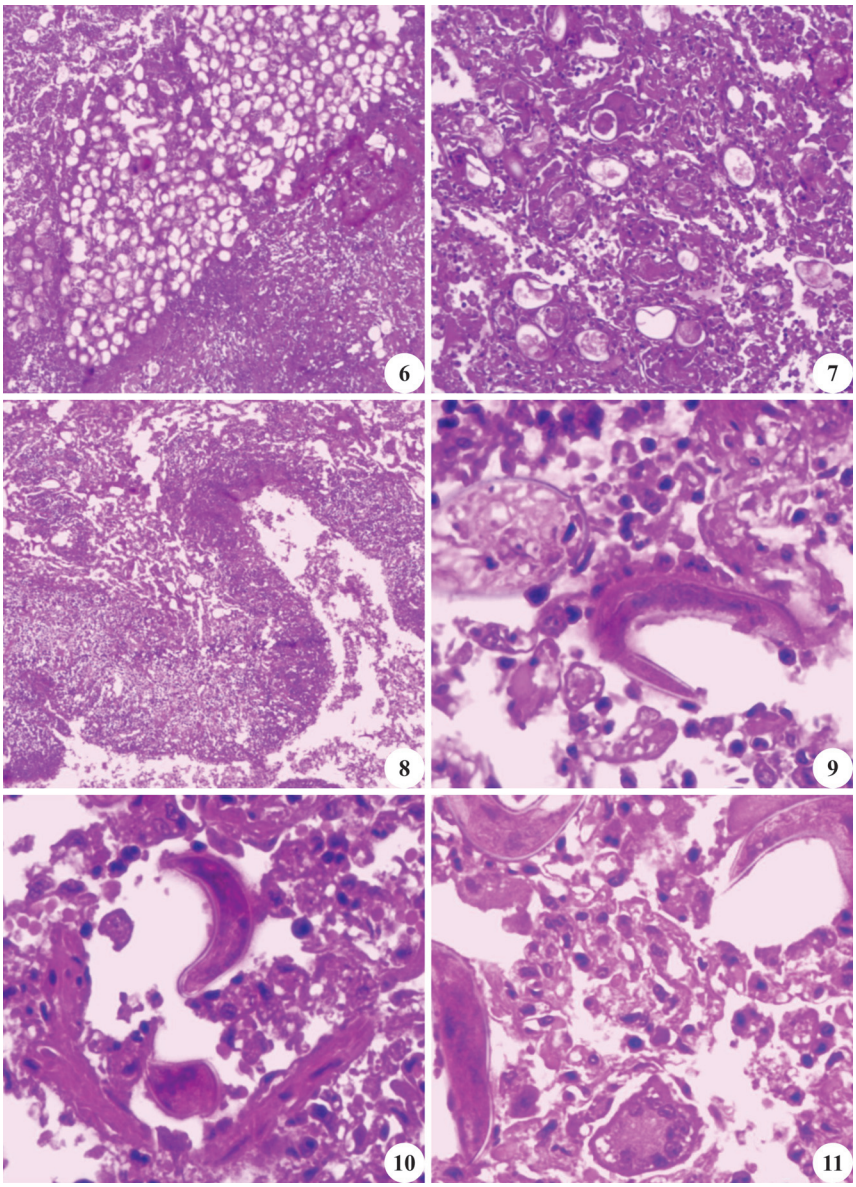

Fig. 6. Lung revealing the presence of huge number of eggs of *Paragonimus* sp (H&E, x40); **Fig. 7.** Lung revealing the presence of eggs of *Paragonimus* sp (H&E, x100); **Fig. 8.** Lung: Chronic bronchitis with infiltration of mononuclear cells (H&E, x40); **Fig. 9.** Lung showing the presence of immature eggs and miracidium without egg shell (H&E, x400); **Fig. 10.** Lung showing the presence of miracidium without egg shell (H&E, x400); **Fig. 11.** Lung revealing the multinucleated giant cell around the miracidium (H&E, x400).

but some time more than two parasites can be present in a cyst. The damage to the lungs is caused by migration of flukes, toxic metabolites of flukes, and also by fluke eggs wherein host's immune response induces severe inflammation[20]. The excretory and secretary products of adult *P. westermani* contain cysteine protease enzymes responsible for invoking immunological process during infection[21-22]. The present case is documented as the very rare incidence of combined infection of pulmonary paragonimiasis and spirocercosis in a Chippiparai dog.

REFERENCES

1. Garcia LS. 2007. Lung flukes. In: Diagnostic Medical Parasitology 5th ed., pp. 438-444. AMS Press, Washington, DC.
2. John DT and Petri WA. 2006. The lung flukes. In: Markell and Voge's Medical Parasitology, ed. Wilson L, 9th ed., pp. 197-202. Elsevier Saunders, Philadelphia, PA.
3. Caswell JL and Williams KJ. 2007. *Paragonimus kellicotti*. In: Pathology of Domestic Animals, ed. Maxie MG, 5th ed., vol. 2, pp. 652-653. Elsevier Saunders, Philadelphia, PA.
4. Blair D, Xu ZB and Agatsuma T. 1998. Paragonimiasis and the genus Paragonimus. In: Advances in Parasitology, ed. Baker JR, Muller R, Rollinson D, vol. 42, pp. 113-222. Academic Press, San Diego, CA.
5. Matumine H and Araki K. 1985. A case of *Paragonimiasis miyazakii* appearing with bilateral pneumothorax, effusion and alternating chest pain-a review of 82 cases reported in Japan. *Nippon Naika Gakkai Zasshi* **74:** 597-605.
6. Singh TS, Sugiyama H and Rangsiruji A. 2012. Paragonimus and paragonimiasis in India. *Indian J Med Res* **136:** 192-204.
7. Miyazaki I. 1974. Lung flukes in the world: Morphology and life history. In: Symposium on Epidemiology of Parasitic Disease. *Int Med Found Japan* 101-134.
8. Quan L, Feng W, Wensen L, Songtao Y and Xichen Z. 2008. Paragonimiasis: an important food-borne zoonosis in China. *Trends Parasitol* **24:** 318-323.
9. Velez I. 2003. Morphological description and life cycle of *Paragonimus spp*. (Trematoda: Troglotrematidae): causal agent of human paragonimiasis in Colombia. *J Parasitol* **89:** 749-755.
10. Guan XH. 2005. Paragonimiasis: In Human Parasitology (Li YL, Guan XH eds), pp. 109-113, People's Public Health Press.
11. Mazaki TM, Baneth G, Aroch I, Harrus S, Kass PH, Ben AT, Zur G, Aizenberg I, Bark H and Lavy E. 2002. Canine spirocercosis: clinical, diagnostic, pathologic and epidemiologic characteristics. *Vet Parasitol* **107:** 235-250.
12. Hu CH and Hoeppli RJC. 1936. The migration route of *Spirocerca sanguinolenta* in experimentally infected dogs. *Chin Med J Supplemet* **1:** 293-311.
13. Bailey WS. 1963. Parasite and cancer: sarcoma in dogs associated with *Spirocerca lupi. Ann NY Acad Sci* **108:** 890-923.
14. Dharanesha NK, Shivshankar BP, Ramesh KR, Kshamaa LM, Umashankar KS, Ananda KJ, Giridhar P and Byregowda SM. 2017. Pulmonary paragonimiasis in a royal Bengal tiger - A case report. *Indian J Vet Pathol* **41:** 143-145.
15. Liesel LM, Kirberger RM, Clift S, Williams M, Keller N and Naidoo V. 2008. *Spirocerca lupi* infection in the dog: A review. *Vet J* **176:** 294-309.
16. Madarame H, Suzuki H, Saitoh Y, Tachibana M, Habe S, Uchida A and Sugiyama H. 2009. Ectopic (Subcutaneous) *Paragonimus miyazakii* infection in a Dog. *Vet Pathol* **46:** 945-948.
17. Yoshimura A, Azakami D, Kishimoto M, Ohmori T, Hirao D, Morita S, Hasegawa S, Morita T and Fukushima R. 2023. A case of a dog with paragonimiasis after consumption of raw deer meat. *J Vet Med Sci* **5:** 541-545.
18. Shibahara T, Nishida H and Sasaki N. 1985. A Case of Multiple Lung Fluke (*Paragonimus westermani*) Infection of a Raccoon Dog in Japan. *Jpn J Parasitol* **34:** 513-516.
19. Presidente JAA and Ramsden RO. 1975. *Paragonimus kellicotti* infection in wild carnivores in southwestern ontario: histopathologic features. *J Wild Dis* **11:** 364-375.
20. Blair D, Xu ZB and Agatsuma T. 1999. Paragonimiasis and the genus Paragonimus. *Adv Parasitol* **42:** 113-222.
21. Lee EG, Na BK, Bae YA, Kim SH, Je EY, Ju JW, Cho SH, Kim TS, Kang SY, Cho SY and Kong Y. 2006. Identification of immunodominant excretory-secretory cysteine proteases of adult *Paragonimus westermani* by proteome analysis. *Proteomics* **6:** 1290-1300.
22. Na BK, Kim SH, Lee EG, Kim TS, Bae YA, Kang I, Yu JR, Sohn WM, Cho SY and Kong Y. 2006. Critical roles for excretory secretory cysteine proteases during tissue invasion of *Paragonimus westermani* newly excysted metacercariae. *Cell Microbiol* **8:** 1034-1046.

Indian J. Vet. Pathol., 48(2) : 185-187, 2024: DOI: 10.5958/0973-970X.2024.00028.6

SHORT COMMUNICATION

Clinico-cytopathological changes in pyogranulomatous pododermatitis in dogs

Gulshan Kumar Singh[1], Jeny K. John*, T.K. Sarkar[2], Manish Shukla, Tareni Das[3], Vikas Jaiswal[1], Naresh Chandra[1], M.V. Jithin, Ajit K. Singh and V.K. Varun

[1]Department of Veterinary Pathology, [2]Department of Veterinary Medicine, [3]ICAR-DFMD-International Center for Foot and Mouth Disease, Odisha, Department of Veterinary Clinical Complex, COVAS, Sardar Vallabhbhai Patel University of Agriculture and Technology, Modipuram-250 110, Meerut, India

Address for Correspondence

Jeny K. John, Assistant Professor, Department of Veterinary Clinical Complex, COVAS, Sardar Vallabhbhai Patel University of Agriculture and Technology, Modipuram-250 110, Meerut, India, E-mail: jenykjohn.vet@svpuat.edu.in

Received: 22.1.2023; Accepted: 27.12.2023

ABSTRACT

Pododermatitis is a complex and multi-etiological inflammatory skin condition of footpads, inter-digital spaces, nails and its fold. The dog breeds with flat foot, wide based paws and scoop shaped feet are more susceptible to pododermatitis. Four cases were presented to Veterinary clinical complex (VCC), College of Veterinary and Animal Sciences, Meerut with the history of chronic skin lesions in paws. Skin scrapings, multiple impression smears and swabs were collected from the affected area and sent to Diagnostic section of VCC. In skin scraping examination, typical cigar shaped *Demodex canis* was noticed in one case. On cytological examination smears, revealed presence of large number of degenerate neutrophils with good fraction of activated macrophages. Large number of round small epithelial cells with large big round nucleus were seen scattered throughout the sections indicates acantholysis. Many of the round epithelial cells exhibit cytoplasmic melanin granules, suggesting hyperpigmentation in the affected area. In three other cases, the cytological analysis of an impression smear from the paw region revealed a substantial presence of neutrophils containing intracytoplasmic cocci. Considering the clinical manifestations, cytological examination, and skin scraping analysis, the aforementioned cases were conclusively diagnosed as pododermatitis.

Keywords: Canine, demodex, pododermatitis, pyogranulomatous

Pododermatitis is a complex and multi-etiological inflammatory skin condition of paw. It is also known as pedal folliculitis/furunculosis[1]. In paws, footpads, inter-digital spaces, nails and its fold can be affected. Lesions can be seen in one foot or more than one feet. Its occurrence is acute, recurrent or chronic[2]. Pododermatitis is a clinical presentation rather than a final diagnosis. Considering the multifaceted nature and the potential for pododermatitis development arising from various causes such as simple trauma or secondary bacterial infections, it is essential to examine each case. The front feet are more susceptible to pododermatitis than hind feet due to more chance of trauma in front feet. The dog breeds with flat foot, wide based paws and scoop shaped feet are more susceptible to pododermatitis[3,4]. Clinical presentation includes itching, constant licking of affected paw, erythema, swelling with or without nodules, hair fall, paronychia, with exudation usually serosanguineous or seropurulent, pain and lameness. It is not necessary to have all these presentations in all cases, some cases may exhibit only a single clinical sign and might affect either a single paw or, in certain situations, multiple paws.

Different forms of pododematitis can be seen in dogs such as allergic pododermatitis with secondary infection, parasitic pododermatitis and sterile pyogranulomatous pododermatitis[5]. A very systematic approach in arriving diagnosis is needed due to multi-etiology, multiple clinical presentation and other diseases with similar clinical presentations. Diagnosis can be made by evaluating history, clinical signs, cytology of impression smear, skin scrapings, hair pluckings and bacterial and fungal cultures[5]. In this paper, we are discussing about clinical and cytopathological changes in a dog with pododermatitis.

Total of 4 cases were presented to Veterinary clinical complex (VCC), College of Veterinary and Animal Sciences, Meerut with the history of acute/chronic skin lesions in paws. Clinical signs noticed in these cases were alopecia, licking, nodules on the paw, erythema, exudation, crust formation and hyper pigmentation. Skin scrapings, swabs and multiple impression smears were collected from the affected area and sent to Diagnostic section of VCC. The skin scrapping were digested in 10% potassium hydroxide and examined under 10X objective of microscope. The impression smear was air-dried and stained with Field stain. The impression

How to cite this article : Singh, G.K., John, J.K., Sarkar, T.K., Shukla, M., Das, T., Jaiswal, V., Chandra, N., Jithin, M.V., Singh, A.K. and Varun, V.K. 2024. Clinico-cytopathological changes in pyogranulomatous pododermatitis in dogs. Indian J. Vet. Pathol., 48(2) : 185-187.

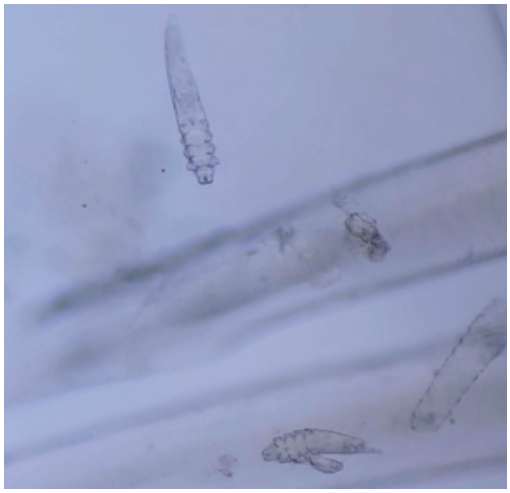

Fig. 1. Cigar shaped *Demodex canis* in skin scraping (100x).

smear was fixed in methanol for 5 minutes. The slides were then washed, and each slide was dipped in Field stain solution B for 10 seconds. Afterward, the slides were rinsed in running tap water and subsequently immersed in Field stain solution A for 20 seconds. The slides were once again washed, air-dried, and examined under an oil immersion (100X) objective. Swabs were used for isolation of bacterial organism and further characterization was done based on catalase and oxidase test.

In skin scraping examination and in impression smear, typical cigar shaped *Demodex canis* was noticed in one case (Fig. 1). In the cytological examination of smears from the above case, the presence of a large number neutrophils, cocci (Fig. 2A), degenerate neutrophils with a significant fraction of activated macrophages was revealed (Fig. 2B). Many of the neutrophils and macrophages exhibit phagocytic activity. Degenerate neutrophils are characterised by lightly stained and swollen nucleus. Presence of degenerate neutrophils indicate presence of infectious agent usually bacteria. In this case, we noticed cocci in group, both extracellularly and intracellularly in neutrophils (Fig. 2C). Phagocytic neutrophils and macrophages contain some necrotic materials also in cytoplasm. Many neutrophil nuclei were condensed into a single large, dark structure, usually round, and a few showed mild indentation. Numerous large mononuclear cells with abundant pale grey foamy cytoplasm was also noticed and in few cytoplasmic vacuoles were seen. Multiple multi-nucleated cells with dark blue granular cytoplasms also observed. Few small lymphocytes were noticed. Most of these round epithelial cells of stratum spinosum contain cytoplasmic melanin granules indicates hyper pigmentation of the affected region. A large number of small, round epithelial cells with large, round nuclei were seen scattered throughout the sections, indicating acantholysis (Fig. 2D).

Skin scraping examination from the paw region was negative for any mites in other 3 cases. Cytological examination of impression smear from the paw

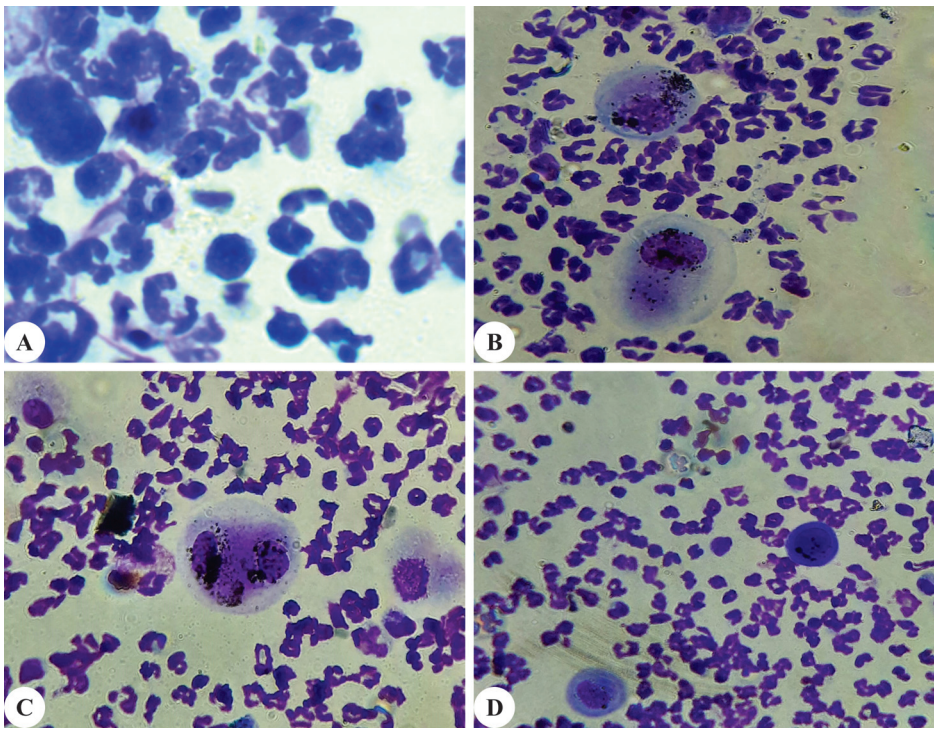

Fig. 2A. Large number of neutrophils cocci (Field stain, 1000x). **B.** Large number of degenerate neutrophils and macrophages (Field stain, 1000x). **C.** Large number of neutrophils and cocci in groups (Field stain, 1000x). **D.** Large number of neutrophils and acanthocytes (Field stain, 1000x).

region showed large number of neutrophils with intracytoplasmic cocci. Cocci were seen outside the neutrophils also in groups of two, four and more. Bacterial isolation was done in nutrient agar. After 24 hrs of incubation at 37^{O}C, small cream colored colonies were seen on nutrient agar. Gram staining and other biochemical tests such as oxidase and catalase were done and the bacteria isolated was identified as *Staphylococcus* spp.

Pododermatitis is any inflammatory condition of the skin of paws. Pedal folliculitis is a complex and multifactorial, and may be frustrating to diagnose and treat[1.] It may arise due to many underlying etiology such as bacteria, viruses, fungi, parasites, allergies, foreign bodies, genetics, hormonal and immunological conditions. In this present case, the etiology was bacteria and parasitic infection. Cocci were found in groups suggestive of staphylococcus species and *Demodex canis* was noticed in skin scraping examination. In this case, the animal was under treatment for a long time. In a study, suggested that *Staphylococcus aureus* is a major pathogen associated with pododermatitis[6]. Though other bacteria's are also involved in causing pododermatitis. Granulomatous pododermatitis was reported from cats and dogs[7]. In this present study, cytological examination revealed presence of neutrophils, macrophages, multinucleated cells, acanthocytes and epithelial cells with melanin granules suggesting pyogranulomatous infection, spongiosis and hyperpigmentation. Diagnosis of pododermatitis can be done by taking history, physical examination, clinical signs, skin scraping examination, cytology, bacterial isolation and identification[5]. By correlating the clinical signs, cytological examination and skin scraping examination, above cases were diagnosed as pododermatitis.

ACKNOWLEDGEMENTS

The authors are thankful to SVPUAT, Meerut for granting permission and providing facilities to carry out this study.

REFERENCES

1. Miller WH, Griffin CE and Campbell KL. 2013. Muller and Kirk's Small Animal Dermatology. 7th ed. St. Louis, Missouri, Elsevier. 201-203.
2. Hnilca KA. 2011. Small Animal Dermatology: A color Atlas and Therapeutic Guide. 3rd ed. St. Louis, Missouri, Elsevier Saunders. 60-62.
3. Besancon MF, Conzemius MG, Evans RB and Ritter MJ. 2004. Distribution of vertical forces in the pads of greyhounds and Labrador retrievers during walking. *Am J Vet Res* **65:** 1497-1501.
4. Duclos DD, Hargis AM and Hanley PW. 2008. Pathogenesis of canine interdigital palmar and plantar comedones and follicular cysts, and their response to laser surgery. *Vet Dermatol* **19:** 134-141.
5. Bajwa J. 2016. Canine pododermatitis. *The Canadian Vet J* **57:** 991.
6. Heidemann Olsen R, Christensen H, Kabell S and Bisgaard M. 2018. Characterization of prevalent bacterial pathogens associated with pododermatitis in table egg layers. *Avian Pathol* **47:** 281-285.
7. Sugahara G, Kiuchi A and Usui R. 2014. Granulomatous pododermatitis in the digits caused by Fusarium proliferatum in a cat. *J Vet Med Sci* **76:** 435-438.

Indian J. Vet. Pathol., 48(2) : 188-190, 2024: DOI: 10.5958/0973-970X.2024.00029.2

SHORT COMMUNICATION

Pathology of mucometra in a Queen cat

G. Swetha, A. Nasreen[1*], A. Anand Kumar, K. Rajesh[1] and M. Raghunath[1]
[1]Department of Veterinary Clinical Complex, Department of Veterinary Pathology, College of Veterinary Science, Tirupati-517 502, Sri Venkateswara Veterinary University, Andhra Pradesh, India

Address for Correspondence
A. Nasreen, Assistant Professor, Department of Veterinary Clinical Complex, Department of Veterinary Pathology, College of Veterinary Science, Tirupati-517 502, Sri Venkateswara Veterinary University, Andhra Pradesh, India,
E-mail: nashreen7@gmail.com

Received: 2.11.2023; Accepted: 23.11.2023

ABSTRACT

Mucometra is accumulation of sterile mucoid fluid in the uterine lumen without any significant systemic clinical signs. A queen cat of two years age without any apparent clinical signs was brought to clinical complex for elective spaying. After ovario-hysterectomy, ovarian and uterine tissues were submitted for histopathology. Grossly, uterus was distended with fluid which was slightly cloudy and viscous. Ovary revealed multiple clear cystic structures on the surface. The microscopic examination of the uterine tissue revealed marked edema with few hyperplastic endometrial glands and ovary revealed cystic structures lined by layers of granulosa cells in the cortical region.

Keywords: Follicular cyst, histopathology, mucometra, Queen cat

How to cite this article : Swetha, G., Nasreen, A., Kumar, A.A., Rajesh, K. and Raghunath, M. 2024. Pathology of mucometra in a Queen cat. Indian J. Vet. Pathol., 48(2) : 188-190.

Queen cats are induced ovulators, but sometimes spontaneous ovulations are also noticed[1]. Mostly, the ovarian changes are non-malignant and do not interfere with fertility of queen, but some hormonal changes may raise concern for queen's overall health and decrease prognosis for future fertility[2]. Ovarian hormones have an impact on the morphological changes that uterus undergoes and results in uterine pathologies such as sub-clinical endometritis, cystic endometrial hyperplasia and mucometra. Mucometra is defined as build-up of sterile fluid in the uterine cavity typically clear to slightly cloudy and can vary in viscosity. This condition occurs sporadically[3] as a result of excessive production of uterine fluid following endometrial hyperplasia, or an obstruction in the uterine lumen, cervix or vagina[4].

Cats are known to frequently develop ovarian cysts, which arise from either mature or degenerating follicles and the occurrence of these cysts tends to increase as they get older[3]. The cysts fail to discharge ova and remain persistent in the ovary, inhibiting the folliculogenesis and is a primary factor contributing to infertility of cats[5]. The most common among them is follicular cyst, which is known to secrete oestrogens[2].

An intact two-year-old queen cat was admitted to the Veterinary clinical complex, College of Veterinary Science, Tirupati for ovariohysterectomy. The queen cat was presented with no apparent clinical signs and the hematological parameters were with in normal range before performing the ovario-hysterectomy. The uterus and ovaries were separated and directed for laboratory for detailed gross and microscopic examination. Tissue samples from uterus and ovaries were processed for histopathological studies by following the standard procedures[6].

On macroscopic examination the uterine horns were bilaterally distended with accumulation of mucoid fluid[3,7]. The lumen of uterine horns revealed, about 50 ml mucoid fluid which was slightly viscous to cloudy and light yellow in colour in accordance with earlier reports[8,9]. There was severe congestion of blood vessels on serosal layer of uterine horns (Fig. 1). The ovaries had a smooth and glistening surface with multiple small size cysts with clear fluid on the surface[2,8,9] (Fig. 2).

Histopathological examination of uterus revealed decreased endometrium to myometrium ratio and mild hyperplasia of endometrial glands. The endometrial stroma showed diffuse oedema and mild fibroplasia[8,9] (Fig. 3). The glands were dilated and lined by single layer columnar epithelial cells. The cells were showing mild hyperplasia with basal nuclei and few nucleoli[7] (Fig. 4). In the myometrium, stratum vasculature showed great dilation of blood vessels with severe congestion[2]. Ovaries revealed few primordial follicles with follicular cyst in the cortex region. The cyst wall showed more than two layers of granulosa cells, few areas revealed exfoliation of the lining granulosa cells into the cystic lumen[7] (Fig. 5). Diffuse

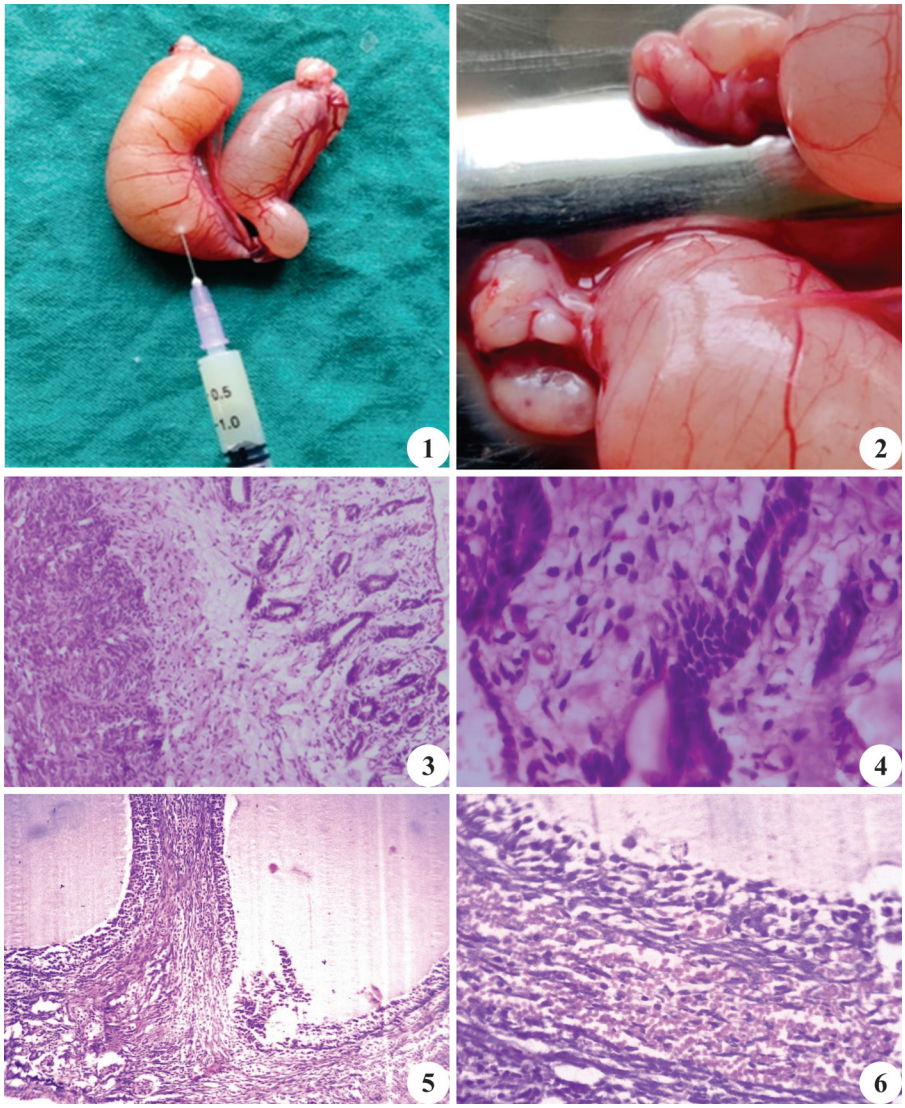

Fig. 1. Mucometra: Symmetrically distended uterine horns with mucoid fluid. Congestion of blood vessels on serosal layer; **Fig. 2.** Follicular cyst: Ovaries showed smooth, glistening surface with multiple cystic structures; **Fig. 3.** Mucometra: Endometrial stroma showed diffuse oedema and fibroplasia with mild increase in glandular structures (H&E X100); **Fig. 4.** Mucometra: Hyperplasia of endometrial glandular epithelial cells and fibroplasia (H&E X400); **Fig. 5.** Follicular cyst, Ovary: Exfoliation of granulosa cells into cystic lumen (H&E X100); **Fig. 6.** Follicular cyst: Diffuse haemorrhages and congestion of blood vessels around the cyst (H&E X400).

haemorrhages and congestion were noticed around the follicular cyst along with mild interstitial endocrinal cell hyperplasia[10] (Fig. 6). Mucometra is usually reported as an incidental finding without any prominent clinical signs[1]. Though the condition is not life threatening it plays a major role in causing infertility in queen cats. Follicular cyst mainly contributes to the development of mucometra through oestrogen stimulation. The chronic stimulation by estrogen causes diffuse accumulation of fluid in the uterus leading to distension of uterine lumen[2]. This is accompanied with endometrial hyperplasia due to progesterone stimulation later aggravated by estrogen finally result in mucometra[11].

REFERENCES

1. Fontbonne A. 2011. Infertility in bitches and queens: recent advances. *Rev Bras Reprod Anim* **35:** 202-209.
2. Johnston SD, Kustritz MVR and Olson PNS. 2001. Disorders of the Feline Uterus and Uterine Tubes. In: Canine and Feline Theriogenology, WB Saunders Company, Philadelphia. pp. 463-471.
3. Polat B and Salmanoğlu MR. 2007. Hydrometra and endometrial hyperplasia in a cat with follicular cyst. *J App Bio Sciences* **1:** 109-110.
4. Jubb KVF and Kennedy PC. 1970. The uterus. In: Pathology of Domestic Animals. New York: Academic press. Pp. 515.
5. Gharagozlou F, Youssefi R, Akbarinejad V, Sasani F, Taghizadeh-Jahed M, Shahpoorzadeh T, Valaie Moradipor H, Hasani N and Atashbaste M. 2014. Evaluation of serum anti-Müllerian hormone (AMH) in a Persian queen cat with bilateral cystic ovarian disease. *Comp Clin Pathol* **23:** 237-239.

6. Bancroft DJ and Cook CH. 1994. Fundamentals of normalhistology and histopathology. Manual of histopathological techniques and their diagnostic application, Edinburgh: Churchill Livingstone: pp. 1-17.
7. Payan R, Pina J, Costa M, Seixas F and Pires MA. 2006. Oestrogen receptors in a case of hydrometra in a bitch. *Veterinary Record* **58:** 487.
8. Rangasamy S, Jemimah ER, Thangapandian P, Sarath T, Nag BSPK and Sridevi P. 2017. Hydrometra with concurrent cystic endometrial hyperplasia and cystic ovary in a queen cat. *Ind Vet J* **94:** 59-61.
9. Nash AS, McCandlish IAP and Renton JP. 1986. Hydrometra in two cats. *J Small Ani Prac* **27:** 265-271.
10. Shiyamala S, Ramesh S and Hemalatha S. 2020. A case study of reproductive pathology in bitches. *J Ent & Zoo Sci* **8:** 1527-1531.
11. Barrau MD, Abel JH and Verhage HG. 1975. Development of the endometrium during the estrous cycle in the bitch. *Am J Anat* **142:** 47-66.

Indian J. Vet. Pathol., 48(2) : 191-195, 2024: DOI: 10.5958/0973-970X.2024.00030.3

CASE REPORT

A case of Paratuberculosis (Johne's Disease) in Vrindavani cattle

C.P. Singh, S.D. Vinay Kumar, Sourabh Babu, Hiteshwar Singh Yadav, Neha, Pawan Kumar and Vidya Singh*

Division of Pathology, ICAR-Indian Veterinary Research Institute, Izatnagar, Bareilly-243 122, Uttar Pradesh, India

Address for Correspondence

Vidya Singh, Senior Scientist, Division of Pathology, ICAR-Indian Veterinary Research Institute, Izatnagar, Bareilly-243 122, Uttar Pradesh, India, E-mail: vidyasingh100@gmail.com

Received: 13.4.2023; Accepted: 7.3.2024

ABSTRACT

An adult female crossbred cattle was presented for necropsy at post mortem facility of Division of Pathology, ICAR-IVRI, Izatnagar with clinical history of chronic diarrhoea, progressive weight loss, reduction in milk yield and poor response to therapy. External examination of carcass revealed poor body condition with skin abrasions at dorsal surface of left metacarpal area and near to perineal area. Gross examination of the carcass revealed transverse corrugation in jejunum and ileum and enlarged mesenteric lymph nodes. Cut sections of the intestine and lymph nodes revealed congestion, edema and granulomatous lesions. Ziehl- Neelsen staining of impression smear and tissue section from jejunum, ileum and lymph nodes depicted pink-red, short, stumpy acid fast bacilli. Microscopic examination revealed desquamation of enterocytes, flattening of villi and presence of large number of macrophages, epitheloid cells multinucleated giant cells in the mucosa and submucosa of jejunum& ileum. Lymphoid depletion with infiltration of multinucleated giant cell was seen in subcapsular spaces of mesenteric lymph nodes. Molecular diagnosis with PCR revealed amplification of 400bp for IS900 gene specific for Johne's bacilli. The case was found to be confirmatory for paratuberculosis based on gross, histological, and molecular analysis.

Keywords: Cattle, Johne's disease, MAP, Paratuberculosis

Johne's disease (Paratuberculosis) is a chronic granulomatous inflammation of distal portion of the jejunum, ileum and the ileocecal valve. It is caused by *Mycobacterium avium subsp. Paratuberculosis* (MAP) in cattle and sheep and goat[1]. *Mycobacterium avium subsp. paratuberculosis*, is a facultative intracellular acid-fast bacterium. It is an extremely slowly growing mycobactin-dependent organism that replicates within the macrophages in gastrointestinal tract and associated lymphoid tissues[2]. Fecal-oral infection in young calves results in protracted periods of subclinical infection during which low titers of organisms are discharged before the infection progresses to its terminal state[3].Johne's disease progresses through several stages and in the majority of cases, takes several years from infection to manifest clinical signs[4]. They reported that infected animals pass through three main disease stages classified as: (1) subclinical, non-shedding; (2) subclinical, shedding; (3) clinical, intermittently or permanently shedding. Each of the stages is marked by specific pathological changes which are best recognized at the microscopic level[5]. The major route of MAP infection in ruminants is *via* ingestion, so the first step in infection is uptake of MAP through mucosal surfaces primarily in the ileum, *via* M cells (specialized absorptive mucosal cells called Microfold cells) residing in the Peyer's patches and then phagocytosed by sub epithelial macrophages. Eventually, the infected macrophages migrate into local lymphatics and the infection spread to regional lymph nodes[6].

An emaciated, hidebound carcass of adult crossbred cattle was received for necropsy at the postmortem facility of the Division of Pathology, ICAR-IVRI, Izatnagar, Bareilly. It had the history of chronic diarrhoea, progressive weight loss, reduction in milk yield and poor response to therapy. External examination of the carcass revealed poor body condition with soiled hind quarters and skin aberrations at the dorsal surface of the body and perineal region.

Gross examination of the carcass revealed multifocal ecchymotic haemorrhages in the lungs with patchy areas of consolidation and thickening of the pleura. Transverse corrugations of the intestinal mucosa was seen in the distal part of jejunum and ileum and in the region around illeocaecal valve. Mesenteric lymph nodes were found enlarged and edematous. Cut sections of the intestine and lymph nodes revealed congestion, edema and granulomatous lesions. Representative tissue samples of the intestine and lymph nodes were collected in 10% neutral buffered formalin (NBF) as well as in ice for histopathology and molecular pathology studies. Also, impression smear of the intestine and mesenteric lymph nodes were collected for Ziehl-Neelsen (ZN) staining.

Impression smears of tissue were dried, fixed in methanol and

How to cite this article : Singh, C.P., Kumar, S.D.V., Babu, S., Yadav, H.S., N., Kumar, P. and Singh, V. 2024. A case of Paratuberculosis (Johne's Disease) in Vrindavani cattle. Indian J. Vet. Pathol., 48(2) : 191-195.

Fig. 1. Gross pictures of the cattle carcass with **(A)** emaciated and dehydrated body condition with visibility of prominent ribs; **(B)** Intestine showing congestion and haemorrhages; **(C)** Transverse corrugations, congestion, petichae and thickening of mucosa in the large intestine; **(D)** Enlarged congested mesenteric lymph nodes.

stained with Ziehl Neelsen staining[7] and examined under oil immersion microscopy. Tissue fixed in NBF were processed for routine histopathology and tissue sections (4-5µm) were examined under microscope[8]. Fresh tissue samples were cut into small pieces using sterile scissors and forceps and homogenized with 200µl of 1X PBS using a hand held homogenizer at 5,000 to make 10% suspension. Total DNA was extracted from the tissue suspensions using DNeasy mini kit (Qiagen) as per the manufacturer's instructions. Concentration of the eluted DNA was quantified at A260/ A280 and checked for its purity and was subjected screening with previously described PCR primers of MAP, IS900 primers P90 (5' -GAAGGGTGTTCGGGGCCGTCGCTTAGG-3') and P91 (5'-GGCGTTGAGGTCGATCGCCCACGTGAC-3'), which amplifies a 400bp fragment of IS900 insertion sequence specific for MAP[9]. The reaction was carried out in 25 µL volume, containing 12.5µL Green dream Taq master mix, 0.5µL each of the forward and reverse primers, 1.0µL DMSO, 1.0µL of template DNA and 9.5 µL of NFW. Thermal cyclic conditions included initial denaturation for 5 min at 94^{O}C followed by 40 cycles of denaturation for 1 min at 94^{O}C, annealing for 30 sec at 65^{O}C and extension for 1min at 72^{O}C, and final extension of 10 min at 72^{O}C. Agarose gel (1%) gel electrophoresis of the amplified product in Tris-acetate EDTA (1%) buffer revealed a product of expected size of 400bp.

Major gross findings are depicted in Fig. 1. The animal had history of chronic diarrhoea and gross examination of the carcass revealed severe emaciation as subcutaneous fat was completely gelatinized and the hide was closely attached to the underlying bony skeleton. Hind quarters were soiled; transverse corrugations were seen in the distal part of jejunum, ileum and ileocecal valve. Mesenteric lymph nodes were found enlarged and edematous Fig. 1A-D.

Microscopic findings are depicted in Fig. 2A-H. Examination of ZN stained impression smear revealed multiple short, stumpy, comma shaped acid fast bacilli were observed in colony. Microscopic examination of the tissue sections of the jejunum, and ileum revealed extensive thickening, villous atrophy with flattening of the villi. There was infiltration of mononuclear cells (MNCs) including macrophages, epitheloid cells, lymphocytes, plasma cells and multinucleated giant cells in the lamina propria of mucosa and upper portion of the submucosa. Infiltration of MNCs was extensive in the lamina propria giving it a puffed up appearance. The crypts of Lieberkuhn, which are the intestine's mucosal glands, showed signs of atrophy, and the glandular lumen was stuffed with exfoliated cells and mononuclear cells. Infiltration of MNCs was also seen in the wall of the crypts. Mild infiltration of MNCs were also seen in the serosa layer. Epitheloid cells were observed to have foamy cytoplasm with dark round to oval shaped eccentric nuclei. Ziehl-Neelsen staining of the tissue

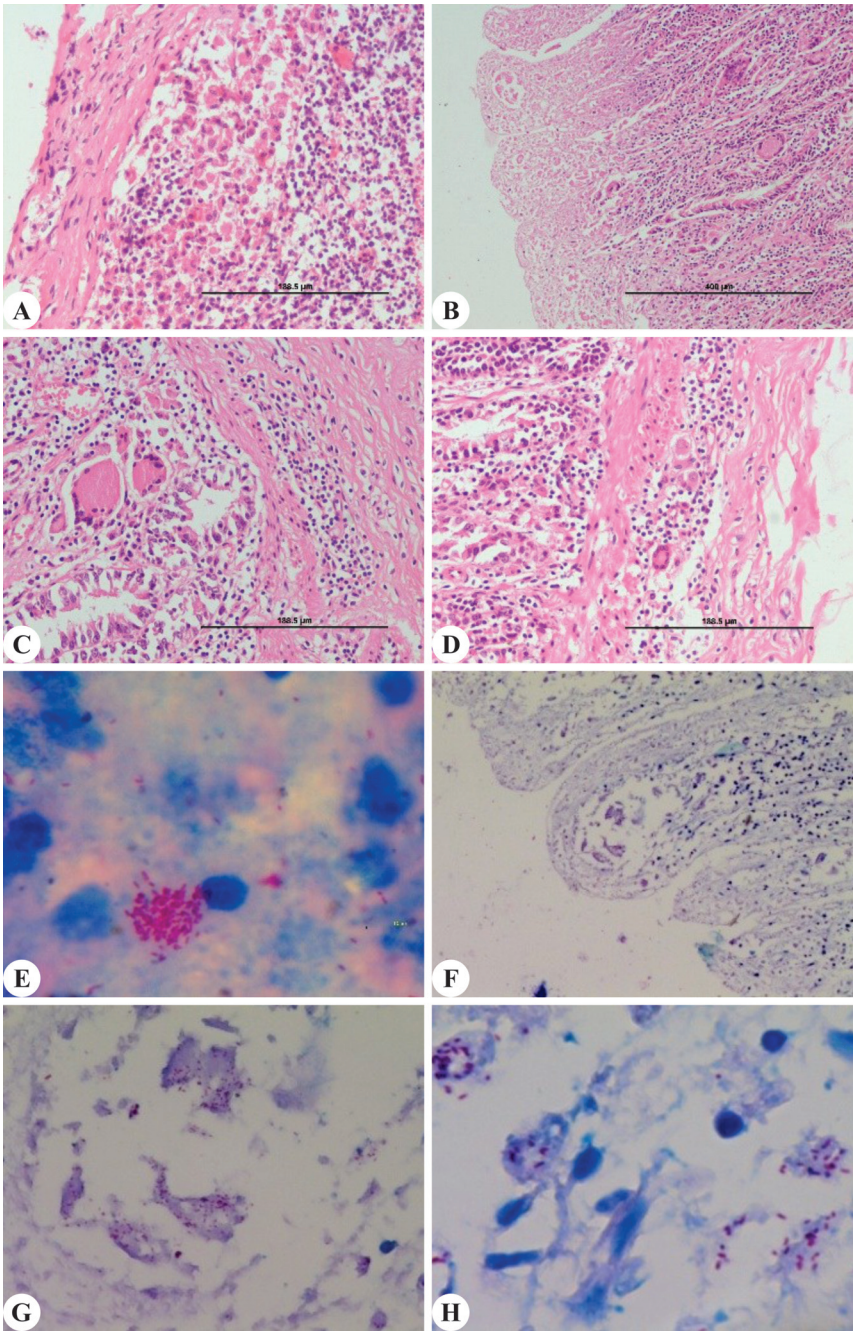

Fig. 2. Section of the mesenteric lymph node and intestines showing **(A)** infiltration of mononuclear cells, epithelioid cells and giant cells in subcapsular space of mesenteric lymph nodes (100X, H&E); **(B)** Villous atrophy causing flattening of the villi in intestine (40X, H&E); **(C and D)** Infiltration of mononuclear cells, epithelioid cells and giant cells (arrow) in the lamina propria of mucosa and sub mucosa of intestine (100X, H&E); **(E)** Colony of short, stumpy, comma shaped acid fast bacilli in impression smear of ileum (1000X, ZN staining); **(F)** Tissue section of ileum showing presence of comma shaped acid fast bacilli (100X, ZN staining); **(G and H)** Pinkish-red acid fast bacilli within degenerating foamy macrophage and epithelioid cells at 400X and 1000X, respectively (ZN staining).

sections revealed epithelial macrophages stuffed with short, stumpy, comma shaped acid fast bacilli. There were multiple microgranulomas visible in the parenchyma of the mesenteric lymph nodes, thick fibrous connective tissue capsules, and an abundance of epithelioid cells in the cortical region. Fibrous connective tissue followed by a rim of MNCs was also seen around the granulomas.

Agarose gel electrophoresis (1%) of the PCR amplified products revealed product of expected size of 400 bp for IS900 insertion sequence specific for *Mycobacterium avian subsp. paratuberculosis* (Fig. 3).

Johne's disease is one of the important infectious diseases affecting the ruminant population. In cattle,

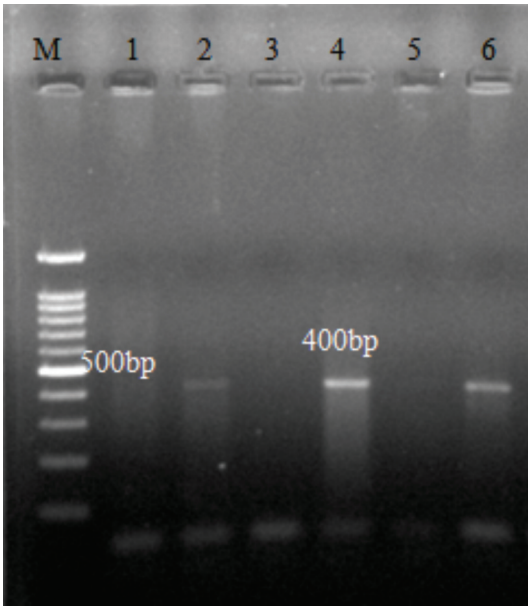

Fig. 3. Agarose gel electrophoresis (1.0) showing positive PCR amplicon of MAP (400 bp) in mesenteric lymph node (L2) and intestine tissue (L4) along with positive control (L6), negative control (L1, L3, L5) and 100 bp DNA ladder (M).

it is characterized by gradual weight loss and chronic diarrhoea in the later stages. Paratuberculosis is highly prevalent in north India and has been reported as 28.6% and 29.8% in buffaloes and cattle, respectively[9]. In the present study, an adult cross-bred cow with clinical history of chronic diarrhoea, gradual weight loss and emaciated body condition was necropsied and investigated using histopathology, ZN staining and molecular methods.

Grossly, the carcass had characteristic lesions like congested and hemorrhagic intestinal mucosa with transverse corrugations and thickened intestinal wall. Mesenteric lymph nodes were enlarged and congested. Microscopically, desquamation and necrosis of the intestinal epithelial cells was seen in the distal segment of jejunum and ileum. Granulomatous inflammation was seen in the mucosa and submucosa of distal intestine with infiltration of MNCs, epitheloid cells and multinucleated giant cells. ZN staining revealed acid fast bacteria. The results observed in the study were in congruence to those of findings of earlier scientists[10,11]. They reported diffuse thickening of the intestinal wall with transverse corrugations. Caseative necrosis and calcification was not seen in the present case, which is in contrast to the previous findings[12]. Mucosal corrugations observed in the current study are in conformity with the findings of other scientists[13]. Genomic detection of MAP by PCR using IS 900 sequence specific primers led to amplification of 400 bp amplicons, which is in line with the earlier observations[14]. In the present investigation, the clinical history, gross and microscopic changes, and PCR amplifications all supported the diagnosis of paratuberculosis.

ACKNOWLEDGEMENT

The authors are thankful to the Director, ICAR-IVRI for providing the facilities for carrying out the above research work and also for providing Institutional fellowship to the first author. The authors also sincerely acknowledge the funding provided by the SERB-DST for providing financial support in the form of research project under core research grant scheme of SERB to the corresponding author.

REFERENCES

1. Gulliver EL, Plain KM, Begg DJ and Whittington RJ. 2015. Histopathological characterization of cutaneous delayed-type hypersensitivity and correlations with intestinal pathology and systemic immune responses in sheep with paratuberculosis. *J Comp Pathol* **153:** 67-80.
2. Klausen J, Huda A, Ekeroth L and Ahrens P. 2003. Evaluation of serum and milk ELISAs for paratuberculosis in Danish dairy cattle. *Prev Vet Med* **58:** 171-178.
3. Stabel JR, Wells SJ and Wagner BA. 2002. Relationships between fecal culture, ELISA, and bulk tank milk test results for Johne's disease in US dairy herds. *J Dairy Sci* **85:** 525-531.
4. Buergelt CD, Layton AW, Ginn PE, Taylor M, King JM, Habecker PL and Collins MT. 2000. The pathology of spontaneous paratuberculosis in the North American bison (*Bison bison*). *Vet Pathol* **37:** 428-438.
5. Collins MT, Lisby G, Moser C, Chicks D, Christensen S, Reichelderfer M and Binder V. 2000. Results of multiple diagnostic tests for Mycobacterium avium subsp. paratuberculosis in patients with inflammatory bowel disease and in controls. *J Clin Microbiol* **38:** 4373-4381.
6. Tiwari A, VanLeeuwen JA and McKenna SLB. 2006. Johne's disease in Canada Part I: Clinical symptoms, pathophysiology, diagnosis, and prevalence in dairy herds. *Can Vet J* **47:** 874-882.
7. Huntley JFJ, Whitlock RH, Bannantine JP and Stabel JR. 2005. Comparison of diagnostic detection methods for *Mycobacterium avium subsp. paratuberculosis* in North American bison. *Vet Pathol* **42:** 42-51.
8. Bancroft JD, Harry CC and Stirling RW. 2007. Manual of Hisological Techniques and their Diagnostic Application. Churchill Livingstone, London. pp. 17-34.
9. Singh SV, Singh AV, Singh R, Singh S, Sharma N, Shukla S, Misra PK, Singh JS, Sohal H, Kumar PK, Patil P and Sandhu KS. 2008. Sero-prevalence of Bovine Johne's disease in buffaloes and cattle population of North India using indigenous ELISA kit based on native *Mycobacterium avium subspecies Paratuberculosis* 'Bison type' genotype of goat origin. *Comp Immunol Microb Infect Dis* **31:** 419-433.
10. Maxie MG, Jubb KVF, Kennedy PC and Palmer NC. 2007. Pathology of Domestic Animals, 5th Ed. Vol. 2. Saunders Elsevier, London. pp. 222-225.
11. Alharbi KB, Al-Swailem A, Al-Dubaib MA, Al-Yamani E, Al-Naeem A, Shehata M, Hashad ME, Albusadah KA and Mahmoud OM. 2012. Pathology and molecular diagnosis of paratuberculosis of camels. *Trop Anim Health Prod* **44:** 173-177.
12. Sikandar A, Cheema AH, Younus M, Aslam A, Zaman MA and Rehman T. 2012. Histopathological and Serological Studies on Paratuberculosis in Cattle and Buffaloes. *Pak Vet J* **32:** 547-551.

13. Rhodes G, Henrys P, Thomson BC and Pickup RW. 2013. *Mycobacterium avium subspecies paratuberculosis* is widely distributed in British soils and waters: Implications for animal and human health. *Environ Microbiol* **15:** 2761-2774.
14. Stanley EC, Mole RJ, Smith RJ, Glenn SM, Barer MR, McGowan M and Rees CE. 2007. Development of a new, combined rapid method using phage and PCR for detection and identification of viable Mycobacterium paratuberculosis bacteria within 48 hours. *App Environ Microbiol* **73:** 1851-1857.

Indian J. Vet. Pathol., 48(2) : 196-198, 2024: DOI: 10.5958/0973-970X.2024.00031.X

CASE REPORT

Mixed infection of ovine pulmonary adenocarcinoma and maedi in sheep - A case study

Hiteshwar Singh Yadav, Neha, S.D. Vinay Kumar, Chandra Pratap Singh, Chandrakanta Jana, Vidya Singh and Pawan Kumar*
Division of Pathology, ICAR-Indian Veterinary Research Institute, Izatnagar, Bareilly-243 122, Uttar Pradesh, India

Address for Correspondence
Pawan Kumar, Senior Scientist, Division of Pathology, ICAR-Indian Veterinary Research Institute, Izatnagar, Bareilly-243 122, Uttar Pradesh, India, E-mail: chauhan2k1@gmail.com

Received: 10.8.2023; Accepted: 6.3.2024

ABSTRACT

Ovine pulmonary adenocarcinoma (OPA) and maedi are retroviral diseases of small ruminants caused by jaagsiekte sheep retrovirus (JSRV) and maedi visna virus (MVV), respectively. A case of mixed infection of OPA and maedi in slaughtered sheep is being presented in this paper. The lung tissue samples from the different lobes were collected in 10% neutral buffered formalin for histopathological evaluation and at -20^{O}C for molecular work, respectively. Histopathologically, the lung tissue sections showed presence of proliferated pneumocytes, hyplerplastic BALT, interstitial pneumonia with infiltration of mononuclear cells and smooth muscle hyperplasia in interalveolar septa. PCR assays were found to be positive for both JSRV and MVV nucleic acid suggesting mixed infection of OPA and maedi in sheep.

Keywords: JSRV, maedi, MVV, ovine pulmonary adenocarcinoma, sheep

Retroviral diseases of sheep include ovine pulmonary adenocarcinoma (OPA) and maedi visna. Both diseases have long incubation period causing production losses to farmers. OPA is caused by jaagsiekte sheep retrovirus (JSRV) and produce neoplastic proliferation of the type II pneumocytes of alveoli and Clara cell of bronchioles[1,2]. Maedi is caused by maedi visna virus (MVV) producing inflammatory conditions like interstitial pneumonia, encephalitis, mastitis and arthritis[3,4]. Clinical diagnosis of the diseases usually possible at later stage, when animal starts to show the clinical signs and symptoms. Characteristic gross and microscopic lesions in the lungs provide definitive diagnosis in case of OPA[5]. PCR assays have been reported by earlier workers to diagnoses the viral nucleic acid in tissue samples, blood, milk and nasal swabs[6,7]. Mixed infection of both JSRV and MVV is usually rare and very few reports are available[8]. The present case reported the rare case of mixed infection of JSRV and MVV diagnosed based upon histological lesions and PCR assay.

In the present case, the lung sample from slaughtered sheep was collected from different lobes in 10% neutral buffered formalin for histopathology and at -20°C in sterile tube for molecular work. Lung tissue sample fixed in formalin was processed for hematoxylin and eosin staining (H & E) by following standard protocol. Briefly, the tissue sections were dehydrated, embedded in paraffin blocks and sections of 4-5 µm thickness were cut and placed on glass slides and stained with H & E. The stained slides were examined under light microscope for histological alterations. Tissue samples stored at -20°C were processed for DNA extraction by using commercial isolation Kit (Qiagen). Extracted DNA was used to detect the JSRV and MVV nucleic acid by PCR. PCR assay for the JSRV and MVV detection was performed as described in previous report. JSRV nucleic acid was detected by using the specific primers (U3) described in earlier studies[6]. MVV was detected by using nested PCR assay[7]. The contents were mixed thoroughly and spun briefly and the tubes were then placed in a thermocycler (Q-Cycler 96, Hains Lifesciences). PCR products were electrophoresed in 2% agarose gel and examined in Gel Documentation system (c150Azure Biosystem).

How to cite this article : Yadav, H.S., N., Kumar, S.D.V., Singh, C.P., Jana, C., Singh, V. and Kumar, P. 2024. Mixed infection of ovine pulmonary adenocarcinoma and maedi in sheep - A case study. Indian J. Vet. Pathol., 48(2) : 196-198.

Histopathological examination of the lung tissue sections revealed multifocal areas of interstitial pneumonia, lymphoid hyperplasia in the bronchus-associated lymphoid tissue and smooth muscle hyperplasia at interalveolar septa. Interstitial pneumonia was characterized by infiltration of lymphocytes and macrophages. These changes were indicative of the maedi as reported by earlier workers also[7,9]. Along with these changes, areas of bronchiolar epithelial hyperplasia were also observed at few locations forming small projections and were indicative of OPA reported earlier[1] (Fig. 1A-D).

PCR assay for JSRV and MVV were found positive. Nested PCR for MVV amplified specific product of 199 bp and 276 bp

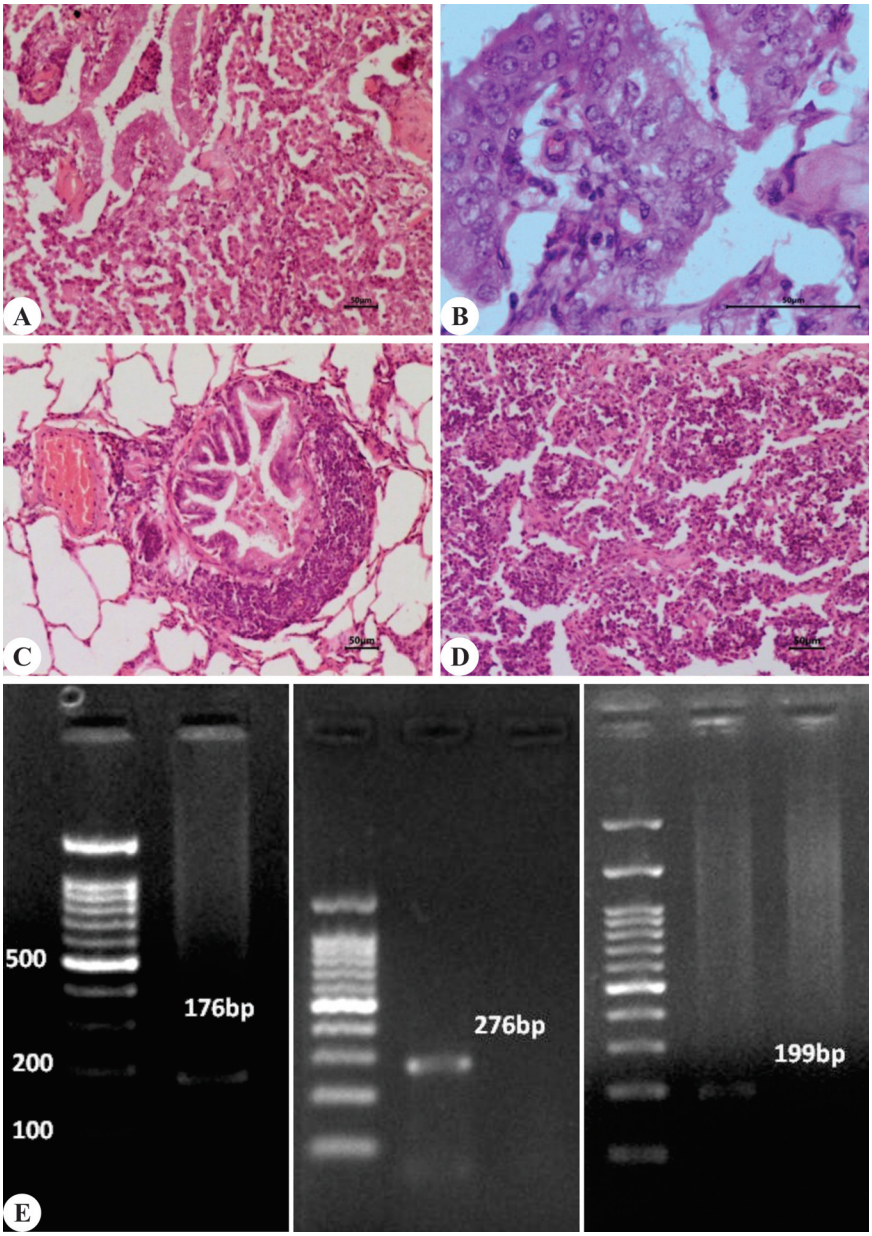

Fig. 1A. Lung tissue section showed presence of bronchiolar epithelial cell proliferation, mononuclear cell infiltration in the interstitial tissue and smooth muscle hyperplasia (H&E x100). **B.** Higher magnification showing bronchiolar epithelial cells proliferation (H&E x100). **C.** Hyperplastic change in the BALT (H&E x100). **D.** Interstitial infiltration of MNCs and smooth muscle hyperplasia in interalveolar septa (H&E x400). **E.** Agarose gel electrophoresis (2%) showing specific PCR amplified products of JSRV (176 bp) and MVV (276 bp & 199 bp).

of MVV LTR (Fig. 1E). PCR assay for JSRV amplified a sequence of 176 bp from U3 region of LTR (Fig. 1E). PCR was used by many worker to detect the presence of retroviral agents in various types of samples i.e. milk, nasal swabs, synovial fluid, etc.[7] Similar cases of mixed infection of JSRV and MVV were reported earlier[8]. Although, the occurrence of these mixed infections are rare, yet there is a need to screen the pneumonic lung samples of small ruminants for multiple samples for the multiple pathogens.

ACKNOWLEDGEMENTS

The authors are thankful to the SERB-DST, Govt. of India and Director, ICAR-Indian Veterinary Research Institute, Izatnagar for providing the necessary facilities.

REFERENCES

1. Griffiths DJ, Martineau HM and Cousens C. 2010. Pathology and pathogenesis of ovine pulmonary adenocarcinoma. *J Comp Pathol* **142:** 260-283.
2. Mishra S, Kumar P, Dar JA, George N, Singh V and Singh R. 2021. Differential immunohistochemical expression of JSRV capsid antigen and tumour biomarkers in classical and atypical

OPA: a comparative study. *Bio Rhy Res* **52:** 946-956.
3. MacLachlan NJ, Dubovi EJ, Barthold SW, Swayne DE and Winton JR. 2011. eds. Fenner's Veterinary Virology. United States: Elsevier.
4. Mishra S, Kumar P, Dar JA, George N, Singh R, Singh V and Singh R. 2020. Detection and prevalence of small ruminant lentiviral (SRLV) infections in indian sheep and goats. *Indian J Vet Pathol* **44:** 207-211.
5. Kycko A, Jasik A and Reichert M. 2008. Detection of jaagsiekte sheep retrovirus in respiratory tract fluid and lung tissue of experimentally infected lambs. *Bull Vet Inst Pulawy* **52:** 9-13.
6. Palmarini M, Holland MJ, Cousens C, Dalziel RG and Sharp JM. 1997. Jaagsiekte retrovirus establishes a disseminated infection of the lymphoid tissues of sheep affected by pulmonary adenomatosis. *J Gen Virol* **77:** 2991-2998.
7. Kumar K, Kumar P, Sindhoora K, Valecha S, Kumar R, Singh V and Singh R. 2022. Detection and immune cell response of natural maedi visna virus (MVV) infection in Indian sheep and goats. *Microb Pathog* **165:** 105-467.
8. Valecha S, Roopa N, Yadav HS, Singh R, Singh V and Kumar P. 2022. Co-infection of maedi visna virus (MVV) with jaagsiekte sheep retrovirus (JSRV) and mycoplasma in Indian sheep and goats. *Indian J Vet Pathol* **47:** 13-17.
9. Preziuso S, Taccini E, Rossi G, Renzoni G and Braca G. 2003. Experimental maedi visna virus infection in sheep: a morphological, immunohistochemical and PCR study after three years of infection. *Euro J Histo Chem* **47:** 373-378.

Indian J. Vet. Pathol., 48(2) : 199-200, 2024: DOI: 10.5958/0973-970X.2024.00032.6

CASE REPORT

Melanosis of the thyroid gland in sheep - A case report

M.V.S. Sudarsan Reddy, N. Sailaja*, P. Amaravathi and M. Sravanthi[1]
[1]State Level Diagnostic Laboratory, SVVU, Department of Veterinary Pathology, College of Veterinary Science, Tirupati-517 502, Sri Venkateswara Veterinary University, Andhra Pradesh, India

Address for Correspondence
N. Sailaja, Professor, Department of Veterinary Pathology, College of Veterinary Science, Tirupati-517 502, Sri Venkateswara Veterinary University, Andhra Pradesh, India, E-mail: sailajapath@gmail.com

Received: 31.10.2023; Accepted: 10.12.2023

ABSTRACT

Thyroid gland of a sheep, collected from a slaughterhouse in Tirupati, revealed a cyst in the right lobe filled with inspissated material and surrounded by a black discoloured area. Histopathological, examination revealed multifocal deposition of brown to black pigment within and outside the interfollicular cells and the presence of an ultimobranchial cyst on the periphery of the thyroid gland. Melanin bleach staining confirmed the pigment as melanin.

Keywords: Melanin, sheep, ultimobranchial cyst

How to cite this article : Reddy, M.V.S.S., Sailaja, N., Amaravathi, P. and Sravanthi, M. 2024. Melanosis of the thyroid gland in sheep - A case report. Indian J. Vet. Pathol., 48(2) : 199-200.

Sheep play an important role in the lives of poor farmers in India, providing them with a range of socio-economic benefits that contribute to their livelihoods and well-being. India has the third largest sheep population in the world, with a population of 74.26 million[1]. The thyroid glands play a vital role, in the reproduction, productivity, and growth in domestic animals[2]. The occurrence of melanin pigmentation in the thyroid is rare. Normally, melanin, responsible for skin and hair colour, is found in the epidermis, retina, and iris. In limited quantity, it exists in the pia-arachnoid and in the oral mucous membrane of animals. During embryonic development, the ultimobranchial body derived from the fifth pharyngeal pouch fuses with the lateral thyroid lobes to form the parafollicular cells. However, in some cases, remnants of the ultimobranchial body can give rise to ultimobranchial cysts within the thyroid gland[4].

A thyroid gland of a sheep was collected from a municipal slaughterhouse located in Tirupati. After a detailed gross examination, the tissues were subjected to fixation, dehydration, clearing, paraffin embedding and further sectioning and staining with routine H & E stain[5]. van-Gieson's and melanin bleach technique were performed for further confirmation of melanin pigment[5].

The right lobe of the thyroid gland appeared slightly larger than the left lobe and normal in colour and consistency. Upon longitudinal section, a cyst with inspissated material was identified on the hilar region in the right lobe. On both sides of the cyst, a 0.5 cm black discolouration in the parenchyma was noticed (Fig. 1).

Histopathologically, the follicles were lined by cuboidal epithelium and the colloid contained resorption vacuoles on the periphery. In multiple areas, interfollicular cells had undergone metaplasia into melanocytes, resulting in the accumulation of brown-black granular pigment within their cytoplasm, along with the presence of black-coloured granules outside the cells (Fig. 2). On van Gieson's staining, the cells appeared spindle-shaped and filled with brown to black pigment and surrounded by pink-coloured collagen tissue (Fig. 3). After the melanin bleach technique, the pigment in the cells was completely bleached confirming it as melanin (Fig. 4). From gross and histopathology, the above case was confirmed as melanosis of the thyroid gland.

In addition to melanin pigmentation, an ultimobranchial cyst was noted on one margin. The cyst was lined by stratified squamous epithelium and filled with concentric layers of eosinophilic keratinised material and follicles surrounding the cyst were collapsed due to pressure atrophy[6-8]. In addition to these, the multifocal follicular hyperplasia was observed in which the follicles were lined by more than one layer of cells partially reducing the lumen of the follicle. Melanocytes, found in the basal skin layer of animals, produce melanin through the oxidation of tyrosine, transferring the pigment to neighbouring keratinocytes via dendritic processes, where it forms a protective cap over the nucleus to shield against ultraviolet radiation. Abnormal or excessive accumulation of melanin pigment in tissues, cells, or organs is known as melanosis. In laboratory animals melanosis in thyroid follicular epithelium associated with minocycline antibiotic usage has been first

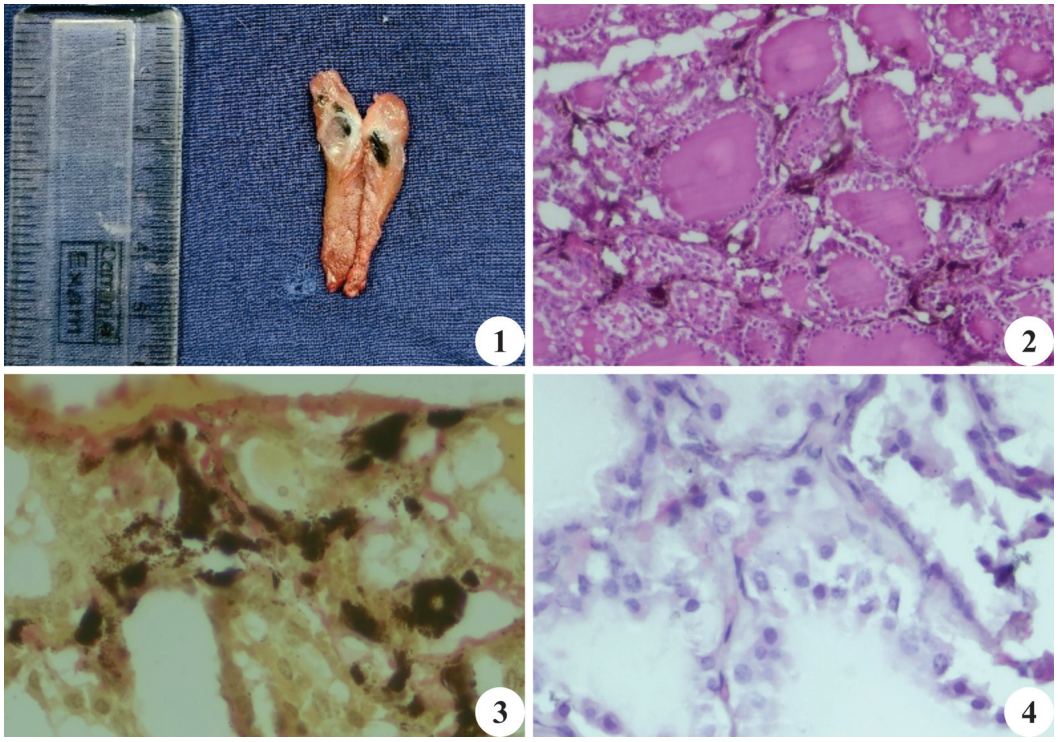

Fig. 1. Melanin pigmentation in right lobe of thyroid gland-longitudinal section; **Fig. 2.** Melanin pigment deposition in interstitium of thyroid gland (H&E x100); **Fig. 3.** Interstitial melanin pigment deposition in the thyroid parenchyma (van Gieson's stain x400); **Fig. 4.** Loss of melanin pigmentation from interstitium (Melanin bleach technique x400).

reported[9]. Further black-brown pigmentation within the follicular epithelium and colloid associated with long-term minocycline therapy was reported by[10]. The melanin deposition in the interstitium and capsule of thyroid parenchyma in a goat of unknown aetiology has been reported by[11]. Ultimobranchial cysts were congenital anomalies of the thyroid gland derived from remnants of the ultimobranchial body, which forms from the fusion of the lateral thyroid lobes and the fifth pharyngeal pouch[4].

ACKNOWLEDGEMENTS

The authors are thankful to Sri Venkateswara Veterinary University for providing facilities to carry out this study.

REFERENCES

1. 20th Livestock Census. 2019. Government of India. Ministry of Fisheries, Animal Husbandry and Dairying; Department of animal husbandry and dairying, Krishi Bhawan, New Delhi.
2. Todini L, Malfatti A, Valbonesi A, Trabalza-Marinucci M and Debenedetti A. 2007. Plasma total T3 and T4 concentrations in goats at different physiological stages, as affected by the energy intake. *Small Ruminant Res* **68:** 285-290.
3. McGavin MD and Zachary JF. 2007. Pathological Basis of Veterinary Disease, 4th edn. Mosby Elsevier. 724-726.
4. Jubb, Kennedy and Palmer. 2016. Endocrine glands. In: Pathology of domestic animals, Vol III, 6th edn. Mosby Elsevier. 292-309.
5. Bancroft, John D and Marilyn Gamble. 2008. Theory and practice of histological techniques. Elsevier health sciences. 44-47 and 126-131.
6. Nouri M, Mohammadian B and Pourjamshid R. 2010. An abattoir study of thyroid histopathology in ewes and their fetus in Ahvaz city of Iran. *Vet Res Forum* **1:** 50-53.
7. Darakhshesh M, Nouri M, Rezaei A and Barati F. 2011. An Abattoir Study of Ovine Maternal and Fetal Thyroid Lesions and the Respective Serum T3 and T4 Levels in an Endemic Goiter Region in Iran. *Vet Res Forum* **2:** 167-175.
8. Poobitha S, Nair M, Kumar R, Sivakumar M, Varshney KC, Umamaheswari D and Aw L. 2020. Ultimobranchial cysts in the thyroid of goats. *J Entomol Zool Stud* **8:** 1794-1797.
9. Benitz KF, Roberts GK and Yusa A. 1967. Morphologic effects of minocycline in laboratory animals. *Toxicil Appl Pharmacol* **11:** 150-170.
10. Bann DV, Goyal N, Crist H and Goldenberg D. 2014. Black thyroid. *Ear, Nose & Throat J* **93:** 10-11.
11. Poobitha S, Nair M, Kumar RR, Varshney KC, Uma Maheswari D and Lakkawar AW. 2021. Neoplasms of the thyroid gland in goats (*Capra hircus*) - A slaughterhouse-based study. *Indian J Vet Pathol* **45:** 209-211.

Indian J. Vet. Pathol., 48(2) : 201-203, 2024: DOI: 10.5958/0973-970X.2024.00033.2

CASE REPORT

Aspergillosis in a Blue and Yellow Macaw (*Ara ararauna)* - A case report

M. Sathish Kumar, S. Uma, S. Poobitha, M.V. Srinivas[1], A.W. Lakkawar, R. Kumar* and M.G. Nair
[1]Department of Veterinary Microbiology, Department of Veterinary Pathology, Rajiv Gandhi Institute of Veterinary Education and Research (RIVER), Kurumbapet-605 009, Puducherry, India

Address for Correspondence
R. Kumar, Professor & Head, Department of Veterinary Pathology, Rajiv Gandhi Institute of Veterinary Education and Research (RIVER), Kurumbapet-605 009, Puducherry, India, E-mail: kumarpath70@gmail.com

Received: 21.9.2023; Accepted: 14.12.2023

ABSTRACT

The carcass of a female Macaw (two-and-a-half-month-old) was referred for a necropsy to the Department of Veterinary Pathology, RIVER, Puducherry with a history of anorexia and respiratory distress from an organised pet bird farm. On necropsy, varying-sized grayish-white nodules (<1 cm diameter) were observed in the thoracic cavity. The entire lung parenchyma had multi-focal caseous nodules (miliary to 1 cm) along with congestion and consolidation. Other gross lesions included a moderate degree of pericarditis, hepatic congestion, and splenomegaly. Representative tissues fixed in 10% neutral buffered formalin were processed by routine paraffin embedding technique and sections were stained with H&E. Histopathology revealed multiple necrotizing variable-sized granulomatous lesions in the lungs, characterized by an extensive area of caseous necrosis with the presence of fungal conidiophores and hyphae surrounded by a zone of lymphocytes, macrophages, epithelioid cells, and fibrous connective tissue. Further, on cultural examination with Saboraud's dextrose agar, fungal colonies with morphological features of *Aspergillus* spp. were recorded. PCR carried out using species-specific primer showed an amplified product of 310 bp confirming *A. fumigatus*. Based on gross, histopathogical, cultural characteristics, and molecular findings, the case was diagnosed as Aspergillosis.

Keywords: Air sac, aspergillosis, caseating granuloma, lungs, macaw

Aspergillosis is an infectious and non-contagious fungal disease of the respiratory system, which affects Aves including poultry, captive and wild birds[1]. *Aspergillus* spp. is a ubiquitous, saprophytic mould that has worldwide distribution except in Antarctica. Of the 340 species of Aspergillus, *A. fumigatus* is the most prevalent species representing 95% of the cases in both domestic and wild birds, and considered as major respiratory pathogen in birds causing high morbidity and mortality[2]. First identified in the lungs of a bustard by Fresenius[3] in 1863, captive birds are highly susceptible to aspergillosis due to several factors that include environmental, host immunity and the unique respiratory anatomy of birds[4,5]. Even though cases of aspergillosis have been reported in several avian species, the present study highlights the pathology and molecular confirmation of pulmonary aspergillosis caused by *Aspergillus fumigatus* in a Blue and Yellow Macaw (*Ara ararauna*).

A female Blue and Yellow Macaw aged two and half months maintained at a private farm at Puducherry was referred for necropsy to the Department of Veterinary Pathology, RIVER, Puducherry with a history of anorexia, depression, and respiratory distress. The farm has been experiencing random mortality in Macaws. Following the necropsy and recording of gross lesions, representative tissue samples were collected for histopathological and microbiological examination. Tissue samples were fixed in 10% Neutral Buffered Formalin (NBF) and processed by routine paraffin embedding techniques. The 4-5 µm thick sections were stained by Hematoxylin and Eosin (H&E), Periodic Acid Schiff's and Grocott's methenamine silver staining[6]. For mycological studies, a small piece of lung sample was inoculated in Sabouraud Dextrose agar (SDA) and incubated at 37°C for 72 hours. Further, the sample was subjected to PCR using species-specific primer sequences of internal transcribed spacer 1 (ITS1) ribosomal DNA and its flanking regions (ACTACCGATTGAATGGCTCG and CATACTTTCAGAACAGCGTTCA) of A. *fumigatus.* In addition, PCR was also carried out for *A.niger* (ACTACCGATTGAATGGCTCG and ACGCTTTCAGACAGTGTTCG) and *A. flavus* (ACTACCGATTGAATGGCTCG and TTCACTAGATCAGACAGAGT) using the species-specific primers[7].

How to cite this article : Kumar, M.S., Uma, S., Poobitha, S., Srinivas, M.V., Lakkawar, A.W., Kumar, R. and Nair, M.G. 2024. Aspergillosis in a Blue and Yellow Macaw *(Ara ararauna)* - A case report. Indian J. Vet. Pathol., 48(2) : 201-203.

Necropsy revealed copious amount of caseous material in the thoracic and abdominal air sacs. Varying-sized grayish-white nodules (<1 cm diameter) were adherent to the rib cage (Fig. 1). The entire lung parenchyma had multi-focal grayish-white caseous nodules (miliary to 1 cm) along with congestion and

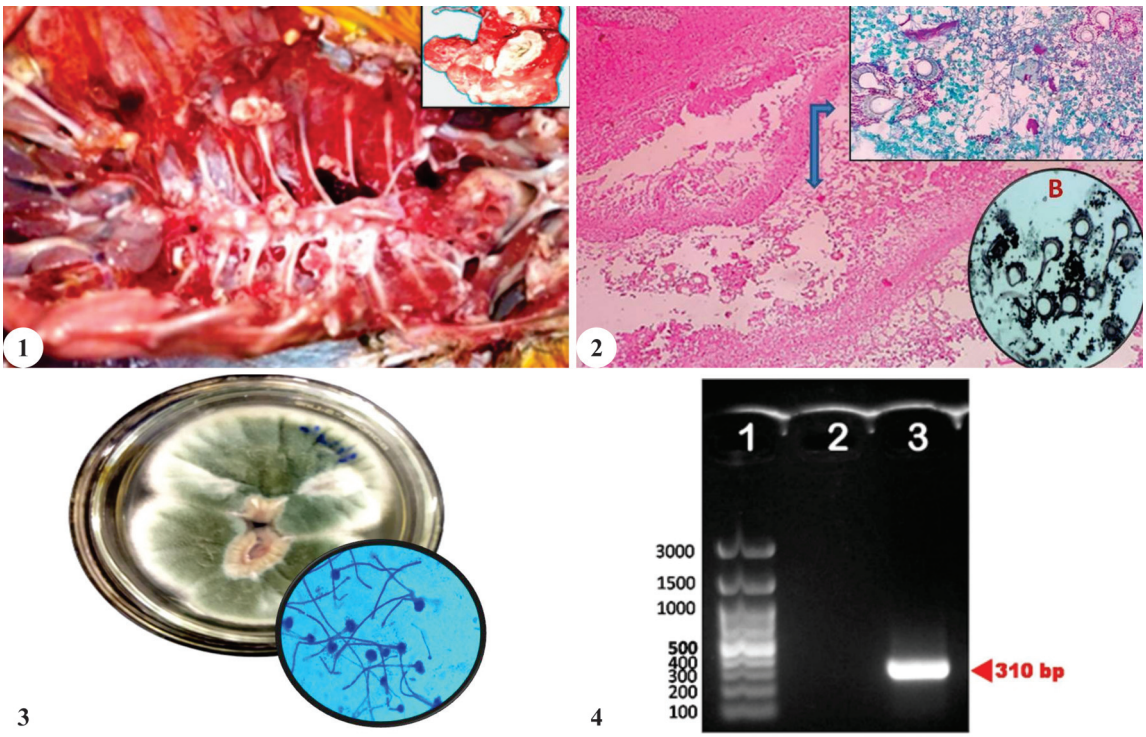

Fig. 1. Varying-sized grayish-white nodules (arrows) adhering to the rib cage. (Inset - Cut surface of a nodule showing caseation necrosis with cavitation); **Fig. 2.** Lung showing extensive area of caseous necrosis with the presence of fungal conidiophores and hyphae surrounded by inflammatory cells and fibrous connective tissue (H&E 400x) (Inset - A: Fungal conidiophores (pink stained). Periodic Acid Schiff (PAS) 400x; Inset - B: Fungal hyphae (black stained). Grocott's methenamine silver (GMS) 200x); **Fig. 3.** Growth of fungal mycelium in Sabouraud's Dextrose Agar with the cultural characteristics of Aspergillus spp. (Inset - Cello tape impression of SDA cultures showing characteristic fungal hyphae and conidiophores (blue stained) of Aspergillus spp. Lactophenol cotton blue stain, 200x); **Fig. 4.** PCR; 1% agarose gel. Lane 1: 100 bp base marker; Lane 2: Negative control; Lane 3: *Aspergillus fumigatus* isolate from the lungs of the Blue and Yellow Macaw.

consolidation (Fig. 1-inset). Other gross lesions included a moderate degree of pericarditis, hepatic congestion and splenic enlargement. Microscopically, multiple necrotizing varying-sized granulomatous lesions in the lungs and air sacs were observed. These lesions were characterized by large areas of encapsulated and clearly demarcated caseous necrosis with fungal conidiophores and hyphae surrounded by lymphocytes, macrophages, and epithelioid cells in the lung parenchyma (Fig. 2). The presence of fungal conidiophores in the lungs was further confirmed by Periodic Acid Schiff's (Fig. 2-inset A) and Grocott's methenamine silver staining methods (Fig. 2-inset B). In the present case report, Aspergillus hyphae were found in lungs associated with necrosis and inflammation suggesting that the route of infection was through inhalation[1]. Aspergillus infection can induce two types of lesion a deep nodular form and a superficial diffused form. In the granulomatous form, neither exudative inflammation nor vascular lesions in the neighbouring tissues are seen. This type of encapsulated reaction develops both in non-aerated and aerated organs (lungs and air sacs). In the non-encapsulated infiltrative type, the fungus frequently invades blood vessels. In aerated organs, the fungus may form aggregates of radiating hyphae containing large numbers of conidiophores and conidia in the absence of a structured granuloma formation. A mixed type composed of both tissue reactions may also occur[1,3]. In the present case, a granulomatous form was observed in the lungs with vascular lesions in the liver.

Inoculation of suspected material in SDA revealed characteristic morphological features of *Aspergillus* spp. (Fig. 3) that appeared as blue fungal hyphae and conidiophores on Lactophenol cotton blue staining (Fig. 3-inset). Although, the sample from the lung lesion inoculated in the SDA showed cultural and morphological characteristics of Aspergillus spp, it is important to mention that isolation of the fungus alone does not confirm the infection because of the ubiquitous nature of the organism[7]. In addition, the identification of species is important in drug susceptibilities and treatment procedures, which may vary among fungal species[8].

Aspergillosis is the most commonly occurring respiratory disease in captive wild birds. Of the psittacine species, the African grey parrot (*Psittacus erithacus*) and pionus parrots (*Pionus spp.*) are reported to have an increased susceptibility to the development of disease[9].

Among 340 accepted Aspergillus species, *Aspergillus fumigatus* is the most prevalent species accounting for 95% of cases in birds, followed by *A. flavus* and *A. niger*[2]. Species identification of fungus using histopathology and fungal culture morphology is not always successful due to atypical microscopic architecture and atypical fungal colonies. The PCR-based identification system is the most reliable and powerful tool that facilitates the diagnosis of infection at an early stage and controls the spread of infection by effective treatment. Hence, PCR carried out on DNA extracted from the culture resulted in the expected product size of 310 bp confirming *A. fumigatus* (Fig. 4).

In general, caudal air sacs are the primary site of infection, but later it spreads to the lungs. Inside the lungs, the organism localizes in the atria and parabronchus, germinates under favourable conditions produces spores, which are eliminated by phagocytic cells. However, when more conidia accumulate or the bird had a weak immune system, the defence mechanism cannot eliminate them, and the infection progress, with subsequent inflammation and necrosis[5]. Captive birds housed in aviaries are more predisposed to develop aspergillosis, due to high concentrations of spores, dirty and poorly ventilated environments, and long-term storage of food. Ambient temperature and humidity play important role in the life cycle of fungi and the level of a bird´s exposure to fungal spores[3]. In the present case, the birds were housed in aviaries suggests that the birds were exposed to spores due to improper housing management.

The present case report highlights the confirmation of mycotic pneumonia caused by *Aspergillus fumigatus* and the systemic effects in a Macaw. Aspergillosis is a potentially important cause for failure of conservation of captive and wild birds, due to ubiquitous presence of conidia in the environment and organic substrates which favours the inhalation of spores by birds[2]. Even though, the therapeutic options are available, it is essential that pet breeders, owners and veterinary practitioners should implement the adequate measures to prevent the spread of ubiquitous fungi, *Aspergillus* spp. from causing infections in aviaries.

ACKNOWLEDGMENT

The authors gratefully acknowledge the Dean, Rajiv Gandhi Institute of Veterinary Education and Research, Puducherry for providing the necessary facilities during the study.

REFERENCES

1. Kannoju A, Veldi P and Kumar V. 2020. An overview of aspergillosis in poultry: A review. *J Entomol Zool Stud* **9:** 685-688.
2. Arne P, Castillo VR, Jouvion G, Le Barzic C and Guillot J. 2021. Aspergillosis in Wild Birds. *J Fungi* **7:** 241.
3. Arne P, Thierry S, Wang D, Deville M, Le Locch G, Desoutter A, Femenia F, Nieguitsila A, Huang W, Chermette R and Guillot J. Aspergillus fumigatus in Poultry. *Int J Microbiol*.
4. Talbot JJ, Thompson P, Vogelnest L and Barrs VR. 2017. Identification of pathogenic Aspergillus isolates from captive birds in Australia. *Med Mycol J* **56:** 1-4.
5. Munir MT, Rehman ZU, Shah MA and Umar S. 2017. Interactions of *Aspergillus fumigatus* with the respiratory system in poultry. *Worlds Poult Sci J* **73**.
6. Luna LG. 1968. Manual of Histological Staining Methods of the Armed Forces Institute of Pathology. McGraw-Hill, New York, USA.
7. De-Oca VM, Martinez SE, Salinas EM, Olivare RA and Godoy FS. 2022. Pathological and mycological characterization of pulmonary *Aspergillus fumigatus* infection producing gliotoxin in a captive African grey parrot (*Psittacus erithacus*). *Braz J Vet Pathol* **15:** 93-98.
8. Sugita C, Makimura K, Uchida K, Yamaguchi H and Nagai A. 2004. PCR identification system for the genus Aspergillus and three major pathogenic species: Aspergillus fumigatus Aspergillus *flavus* and Aspergillus *niger*. *Med Mycol J* **42:** 433-437.
9. Redig PT. 2000. Aspergillosis. In Samour J (ed): Avian Medicine. Mosby, Philadelphia, USA: 275-287.

Title of Thesis	:	Pathomorphological and Immunohisto-chemical studies on thyroid glands of sheep
Name of the Student	:	**Dr M.V.S. Sudarsan Reddy**
Name of the Guide	:	Dr N. Sailaja
Degree/Year	:	MVSc/2024
Name of the University	:	Sri Venkateswara Veterinary University, Tirupati, Andhra Pradesh-517 502

Sheep hold immense significance for impoverished farmers in India, offering vital socio-economic benefits. Understanding the role of sheep thyroid glands is crucial for optimal livestock management as they influence metabolic regulation, reproduction, and growth. Pathological studies on sheep thyroid glands in India are crucial for identifying and managing disorders that impact reproduction, nutrition, and overall flock health. This enhances farmer awareness, promotes sustainable practices, and contributes to the economic success of sheep production. Limited information was available regarding cytological, pathomorphological, and immunohistochemical changes on thyroid lesions in the sheep thyroid glands. The current study addresses this gap, contributing to a more comprehensive understanding of thyroid lesions.

The present study involved the collection and examination of thyroid glands from 100 sheep to investigate pathological conditions. Among these, 13% showed no abnormalities, while congenital anomalies constituted 46% of the cases, including the ultimobranchial cysts (37%), thyroglossal duct anomalies (6%), and branchial cysts (3%). Degenerative changes were observed in 40% of sheep, with follicular degeneration (21%) being the most common. Vascular disturbances (30%), growth disturbances (52%), goitre (41%), pigmentation (1%) and neoplastic conditions (10%) were documented.

Macroscopic examination revealed marked conditions such as ultimobranchial cysts, colloid goiter, follicular adenomas, C-cell adenomas, congestion, and melanosis. The cytological examination showed distinct feature of pathological conditions which correlated with histopathology. Polyhedral keratinized cells with clear vacuolations in ultimobranchial cyst and foamy cytoplasm and dark condensed nuclei in follicular cells in follicular degeneration were observed. While follicular hyperplasia, features uniform size and shape of cohesive groups of cells having basophilia cytoplasm with occasional tyrosine granules, the follicular adenoma showed increased cellularity of round to oval cells with anisocytosis and anisokaryosis. In C cell adenoma, varied degree of cellular atypia, irregular nuclei and calcitonin granules were observed.

The cytological examination involved impression smears, with distinct features noted in various thyroid conditions, including ultimobranchial cysts, follicular degeneration, follicular hyperplasia, and neoplastic conditions.

The microscopic examination of sheep thyroid conditions revealed diverse pathologies. Ultimobranchial cysts, distributed throughout the thyroid parenchyma, exhibited stratified squamous epithelium and eosinophilic keratin debris. Thyroglossal duct cysts revealed cuboidal or stratified squamous epithelium with colloid-containing follicles. Branchial cysts featured ciliated cuboidal/columnar epithelium with cavities filled by eosinophilic fluid. Follicular degeneration ranged from mild to severe, with profound alterations, including desquamation and nuclear abnormalities. Corpora amylacea appeared as concentric basophilic granules, while cystic degeneration presented cystic dilatation with necrosed content. Epithelial hyperplasia and hypertrophy revealed increased cell layers and metaplasia, while atrophy showed fibrous proliferation, diminishing follicle size. C cell hyperplasia, lymphocytic thyroiditis, colloid goiter, and mixed goiter exhibited distinct microscopic features. Vascular anomalies included congestion, hemorrhage, and thrombus, while melanin deposition, capsular thickening, and fibrosis showed characteristic patterns.

Immunohistochemical analysis revealed cytokeratin positivity in follicular adenoma, VEGF immunoreactivity in hemangioma, intense thyroglobulin immunoreaction in thyroid hyperplasia and adenoma, and moderate calcitonin positivity in parafollicular adenoma and hyperplasia.

In conclusion, the cytological examination served as an initial screening for thyroid conditions in sheep, while detailed histopathological studies were essential for confirmation. Immunohistochemical findings aided in differentiating various tumors.

SUPERANNUATION

Dr G.A. Balasubramaniam

Dr Gurusamipalayam Amirthalingam Balasubramaniam, Professor and Head, Department of Veterinary Pathology, Veterinary College and Research Institute, Namakkal, Tamil Nadu was born on 1st May 1964 at Gurusamipalayam village at Rasipuram Taluk of Namakkal District, Tamil Nadu. He completed his graduation from Madras Veterinary College, Chennai in 1987, and MVSc and PhD, in 1989 and 1998, respectively.

He started his career as Assistant Professor in Veterinary University Training and Research centre (VUTRC) then Livestock Research & Development Centre (i.e. LRDC), Dharmapuri in 1989 and worked there for three years. Subsequently he moved to Department of Pathology, Veterinary College and Research Institute, Namakkal and served as a teaching faculty from 22.01.1993 to 30.04.2024. Totally, he was having 34 years of service in academics and research area. He guided 7 PhDs and 15 MVSc students in Veterinary Pathology and more than 60 students as minor guide in Veterinary Pathology and allied disciplines. He served as Dean in-charge of Veterinary College and Research Institute, Namakkal for a short period (from 06.06.2017 to 28.08.2018).

He organized a south zone conference of Indian Association of Veterinary Pathologists (IAVP) and symposium on "Pathobiology of Poultry and laboratory diseases" in 2010 at VCRI, Namakkal. He also organized an international workshop on "Avian Diseases" by inviting eminent poultry pathologist Dr H.L. Shivaprasad, Georgia (USA) in 2013 at VCRI, Namakkal. As Co-organising secretary he organized a national Symposium on, "Innovative Research Approaches for Diagnostic Pathology" at MVC, Chennai in 2011. As a member he organised the workshop on," Toxicologic pathology" at MVC, Chennai in 2011.

He organized several training programmes which includes, "Clinical Pathology" for field veterinarians in 2000, "Postmortem diagnosis of livestock and poultry diseases and their importance" in 2007. VCI Sponsored Continuing Veterinary Education on "Post-mortem examination and Vetero-legal cases".

He received Dr Ganti A. Sastry Memorial Medal for the publication of the article "Pathology of Endosulfan toxicity in chicken" and Dr A. Sundararaj Medal for the publication of the article, "Natural occurrence of Ochrotoxiciosis due to water contamination in chicken, for the best paper publications in Indian Veterinary Journal in 2000. Two more gold medals for the best paper presentation in ISVS in 2013.

Regarding the awards from Indian Association of Veterinary Pathologists, he received IAVP Achievement Award - Best Poultry Pathologist Award in 2012, IAVP President Best Worker Award (2016) - For Best Zonal Secretary (South), Fellow of IAVP in 2016 for effective contribution in Veterinary Pathology and he also obtained best poster awards. Apart from that he also received best oral and poster awards from various societies (16 Nos) in various years and Certificate of commemoration for unblemished service in TANUVAS in 2015.

He has more than 200 publications to his credit in national and international journals of repute. He has also produced colour atlases on "Post-mortem observations of livestock, poultry and laboratory animals" and "Animal tumors". He developed course content for the course "VPP 321 - Avian Pathology" in E-learning programme under National Agricultural Innovation Project (ICAR) and received a certificate of appreciation for task accomplishment. **At present he is acting as Secretary General of IAVP for the period of 2023-25.**

SUPERANNUATION

Dr S. Vairamuthu

Dr S. Vairamuthu was born in Nanguneri, Tirunelveli district in 1964, he pursued his early education at Shankar Reddiar School, Nanguneri. He obtained his undergraduate degree (BVSc) in 1988 followed by a postgraduate degree (MVSc) in 1991.

His professional journey began as a Veterinary Assistant Surgeon in Thanjavur district, subsequently serving as an Assistant Professor at AC & RI Madurai from June 1994 to March 1997. He then joined TANUVAS as an Assistant Professor at VC & RI, Namakkal in April 1997. In June 2000, he transitioned to the Department of Pathology, MVC, Chennai, concurrently pursuing a PhD in poultry pathology, which was completed in 2001.

In December 2006, he was promoted to Associate Professor in the Department of Pathology, later assuming the role of Associate Professor and Head at CCL in July 2007. In December 2012, he was further promoted to Professor and Head of CCL until March 31, 2024.

Throughout his career, he served as a Research Guide for 15 MVSc students and 4 PhD research scholars. Additionally, he contributed as a member of the advisory committee for over 50 PG and PhD research scholars, guided 12 PG Diploma online programs in Veterinary Clinical Laboratory Diagnosis, and conducted annual training programs for field veterinarians on Clinical Laboratory Diagnosis from 2010 to 2023.

He has published more than 160 research papers. He presented seven lead papers during the Professional Society Conference.

He also lead some overseas research programmes. Under the BBSRC project he visited the University of Pretoria, South Africa and ILRI, Kenya during July 2012. He completed three months short term training program on Veterinary Virology and Laboratory Diagnostics at University of Maryland, USA during August - October 2013. He attended a two week training program at University of Bari, Italy during February - March 2023 under NAHEP Project.

He also received gold medals from two Universities for PhD in Veterinary Pathology and 12 professional society awards for clinical and veterinary pathology aspects. He is a active member in five professional societies.